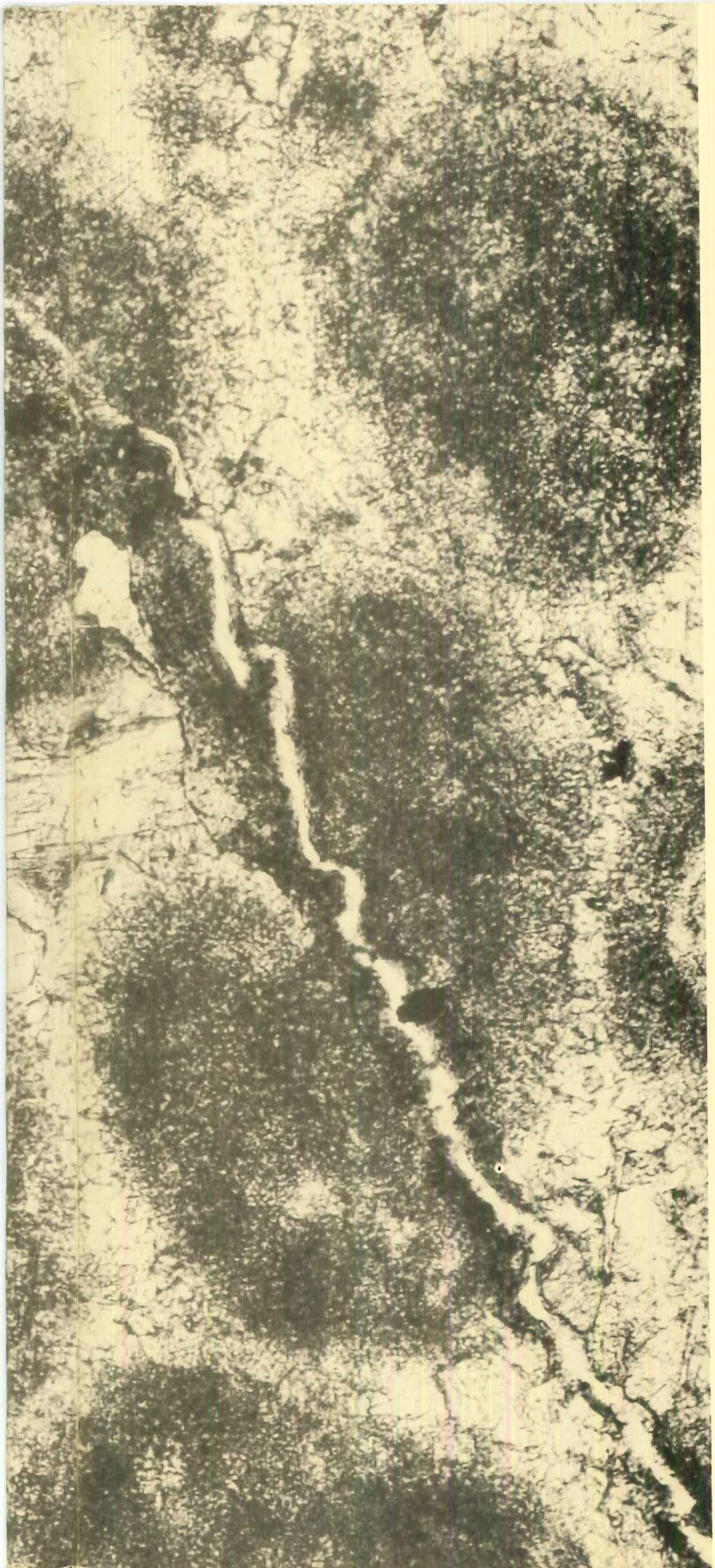

WEATHERING AND SOIL FORMATION IN A LIMESTONE AREA NEAR PASTENA (Fr., Italy)

O. C. Spaargaren

Errata

going with "Weathering and soil formation in a limestone area near Pastena (Fr., Italy)", by O.C. Spaargaren.

Page	Line	
10	24 from bottom	omit "haoliniet"
36	14 from top	read "X-ray diffraction analyses"
38	5 from bottom	read "(see 2.2.1, table 2.1)"
39	9 from bottom	read "iron compounds, ferrihydrite,"
40	23 from bottom	fromboidal = framboidal
41	6 from bottom	$(110.25)Mg^{2+}$ = $(110.25\text{-c-d})Mg^{2+}$
49	8 from top	fertizers = fertilizers
50	8 from bottom	appendix 5.2 = appendix 6.1
53	3 from bottom	read "$\lg[Mg^{2+}]$ + 2pH and $\lg[H_4SiO_4^o]$"
54	25 from bottom	idem
57	14 from top	read "(Sp/227b and a, respectively)"
61	6 from top	of = or
	4 & 41 from bottom	2Bt = 2Bt3
66	13 from bottom	table 2.21 = table 2.19
67	15 from bottom	read "(Sp/118, a chromic luvisol and Sp/119a, a chromic cambisol)"
75	8 from top	read "Fe(II)"
	17 from bottom	omit "2.29 and"
	8 from bottom	(fig. 2.30) = (fig. 2.29)
79		omit last line
81	21 from top	(Sp/183e) = (Sp/68a)
84	25 from top	read "tinuous process of rubefaction"
88	21 from bottom	read "(slightly affected by erosion)"
93	1 from top	read "Sp/22; Sp/41, an orthic acrisol;"
	2 from top	read "C7, a ferric luvisol)."
	5 from top	omit "and this was"
	13 from bottom	in = on
94	4 from bottom	accretionar = accretional
97	2 from top	$SiO_2Al_2O_3$ = SiO_2/Al_2O_3
	13 from top	C' = C7
	18 from bottom	omit "big"
104	4 from bottom	read "erosion processes cannot be held"
105	3 from top	thick = broad
112	22 from top	coincidence = coincide
114	24 from bottom	Sp/98 = Sp/97
115	22 from top	characteristics = characteristic
116	17 from bottom	modality = molality
118	21 from top	dell7 = della
	24 from bottom	Blanc = Blanck
166	7 from top	read "E80 (from Sevink et al., 1979)"
182	first line	read "(pX = -lg[X])"

Page	Table	
58, 59 & 60	2.11, 2.12, 2.13 & 2.15	Profile Sp/122: 2Bt = 2Bt3 Profile Sp/123: 2B = 2Bw1; 3B = 3Bw2
58, 65, 70, 73 & 79	2.11, 2.19, 2.25, 2.28 & 2.32	Qtz % indicated as 1 must be read as <1
62	2.16	2 µm = <2 µm
76	2.30	A = Å
94	3.5	Q % = Qtz %

Stellingen

behorende bij: Weathering and soil formation in a limestone area near Pastena (Fr., Italy), door Otto Coenraad Spaargaren (1979)

1. Valeton (1972) stelt ten onrechte dat terra rossa een intermediair verweringsproduct van kalksteen is, dat zich in de richting van bauxiet ontwikkelt.
   Valeton, I. (1972): Bauxites. Developments in Soil Science 1. Amsterdam-London-New York. 226 pp.

2. Het nemen van "bulk samples" van bodemhorizonten is in vele gevallen onvoldoende om de pedogenetische processen te ontrafelen.

3. Bij het bestuderen en interpreteren van bodemwater gegevens uit mediterrane gebieden dient men rekening te houden met de invloed van uitdroging op de activiteit van water.

4. Het verdient aanbeveling de klassificatie van bodems met een mollic horizont op kalksteen in gebieden waar een "xeric moisture regime" heerst, in de Soil Taxonomy (1975) te wijzigen van Xerolls in Xeric Rendolls.
   Soil Survey Staff (1975): Soil Taxonomy. Washington D.C. 754 pp.

5. Statistische verwerkingsmethoden dragen het gevaar in zich dat "uitzonderingsgevallen" niet nader onderzocht worden.

6. Omdat de pH een logaritmische grootheid is, is deze als zodanig niet geschikt om onbetrouwbaarheidsgrenzen van activiteiten aan te geven.

7. Sociale en politieke factoren mogen bij de aanleg van cultuurtechnische werken eerst in beschouwing genomen worden nadat op grond van natuurwetenschappelijk onderzoek de mogelijkheid van verwezelijking van de gestelde doeleinden voldoende is vastgesteld.

8. Gezien de groeiende schaarste in de wereld aan gronden voor de voedselproductie is in daarvoor geschikte gebieden irrigatie met zout water te verkiezen boven niet geirrigeerd landgebruik.

9. Het onderzoek van de holocene landschapsgenese heeft dringend behoefte aan goede determinatiemethoden van potscherf fragmenten met een doorsnede van minder dan 10 mm.

10. Daar nog steeds vele fysisch geografen hun werk vinden bij internationale organisaties verdient het aanbeveling dat zij tenminste eenmaal tijdens hun studie een verslag schrijven in een van de internationaal meest gangbare buitenlandse talen.

11. De schaatsminnende bevolking van Wageningen e.o. zou er zeer bij gebaat zijn indien de hoogte van het prikkeldraad in de uiterwaarden met ca. 10 cm verlaagd werd.

5714 - pdf

APPENDIX 1: SOIL MAP, going with "Weathering and soil formation in a limestone area near Pastena (Fr., Italy)", by O.C. Spaargaren.

SOIL MAP OF AN AREA SOUTH OF THE SACCO RIVER NEAR PASTENA (Fr., Italy)

scale 1:50 000

LEGEND

SOILS ON MESOZOIC CALCAREOUS ROCKS

- A1 Complex of medium textured LITHOSOLS, excessively drained and medium textured RENDZINAS, shallow, somewhat excessively drained.
- A2 Complex of medium textured RENDZINAS, shallow, somewhat excessively drained and medium textured LITHOSOLS, excessively drained.
- A3 Medium textured RENDZINAS, shallow, somewhat excessively drained.
- A4 Association of medium textured LITHOSOLS, excessively drained and fine textured CHROMIC LUVISOLS and EUTRIC NITOSOLS, deep, (moderately) well drained.
- A5 Association of fine textured CHROMIC LUVISOLS and EUTRIC NITOSOLS, deep, (moderately) well drained and medium textured LITHOSOLS, excessively drained.
- A6 Complex of fine textured CHROMIC LUVISOLS and EUTRIC NITOSOLS, deep, (moderately) well drained.
- A7 Complex of fine textured CHROMIC LUVISOLS and EUTRIC NITOSOLS, moderately deep to deep, (moderately) well drained and medium textured RENDZINAS, shallow, somewhat excessively drained.
- A8 Complex of fine textured CHROMIC VERTISOLS, deep, moderately well drained and medium textured LITHOSOLS, excessively drained.

SOILS ON CALCAREOUS SHALES AND SANDSTONES OF MIOCENE AGE

- B1 Medium textured CALCARIC REGOSOLS, shallow, moderately well drained.
- B2 Association of medium textured CALCARIC REGOSOLS, shallow, moderately well drained and fine textured CALCIC CAMBISOLS, moderately deep to deep, imperfectly drained.
- B3 Association of fine textured CALCIC CAMBISOLS, moderately deep to deep, imperfectly drained and medium textured CALCARIC REGOSOLS, shallow, moderately well drained.
- B4 Fine textured CALCIC CAMBISOLS, moderately deep to deep, imperfectly drained.

SOILS ON SANDSTONES AND CONGLOMERATES OF PLIOCENE/OLD QUATERNARY AGE

- C1 Medium textured FERRIC ACRISOLS, deep, moderately well drained.
- C2 Complex of medium textured FERRIC and GLEYIC ACRISOLS, deep, moderately well drained.
- C3 Medium textured ORTHIC ACRISOLS, deep, well drained.
- C4 Complex of medium textured FERRIC and ORTHIC ACRISOLS, deep, (moderately) well drained.
- C5 Association of medium textured FERRIC ACRISOLS, deep, moderately well drained and coarse textured LITHOSOLS, excessively drained.
- C6 Medium textured LUVIC PHAEOZEMS, deep, well drained.

SOILS ON ALLUVIAL DEPOSITS OF THE SACCO AND LIRI RIVERS AND THEIR TRIBUTARIES.

- D1 Medium to coarse textured CALCARIC FLUVISOLS, shallow, (somewhat) excessively drained.
- D2 Medium textured CHROMIC LUVISOLS, moderately deep, well drained.
- D3 Complex of medium textured ORTHIC LUVISOLS and EUTRIC CAMBISOLS, moderately deep to deep, (moderately) well drained.
- D4 Association of medium textured CALCIC CAMBISOLS and ORTHIC LUVISOLS, deep, (moderately) well drained.

SOILS ON COLLUVIO - ALLUVIAL DEPOSITS

- E1 Complex of fine textured CHROMIC and VERTIC LUVISOLS, deep, moderately well drained.
- E2 Fine textured CHROMIC LUVISOLS, deep, moderately well drained.
- E3 Complex of fine textured CHROMIC LUVISOLS, deep, moderately well drained and medium textured LITHOSOLS, excessively drained.
- E4 Complex of gravelly fine textured CHROMIC LUVISOLS and CHROMIC CAMBISOLS, deep, (moderately) well drained.
- E5 Association of fine textured CALCIC KASTANOZEMS, moderately deep to deep, imperfectly drained and fine textured CALCARIC PHAEOZEMS, moderately deep, moderately well drained.
- E6 Fine textured CALCARIC FLUVISOLS, shallow, moderately well drained.

SOILS ON VOLCANIC DEPOSITS

- F1 Medium textured CALCARIC PHAEOZEMS, shallow, somewhat excessively drained.

Base map derived from Carta d'Italia 1 : 25 000
(F° 159 I S.E. & II N.E. and F° 160 III S.O. & IV S.O.)

ISN 5714-2pdf 58X22

APPENDIX 6.1 Lg $\left(\frac{IAP}{K}\right)$ VALUES AT 15°C OF THE KARSTIC WATERS FOR A NUMBER OF MINERALS (going with: "Weathering and soil formation in a limestone area near Pastena (Fr., Italy)" by O.C. Spaargaren).

[1] Lg K at 25° C. [2] Lg K calculated from HELGESON (1969).

Origin of sample	Sample number	Adularia Lg K = 1.58	Microcline Lg K = 1.60	Sanidine Lg K = 1.86	Albite Lg K = 4.40	Plagioclase Lg K = 26.65	Leucite Lg K = 10.48	Nepheline Lg K = 15.54	Analcime Lg K = 10.02	Laumontite Lg K = 13.06	Phillipsite Lg K = -6.90[1]	Kaolinite Lg K = 8.62	Halloysite Lg K = 12.41	Illite Lg K = 11.53	Muscovite Lg K = 18.67[2]	Ca-montmorillonite Lg K = 7.27	Mg-montmorillonite Lg K = 7.18	K-montmorillonite Lg K = 6.92	Na-montmorillonite Lg K = 7.20	Pyrophyllite Lg K = 42.10	Mg-chlorite Lg K = 62.34	Phlogopite Lg K = 43.70[1]	Annite Lg K = 28.16	Chrysotile Lg K = 33.56	Greenalite Lg K = 23.80[1]	Sepiolite Lg K = 19.00	Talc Lg K = 19.91	Boehmite Lg K = 9.31	Gibbsite (cc) Lg K = -32.77	Gibbsite (cr) Lg K = -33.14	Brucite Lg K = -11.24	Calcite Lg K = -8.29	Aragonite Lg K = -8.26	Magnesite Lg K = -7.90	Dolomite Lg K = -16.81	Siderite Lg K = -10.57	Quartz Lg K = -4.13	Chalcedony Lg K = -3.67	α - Cristobalite Lg K = -3.47	β - Cristobalite Lg K = -2.90	Silica (am) Lg K = -3.13	Silica (gel) Lg K = -2.80
SPRINGS	Sp/ 19a	0.12	0.10	-0.16	-1.52	-2.14	-5.06	-5.19	-3.41	3.99	9.19	4.61	0.82	3.28	3.73	5.00	4.91	4.34	4.44	3.67	- 1.80	-11.38		-10.40		-10.33	- 4.22	1.04	0.06	0.44	-7.25	-0.09	-0.13	-1.56	-1.02		0.40	-0.06	-0.26	-0.83	-0.60	-0.94
	/ 19b	0.66	0.64	0.38	-1.22	-1.51	-4.52	-4.90	-3.11	4.63	9.61	5.22	1.43	4.14	4.87	5.72	5.64	5.13	5.15	4.29	- 0.85	-10.63		-10.19		-10.18	- 3.99	1.34	0.36	0.74	-7.18	-0.05	-0.09	-1.48	-0.90		0.40	-0.06	-0.25	-0.83	-0.59	-0.93
	/ 19c																							- 9.18	- 8.95	- 9.33	- 3.49											-6.68	-0.28	-0.32	-1.42	-1.08	-1.92	0.15	-0.31	-0.50	-1.08	-0.85	-1.18
	/ 19d	0.62	0.60	0.34	-1.01	-0.19	-4.42	-4.42	-2.27	5.68	9.70	5.91	2.11	4.90	5.78	6.45	6.39	5.71	5.82	4.70	3.71	- 8.27	0.56	- 8.05	- 5.00	- 8.38	- 2.13	1.81	0.84	1.22	-6.38	0.08	0.04	-1.18	-0.48	-0.74	0.27	-0.19	-0.39	-0.96	-0.73	-1.06
	Sp/ 32a																							0.20		- 3.33	6.29						-3.71	0.56	0.52	0.29	1.48		0.37	-0.09	-0.29	-0.86	-0.63	-0.96
	/ 32b																							- 7.62		- 8.53	- 1.51						-6.30	0.08	0.04	-0.60	0.11		0.37	-0.10	-0.29	-0.87	-0.63	-0.97
	/ 32c	-0.28	-0.30	-0.56	-1.58	-1.51	-5.41	-5.17	-3.43	4.54	8.96	4.88	1.08	3.48	3.67	5.32	5.36	4.45	4.66	3.86	4.21	- 8.31		- 7.01		- 7.33	- 0.90	1.21	0.24	0.61	-6.10	0.19	0.16	-0.47	0.34		0.36	-0.10	-0.30	-0.87	-0.64	-0.98
	/ 32d	-0.37	-0.39	-0.65	-1.91	-2.27	-5.49	-5.49	-3.75	3.75	8.75	4.13	0.33	2.87	2.86	4.42	4.47	3.65	3.79	3.08	3.47	- 8.39	- 5.36	- 7.02	- 9.77	- 8.19	- 0.94	0.85	-0.13	0.25	-6.09	0.14	0.11	-0.52	0.24	-2.01	0.35	-0.12	-0.31	-0.88	-0.65	-0.99
	/ 32e																							- 8.75	-10.55	- 9.28	- 2.63						-6.68	-0.12	-0.16	-0.79	-0.29	-1.96	0.37	-0.09	-0.29	-0.86	-0.63	-0.97
	/ 32f																							- 7.47	- 8.43	- 8.41	- 1.33						-6.26	0.07	0.04	-0.58	0.12	-1.47	0.38	-0.08	-0.28	-0.85	-0.62	-0.95
	Sp/108																							-12.08		-11.74	- 6.24						-7.69	-0.61	-0.64	-2.16	-2.14		0.23	-0.24	-0.43	-1.01	-0.77	-1.11
	Sp/168a																							- 9.84	-10.65	-10.60	- 4.43						-6.81	-0.71	-0.74	-1.63	-1.71	-2.47	0.01	-0.45	-0.65	-1.22	-0.99	-1.32
	/168b	-0.93	-0.95	-1.21	-2.80	-2.33	-5.72	-5.70	-4.31	3.02	8.62	4.11	0.31	2.44	2.95	3.95	3.95	3.23	3.25	2.39	1.54	- 9.89		- 8.64		- 9.30	- 3.23	1.17	0.20	0.57	-6.41	-0.23	-0.27	-1.17	-0.78		0.01	-0.45	-0.65	-1.22	-0.99	-1.32
	/168c	-0.13	-0.15	-0.41	-2.26	-1.06	-4.87	-5.06	-3.71	4.21	8.70	4.54	0.74	3.54	4.27	4.52	4.55	3.89	3.83	2.73	7.05	- 6.01		- 5.65		- 7.38	- 0.33	1.43	0.46	0.83	-5.38	0.15	0.11	-0.61	0.16		0.03	-0.50	-0.69	-1.26	-1.03	-1.37
	/168d	-1.70	-1.72	-1.98	-3.30	-2.87	-6.35	-5.93	-4.67	2.22	7.39	4.33	0.53	1.92	2.66	3.90	3.87	3.10	3.22	2.35	- 3.15	-13.53	- 6.21	-11.77	-10.23	-12.11	- 6.62	1.42	0.44	0.82	-7.36	-0.72	-0.76	-1.85	-1.95	-1.91	0.12	-0.58	-0.78	-1.35	-1.12	-1.46
	/168e	-0.66	-0.68	-0.94	-2.18	-2.18	-5.52	-5.55	-4.08	3.31	8.31	4.36	0.56	2.77	3.33	4.32	4.31	3.62	3.65	2.79	0.91	-10.19	- 2.08	- 9.06	- 6.73	- 9.96	- 3.51	1.23	0.25	0.63	-6.60	-0.25	-0.29	-1.28	-0.91	-1.07	0.09	-0.38	-0.57	-1.15	-0.91	-1.25
	Sp/193a	0.48	0.47	0.20	-1.30	-0.42	-4.38	-4.35	-2.88	5.08	9.48	5.37	1.57	4.68	5.83	5.99	5.95	5.36	5.42	4.16	3.63	- 8.24	- 1.52	- 8.25	- 7.31	- 9.41	- 2.68	1.91	0.93	1.31	-6.33	-0.04	-0.08	-1.19	-0.61	-1.45	0.09	-0.37	-0.57	-1.14	-0.91	-1.24
	/193b	1.03	1.01	0.75	-0.92	0.78	-3.85	-4.02	-2.52	6.32	9.94	6.83	3.03	5.97	7.44	7.31	7.27	6.65	6.65	5.30	5.28	- 7.37	- 1.12	- 7.89	- 7.42	- 9.14	- 2.29	2.34	1.46	1.84	-6.22	0.06	0.03	-1.08	-0.39	-1.49	0.11	-0.35	-0.55	-1.12	-0.89	-1.23
WEATHERING ZONES	Sp/ 31a	-0.46	-0.48	-0.74	-2.06	-1.61	-5.41	-5.28	-3.72	4.07	8.63	4.82	1.02	3.38	3.80	5.00	5.03	4.20	4.32	3.43	3.57	- 8.73		- 7.62		- 8.84	- 1.88	1.36	0.39	0.76	-6.18	0.12	0.08	-0.59	0.15		0.18	-0.29	-0.48	-1.05	-0.82	-1.16
	/ 31b	-0.01	-0.03	-0.29	-1.47	-0.93	-5.05	-4.87	-3.22	4.92	9.15	5.93	2.13	4.81	5.18	6.33	6.36	5.51	5.68	4.71	2.57	- 9.59	- 2.51	- 8.76	- 7.46	- 9.46	- 2.85	1.83	0.86	1.23	-6.61	-0.10	-0.13	-0.82	-0.29	-0.96	0.26	-0.20	-0.39	-0.97	-0.74	-1.07
	/ 31c	-0.42	-0.44	-0.70	-1.68	-1.19	-5.42	-5.02	-3.40	4.59	8.84	5.35	1.55	3.82	4.26	5.66	5.70	4.78	5.00	4.06	3.59	- 9.02	- 0.60	- 7.85	- 7.07	- 8.91	- 2.00	1.57	0.60	0.97	-6.29	0.07	0.03	-0.65	0.04	-0.97	0.23	-0.23	-0.43	-1.00	-0.77	-1.11
	/ 31d	-0.71	-0.73	-0.99	-2.20	-2.02	-5.69	-5.41	-3.86	3.63	8.41	4.24	0.45	2.76	2.96	4.34	4.34	3.52	3.68	2.83	3.78	- 8.53	- 2.98	- 7.16	- 7.38	- 8.56	- 1.44	1.09	0.11	0.49	-6.02	0.20	0.16	-0.52	0.30	-1.17	0.17	-0.30	-0.49	-1.07	-0.83	-1.17
	Sp/189a	0.79	0.77	0.51	-0.54	0.40	-4.31	-4.07	-2.37	6.37	10.02	7.30	3.50	5.90	7.23	8.01	7.90	7.20	7.40	6.21	- 0.59	-11.55	1.48	-11.38	- 4.13	-11.10	- 5.34	2.45	1.48	1.85	-7.53	-0.96	-1.00	-2.57	-2.91	-0.72	0.33	-0.13	-0.33	-0.90	-0.67	-1.01
	/189b	0.58	0.56	0.30	-0.80	-0.28	-4.57	-4.41	-2.66	5.79	9.78	6.03	2.23	4.82	5.66	6.68	6.56	5.88	6.07	5.02	0.81	-10.19	0.93	- 9.73	- 4.38	- 9.93	- 3.60	1.77	0.80	1.17	-7.01	-0.76	-0.79	-2.43	-2.57	-1.23	0.37	-0.09	-0.29	-0.86	-0.63	-0.96
	/189c	0.68	0.67	0.40	-0.59	0.44	-4.39	-4.06	-2.38	6.36	9.94	6.37	2.58	5.24	6.25	7.05	6.91	6.22	6.44	5.23	2.30	- 9.35	2.60	- 9.14	- 2.97	- 9.65	- 3.16	2.02	1.05	1.39	-6.76	-0.63	-0.67	-2.43	-2.43	-0.94	0.30	-0.16	-0.36	-0.93	-0.70	-1.04
	/189d	-0.47	-0.49	-0.76	-1.78	-1.59	-5.47	-5.11	-3.50	4.18	8.76	4.31	0.51	2.81	3.18	4.55	4.41	3.72	3.93	3.01	0.54	-10.28	1.17	- 9.06	- 3.39	- 9.73	- 3.23	1.06	0.09	0.46	-6.69	-0.64	-0.68	-2.40	-2.41	-1.08	0.23	-0.24	-0.43	-1.01	-0.77	-1.11
COLLUVIA	Sp/ 59a	-1.22	-1.24	-1.50	-2.76	-2.49	-5.86	-5.36	-4.11	2.58	7.90	2.97	-0.79	1.53	1.84	2.62	2.60	1.92	2.06	0.99	4.44	- 7.69		- 6.44		- 8.57	- 1.32	0.76	-0.21	0.16	-5.58	-0.30	-0.34	-1.36	-1.04		-0.13	-0.60	-0.79	-1.36	-1.13	-1.47
	/ 59b	0.92	0.90	0.63	-1.28	-0.21	-3.98	-4.41	-2.90	5.37	9.70	6.79	2.99	5.65	7.25	7.13	7.11	6.59	6.51	5.30	0.80	-10.16	- 0.32	-10.53	- 6.46	-10.87	- 4.89	2.40	1.43	1.80	-7.11	-0.89	-0.93	-1.98	-2.25	-1.20	0.13	-0.34	-0.53	-1.10	-0.87	-1.21
	/ 59c	1.21	1.19	0.93	-0.98	0.87	-3.61	-3.95	-2.52	6.29	10.00	6.24	2.45	5.77	7.15	6.66	6.44	6.09	6.01	4.59	8.49	- 4.87	4.05	- 5.69	- 2.54	- 7.77	- 0.21	2.21	1.23	1.61	-5.45	0.21	0.18	-0.83	0.01	-0.35	0.05	-0.42	-0.61	-1.18	-0.95	-1.29
	/ 59d																							- 4.03		- 6.70	1.42						-4.89	0.54	0.50	-0.49	0.67		0.03	-0.43	-0.62	-1.20	-0.97	-1.30
	Sp/116a	-0.75	-0.77	-1.03	-2.90	-0.62	-5.01	-4.75	-3.88	3.68	8.06	4.92	1.70	3.69	5.56	4.92	4.84	4.32	4.25	2.74	1.72	-10.13	- 0.52	-10.10	- 6.27	-11.64	- 5.73	2.39	1.42	1.79	-6.54	-0.95	-0.98	-2.34	-2.66	-1.64	-0.51	-0.97	-1.17	-1.74	-1.51	-1.84
	/116b	-0.43	-0.45	-0.71	-2.02	-2.56	-5.54	-5.56	-3.84	3.44	8.67	5.19	1.39	3.20	3.89	5.42	5.33	4.69	4.81	4.12	- 6.18	-14.87		-13.47		-12.48	- 7.41	1.39	0.42	0.79	-8.23	-1.66	-1.69	-3.11	-4.14		0.34	-0.13	-0.32	-0.90	-0.66	-1.00
	/116c	-0.01	-0.03	-0.29	-1.78	-2.22	-5.16	-5.40	-3.64	3.85	8.99	5.81	2.01	3.90	4.84	6.14	6.05	5.47	5.53	4.81	- 6.97	-15.31		-14.26		-12.94	- 8.13	1.66	0.69	1.06	-8.52	-2.05	-2.09	-3.51	-4.94		0.37	-0.09	-0.29	-0.86	-0.63	-0.96
	/116d	0.57	0.55	0.29	-1.22	0.16	-4.34	-4.37	-2.85	5.76	9.56	6.33	2.53	5.19	6.42	6.74	6.69	6.02	6.07	4.85	3.11	- 8.85	1.77	- 8.85	- 4.01	- 9.74	- 3.20	2.16	1.19	1.56	-6.56	-0.65	-0.68	-2.01	-2.03	-0.97	0.13	-0.33	-0.52	-1.10	-0.86	-1.20
	/116e	-0.09	-0.11	-0.37	-1.54	-0.20	-4.93	-4.55	-3.10	5.26	9.07	6.56	2.76	4.82	6.12	6.83	6.74	5.99	6.15	4.95	0.07	-11.44	0.12	-10.91	- 5.13	-11.12	- 5.38	2.34	1.37	1.74	-7.20	-1.12	-1.15	-2.53	-3.02	-1.17	0.07	-0.39	-0.59	-1.16	-0.93	-1.27
	Sp/169a	0.20	0.19	-0.08	-1.55	-1.16	-4.89	-5.07	-3.36	4.82	9.22	4.69	0.89	3.73	4.04	5.14	5.12	4.39	4.45	3.59	4.94	-11.06		- 6.51		- 7.86	- 0.48	1.15	0.18	0.55	-5.91	0.28	0.24	-0.75	0.15		0.32	-0.14	-0.33	-0.91	-0.67	-1.01
	/169b	0.69	0.68	0.41	-1.13	-0.68	-4.49	-4.83	-3.03	5.47	9.67	5.67	1.88	4.75	5.33	6.32	6.31	5.60	5.64	4.76	3.73	- 8.13		- 7.70		- 8.50	- 1.48	1.55	0.58	0.95	-6.36	0.08	0.04	-0.89	-0.23		0.41	-0.05	-0.24	-0.82	-0.58	-0.92
	/169c	-0.79	-0.81	-1.07	-2.51	-3.30	-5.61	-6.21	-4.42	2.85	8.24	3.78	-0.01	1.74	1.43	3.46	3.44	2.67	2.72	2.32	0.16	-10.30	- 0.07	- 8.39	- 3.93	- 8.97	- 2.18	0.34	-0.63	-0.26	-6.59	-0.14	-0.18	-1.16	-0.68	-0.25	0.41	-0.05	-0.25	-0.82	-0.59	-0.92
	/169d	-0.85	-0.87	-1.13	-2.50	-2.96	-5.93	-5.99	-4.30	2.98	8.21	3.64	-0.16	2.03	1.97	3.77	3.75	2.98	3.08	2.50	0.22	-10.50	- 5.39	- 8.74	- 9.41	- 9.38	- 2.74	0.64	-0.33	0.04	-6.64	-0.17	-0.20	-1.17	-0.71	-1.97	0.30	-0.16	-0.35	-0.93	-0.69	-1.03
	Sp/170a	-3.48	-3.50	-3.76	-4.46	-7.20	-8.38	-7.58	-6.08	-1.63	5.92	1.89	-1.91	-1.63	-2.05	1.07	1.08	0.23	0.55	0.39	-13.43	-20.16	-11.29	-16.13	-13.04	-14.61	-10.50	-0.05	-1.02	-0.65	-8.98	-3.19	-3.22	-4.05	-6.61	-3.59	0.12	-0.34	-0.53	-1.11	-0.88	-1.21
	/170b	-1.78	-1.80	-2.06	-1.80	-3.90	-6.83	-5.87	-4.21	1.98	7.82	4.10	0.30	1.55	1.56	4.55	4.04	3.12	3.54	2.91	- 5.65	-15.21	- 5.43	-12.58	- 8.58	-11.98	- 6.64	0.90	-0.07	0.30	-7.90	-2.74	-2.78	-3.60	-5.72	-2.84	0.28	-0.19	-0.38	-0.95	-0.72	-1.06

WEATHERING AND SOIL FORMATION IN A LIMESTONE AREA NEAR PASTENA (Fr., Italy)

ACADEMISCH PROEFSCHRIFT

ter verkrijging van de graad van doctor in de Wiskunde en Natuurwetenschappen aan de Universiteit van Amsterdam op gezag van de Rector Magnificus, Prof. Dr. J. Bruyn, hoogleraar in de Faculteit der Letteren, in het openbaar te verdedigen in de Aula der Universiteit (tijdelijk in de Lutherse Kerk, ingang Singel 411, hoek Spui), op woensdag 19 september 1979, des namiddags om 3.00 uur precies

door

Otto Coenraad Spaargaren

geboren te Haarlem

Promotor : Prof. Dr. Ir. A. P. A. Vink
Co-promotor: Dr. J. M. Verstraten
Co-referent : Prof. Dr. Oen Ing Soen

This thesis will also be published as:
Publicaties van het Fysisch Geografisch en Bodemkundig Laboratorium
van de Universiteit van Amsterdam, no. 30 (1979).

ACKNOWLEDGEMENTS

It is a great pleasure to render my cordial thanks to all those who have contributed in some way to this study by moral, logistic or material support; in particular

- Prof. Dr. Ir. A.P.A. Vink, who supervised the completion of this thesis, for his never lasting encouragement during field work and consecutive elaboration, and for his constructive critical remarks on the text,
- the late Dr. Ir. J. van Schuylenborgh, for teaching me the principles of thermodynamic approaches in soil science and for the many fruitful discussions on their application in this study,
- Dr. J.M. Verstraten, who was willing to take over the co-promotorship of the late Dr. Ir. J. van Schuylenborgh, for his careful reading of the text and his valuble suggestions for its improvement,
- Dr. J. Sevink, for critically going through part of the manuscript and his enthousiastic support of this study,
- Drs. E.A. Kummer and Mr. B. de Leeuw, for their preparation and interpretation of the X-ray diffraction analyses,
- Mrs. M.J. van Wijk-de Groot and Messrs. H. Flohr, L. Hoitinga, L. de Lange, R. Smaal, P. Wartenbergh, N. de Wilde de Ligny (Swami Somadeva) and T. van Wijk, for their careful physical and chemical analyses and for their support during the times spent in the laboratory,
- Mr. C. Zeegers, for preparing the thin sections,
- Drs. M.J. Jansma, for counting and interpreting several diatom samples,
- Drs. D. Verheggen, for his help in the field of statistics,
- Drs. J. van der Greef of the Laboratory for Organic Chemistry of the University of Amsterdam, for analysing the organic substances in the limestone rock,
- Dr. C. Boni of the Geological Institute of the University of Rome, for providing chemical data of some karstic springs,
- Mr. Wen Ting-Tiang and Drs. W.G. Westerveld, for taking additional samples,
- Mrs. P. de With and Messrs. A.J. van Geel and C. Snabilié, for preparing the figures and Messrs. W.C.W.A. Bomer and H.E. Renaud for printing the photographs,
- Mrs. G. Giessen-Peters and J.C. Tijmons, for typing the manuscript,
- and all those unnamed, who, in the field and during the time of elaboration of the data, have contributed to the completion of this study.

I also wish to thank all my collegues of the International Soil Museum at Wageningen for their help, both moral and material, during the last months of the preparation of this thesis.

The author gratefully acknowledges the financial support of the Netherlands Organisation for the Advancement of Pure Research (Z.W.O.) anf the "Consiglio Nazionale delle Ricerche" (C.N.R.) in Rome, which enabled him to visit the research area in February and March 1976.

Finally I am greatly indebted to my wife Jantien, who patiently endured all problems and troubles that accompany the completion of a thesis.

CONTENTS

SUMMARY

The scope of this study is to investigate the weathering and soil-forming processes in a limestone area near Pastena (Fr.) in south-central Italy. Emphasis is given to the study of the mineralogy of the soils and parent materials, the changes that occur and to theoretical weathering models of the limestone.

An outline of the physiography, climate and geology of the research area is given in chapter 1. The investigated area consists largely of limestone and dolomitic limestone of mainly Cretaceous age. Besides these rocks, conglomerates, sandstones and shales of Miocene, Pliocene and Quaternary age occur at several localities.

The physiography of the area is dominantly determined by karstic processes. Three subregions can be distinguished, depending on the degree of karstification and all examples of karstic features (karren, dolines, caves, lapies karst, uvalas, poljes) occur. The physiography of the utmost northern and eastern part of the main research area can be described as a rolling to hilly country, consisting of Miocene shales.

On base of the interpretations of the climatological data it is discussed that most likely a xeric moisture regime may be expected. The limit of dryness, however, set by the Soil Survey Staff (1975) on base of water balance calculations, viz. evapotranspiration of 175 mm moisture from a soil holding 200 mm in the absence of rain, seems to be too restrict. A more appropriate value is 125 mm of evapotranspiration of a similar soil, because the length of the dry period calculated from this figure is rather well in accordance with the field observations.

Chapter 2 deals with the weathering of and soil formation on limestone and dolomite. Based on mineralogical and chemical analyses of some limestone samples, theoretical weathering models at several relevant partial CO_2-pressures are calculated for a dolomitic limestone of which the composition is thought to be representative for the limestone in the area under survey. The results of these calculations are compared with the chemical composition of water samples (liquid phase) and the mineralogy of the soils (solid phase).

The carbonate part of the limestone in the calculations consists of approx. 45 % calcite, 45 % dolomite and 10 % aragonite. The non-carbonate mineralogy is dominated by illite (like in most other samples of the limestone), with as accessory minerals smectite, chlorite, kaolinite (dickite), quartz, albite, pyrite and most probably amorphous iron compounds. For the theoretical calculations these accessory minerals are not taken into account for various reasons.

The results of the calculations indicate that a weathering residue consisting of dolomite and kaolinite may be expected at partial CO_2-pressures between $10^{-2.00}$ and $10^{-0.80}$ bar. This theoretical mineralogical composition agrees rather well with the "dolomitic sands" which are found near Itri and locally in the main research area.

The composition of the water samples from karstic springs is in fair agreement with the theoretical solution with respect to Ca, Mg and HCO_3 content. The amount of K, Al and H_4SiO_4 in the water samples on the contrary is several times higher than the calculated amount. This may be due to: (1) the composition of the limestone used in the calculations is not representative for the survey area as a whole and (2) admixture with allochtonous (volcanic) material influences the actual composition of the karstic waters.

Analyses of the water samples show that kaolinite may form the stable phase in this weathering environment. The composition of water in the weathering zones of limestone and dolomite and in colluvial soils, however, may also be controlled by a partial equilibrium between kaolinite and a montmorillonite.

The mineralogy of the soils on limestone, especially that of the relatively deep "in situ" soils, is discussed comprehensively. Three groups of soils are distinguished: (1) "in situ" soils on limestone (both relatively deep soils on limestone and eroded soils in fissures of the limestone), (2) soils on dolomite and (3) soils developed in colluvial deposits derived from limestone and/or dolomite.

In most of the investigated soils the major constituent is formed by kaolinite, with a relatively large amount of illite. The presence of kaolinite is in accordance with the

theoretical weathering calculations and with the composition of the interstitial waters and is thought to form the stable final product of weathering of the limestone under the given conditions. On the other hand, stability relations indicate that it is not likely that illite forms a (meta)stable phase in this weathering environment. Its presence appears to be a function of admixture with allochtonous material (air-borne volcanic dust) or is related to physical properties of the soil material.

In all soils admixture with volcanic material was observed to various depths. Indicative for this admixture appeared to be a relatively high brown/yellowish brown : colourless garnet ratio in the heavy mineral fraction (50 - 500 μm) . The accompanying increase in illite content towards the top of the profiles studied is interpreted as being caused by this admixture.

Analyses of grey and red mottles of a pseudogleyic soil in colluvial deposits show clear differences in mineralogy between the rim and the inner side of the peds. It is thought that these differences are due to poor permeability of the peds in these heavy clay soils, which often also show vertic features. The clayey character and the vertic properties probably restrict the action of penetrating water to the outer sides of the peds.

A theoretical age of the soils on limestone is calculated from the chemical composition of the karstic spring waters. Under the given conditions and taking into account the relatively long period of time in which weathering and soil formation have been active, it is discussed that for the development of 1 m of soil on limestone 0.5 million years is needed. As "in situ" soils on limestone occur with a thickness of over 4 m, the soil formation must have started in early Quaternary times, but most probably earlier.

The soils on Miocene and Pliocene/old Quaternary deposits are discussed briefly in chapter 3. They have been studied as well because their characteristics appear to be of great help in reconstructing the landscape evolution.

Large differences exist between the soils developed on the Miocene (calcareous) shales and sandstones on one hand and the soils on Pliocene/old Quaternary sandstones and conglomerates on the other hand. The soils of the former group are characterized by a mineralogy dominated by primary (geogene) minerals (smectite, muscovite) and a relatively young profile development. The clay mineralogy in the soils on Pliocene/old Quaternary deposits on the contrary is mainly kaolinitic and the amount of weatherable minerals is relatively low. Most of these soils have a pronounced argillic B horizon and their colours show often redder hues than those on Miocene sediments.

The landscape evolution and soil-forming processes during the Quaternary are discussed in chapter 4. Three main landscape-forming processes have been recognized: (1) tectonical movements accompanied by volcanic activity, (2) karst development and (3) several erosion/denudation phases.

Of great importance for the landscape evolution has been the tectonical movements in early and mid-Pleistocene times which are responsible for the formation of the Valle Latina. These movements are most likely accompanied by volcanic activity. K-Ar datings indicate an important volcanic phase in the region at approx. 0.5 to 0.4 million years ago, as well as one of approx. 1 million years ago.

The beginning of the karst development is uncertain but it is very likely that it started in the late Pliocene. It is discussed that the formation of the poljes near Pastena has to be attributed most probably to the period from the late Tertiary to mid-Pleistocene times. The tectonic movements then may have caused the development of a new subsurface drainage, which has led to new dissolution basins. The rough outline of the present-day limestone landscape is therefore thought to be existing since mid-Pleistocene times.

Three major erosion/denudation phases are recognized. The youngest one is of Holocene age, caused by human activity since pre-Roman times and in the colluvia of this phase pottery fragments are always present. This phase is responsible for the present-day bare character of the limestone mountains. The next older phase is probably related to and induced by the important volcanic activity during the mid-Pleistocene. In the colluvia often tuffaceous layers are found. The oldest phase has only been recognized locally and evidence pointing to volcanic activity has not been found.

The soil-forming and weathering processes during the Quaternary are discussed in the second part of chapter 4. It appears that no specific conclusions may be drawn from

the single mineralogical and pedological features observed in the soils with respect to soil-age, weathering intensity and environmental (i.e. paleoclimatological) implications. However, a combination of characteristics, such as a dominance of kaolinitic minerals in the clay fraction, a relatively low amount of weatherable minerals, a distinct profile development (e.g. a pronounced argillic B horizon) and relatively red hues may give an indication on the relative soil-age, especially when soils developed in the same or similar parent materials are compared.

A synthesis of the landscape- and soil-forming processes and their result is given in tabulary form at the end of chapter 4.

SAMENVATTING

Het doel van deze studie is de verwerings- en bodemvormende processen te onderzoeken in een gebied bestaande uit kalksteen in de omgeving van Pastena (Fr.) in zuid-centraal Italië. De nadruk wordt gelegd op de mineralogische samenstelling van de bodems en het uitgangsmateriaal, de veranderingen die optreden en op theoretische verweringsmodellen van de kalksteen.

Een beschrijving van de fysiografie, het klimaat en de geologie van het onderzoeksgebied wordt gegeven in hoofdstuk 1. Het onderzochte gebied bestaat grotendeels uit kalksteen en dolomitische kalksteen, hoofdzakelijk uit het Krijt. Daarnaast komen ook conglomeraten , zandstenen en schalies van Miocene, Pliocene en Kwartaire ouderdom voor.

De fysiografie van het gebied is bepaald door verkarstingsprocessen. Drie subregio's kunnen onderscheiden worden, afhankelijk van de mate van verkarsting en alle voorbeelden van karstverschijnselen (karren, dolines, grotten, uvalas, poljes) komen voor. De fysiografie van het uiterste noorden van het belangrijkste onderzoeksgebied is een golvend tot heuvelachtig gebied bestaande uit Miocene schalies.

Op basis van de interpretatie van de klimaat gegevens wordt besproken dat naar alle waarschijnlijkheid een xeric moisture regime verwacht kan worden. De droogtegrens, welke door de Soil Survey Staff (1975) uitgaande van waterbalans berekeningen, nl. verdamping van 175 mm. vocht uit een bodem die 200 mm. bevat, vastgesteld is, lijkt te eng te zijn. Een beter hanteerbare waarde is verdamping van 125 mm. vocht uit eenzelfde bodem omdat de lengte van de droge periode, die met behulp van dit cijfer is berekend, redelijk goed in overeenstemming is met de veldwaarnemingen.

Hoofdstuk 2 handelt over de verwering van en bodemvorming op kalksteen en dolomiet. itgaande van de mineralogische en chemische analyses van enkele kalksteen monsters zijn theoretische verweringsmodellen voor enkele relevante partiële CO_2-spanning berekend voor een dolomitische kalksteen, waarvan is aangenomen dat de samenstelling representatief geacht mag worden voor de kalksteen in het onderzoeksgebied.

Het carbonaat-houdende gedeelte ervan bestaat uit ongeveer 45 % calciet, 45 % dolomiet en 10 % aragoniet . De mineralogie van het niet-carbonaat gedeelte wordt overheerst door illiet (evenals in de meeste andere monsters) met als bijkomstige mineralen smectiet, chloriet, kaoliniet, haoliniet, kwarts, albiet, pyriet en waarschijnlijk amorfe ijzer verbindingen. Bij de theoretische verweringsberekeningen zijn deze accessorische mineralen om verschillende redenen niet in beschouwing genomen.

De resultaten van de berekeningen duiden erop dat bij partiële CO_2-drukken van $10^{-2.00}$ tot $10^{-0.80}$ bar een verweringsresidue verwacht kan worden bestaande uit kaoliniet en dolomiet. De mineralogische samenstelling komt redelijk goed overeen met die van de "dolomitische zanden" bij Itri, welke ook lokaal in het hoofdonderzoeksgebied voorkomen.

De samenstelling van de water monsters, afkomstig van bronnen in de kalksteen, komt redelijk overeen met de berekende samenstelling van de oplossing wat betreft het gehalte aan Ca,Mg en HCO_3. De hoeveelheden K,Al en H_4SiO_4 in de water monsters liggen daarentegen vele malen hoger dan de berekende hoeveelheden. Dit kan veroorzaakt worden door: (1) de samenstelling van de gebruikte kalksteen is niet representatief voor het gehele onderzoeksgebied en/of (2) bijmenging van allochtoon materiaal (vulcanisch) beinvloedt de werkelijke samenstelling van het water uit de kalksteen.

De analyses van de water monsters tonen aan dat kaoliniet de stabiele fase in deze verweringsomgeving kan vormen. De samenstelling van het water in de verweringszone van de kalksteen en de dolomiet, en in colluviale bodems kan echter ook mede bepaald worden door een partieel evenwicht tussen kaoliniet en een montmorilloniet.

De mineralogie van de bodems op kalksteen, vooral die van de relatief diepe "in situ" bodems wordt in het kort besproken. Drie groepen bodems zijn onderscheiden: (1) diepe "in situ" bodems op kalksteen (zowel relatief diepe bodems op kalksteen als geerodeerde bodems ontwikkeld in spleten in de kalksteen) (2) bodems op dolomiet en (3) bodems ontwikkeld in colluviale afzettingen afkomstig van kalksteen en/of dolomiet.

In de meeste van de onderzochte bodems vormt kaoliniet de belangrijkste component samen met een relatief grote hoeveelheid dolomiet. De aanwezigheid van kaoliniet is in overeenstemming met de theoretische verweringsberekeningen en met de samenstelling van het interstitiële water en vormt, naar aangenomen wordt, het stabiele eindproduct van de verwering van de kalksteen onder de gegeven omstandigheden. De stabiliteitsverhoudingen, evenwel, tonen aan dat het niet waarschijnlijk is dat illiet een (meta) stabiele fase vormt onder deze verweringsomstandigheden. De aanwezigheid van illiet blijkt een gevolg te zijn van bijmenging met allochtoon materiaal (vulkanisch stof) of hangt samen met de fysische eigenschappen van het bodem materiaal.

In alle bodems is bijmenging met vulkanisch materiaal tot verschillende dieptes waargenomen. Een relatief hoge verhouding van bruin/geel bruine : kleurloze granaat in de zware mineraal fractie (50 - 500 μm) blijkt hiervoor indicatief te zijn. De daarmee samengaande toename van het illiet gehalte naar de top van de bestudeerde profielen wordt verondersteld veroorzaakt te worden door deze bijmenging.

Analyses van grijze en rode vlekken van een bodem met pseudogley in colluviale afzettingen tonen duidelijke verschillen in mineralogie tussen de rand en de kern van de peds. Aangenomen wordt dat deze verschillen aan de slechte doorlatendheid van de peds in deze zware kleibodems toe te schrijven zijn, die ook dikwijls vertische verschijnselen vertonen. Het kleiige karakter en de vertische eigenschappen beperken de rol van het water als verweringsagens tot de buitenkant van de peds.

Een theoretische ouderdom van de bodems op kalksteen is berekend aan de hand van de chemische samenstelling van het water uit de kalksteen bronnen. Onder de gegeven omstandigheden en rekening houdend met de relatief lange tijdsduur waarin de verwering en bodemvorming aktief zijn, wordt besproken dat voor de ontwikkeling van 1 m. bodem op kalksteen 0.5 miljoen jaar nodig is. Daar "in situ" bodems op kalksteen voorkomen met een dikte van meer dan 4 m., moet de bodemvorming begonnen zijn in het vroege Kwartair, maar vermoedelijk nog eerder.

De bodems op Miocene en Pliocene/oud Kwartaire afzettingen worden kort besproken in hoofdstuk 3. Dezen zijn bestudeerd omdat hun kenmerken een belangrijk middel bleken te zijn bij de reconstructie van de landschapsontwikkeling.

Grote verschillen bestaan tussen de bodems ontwikkeld op de Miocene (kalkhoudende) schalies en zandstenen aan de ene kant en de bodems op Pleistocene/oud Kwartaire zandstenen en conglomeraten aan de andere kant. De bodems van de eerste groep worden gekarakteriseerd door een mineralogie die gedomineerd wordt door primaire (geogene) mineralen (smectiet, muscoviet) en een relatief jonge profiel ontwikkeling. De kleimineralogie in de bodems op Pliocene/oud Kwartaire afzettingen is daarentegen voornamelijk kaolinitisch en de hoeveelheid verweerbare mineralen is relatief laag. De meeste van deze bodems hebben een uitgesproken argillic B horizon en de kleuren vertonen meestal rodere hues dan die op de Miocene sedimenten.

De landschapsevolutie en de bodemvormende processen gedurende het Kwartair worden behandeld in hoofdstuk 4. Drie belangrijke landschapsvormende processen zijn onderscheiden: (1) tektonische aktiviteit vergezeld met vulkanische aktiviteit, (2) karstontwikkeling en (3) verscheidene erosie/denudatie fases.

Van groot belang voor de landschapsontwikkeling zijn de tektonische bewegingen geweest gedurende het vroeg- en midden Pleistoceen, die verantwoordelijk zijn voor de vorming van het Valle Latina. Deze bewegingen werden zeer waarschijnlijk vergezeld door vulkanische aktiviteit. K-Ar dateringen tonen een belangrijke vulkanische fase in deze streek aan omstreeks $\pm$ 0.5 tot 0.4 miljoen jaar geleden, alsmede één omstreeks 1 miljoen jaar geleden.

Het begin van de karst ontwikkeling is onzeker maar het is zeer waarschijnlijk dat deze geplaatst moet worden in het Laat - Pleistoceen. Besproken wordt dat de vorming van de poljes bij Pastena toegeschreven kunnen worden aan de periode van het Laat-Tertiair tot midden Pleistoceen.

Drie belangrijke erosie/denudatie fasen zijn onderscheiden. De jongste is van Holocene ouderdom, veroorzaakt door menselijke aktiviteit sinds pre - Romeinse tijden en in de colluvia van deze fase zijn altijd aardewerk fragmenten aanwezig. Deze fase is verantwoordelijk voor het huidige kale karakter van de kalksteenberg-

en. Een oudere fase gaat vermoedelijk samen met de omvangrijke vulkanische aktiviteit gedurende het midden Pleistoceen. In de colluvia zijn dikwijls tuf lagen aangetroffen. De oudste fase is slechts plaatselijk onderscheiden, maar er zijn geen aanwijzingen gevonden dat vulkanische aktiviteit hiervoor verantwoordelijk is.

De bodemvormende-en verweringsprocessen gedurende het Kwartair worden besproken in het tweede deel van hoofdstuk 4. Het blijkt dat er geen specifieke konklusies getrokken mogen worden uit enkelvoudige mineralogische en pedogenetische verschijnselen die in de bodems waargenomen zijn wat betreft bodemouderdom, verweringsintensiteit en paleocondities (Bijv. paleoklimatologisch). Een kombinatie van kenmerken, zoals een dominantie van kaoliniet mineralen in de klei fractie, een relatief laag gehalte aan verweerbare mineralen, een duidelijke profiel ontwikkeling (bijv. een uitgesproken argillic B horizon) en relatief rode hues kunnen daarentegen een indikatie geven over de relatieve bodemouderdom, speciaal wanneer bodems, ontwikkeld in hetzelfde of vrijwel hetzelfde moeder materiaal, vergeleken worden.

Een synthese van de landschappelijke- en bodemvormende processen en hun gevolgen zijn in de vorm van een tabel gegeven aan het einde van hoofdstuk 4.

CHAPTER 1 INTRODUCTION

The soils on limestone have been subject of many investigations in the past. Ever since the research on the formation of karst areas started, the soils in these regions were brought into the discussion. The studies were often directed to the problem of the origin of the soil material, its age and the climatic conditions under which it was formed (e.g. Reifenberg, 1929; Blanck, 1930; Graf zu Leiningen, 1930; Mensching, 1955).

During the last decade a change in emphasis on the approach to soil formation on limestone can be noticed. Emphasis is given on the mineralogy and the mineralogical changes, and on laboratory experiments on the weathering of limestone (e.g. Durand & Dutil, 1971; Miller, 1972; Lamouroux, 1972). A part of the present study will be connected with this approach with particular attention to theoretical weathering models of the limestone.

1.1 Purpose of the study and choice of the research area.

The purpose of the present study is to investigate weathering and soil-forming processes in a limestone area in south-central Italy (see fig. 1.1) and to reconstruct its landscape evolution. This area has been chosen because a previous study pointed out that in the Pastena region various phenomena related to a long period of weathering and soil formation could be studied (Spaargaren, 1974). This previous study was carried out as a part of the post-graduate course in physical geography and soil science at the University of Amsterdam. It covered the present main research area and the adjacent part of the Valle Latina in the north and northeast.

1.2 Location of the research areas.

The main research area is situated in south-central Italy between Rome and Naples, roughly 90 km ESE of Rome. The location is approximately between 41° 25' 00" and 41° 32' 00" N.L. and 13° 24' 50" and 13° 33' 40" E.L. (0° 57' 40" and 1° 06' 30" east of Monte Mario (Rome) respectively) (see fig. 1.1), and covers an area of 140 km^2 which

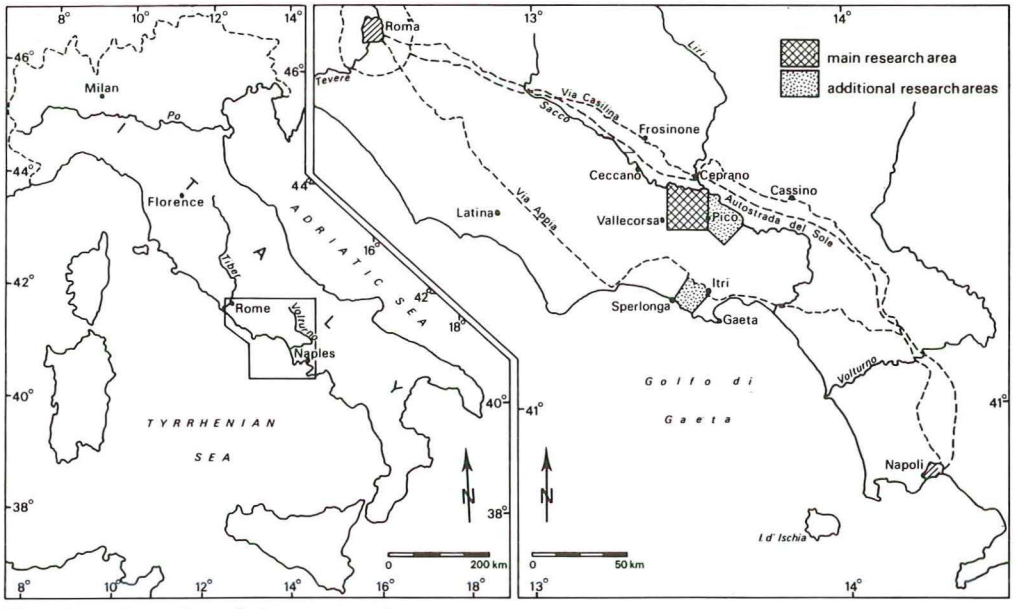

Fig. 1.1 Location of the research areas.

almost completely exists of limestone rocks. Four-fifth of this area is situated in the province of Frosinone and one-fifth in the province of Latina. Both provinces belong to the regio Lazio.

Additional research was carried out in the Itri-Sperlonga region, south of the main area of investigation. This area, located at the Tyrrhenian coast, was studied as part of the survey project "Southern Italy" of the section Soil Mapping of the "Fysisch Geografisch en Bodemkundig Laboratorium" of the University of Amsterdam (Sevink et al., 1979). The area investigated for this project covers approximately the drainage basin of the Sacco River, the lower part of the Liri-Garigliano basin and the adjacent coastal area from Latina to the Monte Massico ridge, east of Gaeta.

The Itri-Sperlonga region was selected because of the predominance of dolomite in this area, which occurs only very locally in the main research area (see 1.6.2).

Additional field studies were carried out in the region east of the main research area. Here Miocene sediments were studied; water samples were collected from these deposits and from karstic springs and limestone-derived colluvium.

1.3 Methods and materials used.

In the summers of 1974 and 1975 field work concentrated on the main research area with emphasis on the weathering of and soil formation on limestone and the landscape evolution of the area under survey. A brief visit was paid to the research area in the winter of 1976 mainly to collect water samples for comparison with those taken during the summer.

During field work the following topographical maps were used: Ceccano and Vallecorsa (sheets 159 I S.E. and II N.E. of the Carta d' Italia) and Ceprano and Pico (sheets 160 IV S.O. and III N.O. of the Carta d' Italia), all at scale 1 : 25 000 (Istituto Geografico Militare, 1961). Also use was made of the geological maps of Frosinone and Cassino (sheets 159 and 160 of the Carta Geologica d' Italia), both at scale 1 : 100 000 (Servizio Geologico d' Italia, 1966). During field work and consecutive elaboration of the data intensive use was made of aerial photographs, numbers 1838-1842, 3412-3416 and 3430-3435 of the Stato Maggiore Aeronautica in Florence. These aerial photographs are at scale of approximately 1 : 35 000.

Profile descriptions were made according to the Guidelines for Soil Profile Description (FAO, 1977). Soil colours were determined with the help of the Revised Standard Soil Color Charts (Oyama & Takehara, 1967) and slopes were measured with an Abney level. Soils were classified according to the Legend of the Soil Map of the World 1 : 5 000 000 (FAO-Unesco, 1974) and the Soil Taxonomy (Soil Survey Staff, 1975).

In order to study the weathering and soil-forming processes, a number of profiles were described and samples were taken for physical, chemical and mineralogical analyses (for analysing procedures see appendix 3). In addition water samples were collected from the weathering zones of limestone and dolomite and from the related soils, as well as from karstic springs and streams. Alkalinity and pH of most of the samples were determined immediately after collection. The samples were filtered by pressure filtration through an 0.45 μm Millipore filter in the field and stored in polyethylene bottles. A part of the filtered sample was acidified with concentrated HNO_3 to pH 2-3, mainly to prevent precipitation of calcium carbonate from the solution.

A physiographic soil map of the main research area was compiled in order to show the relations between the soils and their distribution pattern (see appendix 1). For this soil map about 240 field observations were made. This seems rather low (1.7 km^2), but one should bear in mind that by using aerial photographs the number of observations can be reduced (Vink, 1963). Moreover, approximately 50 % of the area consists of bare to nearly bare rock (units A1 and A2 on the soil map).

1.4 Physiography, vegetation and land use.

The main research area can roughly be divided into two parts: an undulating to rolling area in the utmost northern and eastern parts, with alongside the Sacco River a

number of terraces and a mountainous area in the central and southern parts. This latter area forms the northeastern part of the Monti Ausoni. The elevation ranges from about 75 m a.s.l. near the "Lago di San Giovanni Incarico" up to 1116 m a.s.l. at Monte Calvilli, which is the highest point of the area.

It is possible to subdivide the mountainous area, consisting of limestone and dolomitic limestone, into three physiographic units: the first in the northeast with elevations slightly above 500 m, which in some parts form plateau-like areas (e.g. near Monte Cervaro), the second in the southeast with elevations between 700 and 900 m and a third in the west, which forms a ridge with elevations over 1000 m. These areas are sepatated from each other by large depressions (e.g. Piana Madonna della Macchia, Piana di Ambrifi).

Karst phenomena occur in the whole area. The stage of development of the karstic features from the classical point of view (karren and dolines→uvalas→poljes (Cvijic, 1893) seems to be closely related to the three areas indicated above. In the first area large uvalas (e.g. La Fossa) occur, while in the second area smaller uvalas are found (e.g. San Martino, Valle Vona) and areas where uvalas tend to form (e.g. Monticelli di San Onofrio). In the third area well-developed doline areas (e.g. Visano) tending towards uvala formation occur together with large isolated dolines (e.g. on top of Monte Calvo and at Cimotta Erta).

Some of the large depressions separating the three mountainous subregions can be regarded as poljes (see fig. 1.2) (e.g. Piana Madonna della Macchia). In this large basin also a tortoise-shaped inselberg (Segre, 1948) can be observed. In valleys and at the foot of slopes often "lapies karst" is found (e.g. at La Starza Piana and north of Monte Castello) (see fig. 1.3).

The native vegetation, which is believed to be a decidous forest, still can be found on the eastern slope of Monte Vaglia and north of Monte la Finocchiara. It consists mainly of oak species (principally Quercus ilex and Quercus pubescens) with some elm (Ulmus), chestnut (Castanea), horn beam (Carpinus), maple (Acer) and ash (Fraxinus). These forests are very hard to penetrate because of a heavy undergrowth ("macchia").

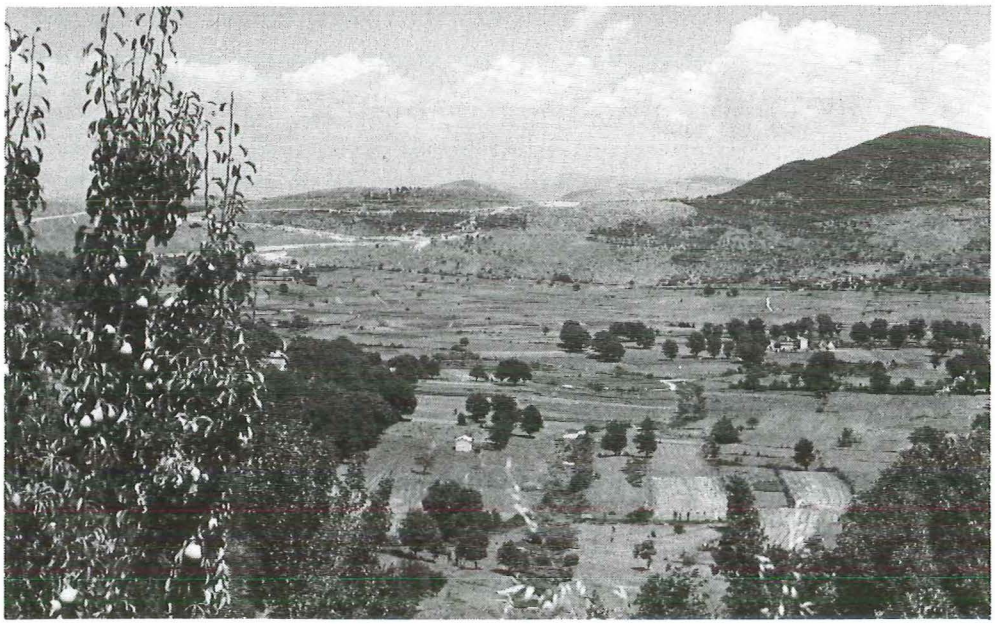

Fig. 1.2 View on the "Piana Madonna delle Macchie" from the south.

Fig. 1.3 Lapies karst at the foot of Monte Castello.

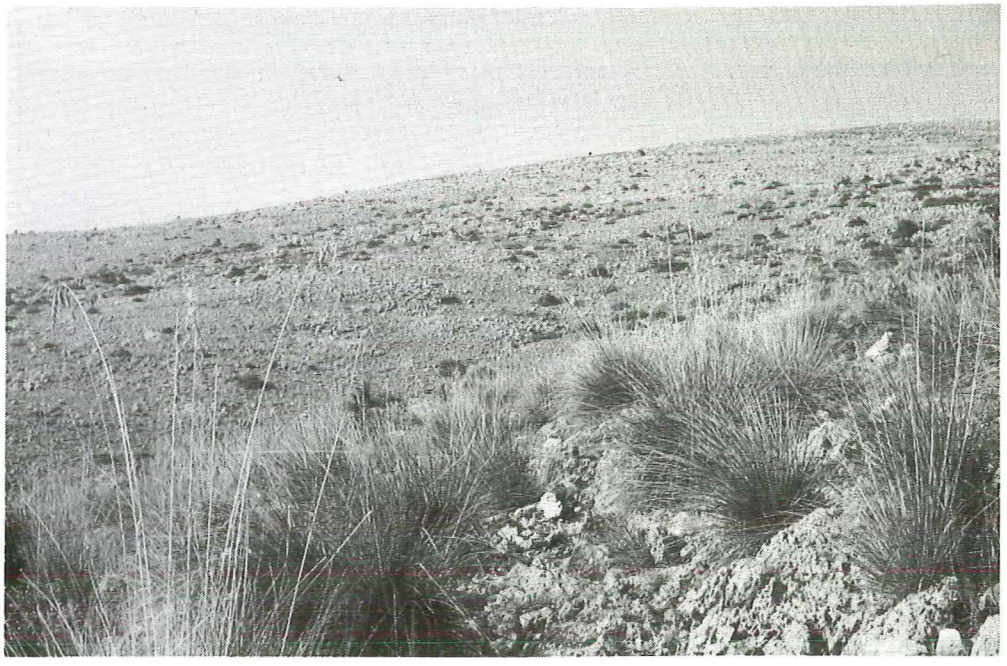

Fig. 1.4 Sparse vegetation on the southwest slope of Monte Cervaro. On the foreground some Ampelodesma tenax Link plants can be observed.

Large parts of the mountainous area are sparsely vegetated, mainly with Ampelodesma tenax Link (see fig. 1.4) (Fenaroli, 1970).

Where possible, the area is cultivated. The main cultures are cereals during winter and spring and maize, tobacco, potatoes and horticulture (tomatoes, melons and beans) during the summer. In the mountainous area the land is not cultivated during the summer because of lack of water. Locally olive trees and vineyards occur, mainly on the terraced parts of the mountain slopes.

1.5 Climate.

The climate can be described as typical mediterranean with cool, moist winters and hot, relatively dry summers (see tables 1.1 and 1.2). According to the Köppen climatic system (1936) it is characterized as a Csa climate. In the FAO-Unesco Bioclimatic Map of the Mediterranean Region 1 : 5 000 000 (Emberger et al., 1962), in which differentiation is based on the xerothermic index, it is described as sub-mediterranean to attanuated mesomediterranean.

Table 1.1 Precipitation in mm of Montecivita Farnese (755 m), Osteria di Castro (155 m), Pico (220 m) and Vallecorsa (350 m) for the years 1921-1950 (Ministerio dei Lavori Pubblici, 1955, 1958).

	J	F	M	A	M	J	J	A	S	O	N	D	Year
Montecivita Farnese	142	130	98	89	66	43	20	27	82	158	176	136	1194
Osteria di Castro	124	142	105	89	116	65	25	34	113	152	189	183	1337
Pico	130	137	104	105	84	55	25	31	102	175	184	171	1303
Vallecorsa	171	193	131	126	92	68	22	42	128	213	210	223	1619

Table 1.2 Temperature in °C of Casamari (250 m) and Montecassino (516 m) for the years 1926-1935 (Eridia, 1942).

	J	F	M	A	M	J	J	A	S	O	N	D	Year
Casamari	5.0	5.7	9.2	12.5	16.1	20.4	23.3	23.3	20.5	15.5	11.4	7.1	14.2
Montecassino	5.8	6.2	9.1	12.1	16.3	22.0	24.2	24.8	21.5	16.7	12.6	8.1	15.0

Important for soil classification purposes is the determination of the soil moisture regime. The Soil Survey Staff (1975) ascribe a xeric moisture regime to Mediterranean climates. They define it as a moisture regime in which (Soil Taxonomy (1975), p. 57):

> "the soil moisture control section is dry in all parts for 45 or more consecutive days within the 4 months that follow the summer solstice in 6 or more years out of 10. It is moist in all parts for 45 or more consecutive days within the 4 months that follow the winter solstice in 6 or more years out of 10. The moisture control section is moist in some part more than half the time, cumulative, that the soil temperature at a depth of 50 cm is higher than 5° C, or in 6 or more years out of 10 it is moist in some part for at least 90 consecutive days when the soil temperature at a depth of 50 cm is continuously higher than 8° C. In addition, the mean annual soil temperature is lower than 22° C, and mean summer and mean winter soil temperatures differ by 5° C or more at a depth of 50 cm or at a lithic or paralithic contact, whichever is shallower."

A soil moisture control section is regarded as dry, if from a soil at field capacity with 200 mm of storage, 175 mm is evapotranspirated in absence of precipitation (Soil Taxonomy (1975), p. 54).

To investigate this, the water balance of a soil with a storage capacity of 200 mm should be examined. For this purpose water balances according to Thornthwaite & Mather (1955) were made for some climatological stations nearby the area studied. The potential evapotranspiration (PE) is calculated also according to Thornthwaite (Grontmij N.V., 1963). This method was used, because calculations of the potential evapotranspiration for Rome according to Penman, Thornthwaite and Blaney & Criddle showed that

the Thornthwaite method gives similar results as the Penman one, while the results of the Blaney & Criddle method deviate considerably. Studies at the "Stazione sperimentale di chimica agraria" of Rome, in which measured maximum evapotranspiration rates were compared with the calculated potential evapotranspiration rates according to Thornthwaite, Turc and Blaney & Criddle respectively, showed that the results of the Thornthwaite method were more close to the real figures than those of Blaney & Criddle (Tombesi et al., 1965).

The water balance of Pico with calculated potential evapotranspiration rates of Casamari, is shown in table 1.3 and figure 1.5.

Table 1.3 Water balance of Pico according to Thornthwaite & Mather (1955), calculated with potential evapotranspiration rates (PE) of Casamari. Storage (ST) = 200 mm.

	J	F	M	A	M	J	J	A	S	O	N	D	Year
P	130	137	104	105	84	55	25	31	102	175	184	171	1303
PE	9	12	30	50	83	115	142	133	96	59	32	16	777
P-PE	121	125	74	55	1	- 60	-117	-102	6	116	152	155	
APWL						- 60	-177	-279					
ST	200	200	200	200	200	148	82	49	55	171	200	200	
ST	0	0	0	0	0	- 52	- 66	- 33	+ 6	+116	+ 29	0	
AE	9	12	30	50	83	107	91	64	96	59	32	16	649
D	0	0	0	0	0	8	51	69	0	0	0	0	128
S	121	125	74	55	1	0	0	0	0	0	123	155	654

P=precipitation, PE=potential evapotranspiration, APWL=accumulated potential water loss, ST=storage, ST=change in storage, AE=actual evapotranspiration, D=deficit. S=surplus.

Water balances were also made for other climatological stations near the main research area. The potential evapotranspiration rates used in the calculations were those obtained for Casamari and Montecassino, depending on the elevation of the station where the precipitation has been measured.

Fig. 1.6 shows the calculated changes in storage of some climatological stations, adjacent to the main investigation area, for a soil with 200 mm of moisture in storage. It indicates that the critical value of 175 mm of evapotranspiration is not reached and that an udic soil moisture regime (Soil Survey Staff, 1975) would be expected.

This, however, does not agree with the general view that a xeric soil moisture regime is typic fot Mediterranean climates. Field observations have shown that from June on the soils can be regarded as dry and that the dry period may extend up to September. In a previous approximation (Soil Survey, 1970) a soil with a storage of 200 mm of moisture was expected to be dry after 125 mm of evapotranspiration. This figure seems to be more appropriate to estimate the length of the dry period with help of the water balance calculations.

The results of the calculations based on 125 mm of evapotranspiration are expressed in fig. 1.6 by a black bar at the bottom of the figures, indicating the length of the dry period. They are in fair agreement with the observed periods during field work. Therefore, in contrast to what is proposed in the Soil Taxonomy (1975) (p. 54), 125 mm of evapotranspiration from a soil holding 200 mm of moisture is taken as the limit beyond which the soil may be regarded as dry.

The length of the calculated dry period, based on an evapotranspiration rate of 125 mm, varies approximately from 40 days to 75 days. Table 1.4 shows this length, together with the expected soil moisture regimes for eigth climatological stations surrounding the main research area. They indicate that in most parts of the area a xeric moisture regime according to this definition may be expected, except for the western part, where locally an udic soil moisture regime may occur.

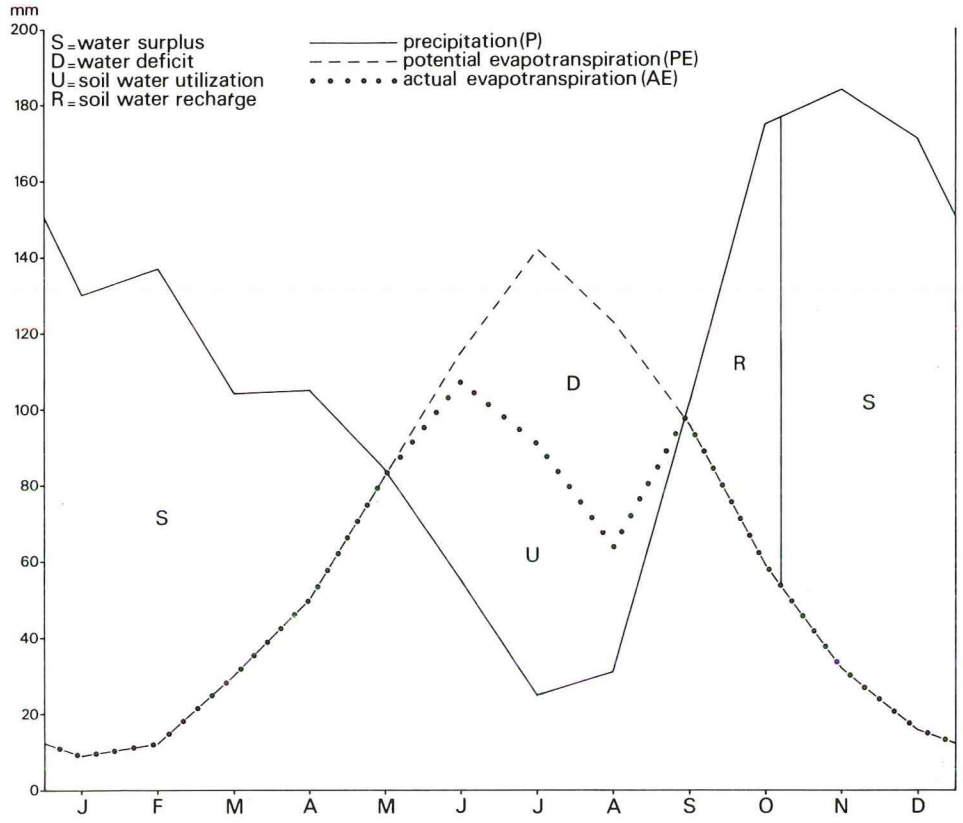

Fig. 1.5 Water balance of Pico according to Thornthwaite & Mather (1955), with calculated evapotranspiration rates (PE) of Casamari.

Table 1.4 Calculated length of the dry period (L.D.P.), based on 125 mm of evapotranspiration from a soil holding 200 mm of moisture, for eigth climatological stations surrounding the main research area and their expected soil moisture regimes (E.S.M.R.).

Climatological stations		L.D.P.	E.S.M.R.
In the north	Osteria di Castro	50 days	xeric
	Ceprano	65 days	xeric
In the west	Vallecorsa	40 days	udic
	Amaseno	55 days	xeric
In the south	Montecivita Farnese	70 days	xeric
	Itri	75 days	xeric
In the east	Pico	60 days	xeric
	Esperia	60 days	xeric

1.6 Geology.

1.6.1 Some structural indications.

The Apennines in Central Italy consist of a number of mountain chains, which are orientated northwest-southeast. These chains are separated from each other by large

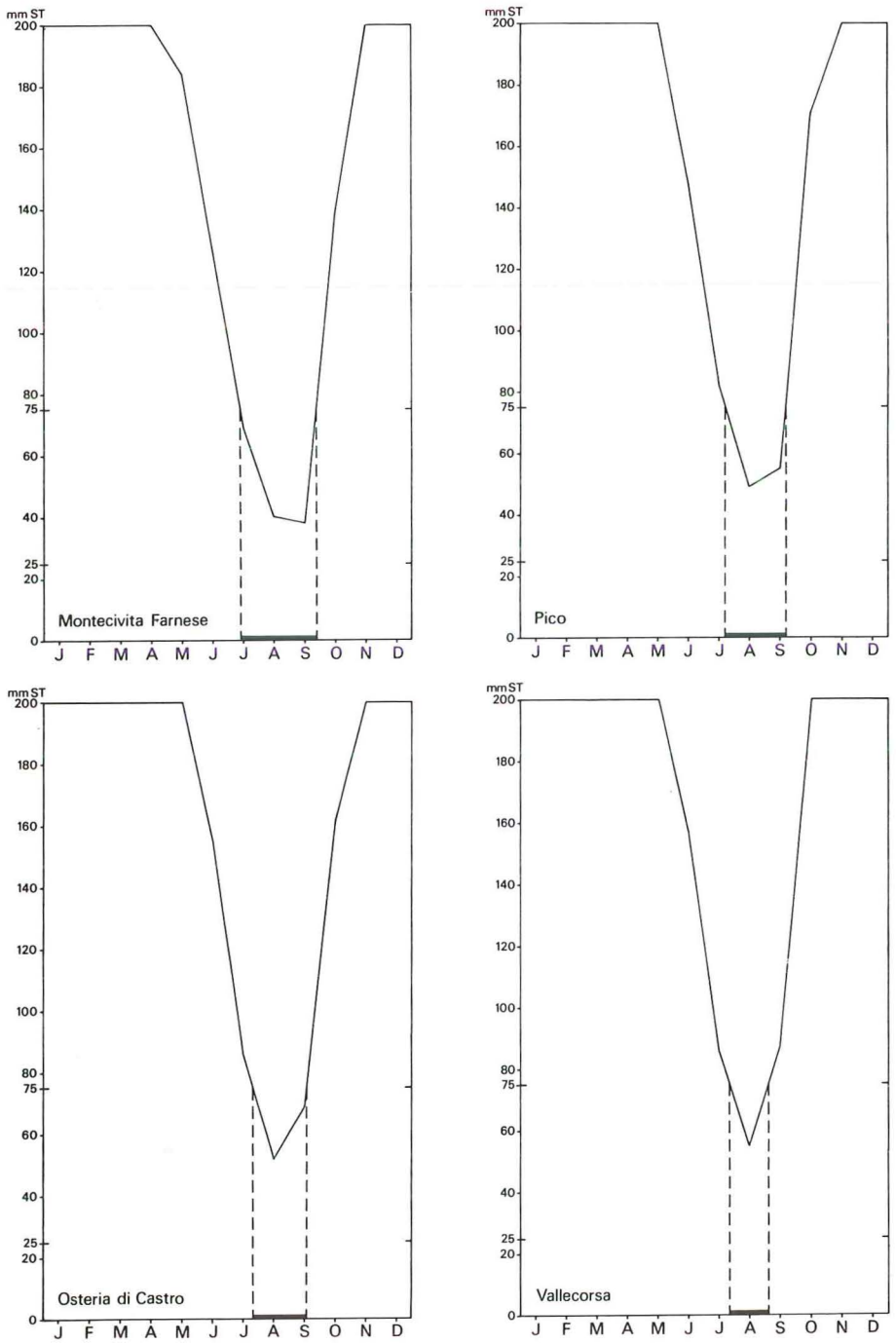

Fig. 1.6 Changes in storage of a soil with storage capacity of 200 mm moisture, calculated for four climatological stations adjacent to the main research area. Black bar indicates dry period after 125 mm of evapotranspiration.

depressions, e.g. the Valle Latina between the chains of the Monti Lepini-Ausoni-Aurunci and the Monte Simbruini-Ernici.

Several ideas about the genesis of this part of the Apennineshave been developed since the last century. The oldest theory is the one of Ponzi, who attributed the chain structure to horsts and grabens. Viola on the contrary ascribed the Valle Latina to a synclinal structure. At the beginning of the twentieth century a new theory was developed by Grzybowski, based on a horizontal displacement of the Mesozoic rocks over Tertiary sediments. Beneo, however, attributes the formation of the Monte Lepini-Ausoni-Aurunci chain to a combination of faulting and folding (Accordi et al., 1967).

A more recent view on the genesis of the Apennines is based on the theory of wave tectonics, as developed amongst others by Merla and Migliorini (Accordi, 1966; Sestini, 1970). This theory is based on the successive uplift of ridges in the Tyrrhenian Sea, thus forming an orogenic wave running from southwest to northeast. The uplift of the ridges caused sedimentation of Flysch deposits in the trough in front of the ridge. When a new ridge was formed, these sediments were displaced in northeasterly direction. This mechanism caused the deposition of chaotically structured sediments (olistostromes), in Italy known as the "argille caotiche" complex. Also larger bodies (olistoliths) could be transported this way. The consolidated conglomerates north of Pico (unit cg, see fig. 1.8), "drifting" on the chaotic clay complex may represent such an olistolith.

These slide movements have also caused displacement of the Mesozoic limestone sediments. Accordi (1966) calculated that the sediments of the Monti Lepini-Ausoni-Aurunci chain have been transported about 50 to 60 km in northern and northeastern direction. He considers the mountain chain indicated above as allochtonous because of this large displacement . This view is supported by the results of a deep drilling in the Monti Simbruini, north of the Valle Latina. Here a Miocene formation was found overlain by 3000 m of Jurassic and Triassic limestone and a Cretaceous overthrust sheet with a thickness of 450 m. The allochtonous character of the Apennines facing the Tyrrhenian Sea has also been recognized in Southern Italy (Grandjacquet, 1963).

Geoelectrical investigations near Pastena showed that in the large karstic depressions "Piana Madonna delle Macchie" and "Piana di San Andrea" most probably the chaotic clay formation is found under a cover of recent sediments (Mancini, 1967). The presence of a large number of springs at the foot of the Monti Lepini-Ausoni-Aurunci chain also indicates most likely an impermeable layer underneath the limestone mountains.

The first "wave tectonic" movements probably occurred in the Upper Jurassic (Accordi, 1966), while the first ridge was formed during the Upper Cretaceous (Sestini, 1970). In the Upper Paleocene a general uplift took place, followed by a continental phase during the Eocene and Oligocene. This is marked by a hiatus in the Latium-Abruzzi succession (Parotto & Praturlon, 1975).

A strong emergence and transgression followed in the Middle Miocene. Sandy-clayey Flysch deposits of Tortonian (Helvetian) and Messinian age, with intercalations of the chaotic clay formation were sedimentated during this period. The tectogenesis of the Monti Lepini-Ausoni-Aurunci chain is in general dated as Upper Miocene. At that time again a ridge was formed, approximately along the present coast line (Sestini, 1970) and transversal movements took place in the north-eastern direction. Evidence of these movements were found in the foot zone of the Monti Ausoni, where tectonical marks on pebbles of a Molasse-like deposit of Pliocene age indicate that the tectogenesis continued at least during part of the Pliocene times (Angelucci, 1966).

The definitive uplift, accompanied by intensive faulting , took place during the Middle and Upper Pliocene (Parotto & Praturlon, 1975) and faulting activity has continued during the Pleistocene. In that time the Valle Latina took its present shape (see chapter 4). Dislocation of Würmian glacial deposits in the Central Apennines (Accordi, 1966) and many earthquakes during historical times show that the faulting activity has not yet ceased.

Associated with these tectonic movements volcanism developed and established the complexes of the Vulsini, Cimini, Sabatini, Tolfa, Albani, Ernici and Roccamonfina. It started mainly during the Upper Pliocene-Early Quaternary times (Negretti et al., 1966), although earlier phases have been recognized (Fazzini et al., 1972). The main

activity of the latter three volcanic complexes , which are important for the area under survey, must be placed in Early to Middle Pleistocene times (see also Remmelzwaal, 1978 and Sevink et al., 1979).

A schematic structural block-diagram of south-central Italy (after Parotto & Praturlon, 1975) is presented in fig. 1.7.

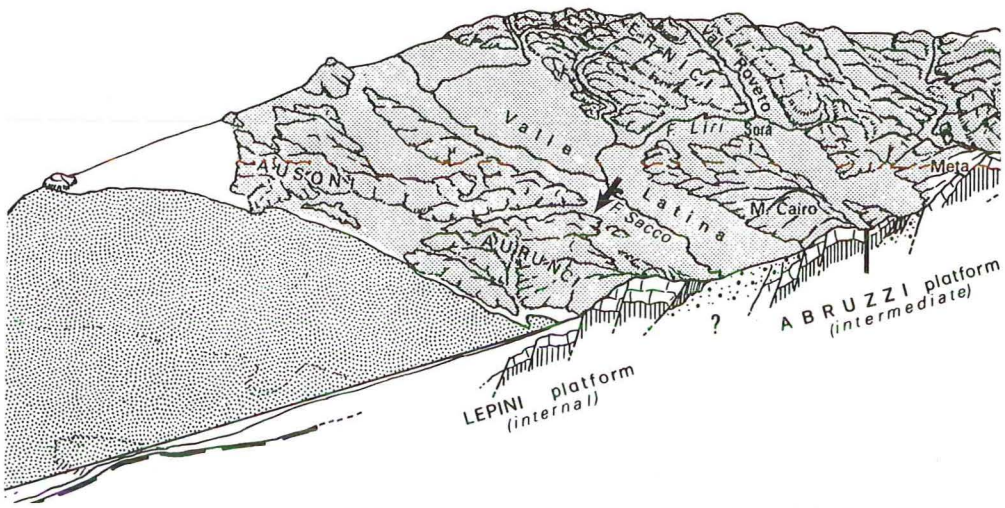

Fig.1.7 Schematic structural block-diagram of south-central Italy (after Parotto & Praturlon, 1975). Black arrow indicates location of the main research area.

1.6.2 Lithology.

The Quaternary sediments consist of alluvial (a), slope (s) and colluvio-lacustrine (f) deposits (fig. 1.8). Alluvial deposits occur in the valley floors of small streams and along the Sacco River. They consist mainly of locally derived material. Slope deposits are found at the fringes of the mountains and basins. The texture is mainly clayey but locally coarser deposits occur. Colluvio-lacustrine sediments are found in the karst basins. They consist of material washed down from the mountain slopes and deposited in a flat to nearly flat position. In most of the Quaternary deposits an admixture of volcanic material can be observed.

The Pliocene sediments (P) are found in the foot zone of the mountains between Pastena and Castro dei Volsci, a small village just outside the main research area in the northwest. They consist of strongly weathered conglomerates grading towards sandstone further away from the mountains. These sandstones do not show any indications of tectonical disturbance as do the conglomerates (Angelucci, 1966); they might therefore be of Early Quaternary age. The conglomerates contain large boulders , mainly of sandstone , elements of Mesozoic limestone and dolomite and very rarely granite. Locally they are cemented by calcium carbonate. North of Pico a cemented conglomerate (cg) occurs. This unit differs from the other conglomerates of Pliocene age, because all limestone elements of local origin are lacking.

The Miocene sediments (M) consist of clay, marl and sandstone. Only small amounts of the sandy and marly formations occur: north of Monte Nero and north of Pico (fig.1.8). The major part of the Miocene sediments consists of the chaotic clay complex ("argille caotiche")(ac). It is formed by a grey scaly clay with olistoliths of marly limestone, cemented rudites and cherty limestone. The microfauna present in this sediment is of Paleocene to Pliocene age. Stratigraphically this formation is interbedded in the top part of the Miocene sediments (M).

Fig. 1.8 Geological map of the main research area (modified after Servizio Geologico d'Italia, 1966).

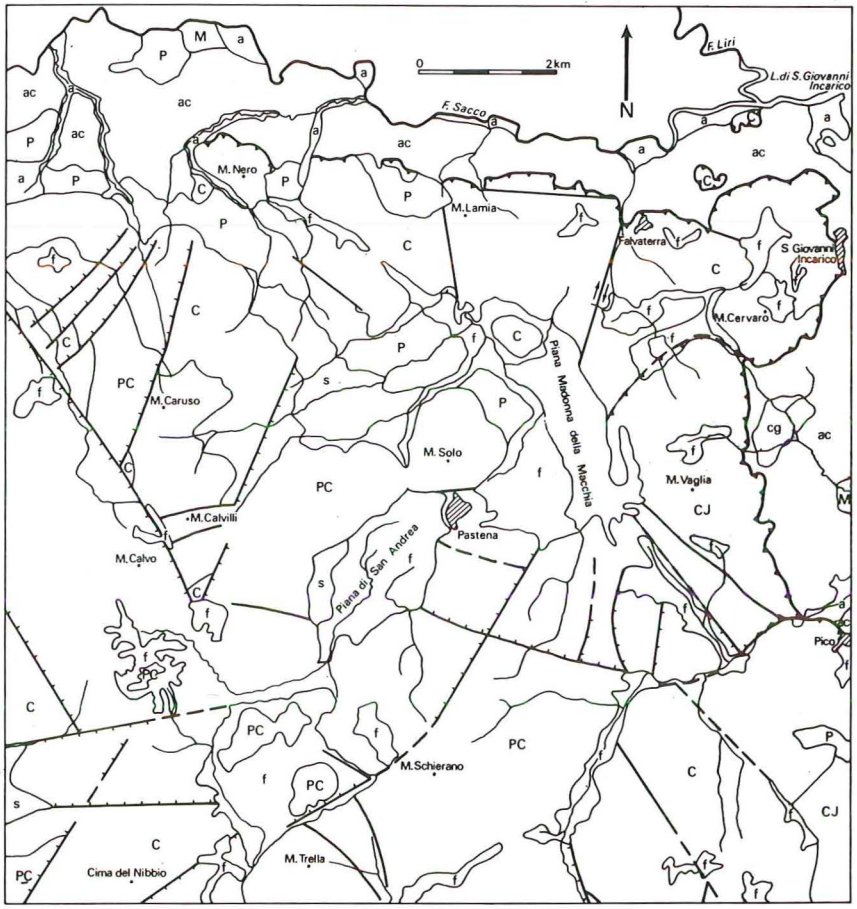

Quaternary		a	alluvial deposits
		s	slope deposits
		f	colluvio-lacustrine basin deposits
Tertiary	Pliocene	? cg	conglomerate
		P	conglomerate and sandstone, strongly weathered
	Miocene	? ac	clay with olistoliths of marly limestone, cemented rudites and cherty limestone ("argille caotiche")
		M	clay, marl and sandstone
	Paleocene	PC	white and brown limestone, locally dolomitic
Cretaceous		C	light brown limestone with intercalations of oolitic beds
Jurassic		CJ	white, gray and light brown limestone with intercalations of dolomite

fault (if dotted uncertain)
idem: overthrust
idem: vertical
idem: horizontal
rivers
village
mountain top

The oldest formations occur in the mountainous area. The mountains themselves consist of limestone and dolomite, in which the entire sedimentation sequence from Jurassic up to Paleocene is represented in shelf facies (Parotto & Praturlon, 1975) and is known as the "Latium-Abruzzi series". The upper part of the sequence (PC) consists of white and brown limestone, which is locally dolomitic. This part is attributed to the Upper Cretaceous and Paleocene. The second formation (C), which belongs to the Cretaceous, consists of light brown limestone with intercalations of oolitic beds and (rarely) dolomitic beds. Also a discontinuous bed of green marly limestone can be found. The lowest part of the sequence consists of white, grey and light brown limestone with intercalations of dolomite. It is attributed to the Lower Cretaceous and the Upper Jurassic. The base of the succession is formed by dolomite and dolomitic limestone of Lower Jurassic and Upper Triassic age. This part of the series is exposed only very locally in the main research area but crops out mainly in the Itri - Sperlonga region, mentioned in 1.2.

Locally volcanic deposits are found in the karst basins. Northeast of Monte Solo a tuff deposit occurs, resting on and interbedded in lacustrine sediments. Also at La Fossa tuff deposits can be found intercalated in lacustrine sediments and in colluvial deposits. These tuff occurences are not indicated on the geological map, because they are too small to be mapped. They belong to the Quaternary volcanism, which developed in the Early and Middle Pleistocene (see Accordi et al., 1967; Remmelzwaal, 1978; Sevink et al., 1979).

CHAPTER 2 WEATHERING OF AND SOIL FORMATION ON LIMESTONE AND DOLOMITE

In this chapter an attempt will be made to obtain insight into the weathering processes in the limestone and dolomite and into the geogenesis and pedeogenesis of the soils found on them. Conformities and differences in weathering and soil formation will be discussed, mainly from the chemical and mineralogical point of view.

The mountainous region in the main research area consists largely of hard limestone rock, locally dolomitic, of Jurassic, Cretaceous and Paleocene age (see 1.6.2). The main soil groups found on these rocks are lithosols, rendzinas and calcaric phaeozems (FAO-Unesco , 1974)(see soil map, appendix 1).

However, also other soils occur. In fissures and cracks in the limestone chromic vertisols are found and on several spots on the mountain slopes deep chromic luvisols and eutric nitosols occur. Where the parent material tends to dolomitic limestone or dolomite, mainly chromic luvisols and chromic vertisols are found. In limestone areas where lapies karst has developed, chromic vertisols dominate between the residual limestone pillars. Special attention will be paid to the deep chromic luvisols and eutric nitosols on the mountain slopes, and also to the chromic vertisols in fissures and cracks in the limestone rock.

In the colluvio-lacustrine deposits of the karstic depressions chromic luvisols, vertic luvisols and chromic vertisols have formed. These soils are studied mainly in relation to the landscape evolution of the area under survey

The profile descriptions made for this study are given in appendix 2, together with the physical and chemical analyses of the soil and rock samples. Analysing procedures are summarized in appendix 3.

2.1 Field observations and soil characteristics.

The soils in the mountainous area can be subdivided into three main groups. related to the parent materials. These groups are:

1) soils on non-dolomitic to slightly dolomitic calcareous rocks
2) soils on dolomitic calcareous rocks
3) soils in colluvio-lacustrine ("colluvial") deposits derived from limestone and/or dolomite.

Fig. 2.1 shows schematicly the position of the main soils in these groups, in relation to parent material and physiography.

2.1.1 Soils on non-dolomitic to slightly dolomitic calcareous rocks.

This group of soils is the most extensive one in the main research area as non-dolomitic to slightly dolomitic calcareous rocks dominate in the mountainous region. According to their profile development, closely related to the degree of erosion, they can be subdivided in:

- shallow soils on mountain slopes: LITHOSOLS and RENDZINAS. They cover most of the limestone area.
- eroded shallow to deep soils in fissures and cracks in the limestone rock: CALCARIC PHAEOZEMS and CHROMIC VERTISOLS. These soils can be considered as erosion remnants of the chromic luvisols and eutric nitosols of group 3. They are found predominantly in the eastern part of the main research area.
- deep, reddish brown soils on mountain slopes: CHROMIC LUVISOLS and EUTRIC NITOSOLS. These soils occur only on small surface areas near Monte la Finocchiara at Il Vallangero, Monte Vaglia, Monte Schierano , Monte Farneto and Monte Pastenese.

In most of the soils admixture of volcanic material was observed. This admixture is the strongest in the lithosols and rendzinas. It has not been observed in the deep-lying

subhorizons of the chromic luvisols and eutric nitosols of the mountain slopes nor in the subsurface horizons of the chromic vertisols in fissures and cracks in the limestone rock.

The shallow soils on the mountain slopes.

These soils, classified as lithosols and rendzinas, were only studied in the field in order to get insight into the soil pattern on limestone. It was considered beyond the scope of this study to investigate these soils thoroughly and therefore no profile descriptions were made nor samples taken of these soils.

The shallow soils consist of a dark Ah horizon of varying thickness, directly overlying hard limestone. The thickness of the Ah horizon of the lithosols varies, according to the definition (FAO-Unesco , 1974), from 0 to 10 cm, that of the rendzinas from 10 to approximately 40 cm. The colour is brownish black to (very) dark brown with hues of 7.5YR and 5YR. The structure is crumb to subangular blocky. It contains calcareous gravel of various sizes and the matrix reacts clearly with HCl (2M). The porosity is high and because of the content of calcareous material the pH must be 7.5 to 8.2. The transition to the hard rock is always abrupt. At this boundary often a thin, whitish layer is observed. It consists of secondary calcium carbonate, which presumably forms during the dry season ("pellicules calcaires"; Lamouroux, 1967).

Because of the strongly varying thickness of the solum and the many rock outcrops, these soils are mainly used for extensive grazing (goats, cattle). At a few places also forestry occurs (e.g. at Piana di Ambrifi) on these soils. This is closely related to the predominance of rendzinas together with rather extreme development of fissures in the limestone rock.

In general, rendzinas dominate the rendzina/lithosol ratio at the foot of slopes, while lithosols prevail on the steeper parts.

The eroded soils in fissures and cracks in the limestone.

These soils are found on mountain slopes in fissures and cracks in the limestone rock. They are classified as chromic vertisols and calcaric phaeozems. The former (profiles Sp/66, Sp/93 and Sp/235) are moderately deep to deep soils with only a thin Ah horizon. In the literature they are often regarded as the classical "terra rossa" (e.g. Buringh, 1970; Mohr et al., 1972), although still no uniformity is reached in the use of this name for the reddish brown, clayey soils in fissures of the limestone rock.

The calcaric phaeozems are shallow to moderately deep soils with a well develloped mollic A horizon. Profile Sp/99 is an example of such a soil.

Fig. 2.1 Idealized sections of slope and karst basin in limestone and dolomite rocks, showing the position and interrelation of the soils found on them and their schematic profile sketches.

A: chromic/vertic luvisols; B: chromic vertisols and chromic luvisols; C: rendzinas; D: chromic luvisols and eutric nitosols; E: lithosols and rendzinas (+ chromic vertisols); F: chromic/vertic luvisols; G: calcic cambisols and calcaric regosols (+ rendzinas); H: chromic vertisols and chromic luvisols; I: lithosols and rendzinas (+ chromic luvisols).

The symbols of the profile sketch are modified after Duchaufour (1977), indicating: 1: mineral soil material with slightly acid, rapidly mineralizing organic matter; 2: accumulation of hydrated oxides of iron; 3: accumulation of dehydrated oxides of iron; 4: diffuse iron-manganese mottles, reflecting hydromorphic conditions; 5: accumulation of calcium carbonate in powdery form; 6: accumulation of calcium carbonate in concretionary form; 7: "dolomitic sands" (weathered dolomitic limestone); 8: calcareous rocks; 9: admixture of volcanic material.

SOILS ON LIMESTONE

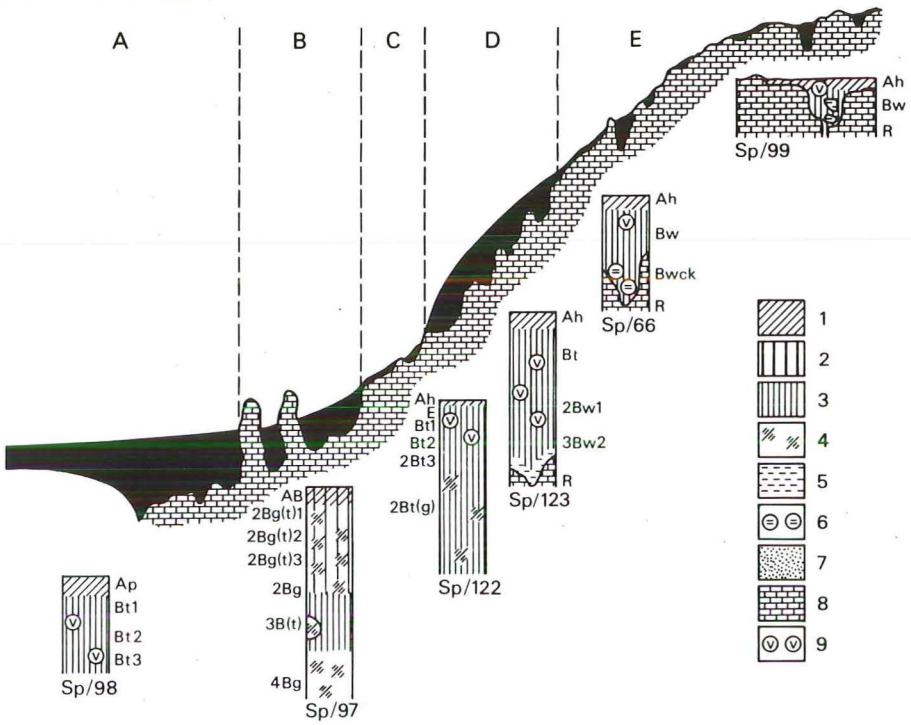

SOILS ON DOLOMITE

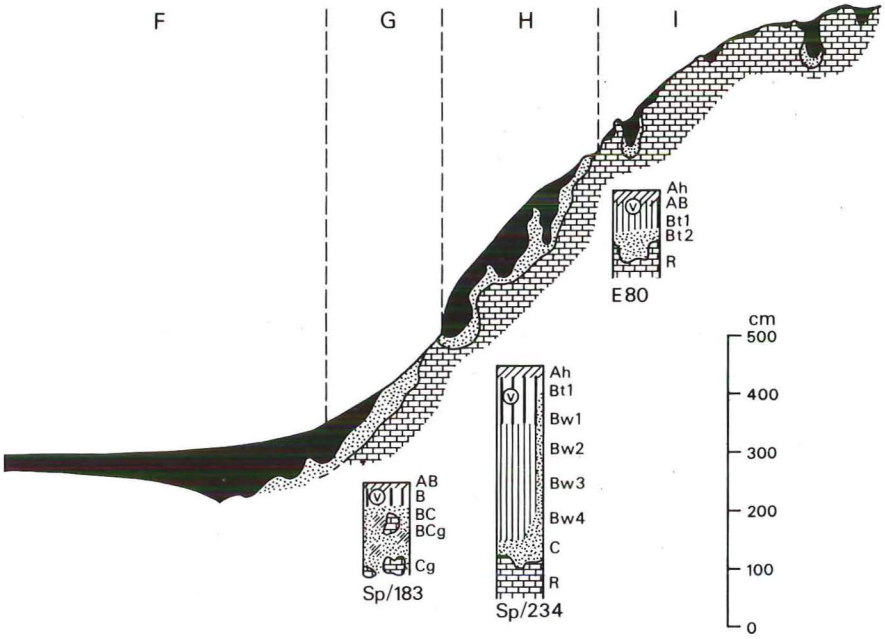

As already mentioned, the Ah horizons of the chromic vertisols are weakly developed. They have either formed in a remnant of the B horizon of a chromic luvisol/eutric nitosol or in colluvial material derived from rendzinas and lithosols. In the first case, the epipedon still bears many characteristics of the original B horizon such as structure and clay cutans. Their colour is dark reddish brown with hues of 5YR. They often contain calcareous gravel and the matrix is non to slightly calcareous. The transition to the Bw horizon is mostly clear.

The epipedons developed in former rendzina or lithosol material have a crumb structure and dark brown to brownish black colours. The matrix is calcareous and slightly weathered limestone fragments are common. The transition to the underlying horizons is mostly abrupt.

The recognition of Bw horizons in these soils needs some explanation. In general, vertisols are described as AC profiles. Both in the Soil Taxonomy, appendix 4 (Soil Survey Staff, 1975) as in the explanatory notes to the Soil Map of the World 1:5 000 000 (FAO-Unesco, 1975a, 1977a, 1977b) this horizon designation is used, although the occurrence of B horizons in vertisols has been indicated in other explanatory notes (FAO-Unesco, 1971, 1975b). The subsurface horizons in the vertisols under discussion, however, do not qualify as C horizon as defined in the Soil Taxonomy (p. 461), because the soil material is relatively highly affected by pedogenic processes. Soil structure is strong and alteration of the non-carbonate part of the limestone is clearly evident, as will be shown later in this study. This is sufficient to meet the requirements for B horizons, mentioned in the Soil Taxonomy (p. 460: B-Horizons, item 4) (see also Remmelzwaal, 1978).

The B horizons in the vertisols have to be regarded as cambic B horizons. They are believed to be remnants of the deeply developed chromic luvisols/eutric nitosols as their morphology and mineralogy is very similar to the deep-lying horizons of these soils. Clay illuviation, however, is too weak to classify them as argillic B horizons.

The Bw horizons have dark reddish brown to reddish brown colours with hues of 5YR and 2.5YR. The structure is subangular blocky in the upper part and angular blocky lower down. Here also, the aggregates are sufficiently wedgeshaped to classify these soils as vertisols. Frequently intersecting slickensides are found and few clay cutans may occur in pores and on pedfaces. They sometimes have very dark brown colours, indicating that these cutans may consist of a mixture of clay, iron and organic compounds. The Bw horizon often contain calcareous gravel, while the matrix can be slightly calcareous. Incidentally yellowish brown calcium carbonate concretions occur in the lower part of what then has been designed as Bwck horizon. Iron-manganese mottles and nodules are common.

In some profiles grey-green coloured soil material was observed near the transition to the hard rock. The mineralogy of this material (e.g. sample Sp/103) is very similar to that of the non-carbonate residue of the limestone (see 2.5.2). It is thought that this material has been recently formed by weathering of the limestone and is not yet affected by the process of rubefaction.

Some general soil characteristics of profiles Sp/66, Sp/93 and Sp/235 are shown in fig. 2.2.

The calcaric phaeozem can be regarded as a still (in the past) stronger eroded chromic member of the sequence that produced the vertisol. The Ah horizon is rather thick (25-30 cm), has a brownish black colour with hues of 5YR and 7.5YR and a crumb structure. Calcareous gravel is common and the matrix is slightly calcareous to calcareous. The boundary to the Bw horizon is abrupt to clear and often an abrupt lateral boundary occurs to the hard rock.

The Bw horizon resembles the Bw horizon of the chromic vertisol, but vertic properties are not pronounced. The colour is dark reddish brown with hues of 5YR and locally 2.5YR and the structure is angular blocky. Thin clay cutans and small slickensides may occur on some pedfaces. The matrix is slightly calcareous and fresh to slightly weathered limestone gravel is common. The boundary between the Bw horizon and the hard rock is abrupt and irregular. At this transition often white soft calcium carbonate layers were observed, similar to those in the lithosols and rendzinas.

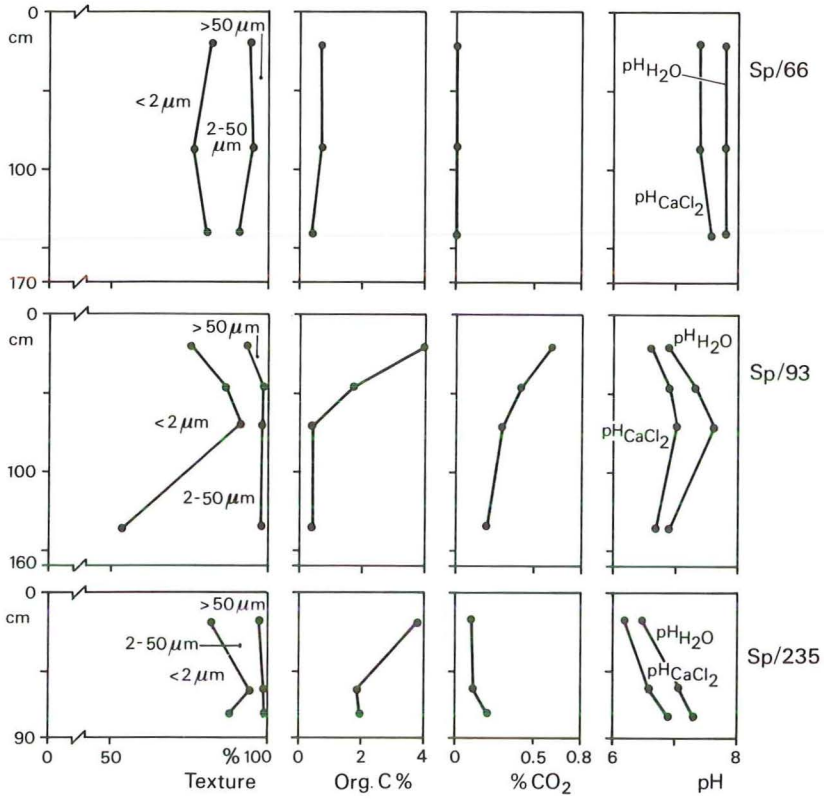

Fig. 2.2 General soil characteristics of the profiles Sp/66, Sp/93 en Sp/235, all chromic vertisols.

The deep reddish brown soils on mountain slopes.

During field work these soils were studied especially at Il Vallangero near Monte la Finocchiara. Two profiles, an eutric nitosol and a chromic luvisol, were described and sampled (see appendix 2, profiles Sp/122 and Sp/123). They are also observed to a minor extent in other parts of the main research area. The soils are very deeply developed, locally to over 4 metres.

The Ah horizons are weakly developed and/or very thin. They show dark to very dark reddish brown colours with hues of 5YR and 2.5YR. Their structure is subangular blocky, locally tending to crumb. The porosity is high and decalcification is complete. The transition to underlying horizons (E or B horizons) is clear and even abrupt boundaries were observed.

E horizons are seldom clearly found and in fact can only be observed when the profile is moist. They are thin, non calcareous and have a subangular blocky structure. Their boundary with the underlying B horizon is clear.

The Bt horizons are very thick and continue down to the lithic contact, which can be very deep. The colour of these horizons is dark reddish brown to reddish brown.

They have hues of 5YR and 2.5YR, while incidentally hues of 10R occur. The structure is angular blocky. In the lower part of the soils the aggregates become more wedge-shaped, due to vertic properties of the soil material. Also medium to large slickensides occur. In the upper part of the Bt horizons patchy to broken moderately thick clay cutans are observed in pores and on pedfaces. They are dark to very dark reddish brown. The entire Bt horizon is decalcified and has a medium porosity. Up to a depth, varying from approximately 1 to 2 metres, volcanic minerals were observed. This allochtonous material was not found in the lower parts of the soils.

Some general soil characteristics of profiles Sp/122 and Sp/123 are shown in fig.2.3.

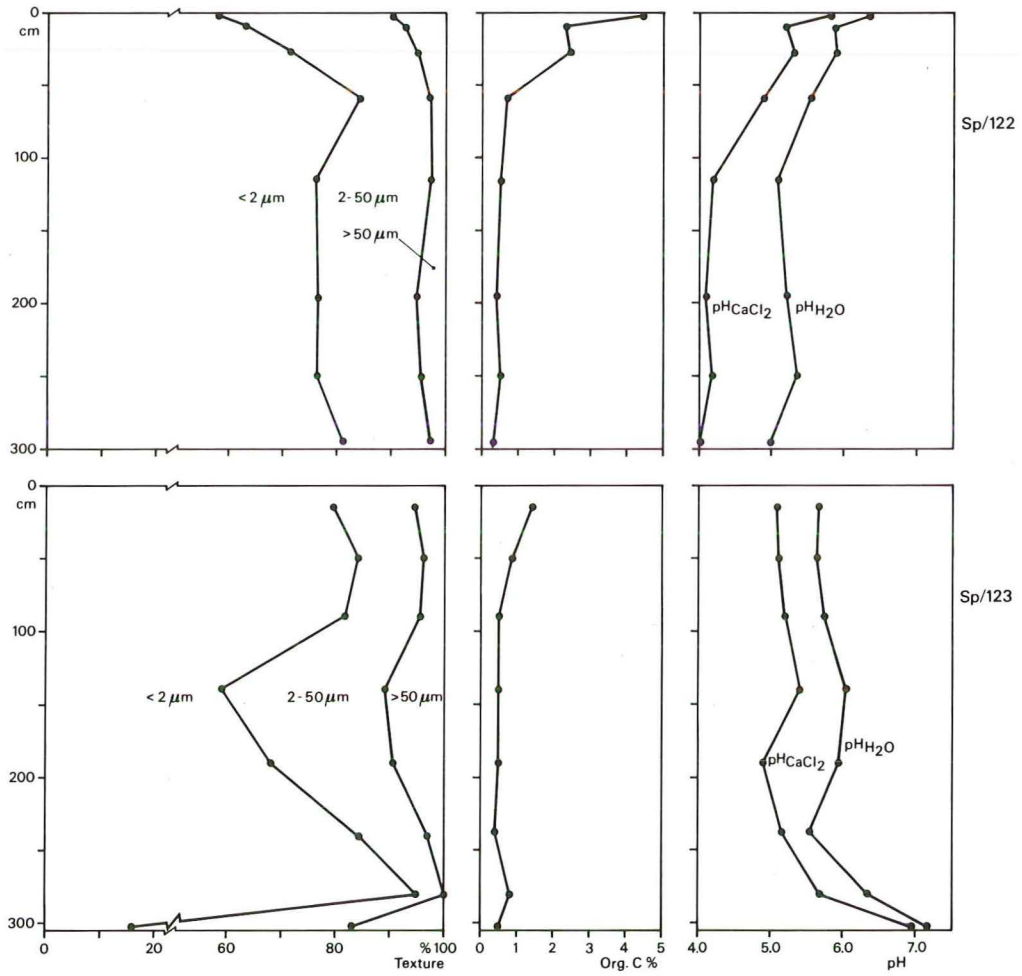

Fig. 2.3 General soil characteristics of profiles Sp/122 (eutric nitosol) and Sp/123 (chromic luvisol).

Besides bluish black iron-manganese mottles, which are often observed in these soils, incidentally mottling due to hydromorphic conditions in the rainy season occurs. These pseudogleyic features resemble the mottling zone ("zone tachetée"; Duchaufour, 1977) of the soils with plinthite in tropical regions, although the latter ones are more pronounced (Mohr et al., 1972). In some colluvial soils in the main research area the

mottling described above also occurs; here it is much more striking, probably due to a more humid physiographic position (see 2.1.3 and fig 2.1).

At the boundary between the soil and the hard rock, which is abrupt and irregular to broken, a transition zone can be observed, consisting of secondary calcium carbonate. This zone varies in thickness from a few millimetres to 5 centimetres.

At Il Vallangero, the soils are nowadays subject to severe gully erosion (see fig. 2.4). V-shaped gullies were observed of more than 4 metres deep, incised down to the underlying limestone. This gullying is caused by deforestation during World War II (local information). In the subsequent years of field work it could clearly be observed, that during heavy rains soil material from this area was washed away. In the winter of 1976 it was actually seen that during a rain storm the soil material was transported in suspension and as small aggregates.

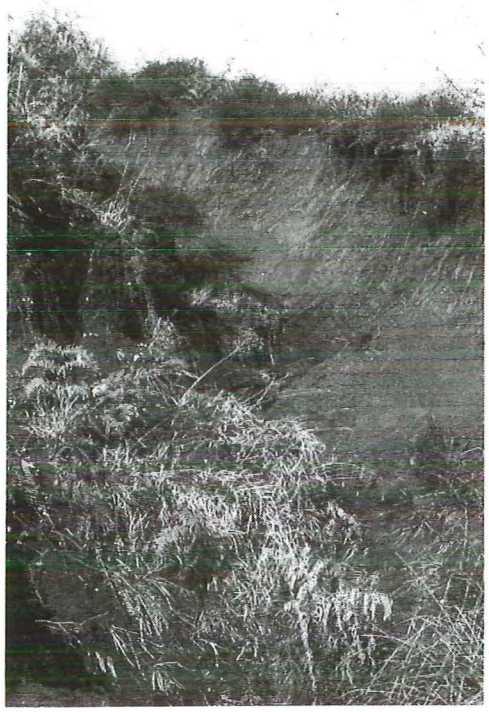

Fig. 2.4 V-shaped gully at Il Vallangero.

Most of the spots with these deep reddish brown soils however, are covered with woods, which is probably the reason that they still exist there.

2.1.2 Soils on dolomitic calcareous rocks.

Dolomitic calcareous rocks only occur to a limited extent in the main research area. They are found northwest of Monte Lamia and as intercalations in the limestone. The soils on them are described here seperately because weathering of and soil formation on dolomite is different from that on limestone.

The solubility product of dolomite in the soil waters of the dolomitic rock area will be reached faster than that of calcite. Also the dissolution of dolomite by percolating (undersaturated) soil water is much slower than that of calcite. This results in residual enrichment of dolomite in a weathering zone between the hard dolomitic rock and the soils. In this zone the calcium carbonate, which cementates the dolomite crystals, is removed. The residue is white fine to very fine sand, which consists mainly of dolomite. An increase in calcium carbonate in this weathering zone towards the hard rock could be sometimes established. Also weathering zones consisting of pure dolomite were found.

Similar to the subdivision made in the soils on non to slightly dolomitic calcareous rocks, the soils on dolomite can ce seperated into three main groups:

- shallow to moderately deep soils on mountain slopes: LITHOSOLS, RENDZINAS and CALCIC CAMBISOLS.
- eroded shallow to deep soils in fissures and cracks in the dolomite: CHROMIC LUVISOLS, VERTIC LUVISOLS and CHROMIC VERTISOLS.
- deep reddish brown soils on mountain slopes: CHROMIC LUVISOLS, VERTIC LUVISOLS, EUTRIC NITOSOLS and CHROMIC VERTISOLS.

This subdivision is mainly based on the field observations in the vast dolomite area between Itri and Sperlonga (see 1.2). Three profiles on dolomite were described (profiles Sp/183, a calcic cambisol; Sp/234, a chromic vertisol and E 80, a chromic luvisol; see appendix 2). The first two profiles are situated in the main research area, while the latter is located near Sperlonga.

The shallow to moderately deep soils on mountain slopes.

The main soils of this group are the lithosols and rendzinas. The lithosols are , according to their definition very thin and occur on hard rock. In contrast to the rendzinas on limestone, the rendzinas on dolomite were found both on hard rock and on loose dolomitic sands. As explained above, the weathering of dolomitic hard rock may lead to the accumulation of dolomitic sands. Thick weathering residues of this kind are found near Itri (Sevink et al., 1979).

Continuing soil formation leads to the development of a cambic B horizon. Profile Sp/183, classified as a calcic cambisol, can be considered as an example of the relatively young but moderately deeply developed soils on mountain slopes.

The colour of this soil is brown with a hue of 10YR. The structure of the solum is subangular blocky. Patchy thin clay cutans were observed on some pedfaces and in the upper part of the profile few dolomitic gravel occurred. Deeper in the profile the colour changes to yellowish brown and yellow, with hues of 10YR en 2.5Y. The texture changes from clay to loamy sand and sand. The structure becomes less pronounced and colour mottling starts due to hydromorphic circumstances. The gravel content increases and the reaction with HCl (2 M) becomes stronger.

The eroded soils in fissures and cracks in the dolomite.

These soils are rather common in the littoral region of the Itri - Sperlonga research area. Here, erosion has resulted into nearly complete truncation of the soils and also thick dolomitic sands residues are very rare. Unlike the soils in the fissures and cracks in the limestone,which nearly all could be classified as chromic vertisols,these soils in dolomite appear to be predominantly chromic luvisols, but also vertic luvisols and chromic vertisols may occur.

Profile E 80 is an example of the chromic luvisols found in this area. The surface horizon has dark reddish brown colours, with a hue of 5YR.

Immediately below the epipedon moderately thick clay cutans were observed. The profile did not show evidence of vertic properties. The matrix is not completely decalcified and very few slightly weathered dolomitic gravels occur.

Besides chromic luvisols, vertic luvisols and chromic vertisols occur. They form a minor group and distinction could only be made on less or more pronounced vertic properties as intersecting slickensides and wedgeshaped aggregates. Both show features of clay illuviation but they differ from the chromic luvisols by complete decalcification of the profile.

The deep, reddish brown soils on mountain slopes.

These soils on dolomite occur to a very minor extent and even less than the deep reddish brown soils on limestone. They have formed locally in the south-eastern part of the main research area, but are not known to occur in the dolomite area between Itri and Sperlonga.

Chromic vertisols are the main soils of this group. Associated with them chromic and vertic luvisols and eutric nitosols occur. The occurence of these soils is related to the thickness of the colluvial cover, in which mostly an argillic B horizon is formed.

Profile Sp/234 is an example of a chromic vertisol. The top part of this profile consists probably of a colluvial cover with a thickness of approximately 45 cm, in which a Bt has developed. Deeper in the soil strong vertic properties, such as medium to large slickensides and wedgeshaped aggregates, occur. Wide cracks existed at time of description, extending towards the surface. The strong vertic properties and insufficient drainage have caused destruction of the road at the location of profile description (fig.2.5).

The colour of the soil varies from (bright) reddish brown to (dark) reddish brown, with hues of 5YR and 2.5YR. The structure is angular blocky, tending to prismatic, in the top part of the profile. The clay illuviation features established in the top part of the Bt horizon disappear deeper in the soil. At the transition to the parent rock a weathered dolomite layer of varying thickness ("dolomitic sand") occurs.

Fig. 2.5 Road near profile Sp/234, destroyed through vertic processes under the road surface and insufficient drainage measures. Note crack at the left side of the picture, extending to the surface and breaking up the road.

The texture of the soil is clayey with a clay content below 1 m of more than 90 %. The pH decreases regularly with depth to a value of 4.9 at approximately 2 m. Organic C content is at its highest in the Ah horizon (1.3 %) and decreases rapidly to about 0.3% deeper in the soil.

2.1.3 The deep colluvial soils in karstic depressions.

In the karstic depressions material has accumulated, which has been washed down from the slopes. Several phases of accumulation can be found, characterized by admixture of allochtonous material. Based on this, the following three groups of soils in colluvial deposits were distinguished:

- soils with admixture of volcanic material and pottery fragments
- soils and paleosols with admixture of volcanic material without pottery fragments
- soils and paleosoils without admixture of volcanic material and pottery fragments

They represent more or less a chronological sequence in colluviation phases, as will be discussed in chapter 4.

Soils with admixture of both volcanic material and pottery fragments.

The soils found in these deposits are very uniform. They are classified as chromic luvisols, while also eutric nitosols may occur. The soils also show in variable proportions vertic properties, so that vertic luvisols and even chromic vertisols may occur. Very locally also chromic cambisols occur (e.g. profile Sp/119a).

Profile Sp/98 is an example of a chromic luvisol. The Ap horizon is weakly developed and has dark (reddish) brown to reddish brown colours with hues of 7.5YR and incidentally 5YR. The structure is subangular blocky to massive and the consistence is hard to very hard when dry. The thickness of the epipedon in these soils varies from

30 to 40 cm. The transition to the underlying horizon is abrupt to clear and smooth

The Bt horizons may extend to a very great depth (more than 2 m). They are very homogeneous and show colours of dark reddish brown to reddish brown, with hues of 5YR.They have subangular blocky to prismatic structures, which often can be broken into angular blocky structures. Clay cutans are commonly found in pores and on pedfaces. Probably two kinds occur: clay-iron-humus cutans, mostly in the top part of the Bt horizon, while deeper in the profile clay-iron cutans prevail. Bluish black iron-manganese mottling is common, together with iron-manganese nodules.

The depth to which pottery fragments may be found is sometimes over 6 metres. The pottery fragments were often weathered and too small to determine, so that archeological dating of these deposits was not possible.

Fig. 2.6 shows some general soil characteristics of profile Sp/98.

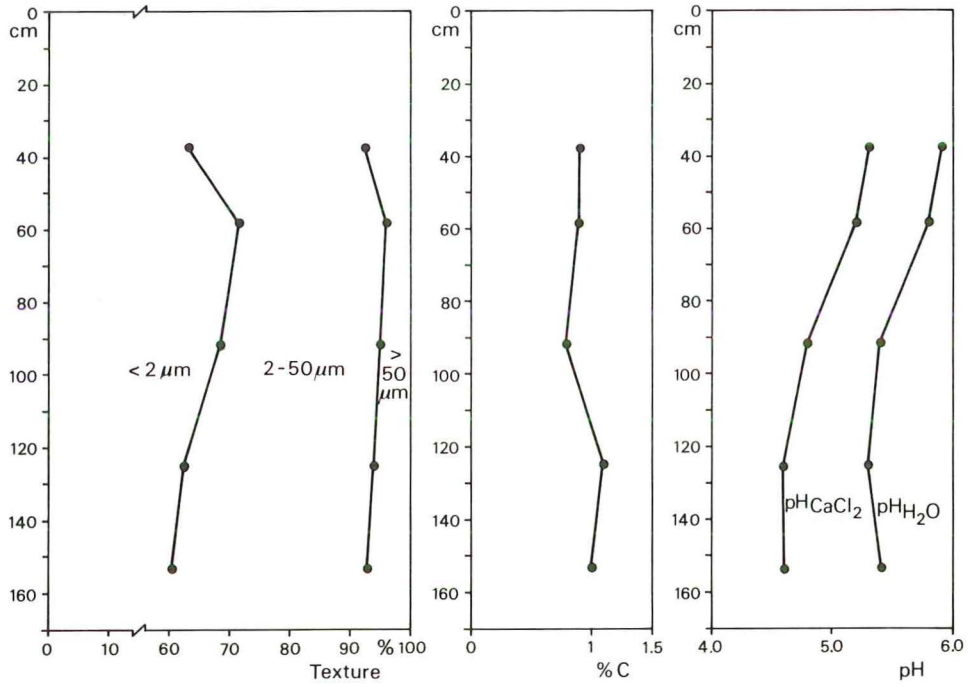

Fig. 2.6 General soil characteristics of profile Sp/98 (chromic luvisol).

Soils and paleosols with admixture of volcanic material without pottery.

These soils were thought to have developed in Pleistocene colluvial deposits because of the lack of pottery fragments. They also differ from the soils of the previous group because the volcanic material is not only present as minerals in the matrix, but also as tuffaceous beds intercalated in the colluvial deposits. Profiles Sp/111 and Sp/118 (both chromic luvisols) are examples of these soils.

The colours of the soils are somewhat redder than the colours in the colluvial soils mentioned above. They are dark to dull reddish brown with hues of 5YR. Common bluish black iron-manganese mottles occur. The structure is medium to coarse prismatic, which can be broken into aggregates with a medium angular blocky structure. They have moderately thick to thick reddish brown to red clay cutans and incidentally slickensides can be observed. They show no reaction with HCl (2 M).

The texture is fine to very-fine and the soil is "strongly acid" (Soil Survey Staff, 1951), with pH varying from 5.7 to 5.1. Similar to the soils of the previous group, the Ap horizon contains a moderate amount of organic C, rapidly decreasing with depth.

The soils and paleosols without admixture of volcanic material and pottery fragments.

Fig. 2.7 Polygonal cracking in chromic vertisols near profile Sp/97.

These sediments are found below the previous groups. This type of deposit is characterized by strong pseudogleyic features. Extreme mottling is observed in profile Sp/97, deeper down in the profiles Sp/111 and Sp/119b and in other colluvial soils in Lazio (Sevink et al., 1979).

In profile Sp/97, a chromic vertisol, it was still possible to establish a matrix colour in the upper part of the profile, which showed to be dark reddish brown. Besides this, common light grey, orange to bright yellowish brown and reddish brown to red mottles occurred. Deeper in the soil no matrix colour could be observed.

The structure is angular blocky, which tends to become wedgeshaped deeper in the profile. Slickensides are very common, while occasionally clay cutans were observed. At the surface near profile Sp/97 wide cracks occurred in the dry season (fig. 2.7), extending downwards to a depth of 70 to 80 cm. Particle size analyses showed a very high clay content in this soil with clay percentages over 90 %. At a depth of approximately 180 cm a some what coarser textured layer occurs with clay percentages of approximately 70 %. Soil reaction is "medium to strongly" acid and organic C content is similar to the soils in the previous groups.

2.2 Composition of the limestone and of the dolomite.

At a number of places fresh limestone and dolomite rocks were sampled for mineralogical and chemical analyses (samples Sp/68a, d and f, Sp/93e and Sp/123i). Of all samples qualitative X-ray diffraction investigations were carried out of the finely ground carbonate rock. The decalcified non-carbonate residue of sample Sp/68a (sample Sp/68b) as well as the clay fractions of the samples Sp/68b, Sp/68e (decalcified non-carbonate residue of sample Sp/68d), Sp/68g (decalcified non-carbonate residue of sample Sp/68f) and of the decalcified non-carbonate residue of the limestone belonging to sampling point Sp/65 were investigated alike.

Thin sections were prepared of the samples Sp/68a, d and f, while an extended physico-chemical and chemical analysis of sample Sp/68a and of its slowly decalcified non-carbonate residue was carried out. This sample has been selected because its mineralogical composition can be regarded as the modal mineralogical composition of the carbonate rocks in the investigated area (see also 1.6.2).

2.2.1 Mineralogical composition of the limestone and of the dolomite.

X-ray diffraction analyses of the samples show a mineralogical composition of the carbonate part of the rocks varying from nearly pure calcite to almost pure dolimite (table 2.1). Besides calcite and dolomite and in one case aragonite, no other carbonate minerals could be detected by X-ray diffraction analyses.

Table 2.1 X-ray diffraction analyses of the samples Sp/68a, d and f, Sp/93e and Sp/123i in approximate estimated percentages.

	% Calcite	% Dolomite	% Aragonite
Sp/123i	97	3	-
Sp/ 68f	95	5	-
Sp/ 68a	45	45	10
Sp/ 93e	45	55	-
Sp/ 68d	5	95	-

X-ray analyses of the non-carbonate residues (both fine earth and clay fractions) show a dominance of 10 Å minerals (illite and muscovite, see table 2.2). An exception to this is sample Sp/68g, which shows besides illite also a considerable amount of 7 Å minerals, probably dickite, a member of the kandite group. The occurrence of mainly 10 Å minerals in the non-carbonate residues of limestone is also reported by other authors (Brugger, 1974; Carroll & Hathaway, 1954; Gal, 1966; Robbins & Keller, 1952; Sinno, 1963). As accessory minerals mainly quartz and traces of smectite, (most probably) chlorite, kaolinite, albite and pyrite occur.

Table 2.2 X-ray diffraction analyses of the samples Sp/68b,e and g and the non-carbonate residue of sample Sp/65c.

Fine earth fraction of sample Sp/68b.

	Sm	14 Å	10 Å	7 Å	Qtz	Ana	Go/Hm	Ab	Pr
Sp/68b	tr	tr	+++(+)	tr	4-6 %	?	-	tr	(x)

Clay fractions (>2 μm)

	Sm	14 Å	10 Å	7 Å	Qtz	Ana	Go/Hm
Sp/68b	tr	-	+++(+)	tr	1-3 %	(x)	-
Sp/68e	?	-	+++	-	$\ll$1 %	tr	-
Sp/68g	+	tr	++(+)	++(+)	4-6 %	?	-
Sp/65c(r)	-	-	+++	?	< 1 %	?	-

Thin section analyses of the various rock samples give the following results:

- Sp/68a: a fine to medium textured, dark grey dolomitic limestone with a few veins of calcite and domains of well crystallized carbonates with crystal sizes between 50 and 400 μm. In voids crystal sizes up to 800 μm were measured. These crystals may be of secondary origin. locally the thin sections show a ground mass of finely divided calcium carbonate.
- Sp/68d: a fine textured grey dolomite with an intricate network of white veins of calcite and a few reddish veins, probably free iron compounds. The thin sections show a matrix of dolomite, with crystal sizes ranging from 35 to 275 μm. Fissures and cavities are filled up with calcite crystals with sizes up to 1000 μm.
- Sp/68g: an oolithic, very fine to fine textured, white to light grey limestone (see cover photograph). Oblong shaped ooliths with a diameter up to 7 mm are more or less parallel orientated, suggesting a fine stratification in the rock. Locally, however, the orientation is more chaotic and "flow" structures were observed. The ground mass consists of very finely divided calcium carbonate. Larger calcite crystals with sizes up to 60 μm in cavities and voids suggest secondary calcium carbonate at these places.

Non-carbonate particles are very sparse in the thin sections. A few quartz, pyroxene, garnet and zircon grains could be established. Also few opaque grains occur which in most of the cases could be determined as haematite or goethite, because of their vivid orange to red colour in oblique striking light. In voids and alongside crystal planes often a dark brown to brownish black coating was observed, which lights up only very slightly in oblique striking light.

The X-ray diffraction analysis of the non-carbonate part residue of the fine earth fraction of sample Sp/68b indicates the presence of pyrite. No evidence was found for the occurrence of haematite or goethite in this sample. Consequently, the considerable amount of Fe_2O_3 and the relative high free iron content in the chemical analyses (see table 2.4) indicates that these coatings probably mainly consist of amourphous iron compounds (most likely ferrihydrite). The samples may also contain an amount of organic substances (see 2.2.2 and appendix 3), part of which may also be found in these coatings.

Of the fraction 50-500 μm of sample Sp/68b a heavy mineral slide was prepared. Besides a very high amount of opaque grains (more than 90 %) mainly green clinopyroxenes (augites and aegerine-augites), garnets and epidotes occur (see table 2.3). The occurrence of dolomite grains in the sample is due to incomplete dissolution of the limestone.

Table 2.3 Heavy mineral composition of the fraction 50-500 μm of the non-carbonate residue of sample Sp/68b.

% opaque grains	Biotite	Dolomite	Green clino-pyroxene	Amphibole	Epidote	Tourmaline	Garnet	Zircon	Rutile	Anatase	Titanite	Staurolite	Apatite	Distheen	Glaucophane	Corund
91.7	6.0	13.0	45.5	4.5	10.0	3.0	10.5	1.5	1.0	0.5	1.0	1.0	0.5	0.5	0.5	1.5

2.2.2 Chemical and normative mineralogical composition of the limestone.

The results of the physical and chemical analyses of the limestone sample Sp/68a and its slowly decalcified non-carbonate residue (sample Sp/68b) are shown in table 2.4.

Table 2.4 Particle size distribution and chemical analyses of the samples Sp/68a and b.

	TEXTURE 2000-50 μm	50-2 μm	2 μm	% CO_2	% Org. C	% "Free" Fe_2O_3
Sp/68a	-	-	-	46.8	0.05	0.1
Sp/68b	3.5	28.5	68.0	2.2	6.1	4.6
Sp/68b (clay)	-	-	-	-	3.2	4.4

Elemental analyses of the fine earth fraction and limestone rock.

	SiO_2	Al_2O_3	Fe_2O_3	FeO	MnO	MgO	CaO	Na_2O	K_2O	TiO_2	P_2O_5	S	L.o.i.
Sp/68a	0.5	0.2	0.1	tr	tr	9.5	44.0	tr	0.1	tr	tr		45.5
Sp/68b	43.4	19.0	8.6	1.4	0.1	3.4	2.2	0.3	4.8	0.9	0.4	0.5	15.3

Elemental analyses of the Ba-saturated clay fraction (< 2 μm) of sample Sp/68b.

	SiO_2	Al_2O_3	Fe_2O_3	FeO	MnO	MgO	CaO	Na_2O	K_2O	TiO_2	P_2O_5	S	L.o.i.	BaO
Sp/68b	46.3	25.4	6.1	1.1	0.1	3.1	tr	0.1	5.6	0.6	0.4	1.2	9.9	2.6

It should be noted that the figures for loss on ignition (L.o.i.) in table 2.4 are the the sum of the loss on ignition due to the volatile constituents (e.g. loss on ignition of sample Sp/68b = L.o.i. due to H_2O^+ + L.o.i. due to $CaMg(CO_3)_2$ + L.o.i. due to FeS_2 +

L.o.i due to C_nH_{2n+2} - weight increase due to oxidation of ferrous iron to ferric iron).

The normative mineralogical composition of the limestone (sample Sp/68a) and the non-carbonate residue (Sp/68b) are presented in table 2.5.

Table 2.5 Normative mineralogical composition of the limestone (Sp/68a) and the non-carbonate residue (Sp/68b) in weight percentages.

	Cc[b]	Dol	Q	Chlor	Ill/Ms	Ab	Hm	Pr	Misc[c]	W[d]
Sp/68a[a]	55	44	0.2	tr	0.6	tr	0.1	tr	tr	tr
Sp/68b	-	-[e]	15	5	61	3	10	3	3	4

[a] It is assumed that the non-carbonate residue of the limestone is 1 %. During the dissolution process of the limestone 3 kg of limestone resulted in 27.5 gr of insoluble residue (≈0.9 %).

[b] Cc stands for calcite + aragonite (see mineralogical composition, table 2.1).

[c] Misc = apatite + strengite + rutile

[d] The figure given for water (W) is the percentage of water used during the normative mineralogical calculation. This procedure was followed because it was not possible to calculate from the value of loss of ignition a proper value of H_2O^+.

[e] Although dolomite is present in the sample (see mineralogical and chemical composition, tables 2.1 and 2.4), the normative mineralogical composition is presented on carbonate-free basis in order ro get insight into the ratios of the non-carbonate minerals in the limestone.

2.3 Calculation of the weathering paths and mass transfer by weathering of the limestone: a theoretical approach.

Weathering of limestone and dolomite is mainly a chemical process, which can be described as the dissolution of carbonate minerals, dissolution, hydrolysis and oxidation of non-carbonate minerals, resulting in precipitation (neoformation) of secondary minerals. Although chemical weathering in itself is an irreversible process, it is possible to apply the classical thermodynamical approach, which follows in the present study, by assuming the existence of partial equilibria,i.e. equilibria are assumed to exist between the aqueous phase and the product minerals and between the species in the aqueous phase mutualy, but not with the reactant minerals. The application of the classical thermodynamic principles in the geosciences gives satisfactory results, as is clear from the literature. Weathering studies, based on thermodynamics allow to predict weathering paths and final products of the weathering and to calculate the mass transfer during the weathering process. The theoretical basis for this approach is given by Helgeson (1968, 1971, 1972), Helgeson et al. (1969, 1970) and Fritz (1975).

Finally the value of the theoretical model and its weathering paths can be tested from the chemical analyses of water samples (aqueous phase) and from the chemical and mineralogical analyses of soil and rock samples (solid phase).

Dirven et al. (1976), in their study on the weathering of serpentinite in Cuba, and Verstraten (1978), in his study on the weathering of low-grade metamorphic shales in Luxembourg, have shown that this approach gives satisfactory results.

2.3.1 Assumptions.

The mineralogical composition of the carbonate part of the limestone rock varies from nearly pure calcite to nearly pure dolomite (see 2.21, table 2.1), whereas the non-carbonate residue is rather homogeneous and consists mainly of illite (muscovite) and quartz. Sample Sp/68a has been selected to serve as the basis for the calculations because its composition holds an intermediate position with respect to the carbonate minerals.

Because of the rapid decrease of the rock forming minerals, with exception of the accessory minerals, with respect to its weathering material (soil) (see normative and actual mineralogical composition of the rock and soils), it is thought that the reaction rates of these rock forming minerals are proportional to their mole fractions. These amount to:

	Mole fractions	Approx. ratios
Cc	0.6922	5070
Dol	0.3006	2200
Q	0.0031	23
Ill	0.0027	20
Chlor	0.0001	1
Ab	0.0001	1
Hm	0.0008	6
Pr	0.0003	2

Chlorite and albite occur only in very minor proportions. Therefore both minerals are neglected in defining the system. This will affect the system not significantly. The contribution of Mg by chlorite to the system is negligible as its Mg-content is totally controlled by dolomite. Also the error made by neglecting albite with respect to the Na-contribution is thought to be very small. The Cl/Na mole ratios in the water samples are rather uniform and indicate that the sodium content in these waters is mainly governed by atmospheric supply by dry fall-out and rainwater (see 2.4.1). Neglecting chlorite and albite has a very minor effect on the Al- and Si-content of the system. The contribution of Al and Si by both minerals is 6 and 8 % of the total Al- and Si-content respectively.

Quartz has been considered as an inert component and has therefore been ignored in the weathering models.

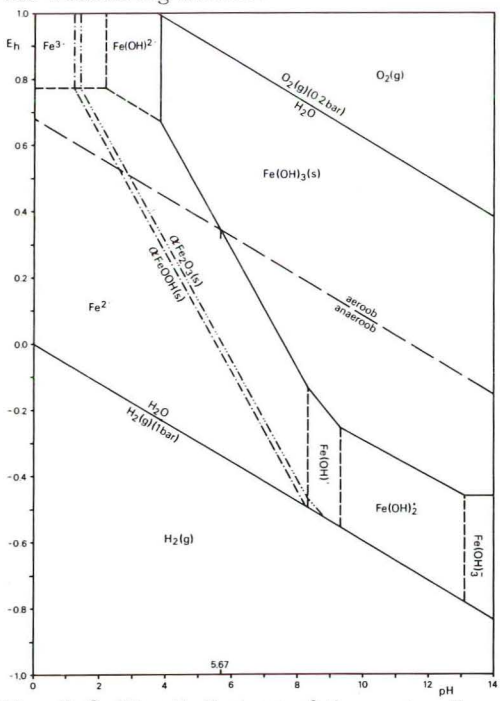

Fig. 2.8 Eh-pH diagram of the system Fe-H_2O-O_2(g) at 25° C and 1 bar pressure and a mobility of the total dissolved Fe-species of 10^{-6} mol/l.

On the following considerations also free iron species in the sample (haematite goethite, ferryhydrite and pyrite) have been left out from the calculations.

It seems reasonable to assume that anaerobic conditions rarely occur in the weathering environment of limestone, as most of the karstic waters are in open connection with the atmosphere through systems of diaclases and caverns. Partial O_2 pressures have not been measured in the water samples, but Langmuir (1971), who investigated 58 water samples from limestone and dolomite in Pennsylvania, records partial O_2 pressures ranging from approximately 0.2 bar (nearly equal to that of the air atmosphere) to approximately 0.08 bar. This indicates aerobic conditions in all his sampled waters.

Using 10^{-6} mol/l for the total dissolved iron species as the limit for the mobility of iron compounds. Ferrihydrite, the most soluble component of the free iron species involved, can be considered as "mobile" at a pH of 5.67 or lower (see fig. 2.8). As the pH of karstic waters apperently increases rapidly (the lowest pH's measured in these waters are in the order of 6.90 in samples taken during or short after storms), it is concluded that

iron oxides and -hydroxides can be regarded as immobile, if organic acids play a subordinate role. The formation of goethite and haematite, often recorded in "terra rossas", from the amorphous iron species is believed to be a process of dehydration, due to the lack of additional iron sources in the rock-forming minerals.

Also the oxidation of pyrite has to be considered. The rate-determining step in this process is the oxidation of ferrous iron to ferric iron, which is believed to be a very slow process (Stumm & Morgan, 1970). The model proposed by these authors, describing the oxidation of pyrite in mineral mine waters, can also be used in the present study (fig. 2.9).

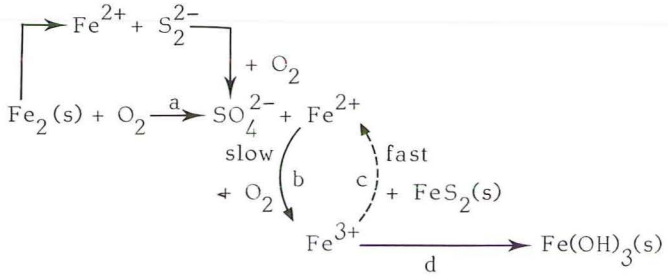

Fig. 2.9 Oxidation model of pyrite in (neutral) karstic environments (modified after Stumm & Morgan, 1970).

After oxidation of sulfide to sulfate (step a), the ferrous iron is oxidized very slowly to ferric iron (step b). Stumm and Morgan report half-times for this oxidation reaction of 1000 days at pH 3. Because of the neutral environments in karstic waters, step c, reduction of ferric iron to ferrous iron by pyrite under formation of elementary sulfur, which is thought to be the driving force of oxidation in acid environments (van Breemen, 1976) can be neglected. Step d can therefore be regarded as the final one. The sluggish oxidation of pyrite at neutral pH's is also reported by Murakami (1966).

The presence of opaque grains with a (fromboidal) pyrite structure in the heavy mineral slides of "terra rossas" supports the view that oxidation of pyrite from limestone and dolomite is a very slow process. Hence it is concluded that kinetic factors act as a brake on the oxidation of pyrite and therefore it is not taken into account in the calculations of the weathering paths of the limestone.

The composition of the now defined reactant part of the rock can be written as $\{5070\,Cc + 2200\,Dol + 20\,Ill\}$ or $\{Ca_{375}Mg_{110}(CO_3)_{475} + Mg_{0.25}K_{0.6}Al_{2.3}Si_{3.5}O_{10}(OH)_2\}$. The Gibbs free energy of formation (ΔG_f°) of the rock, written as solid solution $(Ca_{605}Mg_{185}KAl_4Si_6O_{17}(OH)_3(CO_3)_{790})$ is calculated from the individual rock-forming minerals and amounted to -211296.1 kcal/mol. The contribution of the free energy of mixing, resulting in a slightly more negative value for the Gibbs free energy of formation (Mueller & Saxena, 1977) has been ignored.

The following assumptions were made to calculate the theoretical weathering model of limestone (Dirven et al., 1976; Verstraten, 1978):
- the system is closed with respect to the solid and aqueous phase, but open to the (soil) atmosphere with respect to CO_2,
- during the process of weathering partial equilibrial exist,
- weathering can be considered as a stepwise reaction of incremental addition of small amounts of rock in 1 kg of water,
- formation of crystalline quartz and dolomite is assumed not to occur in this weathering model.

The process of dolomite formation is yet not quite understood. Until now dolomite synthesis has only been achieved under hydrothermal conditions (Graf & Goldsmith, 1956;

Rosenberg et al., 1976; Katz & Matthews, 1977). On the other hand dolomite formation in subrecent and recent sediments (Clayton et al., 1968; Barnes & O'Neil, 1971; Lippmann, 1973) and soils (Kovda et al., 1973) points to the fact that dolomite is not only formed under hydrothermal conditions. Moreover, it is even questionable if hydrothermal environments are the source of the vast dolomite occurrences in the world (Lippmann, 1973).

If Lippmann's suggestion is correct, that the formation of dolomite is analogous to the formation of norsethite, which he succesfully succeeded to synthesize at room temperatures according the reaction

$$BaCO_3 + Mg^{2+} + CO_3^{2-} \longrightarrow BaMg(CO_3)_2$$

an alkaline environment is needed to create a sufficient amount of CO_3^{2-} in the solution. In fact , he started his experiment of norsethite formation in an environment of pH 8.3, which during the experiment dropped to 7.5. His succesful attempt to synthesize $PbMg(CO_3)_2$ showed the same conditions.

As the occurrence of dolomite in sedimentary environments seems to be limited to alkaline conditions (lagoonal and tidal deposits, alkaline soils) it is very unlikely that dolomite formation in weathering environments of limestone occurs. This is also demonstrated by the frequent supersaturation of the karstic waters with respect to dolomite.

The assumption that dolomite is not formed, has been checked by calculating a weathering path (I', see fig. 2.16 and 2.17), in which, after reaching the dolomite saturation point, partial equilibrium with this mineral was maintained throughout the calculation. The unrealistic results of this calculation support the assumption that dolomite is not formed in these weathering environments (see discussion).

Recent investigations (de Boer, 1977; Thorstenson & Plummer, 1977) have shown, that calcite with an Mg-content of 2 to 3 % is, in thermodynamic terms, the most stable form of calcium carbonate. Therefore it has been assumed in the calculations that the chemical composition of calcite as rock-forming constituent is $Ca_{0.98}Mg_{0.02}CO_3$.

Ion activities were determined iteratively. Beforehand an activity coefficient was selected and after the calculation of each part of the weathering path the activity coefficient was computed according the formula of Davies. If the selected ion activity coefficient deviated beyond the (arbitrary) limit of $\gamma_{1\pm} = 10^{-0.002}$, the procedure of calculation was repeated, using the ion activity coefficient obtained after the last calculation. Mostly these then appeared to be correct.

2.3.2 Calculations.

As carbondioxide is the main weathering agens, the weathering paths were calculated for a number of partial CO_2-pressures, representing the whole range of partial CO_2-pressures observed in the weathering environment, viz. $pP_{CO_2} = 3.52$ (0.03 vol. %), 2.80 (0.15 vol. %), 2.00 (1 vol. %), 1.30 (5 vol. %) and 0.80 (15 vol.%) (all partial CO_2-pressures expressed as negative logarithms).

The general reaction equation, showing the congruent dissolution of the limestone rock, can be given as:

$$\left\{Ca_{365}Mg_{110}(CO_3)_{475} + Mg_{0.25}K_{0.6}Al_{2.3}Si_{3.5}O_{10}(OH)_2\right\} + (483-b-d-e-2f-3g-4h-i)\,CO_2(g)$$
$$(485-b-d-i)\,H_2O \longrightarrow (365-a-b)\,Ca^{2+} + a\,CaHCO_3^+ + b\,CaCO_3^o + (110.25)\,Mg^{2+} +$$
$$c\,MgHCO_3^+ + d\,MgCO_3^o + 0.6\,K^+ + (2.3-e-f-g-h)\,Al^{3+} + e\,AlOH^{2+} + f\,Al(OH)_2^+ + g\,Al(OH)_3^o +$$
$$h\,Al(OH)_4^- + 3.5\,H_4SiO_4^o + i\,CO_3^{2-} + (958-a-2b-c-2d-e-2f-3g-4h-2i)\,HCO_3^-.$$

The complexes $CaOH^+$ and $MgOH^+$ are neglected as these are only important at high pH's. Also $H_3SiO_4^-$ is not taken into account, because this species only becomes important with respect to $H_4SiO_4^o$ at a pH 8.4 and higher.

A complete description of the five weathering models as chemical reaction equations is summarized in appendix 4. The results are the weathering paths shown in figures 2.10 to 2.14. The mass transfer along these weathering paths is given in table 2.6. The composition of the ambient solution at the various points along the weathering paths is shown in table 2.7, whereas the theoretical composition of the solution in equilibrium with the limestone rock, compared to the composition of the sampled karst waters is shown in table 2.8.

Table 2.6 Mass transfer along the calculated, theoretical weathering paths, in mg/kg H_2O.

Weathering model	(In)variant point	pP_{CO_2}	Rock diss.	Dol	Q	Mg-chlor	Gibb	Kaol
			mg/kg H_2O					
I	A-C	3.52	64.7	12.8	0.1	0.5	-	-
II	F-H	2.80	113.3	22.95	0.15	0.8	-	-
III	K-N	2.00	208.0	39.4	0.3	-	0.15	0.7
IV	P-T	1.30	369.1	69.5	0.5	-	-	2.0
V	V-Z	0.80	570.3	108.8	0.7	-	-	3.1

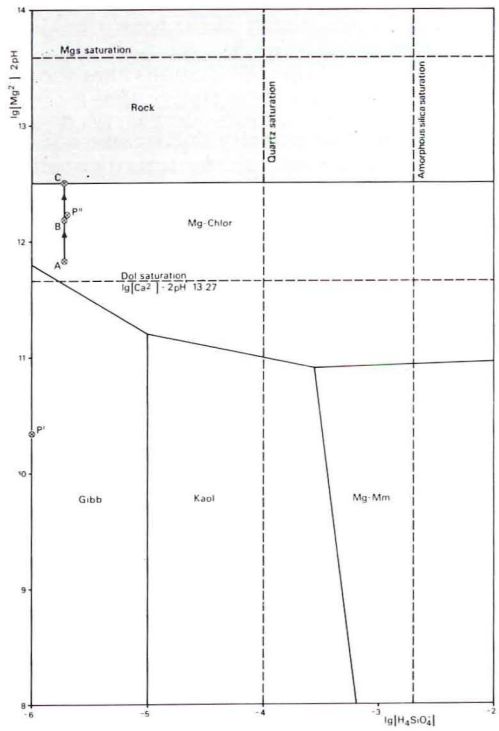

Fig. 2.10 Weathering model I.

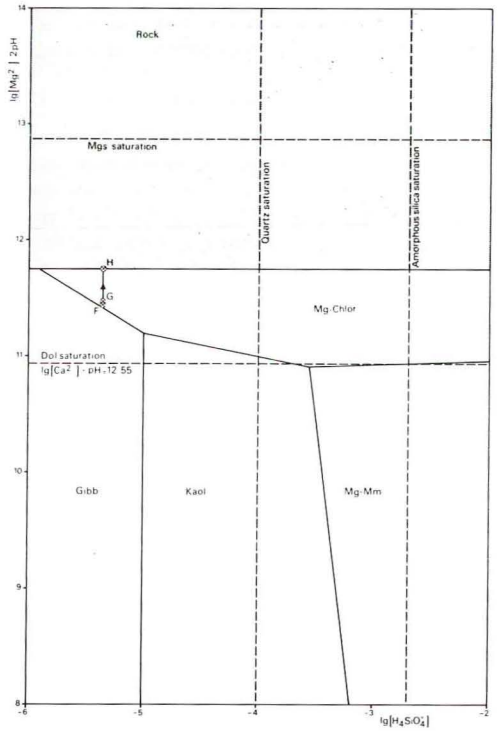

Fig. 2.11 Weathering model II.

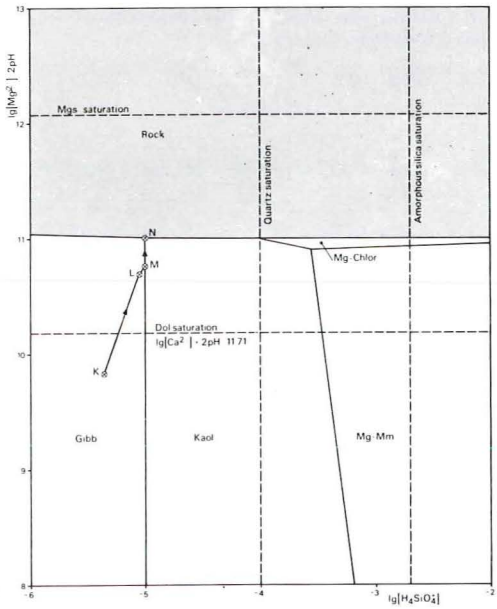

Fig. 2.12 Weathering model III.

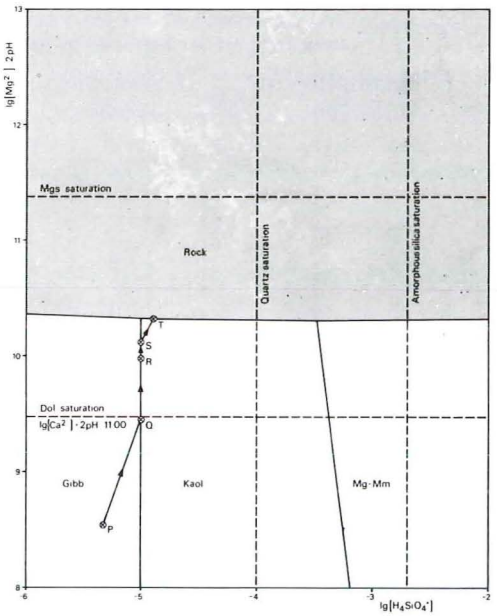

Fig. 2.13 Weathering model IV.

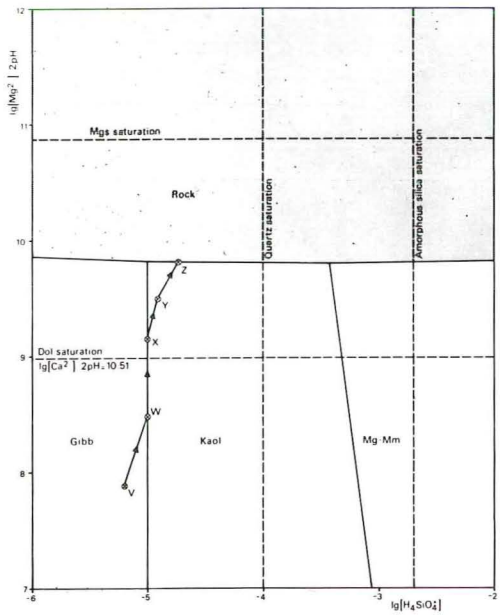

Fig. 2.14 Weathering model V.

Fig. 2.10 to 2.14 Stability fields of the limestone rock, Mg-chlorite (clinochlore), Mg-montmorillonite, kaolinite and gibbsite in the system $MgO - CaO - K_2O - Al_2O_3 - SiO_2 - H_2O - CO_2(g)$ at 25 °C and 1 bar pressure. Conditions in the weathering models are:

I : $lg[Ca^{2+}] + 2pH = 13.27$; $lg[K^+] + pH = 2.28$
$pP_{CO_2} = 3.52$

II : $lg[Ca^{2+}] + 2pH = 12.55$; $lg[K^+] + pH = 2.03$
$pP_{CO_2} = 2.80$

III: $lg[Ca^{2+}] + 2pH = 11.71$; $lg[K^+] + pH = 1.74$
$pP_{CO_2} = 2.00$

IV : $lg[Ca^{2+}] + 2pH = 11.02$; $lg[K^+] + pH = 1.53$
$pP_{CO_2} = 1.30$

V : $lg[Ca^{2+}] + 2pH = 10.51$; $lg[K^+] + pH = 1.38$
$pP_{CO_2} = 0.80$

Points P' and P'' in fig. 2.10 indicate position of the rain water samples Sp/233a and b resp. in the weathering model.

Table 2.7 Ion activities at the (in)variant points along the calculated, theoretical weathering paths, expressed as negative logarithms (-lg[a]).

Weathering model	pP_{CO_2}	(In)variant point	pH	pCa	pMg	pK	pSi	pAl	pCO_3
I	3.52	A	8.06	3.77	4.29	6.51	5.73_5	15.34	5.57
		B	8.18	3.64	4.16	6.37	5.72^5	16.62	5.33
		C	8.35	3.43	4.19	6.07	5.72	17.94	5.00
I'	3.52	A	8.06	3.77	4.29	6.51	5.73_5	15.34	5.57
		B	8.18	3.64	4.16	6.37	5.72^5	16.62	5.33
		C'	8.33	3.39	5.01	5.98	5.71_5	15.73	5.03
		D	9.61	5.95	7.56	1.54	2.70^5	24.10	2.47
II	2.80	F	7.70	3.42	3.95	6.15	5.37	13.83	5.57
		G	7.71	3.41	3.95	6.14_5	5.37	13.94	5.55
		H	7.88	3.21	3.98	5.85^5	5.36	15.24	5.21
III	2.00	K	6.89	3.43	3.95	6.15	5.36	11.46	6.39
		L	7.18	3.16	3.67	5.85	5.06	12.33	5.81
		M	7.22	3.11	3.67	5.79	4.99	12.45	5.73
		N	7.34	2.97	3.67	5.60	4.99	12.81	5.46
IV	1.30	P	6.23	3.40	3.92	6.11^5_5	5.33	9.48	7.01
		Q	6.54	3.10	3.62	5.79^5	5.00	10.41	6.39
		R	6.72	2.94	3.46	5.61_5	5.00	10.95	6.03
		S	6.79	2.86	3.46	5.49^5	5.00	11.16	5.89
		T	6.89	2.75	3.46	5.34	4.89	11.57	5.69
V	0.80	V	5.85	3.29	3.81	6.00	5.21	8.34^5	7.27
		W	6.05	3.10	3.62	5.76	5.00	8.94	6.87
		X	6.28	2.89	3.41	5.56	5.00	9.63	6.41
		Y	6.40	2.78	3.30	5.44	4.92_5	10.07_5	6.17
		Z	6.56	2.61	3.31	5.18	4.72^5	10.74^5	5.85

Table 2.8 Composition of the calculated, theoretical solution at the invariant points, compared with the actual composition of the springs from limestone and dolomite, given as negative logarithm of the ion activities (-lg[a]).

Weath. model	Invar. point	pP_{CO_2}	pH	pCa	pMg	pK	pAl	pSi
I	C	3.52	8.35	3.43	4.19	6.09_5	17.94	5.72
II	H	2.80	7.88	3.21	3.89	5.85^5	15.24	5.36
III	N	2.00	7.34	2.97	3.66	5.60	12.81	5.00
IV	T	1.30	6.88	2.76	3.46	5.36	11.53_5	4.90_5
V	Z	0.80	6.56	2.61	3.31	5.18	10.74^5	4.72^5
Limestone spr.			1.46-2.40	6.90-7.72	2.66-3.09	3.36-3.75	4.20-4.99	9.97-12.42	3.73-4.25
Dolomite spr.			1.28-1.60	6.91-7.27	2.74-2.78	3.02-3.10	4.59-5.15	9.77-11.44	3.75-3.97

2.3.3 Discussion.

The results of the weathering path calculations show that by increasing partial CO_2-pressures the final weathering product shifts gradually from dolomite with Mg-chlorite to dolomite with kaolinite. This is illustrated in fig. 2.15, in which the dashed area can be regarded as the "weathering environment" of the limestone rock under view.

The results also show that the final composition of the solution in the calculations is in good agreement with the calculated activities from the measured composition of the karstic waters with respect to Ca, Mg, pH and P_{CO_2} (see table 2.8 and fig. 2.19).

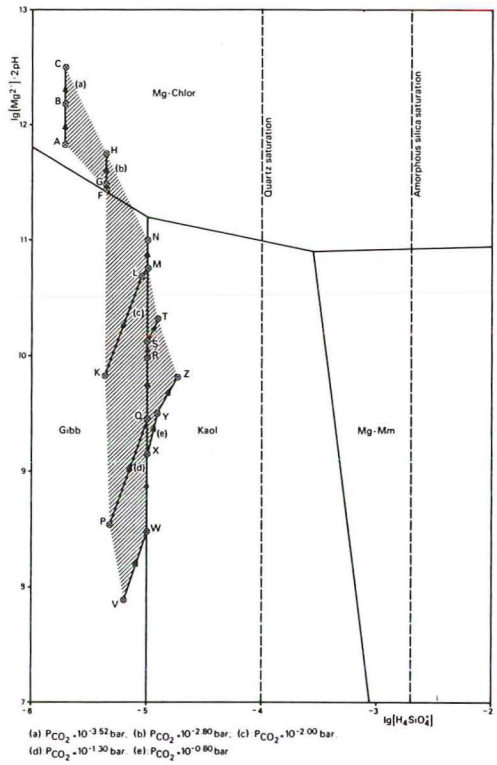

Fig. 2.15 Theoretical "weathering environment" of the limestone (dashed area), as derived from the weathering path calculations and shown in a stability diagram of the system $MgO - CaO - K_2O - Al_2O_3 - SiO_2 - H_2O - CO_2(g)$ at 25 °C and 1 bar pressure. Phases indicated are Mg-chlorite (clinochlore), Mg-montmorillonite, kaolinite and gibbsite. Conditions are the same as in figures 2.10 to 2.14.

The partial CO_2-pressures in the sampled spring waters indicate that the mineral assemblage calculated in the weathering models III and IV can be expected. As will be shown later, this holds good for kaolinite. Dolomite has not been found in the soils on limestone except for the dolomitic limestones. Therefore the limestone used for the calculations may have been too rich in dolomite to obtain results comparable to the observed mineral assemblage in the soils on limestone.

K, Al and H_4SiO_4 content in the karstic waters differ significantly from the activities calculated in the theoretical weathering models. This discrepancy will be discussed in 2.6.2.

The assumption that dolomite is not formed during the weathering process is tested by calculating a weathering path at a partial CO_2-pressure of $10^{-3.52}$ bar, assuming partial equilibrium with dolomite. The subsequent steps of this calculation, expressed as chemical reaction equations, are summarized in appendix 4 (I') and indicated in fig. 2.16 and 2.17.

It was not possible to calculate this weathering path up to the point where the system was fixed (in a theoretical sence), either by reaching overall equilibrium with the rock or by reducing to zero the degrees of freedom according to the phase rule of Gibbs. During the calculations the ionic strength increased above 0.5 M after saturation with amorphous silica was reached. Therefore the formula of Davies, used to calculate the activity coefficients, could no longer be applied.

The situation in point D, in which saturation with amorphous silica was reached (see appendix 4 and fig. 2.16 and 2.17) and partial equilibria exist with Mg-chlorite, dolomite and calcite, already illustrates the unreality of this weathering model.

According to the calculations, in point D 2600.94 g rock is transformed under formation of 35.89 g Mg-chlorite, 1083.39 g dolomite, 1466.87 g calcite and 3.38 g quartz (re-

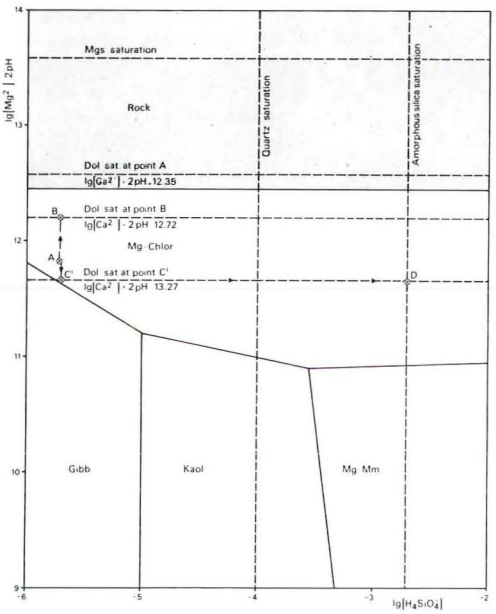

Fig. 2.16 Weathering model I', showing the stability fields of the limestone rock, Mg-chlorite (clinochlore), Mg-montmorillonite, kaolinite and gibbsite in the system $MgO - CaO - K_2O - Al_2O_3 - SiO_2 - H_2O - CO_2(g)$ at 25 °C and 1 bar pressure. $Lg[Ca^{2+}] + 2pH = 13.27$; $lg[K^+] + pH = 8.07$; $pP_{CO_2} = 3.52$.

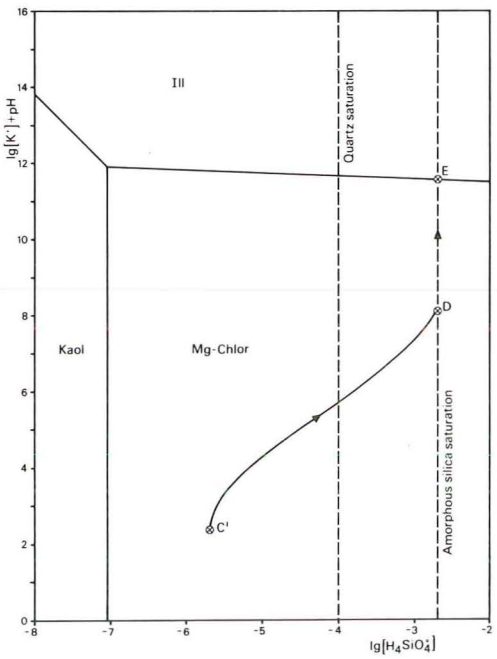

Fig. 2.17 Weathering model I', showing the stability fields of illite, Mg-chlorite (clinochlore) and kaolinite in the system $MgO - CaO - K_2O - Al_2O_3 - SiO_2 - H_2O - CO_2(g)$ at 25°C and 1 bar pressure. $Lg[Ca^{2+}] + 2pH = 13.27$; $lg[Mg^{2+}] + 2pH = 11.66$; $pP_{CO_2} = 3.52$

sidual enriched). Weathering residues containing such considerable amounts of both calcite and dolomite (56.7 and 41.8 % respectively of the total residue) were never found. Moreover, the situation in point D is unrealistic, as it would lead to an increase of the surface. Taking into account the pore volume in both limestone rock and weathering residue (assumed to be 5 and 40 % respectively), it was calculated that the surface was heightened with approximately 40 cm/year.

The composition of the weathering residue as calculated in the weathering models III and IV show fair agreement with the "dolomitic sands" as they occur between Itri and Sperlonga and in a minor extent in the main research area (e.g. profile Sp/183).

2.4 Water chemistry.

During the summer of 1975 and in the winter of 1976 a number of water samples were collected. The samples can roughly be divided into three groups: samples from limestone and dolomite springs, samples from weathering zones of limestone and dolomite and samples from colluvium derived from limestone. In the latter two cases samples were collected by means of porous water samplers (Wood, 1973). Samples were also collected from rivers draining limestone basins. A few samples which were collected previously, main-

ly during the summers of 1971 and 1974, are furthermore taken into account. The water sampling points are indicated in fig. 2.18.

If possible, a soil sample was taken from each sampling point to investigate its mineralogical composition for comparison with the composition of the sampled waters.

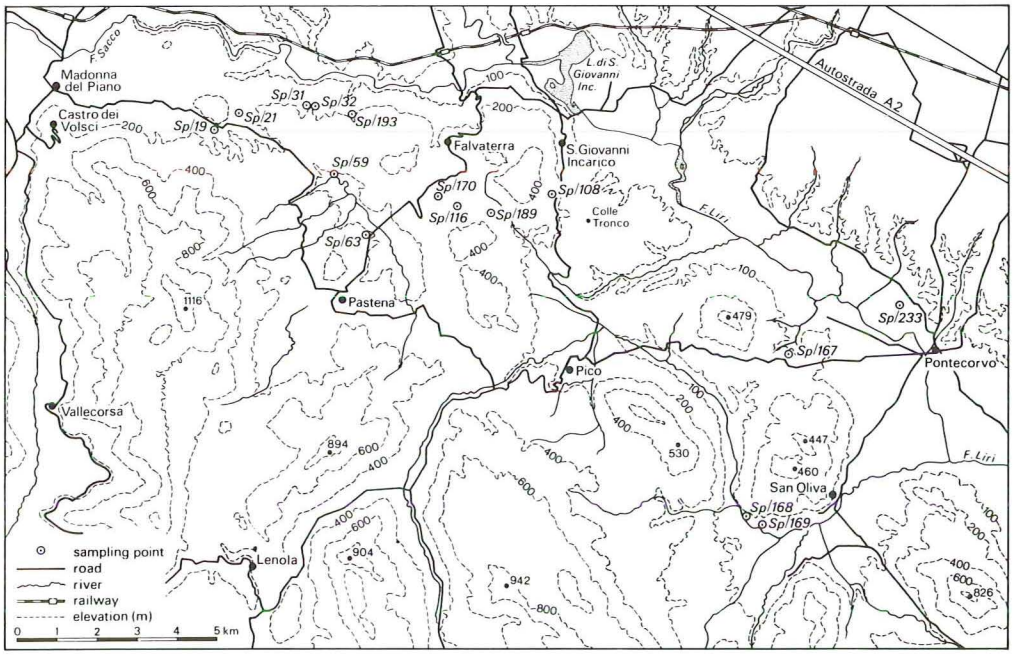

Fig. 2.18 Location of the water sampling points.

2.4.1 Composition of the water samples.

In all samples the following components were determined: Ca, Mg, K, Na, NH_4, Fe_t, Al_t, H_4SiO_4, Cl, SO_4, NO_3, HCO_3, pH and occasionally Mn and orthophosphate. Alkalinity and pH of the samples taken during the summer of 1975 and the winter of 1976 were determined in the field directly after sampling. The results of the analyses, which are described in appendix 3, are given in appendix 5.

Table 2.9 shows the correlation coefficients according to Pearson between a number of species in the water samples. The coefficients were calculated both according Pearson's Product Moment Correlation Test and Spearman's Rank Correlation Test. In general, the Pearson test gave more satisfactory results than the Spearman test. This was mainly due to the distribution free character of the Spearman test, with as result that slight (non-systematic) differences between variables created large differences in the rank numbers. Therefore the results of the Pearson test will be used.

Karstic springs.

The main cations in the spring waters (samples Sp/19, Sp/32, Sp/168 and Sp/193) are Ca, Mg and Na. Ca is the dominant ion and varies from 1.1 mmol/l in sample Sp/168a to 3.5 mmol/l in sample Sp/19b. In the former sample, however, precipitation of calcium carbonate may have taken place as also the HCO_3-content has dropped sharply with respect to the other samples.

Table 2.9 Correlation coefficients between a number of species in the water samples according to Pearson's Product Moment Correlation Test (α= level of significance = 0.10).

Relation	Sp/32	Sp/31	Sp/19	Sp/168	Sp/189	Sp/59	Sp/116	Sp/169
K-Na	0.66	-0.36	0.84	0.16	0.83	-0.98	0.05	0.89
Ca-Mg	0.82	0.75	0.08	0.22	0.99	1.00	0.92	0.91
Na-Cl	0.83	0.95	0.97	0.67	0.99	1.00	0.81	0.83
K-Si	0.46	-0.39	0.82	0.30	0.83	0.91	-0.32	0.55
Mg-Si	-0.56	-0.37	0.01	0.22	0.50	0.12	0.17	0.94
K-Mg	-0.86	0.24	0.44	0.95	0.84	0.50	-0.03	0.61
Si-Al	-	0.95	0.13	-0.64	0.33	0.73	-0.90	0.42
Mg-Al	-	-0.37	0.38	0.22	0.81	-0.20	-0.03	0.57
K-Al	-	-0.10	-0.07	0.31	0.49	0.62	0.45	0.96
Ca-HCO_3	0.99	-0.54	1.00	0.89	0.97	0.98	-0.06	-0.00
Mg-HCO_3	0.83	0.01	0.07	0.64	0.96	0.96	0.27	0.28
Fe-SO_4	-	0.42	-	-	0.92	-	0.82	-
HCO_3-Cl	-0.06	0.35	0.96	0.60	0.98	-0.53	-0.43	0.92
Cl-SO_4	-0.24	0.96	-0.70	0.02	1.00	-0.87	0.36	-0.86

Note: underlined values indicate significant correlation.

The Ca-concentration, like the concentration of the other main components, is rather uniform in the samples Sp/32 and Sp/168. On the contrary the solute concentration levels in sample series Sp/19 deviate strongly. Winter samples of these series are more dilute than the summer samples. Sample Sp/19c was taken shortly after heavy rains, while sample Sp/19d was collected approximately 2 weeks later. The rapid fluctuation of these samples reflects a rapid response to rain and indicates short residence times of the water in the limestone.

These short residence times are due to the geological structure of the Monte Lepini-Ausoni-Aurunci mountain chain. The general dip is approximately northeast-southwest, causing a long flow of the groundwater through the limestone in that direction and short flows in the opposite direction (Boni, 1975), in which zone also the area under survey is situated.

Calculations on the water balance of the Liri-Garigliano drainage basin by Portegies Zwart & Spaargaren (1973) showed that the discharge of the tributaries of the Sacco and Liri rivers from the south side was less than the calculated ones, while the discharge of the northern tributaries exceeds the calculated ones. This indicates that most probably the bulk of the precipitation is drained through the zone of long flow mentioned above and only a small amount through the short flow zone. This will most likely also result in short residence times of the water in the limestone.

As is shown in table 2.9, no or little correlation could be found between Ca and Mg in the samples Sp/19 and Sp/168 (r_p=0.08 and 0.22 respectively). The most plausible explanation for this is mixing of groundwater bodies.

Sample Sp/32 shows a significant positive correlation (r_p=0.82) between Ca and Mg. This spring is issuing from a dolomite area, which also explains the relative high Mg-concentration with respect to the other samples. Ca/Mg molar ratios in these samples vary from 1.87 to 1.99 and are much lower than in the other samples.

Besides Ca and Mg, Na is an important cation in these samples. In most cases a significant positive correlation exists between Na and Cl (see table 2.9) (r_p varying from 1.00 to 0.83). More over, Cl/Na molar ratios are rather constant and in the same order as Cl/Na molar ratios in rain- and seawater (samples Sp/233 and Sp/238 respectively, see appendix 5.1). Na and Cl content therefore is believed to be governed by the input through rainwater and by atmospheric supply as dry fall-out. Na follows the same line as the other ions in the samples, rather constant in samples Sp/32 and Sp/168 and highly varying (0.3 to 0.6 mmol/l) in sample Sp/19.

The main cation is HCO_3. Its occurrence is mainly a function of the electon neutrality of the solution and therefore closely linked to the concentration of Ca and Mg in the samples. This is illustrated by high positive correlation coefficients between HCO_3 and (Ca + Mg) ($r_p = 0.99$, 1.00 and 1.00 for the samples Sp/32, Sp/19 and Sp/168 respectively), indicating CO_2 as driving force for the weathering reactions.

The other anions, NO_3, Cl and SO_4, can be regarded as "pollutants" (Jacobson & Langmuir, 1970). As already mentioned, Cl can be traced back to the input by rainwater. The sources of NO_3 may be twofold. In the first place animal wastes and fertizers are responsible for the NO_3 in the waters. Secondly, oxidation of NH_4 from the rain contributes to the NO_3 content in the waters.

The origin of SO_4 is somewhat obscure. It is not likely that oxidation of pyrite from the limestone is responsible for the amount of SO_4 in the spring waters. The molar ratio in the analysed limestone (sample Sp/68a, see 2.2.2) of Ca and S expressed as SO_4 is approximately 1400 to 1. As these molar ratios in the spring waters are much lower, only a small amount of SO_4 in these waters has to be attributed to the oxidation of pyrite. On the other hand, no significant correlation between Cl and SO_4 could be detected either, as would be expected if SO_4 is derived from rainwater ($r_p = -0.70$, -0.24 and 0.02 for the samples Sp/19, Sp/32 and Sp/168 respectively). However, supply through rainwater cannot be excluded as it carries an amount of SO_4, which is approximately two times smaller than the average amount in the spring waters (31 versus 53 mol/l). The industries near Frosinone and Gaeta (the latter being a petrochemical industry) may account for the SO_4 content in the rainwater.

A third possible source of SO_4 are the Miocene shales. As mentioned in 1.6.1, the limestone mountains are underlain by Miocene shales. Water in contact with these shales has been sampled in a quarry near Pontecorvo (sample Sp/167, see fig. 2.18). This water carries a relatively high amount of SO_4 with respect to the samples from the limestone (up to approximately 130 times higher). As most of the springs issue at the overthrust plane of the limestone and the Miocene shales, it is very likely that these shales will influence the composition of the spring waters.

Mixing with juvenile water cannot be excluded as well. It is believed that at least a number of large springs issuing from the southwestern part of the Monte Lepini-Ausoni range into the Pontinia plain carry a relatively high amount of juvenile water (Boni, personal communication) (see also section 2.6).

H_4SiO_4 content varies from 56 to 187 μmol/l. Samples Sp/168 show the lowest content, while samples Sp/32 show the highest content. H_4SiO_4 content in the latter samples is rather constant and varies only from 164 to 181 μmol/l. As the H_4SiO_4 concentration in the rainwater is rather low (1 to 2 μmol/l), H_4SiO_4 is derived from the weathering of silicate minerals in soils and rocks.

The relatively high H_4SiO_4 content in the samples Sp/32 and Sp/19 with respect to the samples Sp/168 are probably due to the presence of strongly weathered Pliocene/old Quaternary deposits. Samples Sp/21 (see appendix 5.1) show a much higher H_4SiO_4 content (up to 236 μmol/l) than the spring waters (see also chapter 3). These sandstones lack completely in the surroundings of sampling point Sp/168.

Weathering zones of the limestone and dolomite.

From two sampling points water was collected from the weatherings zones of limestone and dolomite (samples Sp/189 and Sp/31 respectively). The samples taken from the weathering zone of dolomite resemble very much those of the spring issuing from dolomite (Sp/32). Ca/Mg molar ratios are somewhat higher (2.16 to 2.22), indicating a relatively smaller amount of Mg in these samples. Though not enough to be significant, a positive correlation exists between Ca and Mg ($r_p = 0.75$), as could be expected in samples drawn from dolomite.

A high positive correlation exists in the samples Sp/31 between Si and Al ($r_p = 0.95$). This might indicate that H_4SiO_4 and Al_t content is controlled by alumino-silicate minerals. This will be discussed in 2.5.4.

In contrast with the samples of the karstic springs, a high positive correlation between Cl and SO_4 was found in the samples Sp/31 and Sp/189 (r_p = 0.96 and 1.00 respectively). This indicates that SO_4 in these samples most probably is derived from rainwater (see also discussion above).

The samples Sp/189 show a decrease in time of the concentration of the main ions. Precipitation, leading to the formation of minerals within the weathering zone is thought to be the cause of this. In crease in time of Cl/Na molar ratios from 1.31 to 1.60 indicates that Na is preferently consumed with respect to Cl, probably due to binding at the adsorption complex. Furthermore, the decrease of Ca and HCO_3 and the increase of pH points to loss of CO_2(g) and consequently to precipitation of calcite.

Colluvial material derived from limestone.

The water collected from the colluvial soils shows a high variation in composition. Some are clearly influenced by neighbouring springs, e.g. samples Sp/169, which shows a relative high content of Ca, Mg and HCO_3. Ca/Mg molar ratios in sample Sp/168 are only slightly lower than those of sample Sp/169 (averages are 3.80 and 4.22 respectively).

In most of these soils Ca and Mg concentration is controlled by limestone gravel in the soils. This is illustrated by significant positive correlation coefficients between Ca and Mg in the samples Sp/59, Sp/116 and Sp/169 (r_p = 1.00, 0.92 and 0.91 respectively). Mean Cl/Na molar ratios are somewhat lower than in the springs and in the weathering zones (1.02 versus 1.17 and 1.34 respectively), indicating release of sodium by weathering of Na-bearing minerals.

H_4SiO_4 content in the colluvial soils varies from 23 μmol/l in sample 116a to 192 μmol/l in sample Sp/169b. The former content may not be illustrative for the high variation in H_4SiO_4 content of the samples. This was the only sample which to preserve it during field work, was frozen. The effect of freezing on the H_4SiO_4 analytical determination, however, is not yet fully understood. Burton et al. (1970) found that after freezing of the sample the silicon content was at its prefreezing level after about 3 hours. On the other hand for acidified samples investigations in our laboratory showed that the initial aqueous silica content was reached after about 6 weeks.

Most of the samples show a relatively high amount of NO_3. Animal wastes and ferti - lizers must be held responsible for this as the sampling points were situated in cultivated areas.

2.4.2 Mineralogical implications.

Ion activities in the water samples have been calculated according the computer program SOLMNEQ (Kharaka & Barnes, 1973). The results are given in appendix 5.2.

In order to establish the (in)stability conditions for the relevant minerals in the weathering environment, their Ion Activity Products (IAP) were calculated. Also for a number of minerals the Saturation Index (SI) of the solution was computed. The SI is defined as the logarithm of the fraction of the Ion Activity Product (IAP) and the Equilibrium Constant (K). If this value equals zero, it is said that the solution in saturated with respect to the mineral under view. Positive values indicate supersaturation, while undersaturation is represented by negative values (see appendix 6.1)

The following mineral groups were checked: feldspars and feldspatoids, a number of the most important clay minerals, several micas, a number of carbonates and the various SiO_2 species. A full list of minerals, their IAP values and the lg $K_{15° C}$ is summarized in appendix 5.2.

Due to analytical limitations, saturation is seldom represented with a SI of zero. Therefore often a tolorance is brought into account. Langmuir (1971) for instance assumes an uncertainty for saturation indices of calcite and dolomite, based on a possible error of 0.05 pH units, or 0.1 SI unit. As, however, the SI is a logarithmic value, the lower boundary of uncertainty is not of equal distance from zero as the upper one. Therefore it is better to recalculate the SI to a value in a linear scale. This can be done by using the equation ΔG_{diff} = RT ln SI (Kharaka & Barnes, 1973). This leads to

a linear value (ΔG_{diff}), which expresses the saturation state of a solution for a certain reaction in kcal/mole. By calculating the Gibbs free energy of reaction and introducing the uncertainty limits of the thermodynamic data for the species involved, tolorance limits for reactions are computed on a linear scale. These can then be compared with the ΔG_{diff} calculated from the SI mentioned before. If the ΔG_{diff} is within the tolerance limits of the reaction ($\Delta G_{tol.r.}$), saturation of the solution for that reaction is assumed.

The tolerance limits were calculated as follows. The Gibbs free energy of reaction is computed from the individual Gibbs free energy of formation (ΔG_f) of the reactant species. These individual Gibbs free energies of formation are mostly given in the literature with their confidence limits. By assuming that the variables are normally distributed and stochastically independant, which holds for most of the species involved, the variance of the sum of the variables can be calculated from the sum of the variances of these variables (van der Grinten & Lenoir, 1973).

As the relations $\Delta G^\circ_r = -RT \ln K_{25°C}$ and $\Delta G_r = -RT \ln K(T)$ are also applicable to the tolerance limits of the Gibbs free energy of reaction, it is possible to compute these limits for the $\Delta G_r(15°C)$ by dividing both relations on each other. This then gives the relation

$$\Delta G_r = \Delta G^\circ_r \frac{T \ln K(T)}{T \ln K_{25°C}} \quad \text{or} \quad \Delta G_{tol.r.} = \Delta G^\circ_{tol.r.} \frac{T \ln K(T)}{T \ln K_{25°C}}$$

The results of these calculations are given in appendix 6.2 and summarized in table 2.10.

All samples appear to be supersaturated with respect to kaolinite, up to approximately 8 kcal/mole, whereas most of the samples are supersaturated with respect to illite and montmorillonite, except for sample Sp/170 a. Supersaturation also occurs frequently for Mg-chlorite (approximately 50 % of the samples).

About 60 % of the samples are supersaturated with respect to gibbsite (cc). The maximum supersaturation (sample Sp/189 a) amounts to 1.62 kcal/mole, while the mean supersaturation is 0.87 kcal/mole. This slight supersaturation might indicate that the Al-content in the samples is controlled by some form of amorphous or cryptocrystaline $Al(OH)_3$ and not by a clay mineral such as kaolinite or montmorillonite, as can be derived from the high supersaturation figures for these minerals.

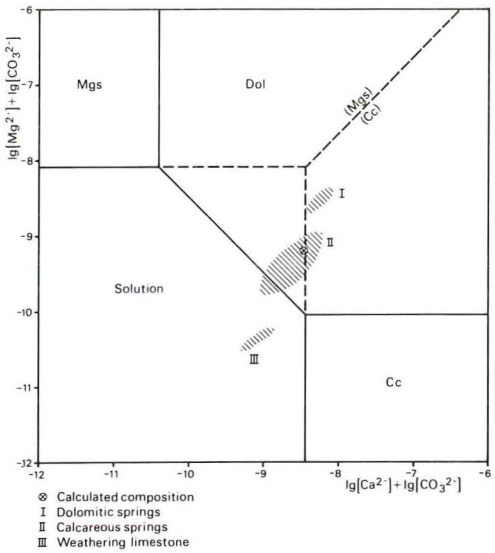

Fig. 2.19 Stability fields of calcite, dolomite and magnesite in the system MgO-CaO-H_2O-CO_2(g) at 25°C and 1 bar pressure. Dashed areas: composition of karstic waters.

As for the carbonates, most of the samples from the springs are saturated with respect to calcite (approximately 80 %), while the spring issuing from a dolomitic area (Sp/32) is also in equilibrium with dolomite (see fig. 2.19).

The samples of the weathering zone of the dolomite show saturation both for calcite and dolomite, like the samples from the spring nearby; on the other hand samples from the weathering zone of the limestone all show undersaturation for calcite and dolomite, indicating that both minerals are unstable in this environment and will be removed gradually.

This undersaturation also obtains for most of the soil water samples of the colluvial soils. Only in the samples Sp/169 saturation is reached with respect to cal-

Table 2.10 Saturation state of the water samples from limestone and dolomite, their weathering zones and colluvia.

Origin of sample		Sample number	Date of sampling	Kaol	Hall	Ill	Ms	Mm	Pyr	Mg-chlor	Bo	Gibb	Cc	Dol	Sid
SPRINGS	Limestone	Sp/ 19a	June 1975	●	◐	●	●	●	●	◐	●	◐	◐	○	
		/ 19b	August 1975	●	●	●	●	●	●	◐	●	●	◐	○	
		/ 19c	16-2-1976										◐	○	○
		/ 19d	28-2-1976	●	●	●	●	●	●	●	●	●	◐	◐	○
		Sp/168a	August 1974										○	○	○
		/168b	June 1975	●	◐	●	●	●	◐	◐	●	◐	◐	○	
		/168c	August 1975	●	◐	●	●	●	●	●	●	●	◐	◐	
		/168d	15-2-1976	●	◐	●	●	●	◐	○	●	●	○	○	○
		/168e	28-2-1976	●	◐	●	●	●	●	◐	●	◐	◐	○	○
		Sp/193a	22-2-1976	●	●	●	●	●	●	●	●	●	◐	○	○
		/193b	28-2-1976	●	●	●	●	●	●	●	●	●	◐	◐	○
	Dolomite	Sp/ 32a	July 1971										●	●	
		/ 32b	June 1975										◐	◐	
		/ 32c	August 1975	●	◐	●	●	●	●	●	●	◐	◐	◐	
		/ 32d	16-2-1976	●	◐	●	●	●	●	●	●	◐	◐	◐	○
		/ 32e	24-2-1976										◐	◐	○
		/ 32f	28-2-1976										◐	◐	○
WEATHERING ZONES	Dolomite Limestone	Sp/189a	22-2-1976	●	●	●	●	●	●	◐	●	●	○	○	○
		/189b	24-2-1976	●	●	●	●	●	●	◐	●	●	○	○	○
		/189c	27-2-1976	●	●	●	●	●	●	●	●	●	○	○	○
		/189d	29-2-1976	●	◐	●	●	●	●	◐	●	●	○	○	○
		Sp/ 31a	June 1975	●	◐	●	●	●	●	●	●	●	◐	◐	
		/ 31b	19-2-1976	●	●	●	●	●	●	●	●	●	◐	◐	○
		/ 31c	24-2-1976	●	●	●	●	●	●	●	●	●	◐	◐	○
		/ 31d	28-2-1976	●	◐	●	●	●	●	●	●	◐	◐	◐	○
COLLUVIA	Young	Sp/ 59a	July 1971	●	◐	●	●	●	◐	●	●	◐	○	○	
		/ 59b	15-2-1976	●	●	●	●	●	●	◐	●	●	○	○	○
		/ 59c	22-2-1976	●	●	●	●	●	●	●	●	●	◐	◐	◐
		/ 59d	29-2-1976										●	●	
		Sp/116a	August 1974	●	●	●	●	●	●	◐	●	●	○	○	○
		/116b	June 1975	●	●	●	●	●	●	◐	●	●	○	○	
		/116c	August 1975	●	●	●	●	●	●	○	●	●	○	○	
		/116d	19-2-1976	●	●	●	●	●	●	●	●	●	○	○	○
		/116e	29-2-1976	●	●	●	●	●	●	◐	●	●	○	○	○
	Old	Sp/169a	June 1975	●	◐	●	●	●	●	●	●	◐	◐	◐	
		/169b	August 1975	●	●	●	●	●	●	●	●	●	◐	◐	
		/169c	19-2-1976	●	◐	●	●	●	◐	◐	◐	○	◐	○	◐
		/169d	29-2-1976	●	◐	●	●	●	◐	◐	●	○	◐	○	○
		Sp/170a	19-2-1976	●	○	○	○	◐	◐	○	◐	○	○	○	○
		/170b	27-2-1976	●	◐	●	●	●	●	○	●	◐	○	○	○

○: undersaturated ◐: saturated ●: supersaturated

cite and in two cases for dolomite. This once more indicates the influence on this sampling point by the spring nearby (Sp/168) as already mentioned in 2.4.1.

Stability phase diagrams (activity diagrams) for the system $MgO - Al_2O_3 - SiO_2 - H_2O$ for 15 °C (288.15 °K) and 1 bar pressure were constructed (fig. 2.20 to 2.22). For the calculation method of the equilibrium equations necessary to construct these diagrams is referred to appendix 7.

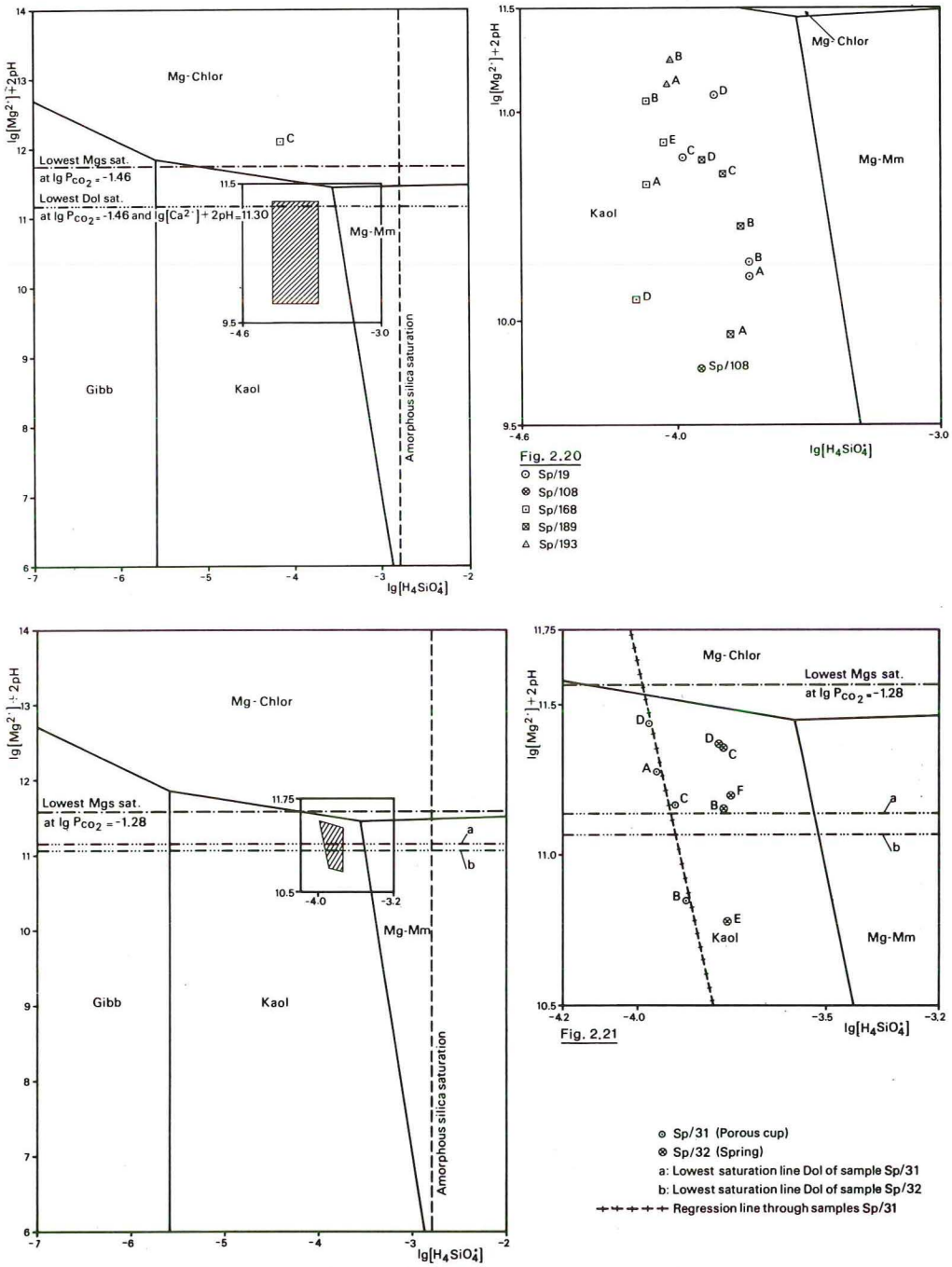

Fig. 2.20 and 2.21 Stability fields of Mg-chlorite (clinochlore). Mg-montmorillonite, kaolinite and gibbsite in the system $MgO - Al_2O_3 - SiO_2 - H_2O$ at 15° C and 1 bar pressure. Indicated are the lg Mg^{2+} + 2pH and lg $H_4SiO_4^0$ plots of the samples of the springs and weathering zone of the limestone (fig. 2.20) and of the dolomite (fig. 2.21).

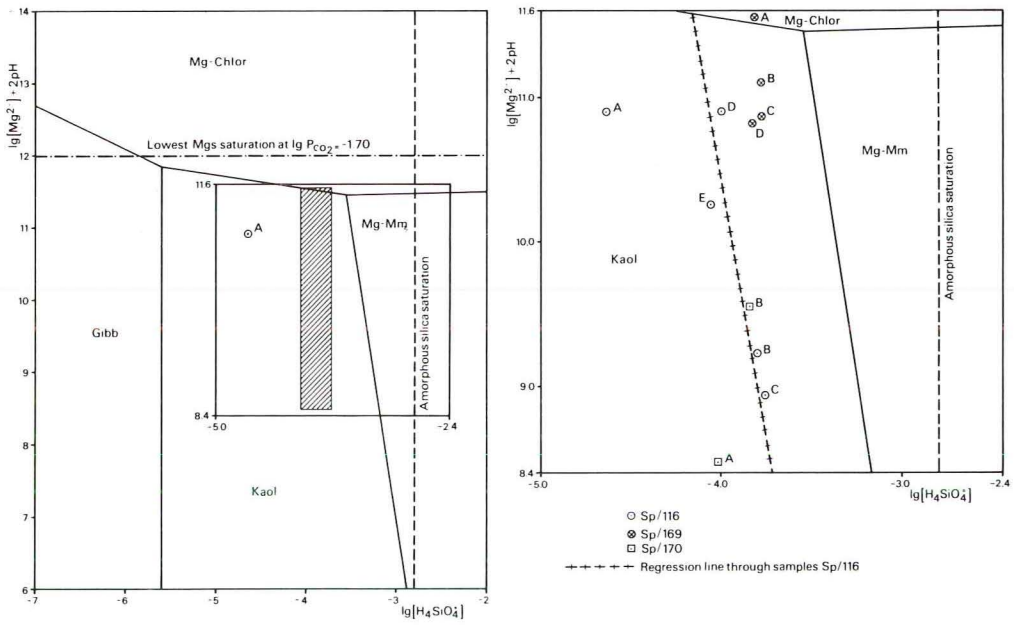

Fig. 2.22 Stability fields of Mg-chlorite (clinochlore), Mg-montmorillonite, kaolinite and gibbsite in the system $MgO - Al_2O_3 - SiO_2 - H_2O$ at 15 °C and 1 bar pressure. Indicated are the lg Mg^{2+} + 2pH and lg $H_4SiO_4^0$ plots of the water samples from the colluvial soils and rivers draining karst basins.

Plotting of the composition of the water samples in these diagrams showed at first glance that kaolinite can be expected to be the stable phase, as nearly all samples are situated in the kaolinite stability field. However, in several samples a negative correlation exists between lg[Mg^{2+}]+ 2pH and lg[$H_4SiO_4^0$]. Moreover, in three cases, viz. in the samples from the weathering zones and in sample Sp/116, this negative correlation is significant (r_p = -0.95, -0.94 and -0.90 respectively). The regression lines through these groups of samples are parallel to the kaolinite-montmorillonite phase boundary. This might indicate that the [$H_4SiO_4^0$] in the samples is controlled by the kaolinite- montmorillonite phase relations, in which the montmorillonite then must have a slightly different Gibbs free energy of formation than used in the computer program SOLMNEQ. It is therefore very likely that besides kaolinite also montmorillonite may form a stable phase.

2.5 Mineralogy of the soils on limestone and dolomite.

When studying the soils on limestone and dolomite, use was made of road cuts, quarries and incisions of gullies. During fieldwork some fresh road cuts were available, e.g. alongside the road Pastena - Falvaterra and soils were studied shortly after their preparation. A number of profile pits were dug as well and augerings down to the underlying rock were made. Samples were taken from soils, weathering - or contact zones and, if possible, from freshly cut rock. A number of soil profiles were described according the FAO Guidelines for Soil Profile Description (FAO, 1977).

Most of the profiles studied are located in the main research area. However, also in other parts of the surrounding area soils were studied and samples taken. Special attention has been paid to the area between Itri and Sperlonga, south of the main research area, and the area east of Pico. In both areas large occurrences of dolomite can be

found and here especially soils on dolomite were studied.

The soils on limestone and on dolomite can roughly be divided into four main groups: deep "in situ" soils, soils in fissures in limestone or dolomite, shallow soils directly on limestone or dolomite (lithosols and rendzinas) and soils developed in colluvial material derived from limestone or dolomite (or both). In the following pages little attention will be paid to the shallow soils, as it was often not clear if these soils had been developed directly from the limestone (monocyclic) or in remnants of older soils (polycyclic).

Soil samples were investigated by means of X-ray diffraction analyses of the clay fraction, heavy mineral slides of the fraction 50 - 500 μm. and thin section analyses of undisturbed soil aggregates. Moreover, physico-chemical and chemical analyses were

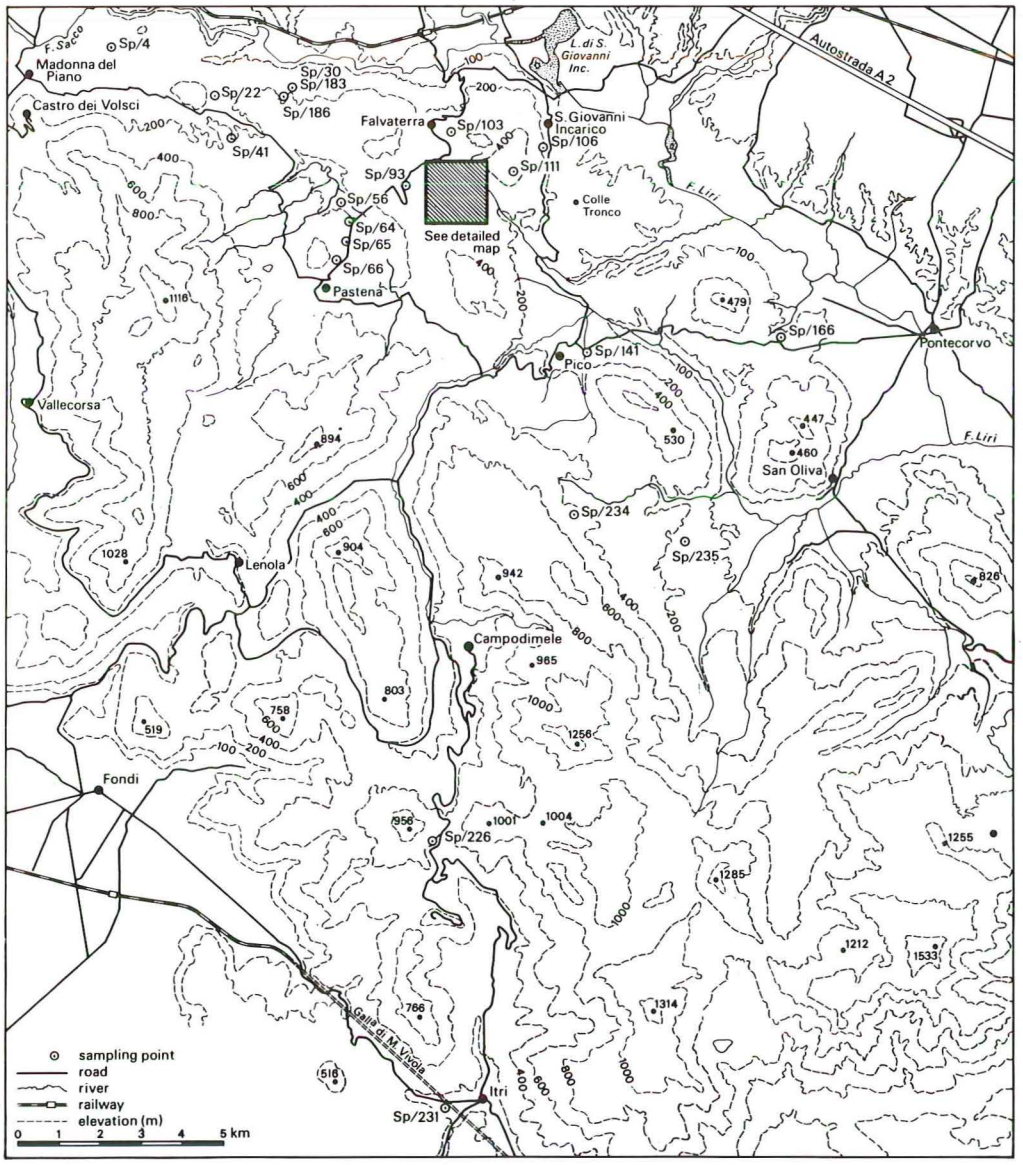

Fig. 2.23 Location of the soil profiles and of isolated sampling points.

Fig. 2.24 Location of the soil profiles and water sampling points at "La Fossa" and "Il Vallangero".

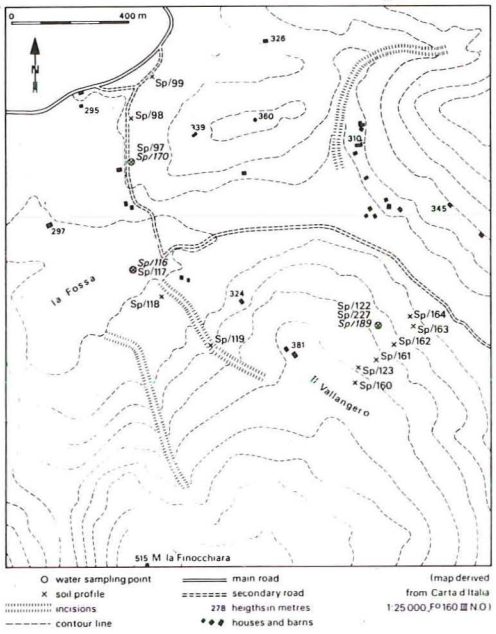

carried out on the fine earth fraction and the clay fraction (<2 μm) of samples from some soil profiles. This was mainly done in order to carry out normative mineralogical calculations to characterize the mineralogy of the soils somewhat more quantitatively and to get an insight into the mineralogical changes within the soil.

The location of the soil profiles and of isolated sampling points is indicated in fig. 2.23 and 2.24.

2.5.1 The deep "in situ" soils, with special attention to the soils at "Il Vallangero".

Deep, reddish brown, clayey soils on limestone are found locally in the eastern part of the main research area and northwest of the "Piana Madonna delle Macchie", the larger polje near Pastena. They occur on steep slopes, e.g. near Monte la Finocchiara and Monte Vaglia, as well as in gently undulating terrains, e.g. west of the "Grotte di Pastena". In association with lithosols they are found southwest of Pico (fig. 2.25) and south and south-

Fig. 2.25 Deep reddish brown soils, west of Monte Pastenese on a slope of approx. 28 %.

west of "Piana di San Andrea", the smaller polje near Pastena. The soils in the Pico/ Piana di San Andrea areas are somewhat more eroded and less deep than the soils in the other areas.

At "Il Vallangero", the north-facing slope of Monte la Finocchiara, the deep soils have been studied intensively. The area is strongly influenced by gully erosion and incisions up to 4 m deep onto the limestone occur (see fig. 2.4). This gully erosion started during World War II after the clearing of the forest (local information).

Two soil profiles were described, one being a chromic luvisol (profile Sp/123) with a depth of 3 m at an altitude of approximately 370 m; the other being an eutric nitosol (profile Sp/122), halfway up slope at an altitude of approximately 325 m (see appendix 2). Limestone was not exposed in the latter profile. But at a location nearby soil water was sampled from the weathering zone of the limestone (Sp/189) and also soil samples were taken of the horizon from which water was sampled and of decalcified soil directly above (Sp/227a and b, respectively).

Moreover from four spots in incisions of gullies soil samples were collected for heavy mineral analyses. These samples (Sp/160 - 163), at each spot four, were taken at certain depths, viz. from 10-20 cm, 50-60 cm, 100-120 cm and 150-170 cm. In addition a profile (Sp/164) at the bottom of the slope was described in which clearly admixture of volcanic material was observed. A sample was taken from the tuff layer in this profile in order to compare the heavy mineral association with those of the other samples.

The location of the profiles and the sampling points is indicated in a schematic section along the slope of "Il Vallangero" (fig. 2.26).

The profiles Sp/122 (eutric nitosol), Sp/123 (chromic luvisol) and samples Sp/227a and b (belonging to water sampling point Sp/189): their mineralogy.

At first sight these soils look rather homogenous. Close examination however, showed at various depths admixture of volcanic material in variable proportions. In profile Sp/122 volcanic material was observed down to a depth of 80 cm, while in profile Sp/123 volcanic minerals were found down to a depth of 220 cm (see also 2.1.1 and appendix 2). No volcanic minerals have been found in the samples Sp/227 a and b.

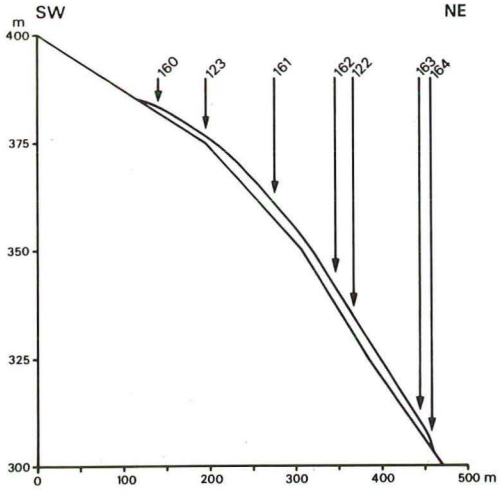

Fig. 2.26 Schematic section along the slope at "Il Vallangero" showing the position of the described soil profiles (Sp/122, Sp/123 and Sp/164) and the sampling points Sp/160-163.

Samples of the profiles were treated for physico-chemical and chemical analyses and the clay fraction (<2 μm) was separated for X-ray diffraction analyses.

Thin sections were prepared from the profiles Sp/122 and Sp/123.

X-ray diffraction analyses of the clay fraction of all the samples show that this fraction can be characterized as a mixture of kaolinite (+halloysite) and and illite Occasionally montmorillonite and 14 Å minerals (chlorite/vermiculite) occur in very small proportions as accessory clay minerals. The dominant free iron species is haematite, whereas quartz content varies from <1 to 4-6 % (see table 2.11).

Quantitative X-ray diffraction analyses were carried out on the samples of profile Sp/122, which were pretreated with Na-citrate and Na-dithionite (Holmgren, 1967) in order to remove interfering iron compounds. The results, shown as intensity percentages (I %) are given in table 2.12.

Table 2.11 Semi-quantitative X-ray diffraction analyses of the fraction<2 μm of the profiles Sp/122 (eutric nitosol) and Sp/123 (chromic luvisol) and of the fraction<1 μm of the samples Sp/227a and b of the water sampling point Sp/189.

		Horizon c.q. sample number	Depth of sample (cm)	Sm	14 Å	10 Å (Ill)	Kaol	Qtz (%)	Hm
Eutric Nitosol	Profile Sp/122	Ah	0-5	tr	-	++	++[1]	4-6	(x)
		E	5-15	tr	-	++	++(+)[1]	4-6	(x)
		Bt1	20-35	tr	-	++	+++[1]	4-6	(x)
		Bt2	50-70	tr	-	+(+)	+++[1]	1-3	(x)
		2Bt	100-120	tr	-	+(+)	++(+)[1]	1-3	(x)
		2Bt(g)	180-210	tr	-	+(+)	++(+)[1]	1-3	(x)
			240-260	tr	-	+(+)	++(+)[1]	1-3	(x)
			290-300	tr	-	+	+(+)[1]	1-3	(x)
		Sp/227a		tr	?	+(+)	++[2]	1	-
		Sp/227b		(+)	tr	++	++[2]	ca.1	-
Chromic Luvisol	Profile Sp/123	Ah	5-25	-	-	++	++[3]	ca.1	(x)
		Bt	40-60	-	-	++	++[3]	ca.1	(x)
			80-100	-	-	++(+)	++[3]	ca.1	(x)
		2B	130-150	-	-	++	++[3]	1-3	x
			180-200	-	-	++	++[3]	1-3	(x)
		3B	230-250	-	-	++(+)	++(+)[3]	ca.1	(x)
			270-290	-	tr	++(+)	++[3]	1	(x)
		3Bk	300-305	-	-	++	++[3]	1	(x)

[1] 7 Å = kaolinite [2] 7 Å = kaolinite + metahalloysite [3] 7 Å = poorly crystalline kaolinite or halloysite

Table 2.12 Quantitative (calculated) X-ray diffraction analyses of the fractions<2μm of profile Sp/122 (eutric nitosol) and samples Sp/227a and b in intensity percentages (I %).

		Horizon c.q. sample nr.	Depth of sample (cm)	Sm (h.ch.)	Sm (l.ch.)	Verm	Chlor	Ill	Kaol	M'hall	Hall
Eutric Nitosol	Profile Sp/122	Ah	0-5	3	tr	2	4	43[1]	48	-	-
		E	5-15	5	tr	tr	5	38[1]	51	-	-
		Bt1	20-35	5	tr	4	5	31[1]	55	-	-
		Bt2	50-70	-	-	-	-	33[2]	67[4]	-	-
		2Bt	100-120	-	-	-	4	33[3]	63	-	-
		2Bt(g)	180-210	-	2	-	4	41[3]	46	7	-
			240-260	-	-	-	4	28	36	32	-
			290-300	-	3	-	5	33	46	13	x[5]
		Sp/227a		6	2	4	-	36	52	x[5]	x[5]
		Sp/227b		4	3	7	-	37	49	x[5]	x[5]

[1] Ill = illite + muscovite [2] Illite poorly crystalline [3] 12 I% swelling illite included [4] Kaolinite poorly crystalline, b-axis disordered [5] Present but quantaty not determined

Some samples contain interstratifications of chlorite-swelling chlorite and in one sample the presence of maghemite (γFe_2O_3) was established despite the treatment with Na-citrate and Na-dithionite.

The results of the chemical analyses carried out on the fine earth fraction and the clay fraction<2 μm are given in appendix 2. These chemical analyses are converted into a normative mineralogical composition of the profiles. The procedure for the "norm" calculations applied to soils has been described by van der Plas & van Schuylenborgh (1970). A modification was introduced by using a Mg-containing illite (Helgeson, 1969), as it appeared that by using this illite the normative mineralogical composition was much closer

Table 2.13 Normative mineralogical composition of profile Sp/122 (eutric nitosol), given in weight percentages.

Fine earth fraction (<2 mm)

Horizon	Depth of sample (cm)	Q	Sm	Ill	Kaol	Hm	Plag	V.G.[1]	Mica[2]	Ru	Misc[3]	W
Ah	0-5	20	6	12	32	9	6	3	10	1.3	1	+3
E	5-15	18	5	12	36	10	5	1	11	1.3	1	+3
Bt1	20-35	13	5	12	44	10	6	4	4	1.2	1	+3
Bt2	50-70	5	6	10	61	10	2	-	4	1.0	1	+3
2Bt	100-120	8	4	8	60	10	2	-	6	1.1	1	+2
2Bt(g)	180-210	10	6	12	53	10	2	-	5	1.0	1	+2
	240-260	10	4	10	57	10	2	-	5	1.1	1	+2
	290-300	11	5	17	49	10	2	-	4	1.0	1	+2

Clay fraction (<2 μm)

Horizon	Depth of sample (cm)	Sm	Ill	Kaol	Q	Gibb	Hm	Ru	Misc[4]	W
Ah	0-5	10	20	55	1	-	11	1.2	2	+3
E	5-15	9	20	56	1	-	11	1.2	2	+3
Bt1	20-35	7	17	61	1	-	11	1.1	2	+2
Bt2	50-70	7	11	69	-	1	10	1.0	1	+3
2Bt	100-120	5	10	72	1	-	10	1.0	1	+2
2Bt(g)	180-210	7	16	64	1	-	10	0.9	1	+2
	240-260	6	13	68	1	-	10	1.0	1	+2
	290-300	7	20	59	2	-	10	0.9	1	+2

[1] V.G. = volcanic glass ($KAlSi_3O_8$) [2] Mica = muscovite + biotite [3] Misc = strengite + apatite [4] Misc = strengite + apatite + albite

Table 2.14 Normative mineralogical composition of the samples Sp/227a and b, given in weight percentages.

Fine earth fraction (< 2 mm)

Sample number	Cc	Dol	Sm + Chlor	Ill	Kaol	Q	Hm	Ms	Ru	Misc	W
Sp/227a	-	-	5	24	56	1.0	10	-	0.7	3[1]	+4
Sp/227b	69	2	2	7	15	0.3	3	0.3	0.7	1[2]	+1

Clay fraction (<2 μm)

Sample number	Sm + Chlor	Ill	Kaol	Q	Hm	Ru	Misc	W
Sp/227a	5	24	57	0.9	10	0.6	2[3]	+4
Sp/227b	8	25	54	0.3	11	0.8	1[4]	+4

[1] Misc = albite + almandine + sillimanite + strengite + apatite [2] Misc.= almandine + sillimanite + strengite [3] Misc = albite + strengite [4] Misc = calcite + strengite

to the mineralogical composition obtained by X-ray diffraction analyses rather than by using muscovite as is done by van der Plas and van Schuylenborgh. A list of "norm" minerals used is given in appendix 8.

The normative mineralogical composition of the profiles Sp/122 and Sp/123 and of the samples Sp/227a and b, which can be regarded as the lower part of profile Sp/122, is given in tables 2.13, 2.14 and 2.15.

On first thought, if tables 2.12 and 2.13 (fraction<2 μm) are compared with each other, considerable differences, especially in the amount of illite can be noted. The cause of this might be fourfold. Firstly, the normative mineralogical composition is given in weight percentages, while in table 2.12 intensity percentages are shown. Secondly, the normative mineralogical composition is calculated for the total clay fraction, whereas in the calculated X-ray diffraction analyses only the alumino-silicate minerals are con-

Table 2.15 Normative mineralogical composition of profile Sp/123 (chromic luvisol), given in weight percentages.

Fine earth fraction (<2 mm)

Horizon	Depth of sample (cm)	Q	Plag	Mica[1]	Sm+Verm[2]	Ill	Kaol	Go/Hm	Cc	Dol	Ru	Misc[3]	W	CO_2
Ah	5-25	6	4	6	5	14	53	11	-	-	1.1	0.4	+1	-
Bt	40-60	4	2	4	5	14	58	11	-	-	1.1	0.5	+2	-
	80-100	5	3	6	4	14	55	11	-	-	1.1	0.6	+1	-
2B	130-150	17	3	10	3	12	42	11	-	-	0.7	0.8	+1	-
	180-200	13	3	7	4	12	49	11	-	-	0.7	0.7	+1	-
3B	230-250	6	3	4	5	16	55	10	-	-	1.0	0.4	+2	-
	270-290	3	1	1	7	21	56	10	-	-	0.9	0.5	+3	-
3Bk	300-305	1	3	0.2	1	2	6	1	85	-	0.2	0.2	+1	-
R		1	1	tr	tr	1	1	0.3	94	2	tr	tr	tr	-0.1

Clay fraction (<2 μm)

Horizon	Depth of sample (cm)	Sm	Ill	Kaol	Q	Hm	Cc	Ru	Misc[4]	W
Ah	5-25	6	17	63	2	10	-	1.0	1	+2
Bt	40-60	6	16	64	2	10	-	1.0	1	+3
	80-100	5	17	64	2	10	-	1.0	1	+3
2B	130-150	6	19	58	3	12	-	1.2	1	+2
	180-200	5	18	61	3	11	-	1.1	1	+2
3B	230-250	6	18	62	3	9	-	0.9	1	+2
	270-290	7	22	57	2	10	-	0.9	1	+3
3Bk	300-305	3	12	29	2	5	48	0.5	1	+2

[1] Mica = biotite + muscovite [2] Sm + Verm : sample of 3Bk includes 0.7 % vermiculite [3] Misc = apatite + strengite + pyrolusite [4] Misc = apatite + strengite

sidered. Thirdly, the actual chemical composition of the minerals may differ from the normative chemical composition, which is idealized.

A fourth factor influencing the difference is found in the difficulty of introducing both smectite and chlorite or vermiculite in the normative mineralogical composition. By this, free silica and kaolinite content may be too low and smectite content too high in table 2.13.

However, the changes in mineralogical composition which can be postulated from both tables show the same trend. From bottom to top of the profile an increase of smectite (in reality an increase of smectite + chlorite + vermiculite) can be noted, an increase followed by a decrease of illite and the reverse for kaolinite.

Not indicated in the normative mineralogical composition but clearly evident from the X-ray diffraction analyses is the presence of (partly dehydrated) halloysite and metahalloysite in the last three samples of this profile. Also the samples Sp/227 a and b contain metahalloysite (see table 2.11 and 2.12). As the chemical composition of halloysite, metahalloysite and kaolinite in general is the same except for their crystal water content (Weaver & Pollard, 1973), it is not possible to indicate this in the normative mineralogical composition. The presence of halloysite and metahalloysite can only be suspected by the high surplus of water.

The sampled waters are highly supersaturated with respect to kaolinite, but only slightly as to halloysite (see appendix 6 and table 2.10). This and the obvious shift in profile Sp/122 (table 2.12) from partly dehydrated halloysite via metahalloysite to kaolinite might indicate that in the weathering process of limestone near the bottom of the profile at first a halloysitic precipitate is formed. Dehydration and aging of the precipitate leads to the formation of metahalloysite. From thermodynamical point of view metahalloysite is unstable with respect to kaolinite (Marshall, 1977, p. 53). Therefore it will disappear or transform gradually into kaolinite. As the structures of kaolinite and meta-

halloysite do not match, recrystallization must take place to achieve this transformation.

Numerous studies on experimental formation of kaolinite have been carried out recently (e.g. de Kimpe et al., 1964; de Kimpe & Fripiat, 1968; de Kimpe, 1969; Kittrick, 1970; Linares & Huertas, 1971; Hem & Lund, 1974). These studies reveal the impossibility of precipitation of kaolinite directly from the soil solution. The presence of alumino-silic gels, organic compounds of crystalline particles (de Kimpe & Fripiat: zeolite ; Kittrick: montmorillonite) were always necessary to obtain kaolinitic material. In this case, the analyses indicate that probably halloysite (or a halloysitic precipitate) may be one of the first weathering products of the limestone.

The transition of halloysite to kaolinite has been studied by several authors (e.g. Tumara & Jackson, 1953; La Iglesia & Galen, 1975; Eberl & Hower, 1975; Wilke & Schwertmann, 1977). The difficulty in this transformation however is the recrystallization (re-ordering of the layer-lattice), which must take place in the transition of metahalloysite to kaolinite. This process is probably very slow as can be deduced from the presence of metahalloysite in a large number of samples.

Tables 2.12 and 2.10 show an overall decrease of illite from the lowermost sample of Profile Sp/122 to the sample of the 2Bt. Moreover the illite content in the samples Sp/227 a and b, which can be regarded as the contact zone with the underlying limestone belonging to profile Sp/122 (eutric nitosol), is still somewhat higher than in the sample of the 2Bt(g) at approximately 3 m depth. The illite content in the fraction <2 μm of profile Sp/123 shows the same decline, though not so striking. This indicates the instability of illite, which is inherited from the limestone rock (see 2.2.2). The theoretical approach in this chapter already showed the instability of illite.

Investigations by Carroll & Hathaway (1954) and Miller (1972) on soil formation on limestone in the U.S.A. indicate the same and confirm the findings of Ross & Hendrick (1945), that kaolinite is a final product of clay mineral formation in soils on limestone. Carroll & Hathaway investigated a soil with a thickness of 66 cm on Lenoir limestone in the Appalachian Mountains. Their clay mineralogical data indicate that hydrous mica, present in the parent rock, has been altered under formation of chlorite and kaolinite.

Miller studied four deep red soils overlying carbonate rocks in Tennessee. His mineralogical analyses of the clay fraction revealed that the illite content, which is at its highest in the rock, rapidly decreases within 20 cm of the rock. It is substituted by kaolinite and to a minor extent by soil vermiculite. In two of the profiles mentioned chlorite is abundant in the rock, but its content is rapidly reduced to zero within 20 cm of the rock surface.

In contrast with the findings of Carroll & Hathaway and Miller, in the top part of profile Sp/122 the illite content increases again, while illite content in profile Sp/123 is rather constant in the Bt and 2B horizons. Mineralogical analyses of the sand fraction and in the thin sections revealed the presence of allochtonous volcanic material in the top horizons, such as biotite and a few particles of volcanic glass. Moreover, in the X-ray diffraction analyses muscovite besides illite was detected in the clay fraction of the E-horizon of profile Sp/122 (see table 2.12). Therefore it is supposed that the increase in illite content in the top horizons of profile Sp/122 has to be attributed to the admixture of volcanic material. This is also the reason why this profile is divided into two parts by horizon designation.

The increase in illite content mentioned above is accompanied by a decrease of kaolinite in the top part of profile Sp/122 (eutric nitosol). This might be due to preferential eluviation of kaolinite (Mohr et al., 1972), which, consequently, may have contributed to a residual enrichment of illite in the upper horizons of this soil. However, transformation of kaolinite into Al-interlayered minerals/Al-chlorite is very likely, as also an increase of 14 Å minerals in the top part of the soil is shown by the X-ray diffraction analyses (see table 2.12).

The illite content in profile Sp/123 (chromic luvisol) does not reach the low contents mentioned for profile Sp/122 (10 and 11 % in the 2Bt and Bt2 respectively, see table 2.5.3). In the field it was possible already to establish a thick horizon (the 2Bw1 horizon) with admixture of volcanic material. This probably accounts for the rather uniform illite content in this soil.

The mineralogical investigations described above indicate that the mineralogy of both profiles cannot be explained solely by weathering of limestone. Although certain mineralogical transformations seem to be caused by pedogenesis, the admixture with airborne volcanic dust to variable depths attributes certainly to the mineralogical assemblage observed in these soils.

The varying depths to which this admixture has been found indicate that also colluviation processes may play an important role in this area and, to a certain extent, may determine the mineralogy of the soils. In order to get an insight into these colluviation processes, a number of samples at fixed depths were collected along the slope at "Il Vallangero" for particle size distribution analyses and heavy mineral composition.

The samples Sp/160 to Sp/164: their particle size distribution and heavy mineral composition.

The samples Sp/160 to Sp/163 were collected along the slope of Il Vallangero (for location on the slope see fig.2.26). Samples were taken at certain depths (i.e. 10-20 cm, 50-60 cm, 100-120 cm and 150-170 cm). Particle size analyses were carried out on the samples and heavy mineral slides were prepared from the fraction 50-500 μm.

The particle size distribution within the silt fraction (2-50 μm) was analysed extensively. The results of the analyses are shown in table 2.16.

Table 2.16 Particle size distribution of the profiles Sp/160 to Sp/163.

Sample number	Depth of sample (cm)	>50	50-32	32-16	16-8	8-4	4-2	2 μm
Sp/160a	10-20	1.5	3.0	2.0	1.5	2.0	4.0	86.0
/160b	50-60	0.5	3.0	1.0	1.0	1.5	2.0	91.0
/160c	100-120	0.2	2.0	1.0	1.0	0.5	1.5	94.0
/160d	150-170	0.1	1.5	1.0	1.0	0.5	1.5	94.5
Sp/161a	10-20	5.0	11.0	3.0	7.5	6.0	4.5	63.0
/161b	50-60	3.5	10.0	3.5	5.5	4.5	4.5	68.0
/161c	100-120	2.5	2.5	5.5	4.5	4.0	3.5	77.5
/161d	150-170	2.0	7.0	2.5	2.0	2.5	2.5	81.5
Sp/162a	10-20	6.0	6.5	2.5	11.0	7.0	10.5	56.5
/162b	50-60	5.5	5.5	3.5	11.0	6.5	13.0	55.0
/162c	100-120	5.5	2.0	6.5	11.0	9.0	11.5	54.0
/162d	150-170	2.0	3.5	1.5	3.0	3.0	8.0	79.0
Sp/163a	10-20	5.0	5.5	6.5	7.5	6.5	11.0	58.0
/163b	50-60	6.0	6.5	10.5	9.5	8.5	19.0	40.0
/163c	100-120	6.0	5.0	9.5	11.5	8.0	14.0	45.5
/163d	150-170	6.0	5.0	10.0	10.0	9.0	16.0	44.0

The particle size distribution shows a progressive "coarsening" of the soils down the slope, although all samples still have a clayey texture except for those of the most downside profile which has a silty clay texture.

This progressive coarsening downslope may very well be due to colluviation processes. Soil forming processes such as clay illuviation can, under the prevailing conditions only account for part of this phenomenon (cf. profiles Sp/122 and Sp/123). Lateral clay eluviation may occur but is thought to be unimportant because of the clayey character of the soils which impedes the necessary throughflow.

The heavy mineral analyses show in all samples a high amount of garnets (>40 %, see table 2.17). The heavy mineral composition is compared with those of the limestone rock (Sp/68) and of a tuff profile (Sp/164) at Il Vallangero.

The latter two samples show a similarity in their mineral association. Both contain mainly pyroxenes and garnets. Differences are found in the epidote and tourmaline content (12 versus 1 and 4 versus 0, respectively).

Table 2.17 Heavy mineral composition in the fraction 50-500 μm of the profiles Sp/160 to Sp/163, compared with the heavy mineral association of profile Sp/164 (tuff) and Sp/68 (limestone).

Profile	Heavy minerals / Depth of sample (cm)	pyroxenes	amphiboles	epidotes	tourmalines	garnets	zircons	rutiles	titanites	staurdites	olivines	misc	% opaque gr
Sp/160	10-20	18	4	13	-	49	10	4	-	2	-	-	90
	50-60	5	3	7	-	63	5	3	7	7	-	-	88
	100-120	6	3	12	2	55	8	1	4	9	-	-	94
	150-170	3	6	13	2	40	6	3	6	13	8	-	94
Sp/161	10-20	9	2	-	-	80	-	1	3	4	-	1	83
	50-60	3	7	4	-	79	1	3	2	1	-	-	86
	100-120	1	1	14	2	54	5	7	4	11	1	-	94
	150-170	5	6	13	3	46	3	3	5	9	6	1	96
Sp/162	10-20	25	7	3	1	51	2	1	5	2	3	-	78
	50-60	38	2	3	-	46	2	1	4	2	2	-	79
	100-120	28	2	5	-	51	1	2	3	7	1	-	83
	150-170	10	-	7	1	64	3	1	5	6	3	-	93
Sp/163	10-20	9	1	11	5	52	10	4	-	4	3	-	93
	50-60	1	1	16	2	54	7	3	1	4	8	-	96
	100-120	1	16	10	3	55	1	5	-	5	4	-	83
	150-170	-	14	16	4	40	6	4	-	10	6	-	90
Sp/164 (tuff)		46	4	1	-	38	1	2	1	3	4	-	65
Sp/68 (limestone)		56	5	12	4	13	2	1	1	1	-	2	94

A difference is also found in the type of garnets in both samples. In the limestone, colourless garnets (grossular) prevail, while in the tuff sample mainly brown and yellowish brown garnets (andradite ?) occur. The ratios brown/yellowish brown : colourless garnets in the samples Sp/68 (limestone) and Sp/164 (tuff) are 0.22 and 5.00 respectively. Because of this large difference, this ratio can be used to indicate volcanic admixture to the soils (table 2.18). In general, the ratio shows a decrease with depth, indi-

Table 2.18 Ratio brown/yellowish brown : colourless garnets in the heavy mineral fraction (50-500 μm) of the profiles Sp/160 to Sp/163.

profile number / depth of sample (cm)	10-20	50-60	100-120	150-170
Sp/160	1.64	7.22	1.29	0.54
Sp/161	4.20	1.55	0.69	0.13
Sp/162	3.31	6.56	3.93	3.50
Sp/163	0.32	0.13	0.26	0.16

cating a growing influence of the colourless garnet, most probably inherited from the limestone. The high ratios in the top horizons of the profiles Sp/160 and Sp/161 and throughout profile Sp/162 might indicate therefore an admixture of volcanic material.

Besides colourless and brown to yellowish brown garnets also green and pink garnets occur in all samples. In most samples green garnets occupy about 20 to 30 % of the total garnet content, whereas the pink garnet content is less than 10 %. The green and

pink garnets lack completely in the limestone sample and the amount in the tuff sample is very low (both 5 % of the total garnet amount). Because of the lack of more data on the heavy mineral composition of the limestone in the research area, it cannot be established if the green and pink garnets are derived from volcanic admixture or from limestone beds containing these garnets.

The rate of admixture of volcanic material to the soils can also be deduced from the varying pyroxene (mainly augite and aegerine-augite) content in the samples. The strong admixture already established in profile Sp/162, is accompanied by a high pyroxene content. The samples of the top horizons of the profiles Sp/160, Sp/161 and Sp/163 show the same trend. Moreover it is striking that tourmaline and epidote, frequently occurring in the limestone, are absent or only present in a small amount in the same samples.

From what preceded it is clear that, though on first thoughts the soils at Il Vallangero are rather uniform thick reddish brown clayey soils derived from limestone, one must take into account a varying influence of admixture with volcanic material and of colluviation processes.

The mineralogical investigations of the profiles Sp/122 and Sp/123 already indicated, that in the uppermost profile (Sp/123) a volcanic influence could be established up to approximately 2.20 m deep. The lower situated profile (Sp/122) showed an admixture of volcanic material to a depth of only approximately 80 cm. The profiles Sp/160 to Sp/163, forming a catena along the slope at Il Vallangero, also reveal a varying volcanic influence: increasing downslope but decreasing again in the lower-most profile.

It therefore can be concluded that the deep soils at Il Vallangero (and probably also in the other areas mentioned in the introduction of this section) are not only a product of limestone weathering and soil formation in the residue. A top layer of variable thickness occurs, locally over 2 m thick, consisting of material derived from limestone weathering and admixture of volcanic deposits. Colluviation processes on a microscale with differences within a few metres in small karstic depressions due to dissolution of the underlying limestone, and overall colluviation processes along the slope must be held responsible for the irregular pattern of this mixed layer.

2.5.2 The soils in fissures and cracks in the limestone rock.

Soils in fissures and cracks in the limestone can be observed throughout the research area. Most of them, however, are shallow, obscured by vegetation and strongly eroded. Thanks to recent roadworks exposures appeared, showing the soils in their natural habitat. Therefore extensive use was made of new road-cuts when studying these soils.

Three profiles, all chromic vertisols, were described, two alongside the new road from Pastena to Falvaterra (Sp/66 and Sp/93) and one alongside the new road from Pico to San Oliva, south of Pontecorvo (Sp/235) (see appendix 2). The location of these profiles is indicated in fig. 2.23.

In addition to the samples of the profiles mentioned above, soil material of the contact zone with the limestone and weathering limestone was collected (samples Sp/65a and b, Sp/68c, Sp/103, Sp/212 and Sp/226). Two samples were taken from freshly cut limestone near profile Sp/93 and sampling point Sp/65 and three types of (freshly cut) limestone were collected together with sample Sp/68c (see section 2.2).

The samples Sp/65a and b and Sp/68c are rubified soil material (hues of 2.5YR) adjacent to the parent rock. The samples Sp/103 and Sp/212 consist of yellowish-grey soil material, which is thought to be weathering products from limestone not affected by rubefaction. Sample Sp/226 represents the initial limestome weathering and is taken from cracks in a strongly fractured limestone at the road pass between Pico and Itri. The location of these sampling points is shown in fig 2.23.

From the samples the fraction $<1\,\mu m$ was separated for X-ray diffraction analyses and chemical analyses were carried out on the samples of profile Sp/66 and sample Sp/68c. The results of the X-ray diffraction analyses are given in tables 2.19 and 2.20.

The soils show the same mineralogical characteristics as the soils discussed in 2.5.1. In most cases the mineralogical association in the fraction $<1\,\mu m$ can be descri-

Table 2.19 Semi-quantitative X-ray diffraction analyses of the fraction <1 μm of the profiles Sp/66, Sp/93 and Sp/235, all chromic vertisols, and of the samples Sp/65, Sp/68c, Sp/103, Sp/212 and Sp/226.

Profile c.q. sample number	Horizon	Depth of sample (cm)	Sm	14 Å	10 Å (Ill)	Kaol	Qtz (%)	Hm	Go	Ana
	AB	15-35	tr	(+)	++	+[1]	1-3	tr	-	-
Sp/ 66	Bw	80-110	tr	(+)	++(+)	+(+)[1]	1-3	tr	-	-
	Bwck	150-165	(+)	+	++	+(+)[1]	1-3	tr	-	-
	AB	10-30	?	-	++	++[1]	ca. 1	-	?	-
	Bt	40-50	?	-	++	++[1]	ca. 1	-	?	-
Sp/ 93	Bw1	60-80	?	-	++	++[1]	ca. 1	-	?	-
	Bw2	120-150	?	-	++	++[1]	ca. 1	-	?	-
	R		tr	-	+++	(+)[1]	1	-	-	-
	AB	10-25	tr	-	+	++[2]	1	-	-	-
Sp/235	Bw	50-70	tr	-	+	++[2]	1	-	-	-
	Bw	70-80	tr	tr	+	++(+)[2]	1	-	-	-
	Bt		?	-	++	++(+)[2]	1	-	-	?
Sp/ 65[3]	B(t)		?	(+)	++(+)	++[2]	1	-	-	?
	R		-	-	+++	?[2]	1	-	-	?
Sp/ 68c			tr	(+)	+(+)	+[1]	ca. 1	-	-	?
Sp/103			tr	-	+++	(+)[1]	-	-	-	(x)
Sp/212			+	-	(+)	+[1]	1	-	x	(x)
Sp/226			+	+[4]	+(+)	+[1]	1	-	-	-

[1] 7 Å = kaolinite [2] 7 Å = kaolinite + metahalloysite [3] Fraction <2 μm [4] 14 Å = mainly vermiculite

Table 2.20 Quantitative (calculated) X-ray diffraction analyses of the fraction <1 μm of profile Sp/66 and samples Sp/68c and Sp/226 in intensity percentages (I %).

Profile c.q. sample number	Horizon	Depth of sample (cm)	Sm (h.ch.)	Sm (l.ch.)	Verm	Chlor	Ill	Kaol
	AB	15-35	3	4	-	6	38	49
Sp/ 66	Bw	80-110	8	4	7	7	33	41
	Bwck	150-170	12	5	13	-	29	41
Sp/ 68c			7	5	10	10	28	40
Sp/226			21	8	16	tr	23	32

bed as a mixture of illite and kaolinite (with or without metahalloysite). Accessory minerals are smectites 14 Å minerals (vermiculite/chlorite), quartz and, occasionally, anatase, haematite and goethite.

However, in comparison with the mineralogy of the soils of the preceding subsection, the samples of the fissure profiles more often show a fair to considerable amount of smectites and 14 Å minerals. Quantitative (calculated) X-ray diffraction analyses of sample Sp/226show for instance a smectite amount (high charge + low charge) of 29 I % together with 16 I % vermiculite.

A higher amount of smectites and 14 Å minerals can also be observed in the lower parts of profiles Sp/123 (chromic luvisol) and the samples Sp/227 a and b (see table 2.11) and in particular in profile Sp/66(chromic vertisol) (see tables 2.19 and 2.20). This gives rise to the supposition that in an initial stage of limestone weathering besides a halloysitic precipitate (see 2.5.1), vermiculite and probably also montmorillonite has formed.

The transition from illite or some other mica mineral to vermiculite is quite common in weathering processes and often recorded in soils (cf. Dixon & Weed, 1977). The occurrence of vermiculite in weathering products of the limestone has been reported by

Khan (1960), Ku & Hsu (1963), Rotini et al. (1965), de Waart (1971) and Miller (1972). Chlorite occurrences are established by Norrish & Rogers (1956) in the lower parts of some profiles on calcareous parent material in South Australia.

Of interest are the analyses of the samples Sp/65 (table 2.19). These samples were taken alongside the road from Pastena to Falvaterra, shortly after the broadening in 1971. About 4 m under the surface dark reddish brown clay (2.5YR, moist) was found. Samples were taken from crumby, very friable material, directly adjacent to the limestone (B(t)) and of material showing a prismatic habitus (Bt), approximately 40 cm above the limestone surface. Also freely cut limestone rock was sampled.

The X-ray diffraction analyses of these samples show clearly the weathering of illite, the dominant clay mineral in the non-carbonate residue of the limestone, giving way to kaolinite (+ metahalloysite). A 14 Å mineral appears in the initial weathering stage, but is not detectable anymore in the sample 40 cm above the limestone. As the sampling point is situated deep under the surface, admixture of volcanic material can be excluded. therefore it is believed that these samples reflect the real process of limestone weathering and support the view established in the preceding section and in section 2.3 that kaolinite is the main weathering product of the limestone under the given conditions.

The chemical analyses of the fractions < 2 mm and < 2 µm of profile Sp/66 (chromic vertisol) were converted into a normative mineralogical composition of this profile (table 2.21). Profile Sp/66 reflects more clearly than other samples or profiles the combined results of the two weathering processes (i.e. limestone weathering and weathering processes influenced by admixture of volcanic material) together.

Table 2.21 Normative mineralogical composition of profile Sp/66 (chromic vertisol), given in weight percentages.

Fine earth fraction (< 2 mm).

Horizon	Depth of sample (cm)	Sm+Chl	Ill	Kaol	Q	Hm	Or	Plag	Epi	Aug	Ru	Misc[1]	W
AB	10-30	4	23	43	11	9	2	4	-	2	0.9	1	+2
Bw	80-100	3	27	42	9	9	2	3	-	3	0.8	1	+1
2Bwck	150-170	8	14	46	9	9	4	5	2	1	0.8	1	+1

[1]Misc = miscellaneous (apatite + pyrolusite).

Clay fraction (< 2 µm).

Horizon	Depth of sample (cm)	Sm+Chl	Ill	Kaol	Q	Hm	Plag	Ru	Misc[2]	W
Ab	10-30	5	28	52	tr	11	2	0.9	1	+3
Bw	80-100	4	36	45	2	11	1	0.8	tr	+3
2Bwck	150-170	10	17	57	4	11	tr	0.7	tr	+1

[2]Misc = miscellaneous (apatite + pyrolusite).
tr = 0.5 %.

The normative mineralogical composition of the fraction < 2 µm is rather well in accordancewith the X-ray diffraction analyses of this profile (see table 2.21), except for the kaolinite and quartz content. The X-ray diffraction analyses show a decrease of kaolinite in the AB-horizon, while quartz content remains constant. The increase in illite content, however, suggests an admixture with volcanic material as is mentioned already in section 2.5.1. Plagioclase has not been detected in the X-ray films and must also be regarded as a calculation method to account for Na_2O and CaO present in the sample.

Volcanic admixture could be directly established in the thin sections by the presence of some volcanic glass particles and augites. In view of this, the difference between the kaolonite and quartz content with respect to the X-ray diffraction analyses can easily be explained. Most probably part of the kaolinite must be regarded as allophane ($Al_2O_3.SiO_2.nH_2O$). In the calculations the transformation of kaolinite to allophane increases the free silica content. The presence of allophanes may also count for the ex-

cess of water in the normative mineralogical composition. A reasonable assumption for e.g. the AB horizon would be 51.4Kaol (+7.2W) → 37.0Kaol + 10.8All + 3.6Q expressed in equivalent percentages. Ultimate excess of water will be 2.4 eq. % (0.5 weight percentage).

Volcanic admixture is also shown in the normative mineralogical composition of the fine earth fraction. Though present in a very small quantity, augite increases from 2Bwck to the Bw and Ab horizons. The absence of epidote in the top horizons fits well in this view as most probably this is inherited from the limestone (see 2.5.1 and table 2.17).

Although it has not always been realized, particularly in the case of limestone weathering, the youngest weathering products are found in the lower parts of an in situ profile. Unless colluviation processes have been active or admixture with allochtonous material has taken place, the age of the soil material decreases therefore with depth in such profiles .

Because of the similar character of the mineralogy in the lower parts of the soils in fissures and of the deep soils discussed in 2.5.1 (e.g. samples Sp/227 a and b, regarded as the lower-most part of profile Sp/122), both most probably reflect the same stage of limestone weathering. The soil material of the 2Bt and 2Bt(g) horizons of profile Sp/122, which most probably have directly resulted from limestone weathering as it is not effected by volcanic admixture, must therefore be still older than that of the soils in fissures and cracks of the limestone.

2.5.3 Soils in colluvial deposits derived from limestone and/or dolomite.

These soils cover the small and large karst basins in the research area. They are mostly developed in young Holocene colluvial deposits as is indicated by the presence of pottery fragments throughout most of the profiles studied. The thickness of these colluvial deposits varies from 35 cm in the case of profile Sp/97, mentioned below, to more than 6 m. In a previous study (Spaargaren, 1974) a deep-drilling in the Piana di San Andrea near Pastena showed pottery fragments to a depth of approximately 6 m. Besides the disappearance of pottery fragments from that point on also the percentage of the frac- < 50 μm dropped sharply (see fig. 4.3)

At a number of locations products of older colluvial phases can be observed under the recent colluvial cover. No pottery fragments have been noticed in these deposits. They are often associated with the presence of volcanic material. Therefore it is assumed that the older phases most probably are induced by volcanic activity in the surroundings (Colli Albani, Roccamonfina, Ernici).

A number of profiles (Sp/97, a chromic vertisol, Sp/98, a chromic luvisol and Sp/111, a chromic luvisol as well), and two profiles in an alluvial fan at "La Fossa" (Sp/118, a chromic cambisol and Sp/119a, a chromic luvisol) have been studied. Also a sample was taken of colluvial material at the water sampling point Sp/116 (Sp/117).

X-ray diffraction analyses were carried out on the fraction <1 μm of the samples of profiles Sp/97, Sp/98 (fraction <2 μm) and Sp/111, as well of sample Sp/117. Moreover, the chemical composition of the fractions < 2 mm and <2 μm of the samples of profiles Sp/97, Sp/98 and of sample Sp/117 has been determined.

The soils developed in young, Holocene colluvial material.

In comparison with the other soils on limestone these soils show a somewhat coarser texture (60-70 % clay versus 80-90 % clay). Admixture of volcanic material as well as the colluvial character of these soils were clearly recognisable in the field. Throughout the profiles dark volcanic minerals could be observed while the occurrence of thin beds of laminated material in some profiles (i.e. Sp/98) indicates the result of a rapid "colluviation" process, sheet deposition.

This process of colluviation has been observed at microscale at Il Vallangero during a heavy storm in the winter of 1976. Material was transported downslope as small aggre-

gates (less than approximately 5 mm) and in suspension. It was deposited in small depressions at the foot of the slope. The result was a layer of loosely stacked aggregates covered by a macroscopically uniform layer, sedimented from the suspension.

Profile Sp/98, a chromic luvisol (FAO-Unesco, 1974), is an example of the soils developed in young colluvial material. At a depth of 35 cm it shows a horizon with a platy structure, most probably due to the process of "sheet deposition" as described above. Below this layer it is rather uniform except for the structure which gradually becomes more prismatic. Because of the colluvial characteristics in this soil, mineralogical differences may partly be due to original heterogeneity of the deposition.

The X-ray diffraction analyses reveal little differentiation between the horizons except for a slight increase in content of 14 Å and 7 Å minerals in the B horizon ("sheet deposition" horizon) (see table 2.22).

Table 2.22 Semi-quantitative X-ray diffraction analyses of the fraction <2 μm of profile Sp/98 and of sample Sp/117 (fraction <1 μm).

Horizon	Depth of sample (cm)	Mm	14 Å	10 Å (111)	7 Å	Qtz %
B	35-40	tr	(+)	++	++(+)	4-6
Bt1	50-70	tr	tr	++	++	3-5
Bt2	85-100	?	tr	++	++	3-5
	120-135	tr	tr	++	++	3-5
Bt3	145-160	tr	tr	++	++	3-5
Sp/117				+(+)	++	1-3

The normative mineralogical composition gives somewhat more information on the mineralogy of this profile (table 2.23).

Table 2.23 Normative mineralogical composition of the fractions <2 mm and <2 μm of profile Sp/98 and of sample Sp/117, in weight percentages.

Fine earth fraction (<2 mm).

Horizon	Depth of sample (cm)	Q	Plag	Mica[1]	Sm	Ill	Kaol	Go/Hm	Ru	Misc[2]	W
B	35-40	16	6	13	6	13	34	10	1.2	1	+3
Bt1	50-70	10	4	9	5	13	47	10	1.1	1	+2
Bt2	85-100	13	4	9	5	13	43	11	1.2	1	+2
	120-135	16	5	10	5	14	38	10	1.3	1	+2
Bt3	145-160	20	5	10	5	14	35	9	1.3	1	+2
Sp/117	60-80	18	4	11	3[3]	13	38	11	1.0	1	+1

Clay fraction (<2 μm).

Horizon	Depth of sample (cm)	Sm	Ill	Kaol	Q	Go	Ru	Misc[4]	W
B	35-40	9	21	54	2	11	1.1	2	+1
Bt1	50-70	8	18	60	1	10	1.0	2	+1
Bt2	85-100	7	19	58	2	11	1.1	2	+1
	120-135	8	22	55	1	11	1.2	2	+1
Bt3	145-160	8	22	54	1	12	1.2	2	+1
Sp/117	60-80	6[5]	25	52	-	14	1.2	2	+2

[1]Mica = biotite + muscovite [2]Misc = albite + strengite + pyrolusite [3]Sm = montmorillonite + chlorite
[4]Misc = strengite + pyrosulite [5]Sm = smectite + vermiculite

It shows a slight decrease of illite and an increase of kaolinite in the fraction <2 μm below the B horizon from bottom to top of the profile. This may be attributed to the weathering of illite and formation of kaolinite, a process also found in the profile mentioned in the previous sections.

Smectite (montmorillonite) shows little variation and therefore appears to be stable in this environment. This is in accordance with the findings in the water samples from

this type of colluvium (see section 2.4, sample Sp/116). The composition of the interstitial pore water of this sample indicates that an equilibrium between kaolinite and a Mg-montmorillonite may exist.

The colluvial character of this soil is illustrated by an increase in free iron content in the fraction <2 μm (see appendix 2) from 7.6 to 8.0 % and an increase in TiO_2-content with depth (Ru in the normative mineralogical composition). Transport of free iron species bound to clay particles cannot account for this increase, nor is it hardly likely that iron would be translocated as free iron species in this soil. These differences are therefore thought to be of geogene origin. This view is also supported by the free silica content in the fraction <2 mm, which also increases with depth. The textural change within the profile (71.5 % clay in the 2Bt1 towards 60.5 % clay in the 2Bt3) can only account for part of the increase in free silica content

The heavy mineral composition of three samples of profile Sp/98 is given in table 2.24. It shows besides a high amount of garnets large quantities of pyroxenes (augites

Table 2.24 Heavy mineral composition of three samples of profile Sp/98 in the fraction 50-500 μm.

Horizon	Depth of sample (cm)	Pyroxenes	Amphiboles	Epidotes	Tourmalines	Garnets	Zircons	Rutiles	Titanites	Staurolites	Olivines	% opaque grains
B (sheet)	35-40	18	15	3	2	51	3	2	2	1	3	66
2Bt2	85-100	16	13	1	-	57	4	1	1	2	5	77
2Bt3	145-160	12	14	7	1	54	2	-	2	1	7	83

and aegirine-augite) and amphiboles (mainly green hornblendes). The garnet group consists of 65 % or more of the brown to yellowish brown garnet.

The observation in the heavy mineral slides reveal clearly the admixture with volcanic material, being more or less constant throughout the profile. The ratio brown/yellowish brown : colourless garnet varies from 4.33 to 17.50.

The soils and paleosols developed in older, Pleistocene colluvial material.

Soils and paleosols developed in older, Pleistocene colluvial material are found under a cover of recent colluvial deposits of varying thickness. They have one feature in common: they all show pseudogleyic characteristics. Examples of these soils are the profiles Sp/97 (a chromic vertisol, see fig. 2.27) and Sp/111 (a chromic luvisol), while near profile Sp/119 probably also remnants of this kind of soil occur (samples Sp/119 g and h).

X-ray diffraction analyses were carried out on a number of samples of these profiles and the results are presented in tables 2.25 .

The mineralogy of the fraction <1 μm of these soils, again, can be described as a mixture of illite and kaolinite (+ metahalloysite). Incidentally montmorillonite occurs, but no 14 Å minerals could be detected. Profile Sp/97 shows a strong decrease with depth of illite and smectite, followed by an increase in the 4Bg sample and the reverse for the 7 Å minerals. The composition of profile Sp/111 is rather constant with only some minor variations, while the samples of profile Sp/119 show an increase with depth of both illite and kaolinite.

The results of the normative mineralogical calculations of profile Sp/97 are given in table 2.26. The figures of the clay fraction (<2 μm) demonstrate clearly the decrease of illite and the increase of kaolinite with depth. Smectite has been introduced in the cal-

Table 2.25 Semi-quantitative X-ray diffraction analyses of the fraction <1 μm of some samples of the profiles Sp/97, Sp/111 and Sp/119.

	Horizon	Depth of sample (cm)	Sm	10 Å (Ill)	7 Å	Qtz %	Ana	Go
Chromic Vertisol Sp/97	2Bg(t)2	90-105	?	++(+)	+(+)[1]	1	-	-
	2Bg	160-170	?	++	++[1]	1	-	-
	3B(t)	180-200	?	+	+++[1]	ca.1	-	-
	4Bg	230-250	?	++(+)	+[1]	1	-	-
Chromic Luvisol Sp/111	Ap	55-20	-	++	++[1]	1-3	-	-
	Bt	30-45	-	++	++[1]	ca.1	-	-
	2BC	50-70	tr	++	++(+)[1]	1	-	-
	3Bg	90-110	-	+(+)	++[2]	ca.1	-	-
		190-210	tr	++	++(+)[1]	ca.1	-	?
		290-310	-	++	++[1]	1	-	-
		390-410	-	++	++(+)[1]	1	-	-
Sp/119	2Bg	80-95	tr	++	++[2]	1	-	-
	2B(g)	100-110	tr	++(+)	++(+)[2]	ca.1	(+)	-

[1] 7 Å = kaolinite + metahalloysite [2] 7 Å = kaolinite

Table 2.26 Normative mineralogical composition of the fine earth fraction (<2 mm) and clay fraction (<2μm) of profile Sp/97 (chromic vertisol) in weight percentages.

Fine earth fraction (<2 mm)

Horizon	Depth of sample (cm)	Q	Sm	Ill	Kaol	Mica[1]	Verm	Plag	Go/Hm	Ru	Str	W
2Bg(t)1	45-65	4	9	31	42	1	1	3	8	0.8	0.5	+3
2Bg(t)2	90-105	3	7	30	46	tr[2]	1	3	9	0.8	0.5	+2
2Bg(t)3	130-150	4	6	24	52	tr[2]	1	2	9	0.9	0.6	+2
2Bg	160-170	4	4	23	54	3	-	2	9	0.7	0.6	+2
3B(t)	180-200	12	3	8	52	10	-	4	9	1.0	0.7	+3
	200-220	11	3	9	53	10	-	3	9	1.1	0.8	+3

Clay fraction (<2 μm)

Horizon	Depth of sample (cm)	Sm	Ill	Kaol	Q	Go	Ru	Misc[3]	W
2Bg(t)1	45-65	9	34	44	3	8	0.8	1	+3
2Bg(t)2	90-105	7	33	48	2	8	0.8	1	+2
2Bg(t)3	130-150	6	26	54	3	9	0.9	1	+2
2Bg	160-170	4	25	56	3	10	0.7	1	+1
3B(t)	180-200	4	11	72	2	8	0.9	2	+1
	200-220	4	12	71	2	9	1.0	1	+1

[1] Mica = biotite + muscovite [2] tr = less than 0.5% [3] Misc = albite + apatite + strengite

culations as the X-ray films of the fraction <1 μm of the samples show a faint indication for the presence of montmorillonite. In the calculations smectite content also shows an increase towards the surface.

On first thought one is disposed to explain the increase of illite towards the surface by admixture of volcanic material as is the case for instance in the profiles Sp/66 and Sp/122, discussed in the previous sections. Volcanic admixture, however, is somewhat doubtful in this profile. The heavy mineral composition of the fraction 50-500 μm of the 3B(t) horizon (table 2.27) differs significantly from those of the samples in which volcanic admixture could be established. The low amount of pyroxenes (augites) is not indicative as this also might be the result of strong weathering. In fact, the high amount zircon and rutile in the sample points in this direction. However, the high amount of epidotes, the relatively low amount of garnets and a ratio brown/yellowish brown : colour-

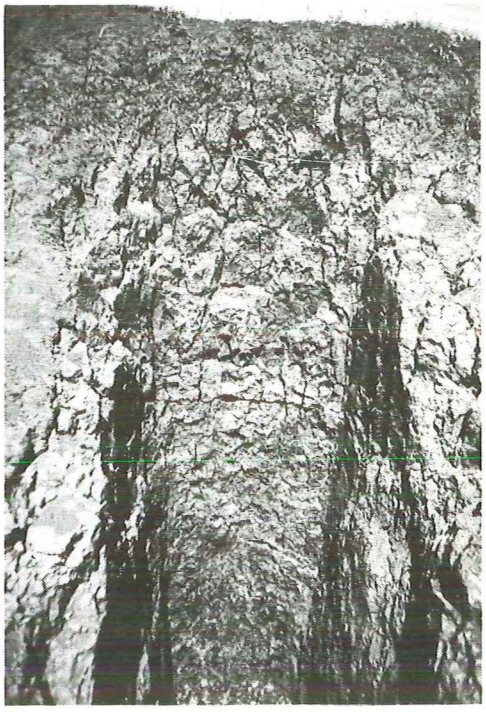

Fig. 2.27 Chromic Vertisol (profile Sp/99) in older, Pleistocene colluvial deposits.

less garnet of 0.52 are more indicative for a limestone origin than for volcanic admixture.

The high illite content of the top horizon seems to indicate that there is little or no weathering of illite, like in the other "in situ" profiles studied. Even the soils in young, Holocene colluvial deposits show indications of weathering of illite (see profile Sp/98 and discussion above). This excludes the factor time which might be a reason.

Increase of illite from bottom to top of the profile is a common feature in vertisols in tropical regions (cf. Mohr et al., 1972, chapter 3). The examples given by these authors show that this increase is accompinied by a decrease of montmorillonitic clay minerals. In fact, the increase is explained by transformation of montmorillonite to illite, because of the increase with depth of the Mg/K activity ratio in the soil solution. The figures presented in table 2.26, however, show besides the increase of illite from bottom to top of the profile also an increase in smectite content in the same direction.

This becomes even more clear, when the phase relations in the system $K_2O - MgO - Al_2O_3 - SiO_2 - H_2O$ are studied. From this it appears that the $lg[K^+]$ + pH value is the important determining factor in the question if illite will be a stable phase and therefore might be formed. A phase diagram constructed for a number of relevant phases at 15 °C and 1 bar pressure, using the relations given in appendix 7, shows a lowest stability point for illite at $lg[K^+]$ + pH = 5.04 (fig. 2.28). Misra (1973), mentioned by Marshall (1977) gives somewhat lower $lg[K^+]$ + pH values, depending on the $lg[Mg^{2+}]$ + 2pH value. At $lg[Mg^{2+}]$ + 2pH = 14.0, his lowest stability point for illite is situated at a $lg[K^+]$ + pH value of approximately 4.35.

The chemical composition of two water samples taken from the 2Bg(t)1 horizon (Sp/170a and b, see section 2.4) shows, that the high values mentioned above are not reached in this soil. Water sample Sp/170a has $lg[Mg^{2+}]$ + 2pH and $lg[K^+]$ + pH values of 8.48 and 0.86 respectively, while sample Sp/170b shows values of 9.56 and 1.15 respectively. Consequently, neoformation of illite in the upper horizons of this soil is not likely to occur.

Interesting results were obtained from mineralogical and chemical analyses of samples of the mottles in the 2Bg(t)1 horizon. The results of the X-ray diffraction analyses of the fraction <1 μm of these samples (table 2.28) show a dominance of K-mica in the

Table 2.27 Heavy mineral composition of the fraction 50-500 μm in the 3B(t) horizon of profile Sp/97 (chromic vertisol).

Pyroxenes	Amphiboles	Epidotes	Tourmalines	Garnets	Zircons	Rutiles	Titanites	Staurolites	Olivines	Disthenes	Anatases	% opaque grains
3	1	24	3	21	23	8	3	2	2	7	3	91

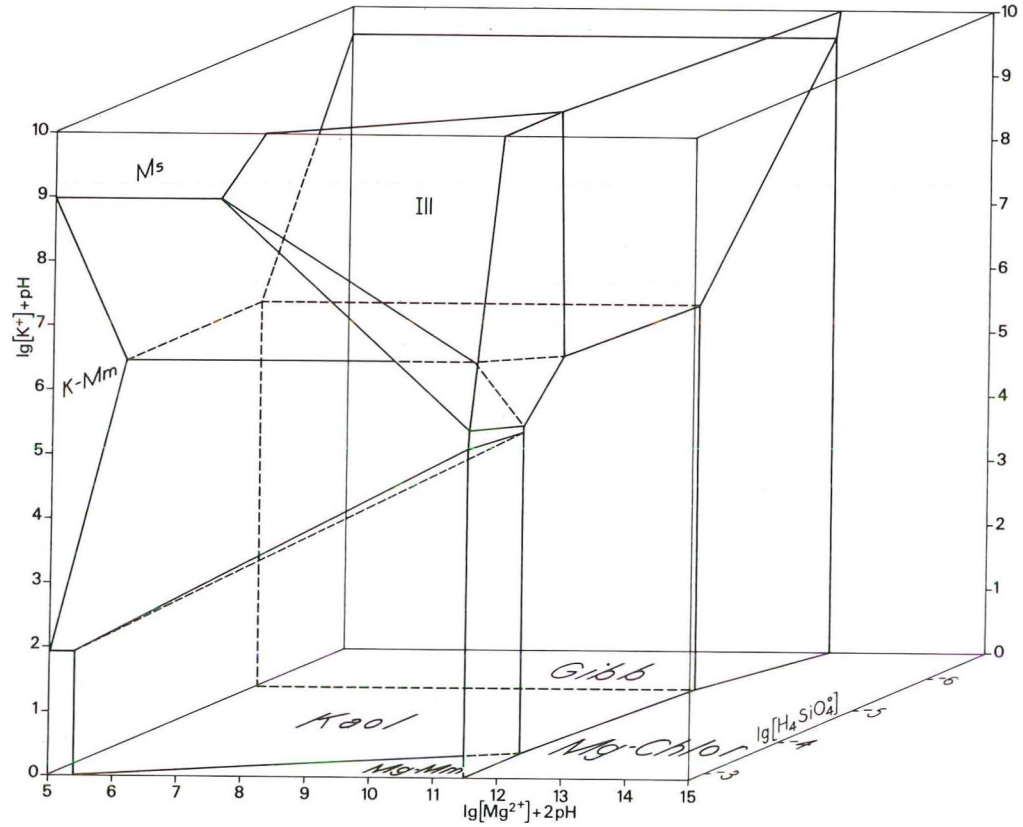

Fig. 2.28 Stability fields of illite, muscovite, K-montmorillonite, Mg-montmorillonite, Mg-chlorite (clinochlore), kaolinite and gibbsite at 15° C (288.15° K) and 1bar pressure in the system $MgO - K_2O - Al_2O_3 - SiO_2 - H_2O$.

light grey mottles, the occurrence of montmorillonite and anatase and a very small amount of kaolinite. The red mottles show the occurrence of both illite and kaolinite in fair amounts. The chemical analyses of these samples, converted to a normative mineralogical composition (table 2.29) show the same trend.

The soils in Pliocene sandstone often also show pseudogleyic characteristics (see chapter 3). To compare the pseudogleyic features in both soils with each other, also samples of the mottles of the Bg horizon of profile Sp/4 (a ferric acrisol) (see appendix 2) were taken. The result of the analyses of these samples, however, do not reveal such striking mineralogical differences as in the case of the samples from profile Sp/97. Besides a more pronounced difference in goethite content (5 and 19 % in the light grey and red mottles respectively) no significant differences can be observed in the normative mineralogical composition, if goethite is expelled from the calculations (see tables 3.10 and 3.11).

Although of coarse differences in mineralogy of both soils exist related to the parent material, the different expression of the pseudogleyic features as result of pedogenetic processes is thought to be caused by differences in texture between both profiles. The Bg horizon of the ferric acrisol in Pliocene sandstones shows a clay loam to sandy loam texture, while the upper horizons of profile Sp/97 have clayey textures with clay percentages of more than 90 %. From this it may be assumed that water penetrating into the soil cannot move as freely as in the case of profile Sp/4. Moreover the vertic character

Table 2.28 Semi-quantitative X-ray diffraction analyses of the fraction <1 μm of samples from light grey and red mottles of the 2Bg(t)1 horizon of profile Sp/97 (chromic vertisol).

	Mm	14 Å	10 Å (Ill)	7 Å [1]	Qtz %	Ana
Light grey	(+)	–	+++(+)	(+) [2]	1	(+)
Red	–	–	++	++	1	–

[1] 7 Å = kaolinite + metahalloysite [2] 7 Å = kaolinite

Table 2.29 Normative mineralogical composition of samples from light grey and red mottles of the 2Bg(t)1 horizon of profile Sp/97 (chromic vertisol) shown in weight percentages.

Fraction <2 mm.

	Q	Sm	Ill	Kaol	Mica [1]	Verm	Go/Hm	Plag	Ru	Misc [2]	W	Free Fe_2O_3
Light grey	2	13	57	13	–	2	7	5	1.0	tr [3]	+3	3.4
Red	3	6	25	50	2	–	9	3	0.8	1	+2	5.6

Fraction <2 μm.

	Sm	Ill	Kaol	Q	Go	Ru	Misc [5]	W	Free Fe_2O_3
Light grey	15 [4]	63	14	–	7	0.9	tr	+3	2.2
Red	7	28	51	2	9	0.9	2	+2	5.7

[1] Mica = biotite + muscovite [2] Misc = apatite + strengite [3] tr = 0.5 % [4] Sm includes 0.4 % vermiculite [5] Misc = albite + apatite + strengite

of profile Sp/97 contributes to the impermeability of the peds as most of the pedfaces are formed by slickensides. It is therefore very likely that water penetrating this soil only affects the outside parts of the peds. This view is supported by the mineralogical composition of the innerside of the peds which is in reasonable accordance with the mineralogy of the other soils on limestone investigated.

The apparent stability of illite and smectite in the outer sides of the peds still needs some explanation. As is described above formation of illite and smectite is not very likely. Also preferential chemical breakdown of kaolinite must be excluded as is appears from the composition of the water samples Sp/170 a and b, that kaolinite can be expected to form the stable phase in this weathering environment (see section 2.4 and fig. 2.22). Therefore the only explanation for the apparent stability of illite and smectite must be found in preferential eluviation of kaolinite (Mohr et al., 1972) The $[K^+] / [H^+]$ ratios in the soil solution are very low. This points to the fact that the transformation of kaolinite to illite mentioned by these authors as a result of increasing $[K^+] / [H^+]$ ratios, is neglegible.

The process of preferential eluviation of kaolinite can only occur upon the moistening of the soils, when the cracks are still open. The profile was described during summertime and the presence of clay cutans has been established in the field. They have also been observed in the thin sections (Fig. 2.31). This indicates that the cutans must be very young as upon closing of the cracks and voids after a long period of moistening the cutans will be destroyed by the vertic processes in the soil (see also Remmelzwaal, 1978).

The present mineral distribution in this soil may therefore be explained best by both geogenetic and pedogenetic processes. The distribution pattern of illite must most probably be related to original differences in the colluvial deposits. If an older "in situ" soil on limestone, comparable to the soils discussed in 2.5.1 (e.g. profile Sp/122, eutric nitosol) is eroded by denudation and erosion processes, the resultant products may reflect the "mother" soil in upside down position. Consequently, the illite distribution in these products will show an increase towards the surface, as in the case of profile Sp/97.

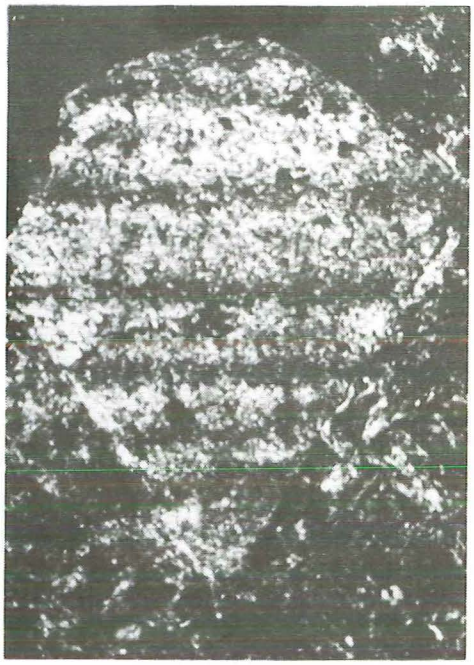

Fig. 2.29

Fig. 2.30

Fig. 2.31

Fig. 2.29 2Bg(t)1 chromic vertisol (profile Sp/97). Sedimentary relict. X-nicols, 70x.

Fig. 2.30 2Bg(t)2 chromic vertisol (profile Sp/97). (Bi-)masepic fabric with diffuse, irregular sesquioxidic nodules. X-nicols, 25x.

Fig. 2.31 3B(t) chromic vertisol (profile Sp/97). Interpedal compound argillan-mangan over clustered pedorelicts. Plain light, 170x.

Pedogenetic processes such as preferential translocation of kaolinite may have strengthened this distribution. Moreover, the sharp decrease in illite content between the 2Bg and 3B(t) horizons might also be partly attributed to a stronger degree of weathering, possibly due to earlier sedimentation of the material which now forms the lower horizons.

The pseudogleyic character of this profile still needs some closer examination. Scheffer & Schachtschabel (1976) describe the formation of pseudogley as diffusion of reduced Fe (III) and Mn (II) from the outer side of the ped to the innerside, followed by oxidation and precipitation of Fe (III) and Mn (III) or (IV) compounds. Others (e.g. Mohr et al., 1972; Bolt & Bruggenwert, 1977) are less specific on the direction of transport of the reduced Fe (II) and Mn (II) species. In general however pseudogleyic formation is regarded as a process by which Fe and Mn are reduced in the outer rim of the ped through low redox potentials due to water saturation in voids and pores and chelating by organic compounds.

The thus mobilized Fe and Mn species are transportated to zones with higher redox potentials. Ultimately oxidation to Fe (III) and Mn (III) or (IV) and precipitation as concretions or mottles takes place.

As mentioned above, the normative mineralogical composition and the X-ray diffraction analyses of the sample of the red mottles show fair agreement with the mineralogical composition of the soils studied. Deferrisation of the outer side of the ped as is shown by e.g. the free iron contents of the mottles (3.4 versus 5.6 % in the fine earth fraction and 2.2 versus 5.7 % in the clay fraction of the grey and red mottles respectively), is apparently not followed by a significant increase of iron in the inner side of the ped.

Fig. 2.32 Deep gully in colluvial deposits in a karst basin near Monte Cervaro. The lighter bands are formed by tuff layers interbedded in the colluvial deposits. Profile Sp/111 (chromic luvisol) is situated left of this picture.

Therefore mobilization of the Fe and Mn species must have been followed by a downward (or lateral through voids and pores) movement of the dissolved species. The increase in normative goethite content in the fraction < 2 μm (table 2.26) supports this view, as well as the increase with depth of the free iron content. Hence the pseudogleyic formation in this profile is a result of a vertical displacement of Fe- and Mn species rather than of a horizontal one. This is also illustrated by the thin sections, in which ferrans and probably mangans (Brewer, 1976) were observed in samples of the 2Bg and 3B(t) horizons (see fig. 2.29 and 2.31).

Besides mineralogical indications of the colluvial character of this soil (the decrease with depth in illite content and the rather irregular behaviour of titanium content for instance), evidence was also found in the thin sections. One of the slides revealed a papule, which through its lamination was interpreted as a sedimentary relict (Brewer, 1976) (fig. 2.30). The fine stratification within the papule also points to a relict of lacustrine origin and indicates that a lake has existed in the karst basin.

Profile Sp/111 (a chromic luvisol) also shows pseudogleyic features. The X-ray diffraction analyses of this profile, how-

ever do not show the decrease with depth of the illite content, which is evident in profile Sp/97. Moreover the grain size distribution reveals a coarser texture (clay content in the 3Bg horizon varies from 55.0 to 69.5 %).

The coarser texture must be caused by admixture of volcanic material throughout this profile. A tuff deposit covers the soil and deeper in the profile also weathered tuff banks occur. They form an irregular or wavy horizon as can be seen in fig. 2.32. Dissolution of the limestone and consecutive subsidence of the soil above must be the cause of the irregular apparence. It supports the view establish in 2.5.1, that variation in thickness of the colluvial cover at distances of a few metres can be explained by local karstic dissolution processes.

The admixture with volcanic material in this profile forms a contrast with profile Sp/97, in which volcanic material could not be established. Therefore it is likely that profile Sp/111 is younger than profile Sp/97. This indicates that the pseudogleyic formation is not tied to a certain time period. The feature can only be used to distinguish recent colluvial deposits from older ones.

2.5.4 The soils on dolomite.

Soils on dolomite differ from those on limestone by the presence in most localities of rather thick sandy weathering residues, consisting of nearly pure dolomite grains ("dolomitic sands"). The transition of the soil to the rock is less abrupt than in the case of soils on limestone. These weathering residues can reach considerable thickness. Near Itri frequently dolomitic sands were found of several metres thick.

The pressence of (more or less) thick weathering zones on dolomite is due to the difference in solubility between calcite and dolomite (see also 2.1.2). Calcium carbonate minerals cementing the dolomite grains are dissolved, leaving a residue of sandy dolomitic grains.

Three soil profiles were described. one situated northwest of Monte Lamia, a relatively young soil on dolomite (profile Sp/183, a calcic cambisol), one situated east of Pico alongside the road Pico - San Oliva, a deep (colluvial) soil on dolomite (profile Sp/234, a chromic vertisol), and one east of Sperlonga, a soil in a fissure in the dolomite (profile E 80, a chromic luvisol). Samples were taken of all soils for mineralogical and chemical analyses.

The relatively young soil near Monte Lamia (profile Sp/183, a calcic cambisol).

This profile is located in between the water sampling points Sp/31 and Sp/32 alongside the road Castro dei Volsci - San Giovanni Incarico (see fig. 2.23). It has been classified as a calcic cambisol (FAO - Unesco, 1974). Given the physiographic position of this profile the top part may have been influenced by colluviation processes. As the profile is situated near the overthrust fault of the limestone over Miocene shales (see section 1.6), water logging occurs, causing gley features in the lower parts of this soil. A cover of mosses along the section indicates the permanent character of this water saturation.

The X-ray diffraction analyses, shown in table 2.30, reveal besides illite and kaolinite a fair amount of smectite and 14 A minerals. The amount of smectite increases

Table 2.30 Semi-quantitative X-ray diffraction analyses of the fraction <2 μm of profile Sp/183 (calcic cambisol).

Horizon	Depth of sample (cm)	Mm	14 A	10 A (111)	7 A[1]	Qtz %	Go	Ana	Dol
AB	0-10	+(+)	+	++	+(+)	3-5	(x)	x	-
B	15-30	+(+)	+	++	+(+)	3-5	(x)	x	-
BC	40-55	+(+)	+	++(+)	+(+)	3-5	(x)	x	-
BCg	70-90	+	+	++	+(+)	3-5	(x)	x	-
Cg	110-130	+	+	++	+(+)	2-4	(x)	x	-

[1] 7 A = kaolinite

towards the surface, indicating most probably the formation of montmorillonite. The possibility that montmorillonite might be a stable phase in this weathering environment was already postulated from the interpretation of the chemical data from water sample Sp/31 (see section 2.4). This sample was taken from weathering dolomite approximately 20 m west of this profile.

Somewhat more insight in the mineralogy of this soil can be obtained from the normative mineralogical composition (table 2.31).

Table 2.31 Normative mineralogical composition of the fraction < 2 mm and < 2 μm of profile Sp/183 (calcic cambisol), given in weight percentages

Fine earth fraction (< 2 mm).

Horizon	Depth of sample (cm)	Dol	Cc	Sm+Verm	Ill	Kaol	Q	Go	Plag	Or	Ru	Misc[1]	W	CO_2
AB	0-10	4	-	7	18	45	16	7	9	5	1.0	3	+5	-
B	15-30	11	1	6	20	30	15	7	4	3	0.8	2	+4	-
BC	40-55	80	3	1	5	7	0.8	2	1	-	0.1	0.2	+0.9	-0.6
BCg	70-90	84	6	0.7	3	4	0.7	1	0.8	-	0.1	0.1	+0.2	+0.1
Cg	110-130	89	7	0.2	1	1	0.3	0.4	0.8	-	tr	tr	+0.1	-0.3

Clay fraction (< 2 μm).

Horizon	Depth of sample (cm)	Dol	Sm+Verm	Ill	Kaol	Q	Go	Ru	Misc[2]	W
AB	0-10	0.3	10	26	45	7	10	0.9	1	+7
B	15-30	0.4	9	30	45	3	11	0.9	1	+5
BC	40-55	1	9	29	43	5	10	0.8	2	+6
BCg	70-90	3	7	34	35	7	12	0.7	1	+2
Cg	110-130	5	6	36	33	7	10	0.7	2	+3

[1] Misc = biotite + epidote + pyrolusite + strengite [2] Misc = albite + pyrosulite + strengite

The figures for the fraction <2 μm show a decrease in illite and free silica content towards the surface and an increase in smectite + vermiculite and kaolinite content in the same direction. This might suggest the weathering of illite to montmorillonite and kaolinite.

The decrease towards the top of the B horizon of free silica needs some explanation. The CaO present in the sample is with an equivalent amount of MgO and CO_2 converted to dolomite. Dolomite nor any other carbonate-bearing mineral could be detected in the X-ray samples while on the other hand chemical analyses of the fraction <2 μm revealed the presence of CO_2. Because dolomite is less soluble than calcite and therefore more likely to persist, the introduction in the normative mineralogical calculations of dolomite has been preferred to that of calcite. If however, calcite is present in the mode, part of the dolomite can be converted with kaolinite and free silica to montmorillonite (or vermiculite) according the equation

$$4\ \text{Dol} + 12\ \text{Kaol} + 10\ \text{Q} \rightarrow 2\ \text{Cc} + 24\ \text{Mm} (+ 2\ \text{W} + 2\ \text{CO}_2)$$

If this variant calculation is introduced, it results in a more or less constant free silica content. This modification however, is accompanied with an abnormal (i.e. decrease from bottom to top of the profile) behaviour with respect to the mode of montmorillonite, together with an excess of CO_2. For these reasons dolomite has been maintained in the calculations accepting the increase with depth in free silica content as inevitable.

The figures of the fraction <2 mm show clearly the persistence of dolomite with respect to calcite as mentioned above and in section 2.4. The occurrence of orthoclase in the top two samples might be attributed to admixture with allochtonous material. Orthoclase and K-bearing volcanic glasses are, chemically, identical (Robie et al., 1978). In the thin sections of this profile no evidence was found of the presence of volcanic

glass particles as was the case in other thin sections. Therefore orthoclase is maintained more to indicate an excess in K_2O or a shortage of Al_2O_3, rather than interpreted as such.

The mineralogy of the clay fraction still needs some more explanation. As mentioned above, table 2.31 shows that kaolinite, montmorillonite and 14 Å minerals appear to be (meta)stable phases. In section 2.4 it was discussed that the soil solution might be controlled by an equilibrium between kaolinite and Mg-montmorillonite. The regression line with an $r = -0.954$, constructed through the $\lg[Mg^{2+}] + 2pH$ and $\lg[H_4SiO_4^0]$ plots of samples Sp/31 in an activity diagram in the system $MgO - Al_2O_3 - SiO_2 - H_2O$ at 15 °C and 1 bar pressure was parallel to the calculated kaolinite - Mg-montmorillonite phase boundary (see fig. 2.21).

Verstraten (1978) recently showed that the area above the kaolinite and montmorillonite stability fields can be occupied by a vermiculite. The phase boundary between kaolinite and vermiculite is situated slightly lower lower in his diagram, than the chlorite - kaolinite phase boundary shown in this study. This might indicate that besides the kaolinite - montmorillonite also the kaolinite - vermiculite partial equilibria could be effective in the weathering of dolomite. If so, it must be attributed to the high $[Mg^{2+}] / [H^+]$ ratio in the soil solution, and explains the apparent stability of 14 Å minerals, probably mainly vermiculite, as is shown in the X-ray diffraction analyses (table 2.30).

The deep (colluvial) soil on dolomite (profile Sp/234, a chromic vertisol).

This soil, located alongside the road Pico - San Oliva, south of Pontecorvo, is classified as a chromic vertisol (FAO-Unesco, 1974). Fig. 2.33 shows the soil at the time of description (summer of 1974) and illustrates the irregular surface that the dolomitic limestone can have.

Fig. 2.33 The deep chromic vertisol on dolomite (profile Sp/234), showing the irregular surface of the dolomite, present as "dolomitic sands".

The top part of the profile might very well be influenced by colluviation. The analyses of the samples indicate that the first metre might be a colluvial cover which probably due to vertic processes cannot clearly be distinguished from the underlying horizons. This was not clearly recognized in the field, but the change in colour from 5YR to 2.5YR in the profile description as well as the rather gradual and irregular transition between the soil and the dolomite may give an indication.

The X-ray diffraction analyses of this profile (table 2.32) show besides illite and 7 Å minerals (kaolinite + metahalloysite) traces of 14 Å minerals. There are some indications that these are vermiculites. The films did not show recognizable reflections of smectite minerals, which are normally common in vertisols.

The content in mineral assemblage varies little. Only in the samples of the top horizons reflections are somewhat stronger compared with the reflections in those of the lower horizons. The small variation is also evident from the normative mineralogical composition (table 2.33).

The increase from the Bw2 horizon upwards in mica and free silica content in the fraction <2 mm is evident. This can

Table 2.32 Semi-quantitative X-ray diffraction analyses of the fraction < 2 μm of profile Sp/234 (chromic vertisol).

Horizon	Depth of sample (cm)	14 Å[1]	10 Å (Ill)	7 Å[2]	Qtz %	Hm
Ah	5-15	tr	++	++(+)	ca. 1	(x)
Bt	25-40	tr-(+)	++(+)	++(+)	ca. 1	(x)
Bw1	70-90	tr-(+)	++(+)	++(+)	1	(x)
Bw2	120-140	tr	++	++	1	(x)
Bw3	200-220	tr	++(+)	++(+)	1	(x)
Bw4	270-290	tr	++	++	1	(x)
C	310-325	tr	++	++	1	(x)

[1] 14 Å = probably vermiculite [2] 7 Å = kaolinite + metahalloysite

Table 2.33 Normative mineralogical composition of the fractions <2 mm and <2 μm of profile Sp/234 (chromic vertisol), given in weight percentages.

Fine earth fraction (<2 mm)

Horizon	Depth of sample (cm)	Dol	Cc	Verm	Ill	Kaol	Q	Hm	Mica[1]	Plag	Ru	Misc[2]	W	CO_2
Ah	5-15	-	-	1	13	53	12	9	6	4	1.0	1	+3	-
Bt	25-40	-	-	1	16	48	14	9	7	3	1.1	1	+2	-
Bw1	70-90	-	-	1	17	58	7	9	3	3	1.0	1	+2	-
Bw2	120-140	-	-	1	18	60	6	9	1	3	1.0	1	+2	-
Bw3	200-220	-	-	1	18	61	5	9	2	2	1.0	1	+2	-
Bw4	270-290	1	-	1	18	62	4	9	tr	3	0.9	1	+3	-
C	310-325	74	19	tr	1	2	3	tr	tr	1	tr	tr	+2	-2
R		80	15	-	-	tr	4	tr	-	1	tr	tr	+3	-2

Clay fraction (<2 μm)

Horizon	Depth of sample (cm)	Dol	Verm	Ill	Kaol	Q	Hm	Ru	Misc[3]	W	CO_2
Ah	5-15	-	1	18	63	5	8	0.9	4	+2	-
Bt	25-40	-	1	23	59	4	9	0.9	3	+2	-
Bw1	70-90	-	1	21	61	4	9	0.9	3	+2	-
Bw2	120-140	-	1	18	62	6	9	0.9	3	+2	-
Bw3	200-220	-	1	20	62	5	9	0.9	2	+2	-
Bw4	270-290	-	1	19	63	4	9	0.9	3	+3	-
C	310-325	1	1	24	58	4	8	0.9	3	+2	-1

[1] Mica = biotite + muscovite [2] Misc = augite + gibbsite + strengite + pyrolusite [3] Misc = plagioclase + strengite + pyrolusite

also be noticed in the fraction <2 μm in which the illite content increases from the Bw2 to the Bt horizon from 18 to 23 %. The same feature was established in the profiles Sp/122 and Sp/123 (see 2.5.1) and has been attributed there to the admixture of volcanic material.

In this view fits also well the trend in the mica content, the increase of which cannot be solely explained by differences in texture between the two horizons.

The admixture of volcanic material is not as evident as in the soils discussed in 2.5.1 (e.g. profile Sp/123, the chromic luvisol). Volcanic minerals have not been noticed at the time of profile description, but a volcanic component could be established under the binocular microscope in the sand fraction of the samples of the Ah, Bt and Bw1 horizon (viz. biotite and augite).

The mineralogy of this profile is quite well comparable with the thick profiles at IL Vallangero (see 2.5.1), except for the presence of (possibly) vermiculite in this soil. Illite and kaolinite content agree rather well but are somewhat more pronounced in profile Sp/122. In fact the mineralogy of profile Sp/123 which is more affected by colluviation processes and admixture of volcanic material is very close to the mineralogy

luviation processes and admixture of volcanic material is very close to the mineralogy of profile Sp/234.

The persistence of 14 Å minerals (possibly vermiculite) has already been discussed in the preceding text. It fits well in the view postulated there that vermiculite is one of the stable phases in soils and weathering products on dolomite due to high $[Mg^{2+}] / [H^+]$ ratios in the soil solution.

The soil in fissure in dolomite near Sperlonga (profile E 80, a chromic luvisol).

Between Itri and Sperlonga a large area occurs with dolomite and dolomitic limestone of Triassic and Lower Jurassic age (Servizio Geologico Italiano, 1966). The area was mapped by the author as part of the soil survey project "Southern Italy" carried out by the section for Soil Mapping of the "Fysisch geografisch en Bodemkundig Laboratorium" (Sevink et al., 1979). During this survey a soil in fissure in dolomite was described approximately 3 km east of Sperlonga. Physico-chemical and chemical analyses were carried out, but because of lack of X-ray diffraction analyses at this moment the normative mineralogical composition (table 2.34) obtained from the chemical analyses, must be regarded as tentative.

Table 2.34 Tentative normative mineralogical composition of the fractions < 2 mm and < 2 μm of profile E 80 (chromic luvisol), given in weight percentages.

Fine earth fraction (< 2 mm)

Horizon	Depth of sample (cm)	Dol	Cc	Q	Plag	Or	Mica[1]	Aug	Go/Hm	Sm	Ill	Kaol	Ru	Misc[2]	CO_2
Ah	5-15	3	tr[4]	10	8	6	1	4	8	4	15	40	0.8	0.5	+2 –
Bt1	20-30	tr[4]	–	5	7	4	2	–	9	7	17	48	0.8	0.5	+2 +0.4
Bt2	35-55	tr[4]	–	2	5	2	1	–	10	8	18	53	0.7	0.5	+1 +0.5
Bt3	80-100	67	6	13	1	2	tr[4]	–	3	1	2	5	0.2	0.3	tr[4] +0.1

Clay fraction (< 2 μm)

Horizon	Depth of sample (cm)	Dol	Sm	Ill	Kaol		Go	Ru	Misc[3]	W	CO_2
Ah	5-15	0.9	6	21	57	2	10	0.7	2	+3	–
Bt1	20-30	0.1	9	21	58	tr[4]	10	0.7	1	+2	+0.5
Bt2	35-55	0.4	9	20	58	1	10	0.7	1	+1	+0.5
Bt3	80-100	0.9	11	21	53	2	10	0.7	1	+2	+0.2

[1] Mica = biotite [2] Misc = strengite + pyrolusite [3] Misc = albite + calcite + strengite + pyrolusite [4] tr = less than 0.1%

The figures of the fraction < 2 μm show little variation except for the Mg-alumino-silicates (Sm) which tend to decrease towards the surface. As for the fraction < 2 mm, an increase in content of free silica, plagioclase and orthoclase can be noted as well as the necessity to convert an excess in CaO, MgO and FeO together with SiO_2 to augite

Some remarks have to be made however, on the FeO/Fe_2O_3 analyses. These analyses for this profile were carried out according to the method of Clemency & Wagner (1961) by dissolving the samples in a mixture of H_2SO_4 (96 %) and HF (48 %) while heating (180° C). Recent investigations by the laboratory section of the "Fysisch Geografisch en Bodemkundig Laboratorium" have shown that the presence of relatively high amounts of organic carbon (A-horizon material) causes reduction of Fe (III) to Fe (II) during this treatment. Consequently, the FeO figures of this profile may be somewhat too high, especially in the upper part and should be partly converted into ferric iron.

This most probably explains the decrease towards the surface in Go/Hm content in the fraction < 2 mm and partly the necessity to introduce augite in the calculations. The presence of augite however, would not be surprising as in a number of top soils in this area admixture of volcanic minerals is noticed (Sevink et al., 1979).

This soil differs from the soils in fissures in limestone by the near absence of vertic features. In the lower part of the deeply developed profile on dolomite (profile Sp/234) however, still relatively strong vertic properties like many wedgeshaped aggregates and slickensides occur. It is thought that differences in profile thickness play an important role in the different behaviour of these soils.

The soil in fissure in dolomite is largely surrounded by the "dolomitic sands". This creates a relatively dry position for the soil because upon the moistening the water will be drained to a great extent through the "dolomitic sand" zone.

This is not the case in both the deeper profiles on dolomite in which the penetrating rainwater has to pass through the soil before reaching the "dolomitic sand" zone, nor in the soils in fissures in the limestone where this highly permeable layer lacks. Moreover lateral supply may play an important role, which of coarse will be only very small in the case of the soils in fissure. These differences may account for the different profile development of this soil.

2.6 Summary, discusion and conclusions.

2.6.1 Summary of the mineralogical and chemical data of the limestone and soils on limestone and the calculated theoretical weathering paths.

In the preceding sections several aspects of the weathering and soil formation on limestone have been discussed. They can be summarized as follows.

The analyses of the limestone rock samples show a varying composition in carbonate minerals. The whole range between limestone (Sp/123i) and dolomite (Sp/183e), according the classification of Cayeux (Chilingar et al. (Ed),1967) occurs. Most of the samples are of intermediate composition and can be described as dolomitic limestone.

The insoluble residue of the limestone consists of a mixture of mainly illite and quartz with small amounts of smectites, chlorites,7 Å minerals, feldspars, pyrites and anastases. One of the samples showed a considerable amount of 7 Å minerals, probably dickite.

The soils on the other hand show a dominance of 7 Å minerals (mainly kaolinite and metahalloysite), together with illite, quartz and ferric oxides and hydroxides (mainly haematite).

The weathering path calculations show that at partial CO_2 pressures higher than 10^{-2} bar, kaolinite is the stable phase in the weathering products of limestone. Partial CO_2 pressures in the water samples from springs vary from $10^{-1.28}$ to $10^{-2.40}$, with a mean value of $10^{-1.71}$ bar (appendix 5.2) and demonstrate that the theoretical result is in accordance with the dominance of 7 Å minerals in the soils. The theoretical chemical composition of the solution is in fair agreement with the chemical composition of the water samples, except for the K, Al_t and H_4SiO_4 content (see 2.3.1, table 2.8).

In most of the soils a decrease in illite content from the surface of the soil downwards is followed by an increase towards the limestone. This decrease is more or less parallel to the occurrence of volcanic minerals and is therefore interpreted as being caused by admixture of volcanic material. It will be shown below that the disagreement between the theoretical and the real composition of the soil solution also points to an influence of volcanic minerals.

Because of this the soils are divided into two parts: (1) a lower part most probably to be purely attributed to the weathering of the limestone and (2) a top part in which admixture of allochtonous material and colluvial processes play an important role. This top part is of varying thickness and differs horizontally within a few metres.

2.6.2 Discussion of the weathering processes.

Illite

The mineralogical analyses of the soils on limestone still leave some questions open. One of the main problems is the apparent stability of illite in the soil.

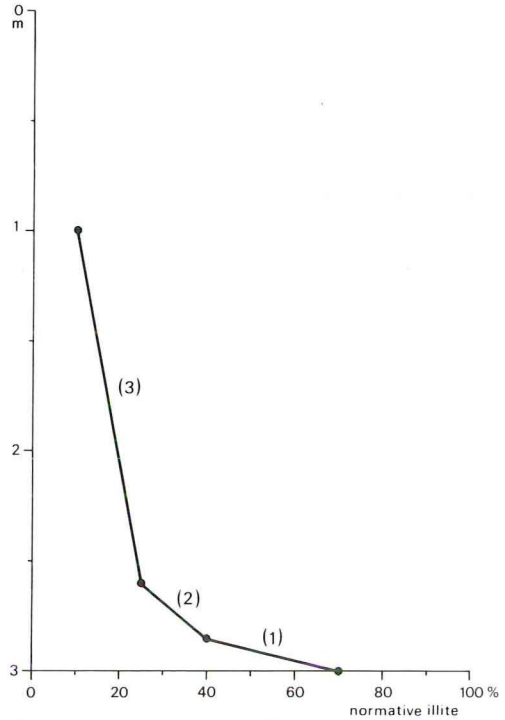

Fig. 2.34 Schematic illite content in an ideal soil profile on limestone.

A close examination of some profiles and samples (Sp/65, Sp/103, Sp/122 and Sp/227) indicates that the illite contents in the weathering zone provide some interesting data. This zone, the bottom half of the profile, may in fact be divided into three separate subzones: (1) a strong decrease (from ± 70 to 40 % normative illite) from the limestone upwards within a few decimetres, (2) a somewhat less strong decrease (from ± 40 to 25 % normative illite) immediately above the first decimetres and (3) a much smaller decrease over 1 or more metres up to the top half of the profile (fig. 2.34). The decrease in illite content within the above mentioned subzone (3) is much less than would be expected from the presumed instability of illite under the given conditions. The illite content within all three subzones also shows variations (see e.g. profile Sp/122, section 2.5.1 and table 2.12/13). Other investigations on soils on limestone show similar features (Caroll & Hathaway, 1954; Miller, 1972). This could be caused by e.g. the physical properties of the soils. Particle size analyses show a high clay percentage, mostly more than 80 %. Moreover, most of the soils show vertic properties, especially in the lower parts of the solum. This together causes slow permeability within the peds and restricts the action of water as a weathering agent mainly to the outer zone of the ped. This differential weathering has been demonstrated in profile Sp/97 by the analyses of the light grey and red mottles (see 2.5.3). Pseudogleyic features also often occur in the non-colluvial soils on limestone. This pseudogley formation is an aspect of the process of differential weathering of the peds.

The relatively low permeability of the peds in these heavy clay soils, although it does not inhibit the preferential leaching of kaolinite, may prevent the decomposition of illite. Moreover, the apparent stability of illite is favoured by the supersaturation of the soil solution with respect to illite (see 2.4.2, table 2.10). The cause for the supersaturation should most likely be explained from the admixture with volcanic material. In this view the disagreement between the theoretical and the actual composition of the solutions with respect to K, Al and Si is interesting

The (K^+), $(Al^{3+})_t$ and $(H_4SiO_4^0)$ in the sampled waters are 3-4, 3-5 and 9-12 times higher than in the theoretical solution (see 2.3.1). The ratio of "disagreement" of these components is approximately 1:1:2 to 3. This ratio is very similar to the element ratio in a number of volcanic minerals, which occur as admixture in the soils on limestone (e.g. biotite, K- containing volcanic glass). As these minerals are unstable in this weathering environment , as indicated for instance by the frequent undersaturation of the soil solutions with respect to biotite (annite + phlogopite, appendix 6), it is thought that their decomposition contributes to the supersaturation of the water samples with respect to illite, and thus prevents the decomposition of illite or even leads to illite formation.

However, also other factors have to be considered in view of the disagreement between the theoretical weathering model and the actual mineralogical composition of the soil as weathering product. This disagreement might result as well from the assumption of equal reaction rates of the rock forming minerals (see 2.2.1). It is very likely that

this assumption is not correct. The carbonates are removed faster than the speed of dissolution and transformation of the minerals in the insoluble residue. This leads to an only partial decomposition of the non-carbonate minerals, e.g. illite, which then are taken up in the soil.

In this view it is of interest that the dissolution behaviour of carbonates is opposite to that of most other minerals. Carbonates become more soluble at decreasing temperatures at a certain partial CO_2 pressure, while most minerals have a higher solubility at increasing temperatures. The effect of temperature on the mineralogical composition of the soils on limestone can be postulated from the literature.

In his study on rendzina formation in Graubünden (Switzerland), Brugger (1974) showed that the illite content from rock to soil only decreased slightly. Chemical analyses of limestone and weathering residues in Switzerland, given by Blanck (1930) (p. 104), can be interpreted the same way as they show a sharp decrease in CaO and CO_2 and occasionally MgO and an increase for the other oxides going from parent rock to the related soil. Lippi-Boncambi et al. (1955) report well crystallized illite in a mountain rendzina in Umbria (Italy), which points to inheritance from the underlying limestone. The sample contained 70 % illite, 5 % kaolinite and 10 % quartz. Also Scheffer & Schachtschabel (1976) report illite and montmorillonite as the main clay minerals in the rendzinas of the mid-latitudes.

On the contrary in soils on limestone in tropical and subtropical regions illite is only present in very small amounts or absent. Mohr et al., (1972), comparing the clay mineralogy of some black earths, rendzinas and chernozems in Australia, give moderate amounts of illite (viz. 30-40 %) for the rendzinas. As the illite content of the parent rock is not known, nothing can be said about a possible decrease in illite content. However, the figures mentioned above are lower compared with the general illite content of limestone rocks.

Analyses of bauxites on limestones of Jamaica did not reveal illite at all (Beaven & Dumbleton, 1966 ; Ahmad et al., 1966). Beaven and Dumbleton report considerable amounts of kaolinite besides varying amounts of gibbsite (+ boehmite) and iron-(hydr)oxides. Kaolinite content is rather low (3-9 %) in the figures given by Ahmad et al. (1966). The investigated samples mainly consisted of gibbsite, boehmite and goethite.

From the literature cited above it can be postulated that temperature plays an important role in the weathering of limestone. In cold and temperate climates the decomposition of illite tends to stay behind the dissolution of the carbonates. In tropical and subtropical climates alteration of illite seems to keep step with the dissolution of carbonates or tends to stay behind only slightly.

Theoretically alternation of warmer and colder periods will thus be reflected by varying amounts of illite content in the soils. In fact this might be an explanation for the variation in illite content observed in some thick soils on limestone. This interpretation however, must be handled very carefully as admixture of allochtonous material and variation in mineralogical composition of the parent rock might also influence the illite content.

Other minerals.

Besides dissolution of illite and precipitation of alumino-silicates (kaolinite, metahalloysite, halloysite), there are indications that during the weathering process of limestone also transformation of illite to some kind of 14 A mineral and/or smectite occurs. This is especially found in the lower parts of the soils and in the weathering cracks. As this appears to be restricted to the neighbourhood of the weathering zones of limestone, the buffering environment, leading to neutral pH's and a moderate $[Mg^{2+}] / [H^+]$ ratio must account for it. The phase relations shown e.g. in fig. 2.10 show that $[Mg^{2+}]$ of 1 mmol/l already brings the lg $[H_4SiO_4^o]$ (e.g. $\pm$ -4), lg $[Mg^{2+}]$ + 2pH (e.g. $\pm$ 11) plot near the phase boundary between Mg-chlorite and kaolinite.

Verstraten (1978) recently showed that above the kaolinite stability field the stability field of a vermiculite is found. The phase boundary between vermiculite and kaolinite in his diagram differs only slightly from that of the phase boundary between

Mg-chlorite and kaolinite, shown in fig. 2.10.

Decalcification and the following decrease in pH cause shifting of the lg $[H_4SiO_4^o]$, lg$[Mg^{2+}]$ + 2pH plot into the kaolinite stability field. This explains the disappearance of 14 Å minerals further away from the weathering zone of the limestone.

When the results of the weathering path calculations are examined, it is clear that (theoretically) gibbsite or kaolinite can be expected as weathering products of nearly pure limestone at partial CO_2 pressures higher than 10^{-2} bar. Which mineral will occur, depends on the point of opening of the system. This can be in the gibbsite stability field if a rapid removal of the solutes like dissolved silica takes place, thus under high rainfall and leaching conditions. In environments with moderate rainfall and/or moderate leaching kaolinite will be the stable phase. These circumstances occur in the mediterrenean climate and hence the presence of large amounts of kaolinite in the red clayey soils on limestone can very well be explained.

Valeton (1972) states, that the "terra rossa" forms an intermediate stage between limestones and bauxites. It has been shown above that kaolinite can form a stable phase in the weathering sequence of limestone. Therefore Valetons statement is incorrect and should be modified: besides bauxite also "terra rossa" as a kaolinite soil can form the final product of limestone weathering.

2.6.3 The age of the soils on limestone and dolomite.

The age of the soils on limestone has been a subject of discussion for many years. Related to this were the polemics in the twenties and thirties of this century on the origin of the red soils on limestone. The opinions on the age are manyfold. They can be summarized as follows:

- Soil formation started in the Pliocene and continued until the present with a discontinuous of rubefaction (Bottner & Lossaint, 1966; Markovic - Marjanovic, 1972).
- The start of the soil formation is uncertain but continues until today, including the rubefaction (Reifenberg, 1947; Klinge, 1957; Maignien, 1959; Lamouroux, 1965).
- The soil formation is restricted to pluvial climates as only during these times enough limestone can be dissolved that correspond with the residues found (Birot, 1953; Mensching, 1955).
- The soil formation has taken place in tropical and subtropical climates during the Quaternary (Demangeot, 1965; Duchaufour, 1970; de Bruin, 1970).
- The red soils in fissures have developed starting in the Würm pluvial period and lasting until today (Mohr et al., 1972).

The results of the weathering calculations (see section 2.3) did not permit an estimation on the age of the soils as the resultant weathering products deviated from the actual composition of the soil material by a relatively high amount of dolomite. As the overall equilibrium composition of the theoretical solution was in fair agreement with respect to Ca, Mg and HCO_3 content, compared with the sampled spring waters, a calculation method was adopted based on the actual content of Ca and Mg in the spring waters.

It has been assumed that the calcium and magnesium in these samples are derived from the carbonate constituents in the limestone rock. As the concentrations of Ca and Mg (in mmol/l) are known, it is possible to calculate the amount of carbonates ($CaCO_3$ + $MgCO_3$) in the limestone rock, dissolved in one liter. Carbonates + insoluble residue is regarded to be the composition of the limestone.

The maximum concentrations of Ca and Mg are found in sample Sp/19b and are equal to 370.4 mg carbonates/l. The mean total (Ca^{2+}) and (Mg^{2+}) in the samples of the springs is approximately 280 mg carbonates/l. Italian investigations of some large springs near the main research area show higher Ca and Mg concentrations (see table 2.35), varying from approximately 445 mg carbonates/l (Ninfa) to approximately 750 mg carbonates/l (Cassino). The cause of these higher amounts has been discussed in section 2.4.1 and is thought to be related to the geological structures.

For the calculations on the theoretical age of the soils on limestone, the following

Table 2.35 Mean annual chemical composition and temperature of samples from springs, issuing from the Monte Lepini – Ausoni – Aurunci into the Pontinia plain and from the spring near Cassino, issuing from the Monte Simbruini – Ernici into the Valle Latina, in mmol/l.

	t °C	pH	Na^+	K^+	Ca^{2+}	Mg^{2+}	Cl^-	SO_4^{2-}	HCO_3^-
Ninfa	13.7	7.8	0.20	0.02	3.70	1.10	0.45	0.22	4.25
Fontana dal Muro	15.4	7.7	3.26	0.13	5.15	2.18	4.06	0.65	6.00
Sardellane	16.2	7.8	2.60	0.15	5.57	2.42	3.95	0.81	6.15
Cassino	13.5	7.5	0.16	0.03	6.48	1.53	0.37	0.27	7.65

(data provided by the Laboratory for Hydrogeology, Geological Institute, University of Rome, 1976)

figures, based on the analyses described in appendix 3, are used:

bulk density of the limestone	2.75 g/cm^3
porosity of the limestone	5 %
amount of insoluble residue	1 %
porosity of the soil	40 %

For varying amounts of solubility of the limestone equations were developed with, as variables, the amount of effective rainfall (p) in dm^3 (=l)/year and the number of years necessary to release an amount of insoluble residue comparable to a soil with a depth of 1 m (t). The obtained equations at the various solubility levels were:

200 mg carbonates/l: $p.t = 8.16 \times 10^6$
250 mg carbonates/l: $p.t = 6.53 \times 10^6$
300 mg carbonates/l: $p.t = 5.44 \times 10^6$
350 mg carbonates/l: $p.t = 4.66 \times 10^6$
400 mg carbonates/l: $p.t = 4.08 \times 10^6$
500 mg carbonates/l: $p.t = 3.26 \times 10^6$

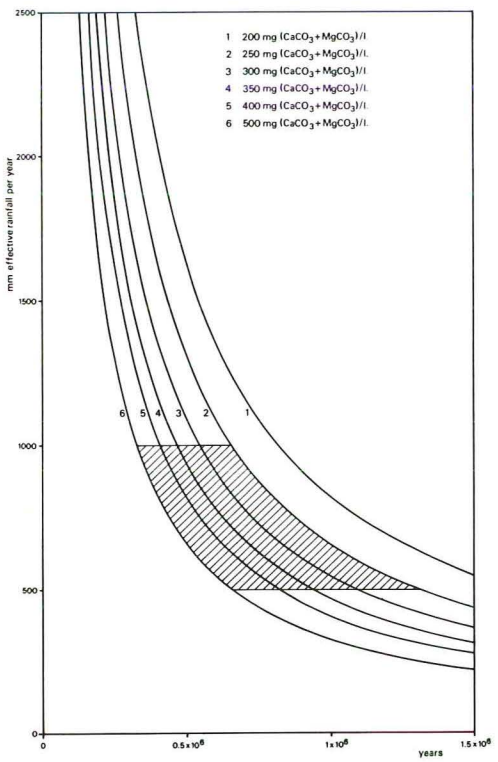

Fig. 2.35 Relation between mm effective rainfall/year and number of years necessary to produce a soil of 1 m depth at various levels of solubility of the limestone. For dashed area see text.

No rectalinear relationship exists between the two variables. This is demonstrated in fig 2.35 showing these relationships, from which it has to be concluded, that at high effective rainfall rates (e.g. 1500 mm), the number of years necessary to obtain a soil of 1 m depth does not decrease as much as at lower effective rainfall rates (e.g. 500 mm).

The present-day effective rainfall is approximately 650 mm/year (see table 1.3, surplus). If it is assumed that during the past the minimum effective rainfall has been 500 mm/year and the maximum 1000 mm/year and the amount of dissolved carbonates, which depends on temperature and partial CO_2 pressures, has varied from 250 mg/l to 500 mg/l, a minimum age of a soil of 1 m thichness is acchieved at 325 000 years and a maximum age at 1 300 000 years. This is indicated in fig. 2.35 by a dashed area.

It seems reasonable to assume that a "regolith" of 1 m thickness on limestone needs at least 500 000 years to be formed under the given conditions. As soils of 4 m

thick occur on mountain slopes, their soil formation must have started at least 1.3 million years ago (4 x 325 000 years), but most probably earlier (4 x 500 000 years).

In this view recent investigations by Remmelzwaal (1978) and Sevink et al. (1979) show interesting results. K - Ar datings on volcanic deposits in the Amaseno basin, west of the main research area appear to be about 1 million years and seem to be the oldest occurring tuff deposits in the neighbourhood.

As mentioned in the previous sections, no admixture with volcanic material could be detected in the lower parts of some soils. This might indicate that the top part of the non-affected soils should be at least older than 1 million years. It is very unlikely that they are younger than the last volcanic eruptions as even the very young soils (the lithosols and rendzinas of the mountain slopes) show a considerable admixture with volcanic minerals (Sevink et al., 1979).

One profile, a chromic vertisol in colluvial deposits (Sp/97) also lacked any evidence of volcanic material. As the mineralogical composition of this soil could only be explained by reversion of an older "in situ" soil and the colluvial character is beyond doubt (see 2.5.3), this must also be older than 1 million years. In fact, the "mother" soil of this profile must have had a relatively long period of soil formation as within the colluvial profile no indications were found of stratification due to periodical colluviation. Therefore the part of profile Sp/97 between 35 and 170/185 cm is regarded as inherited from one "mother" profile. This means in view of the calculations which seem to be not far from the truth, an age for the "mother" soil of at least 500 000 years but most probably more. Together with the age of profile Sp/97, the oldest soil formation period which can be reconstructed, must be between 1.5 and 2 milion years ago.

Most probably these figures are still too low as in the calculations ideal circumstances, i.e. effective rainfall between 500 and 1000 mm, are used. It is questionable if this surplus (precipitation minus evapotranspiration) has always been as high over the long period mentioned and if the total surplus may be taken into account as effective for soil formation.

However, the figures presented above, point to a soil formation, which started most probably not later than in early Quaternary times and continues still today.

2.6.4 Conclusions.

In the foregoing sections the weathering of and soil formation on limestone have been investigated. A theoretical model for the weathering of a particular dolomitic limestone has been developed and is compared with the mineralogical composition of the soils on limestone and with the chemical composition of the soil - and karst waters. The results show a fair agreement between the mineral assemblage given by the theoretical model and the actual one. Differences between them could very well be explained by admixture of allochtonous material, mainly airborne volcanic dust and physical properties such as poor permeability of the peds in these heavy clay soils, which were not taken into account in the theoretical model. The fair agreement between the theoretical model and the reality promises much for investigations in the future, especially if more is known about the reaction rates of minerals.

The mineralogical change during the weathering can be described as follows. Carbonates are removed completely with calcite more rapidly than dolomite. The non-carbonate residue is transformed into kaolinite and free iron compounds with a residual enrichment of the immobile component such as quartz, rutile, anastase etc. The transformation from the weatherable minerals to kaolinite can be direct (hydrolysis and precipitation from the solution) or indirect. Fig. 2.36 presents a diagram of this weathering model.

Differences between the mineralogy of the soils on limestone and those on dolomite are only small. Probably due to a higher $[Mg^{2+}] / [H^{+}]$ ratio in the soil solution of the latter soils, induced by weathering of dolomite, 14 Å minerals like vermiculite may form a stable phase, but their occurrence is only of secondary importance. Kaolinite and illite are still the major constituents in the soils on dolomite.

Of influence on the soil formation may be relatively thick weathering residues of dolomite. In certain cases, viz. if they extend to the surface they may create a more dry environment compared with the soils on limestone, where these "dolomitic sand" layers lack.

Physical properties of the soils on limestone such as the high clay content and the vertic properties considerably influence the mineralogy of the soils. Poor permeability of the peds delimit the active area of water penetrating into the soil.

The age of the soils on limestone cannot be determined accurately, but soil formation started probably 1.5 to 2 million years ago, perhaps earlier, and continues still today.

The weathering of large limestone areas may be of geological importance as through the tremendous loss in weight in a relatively short period tectonical movements may be enhanced.

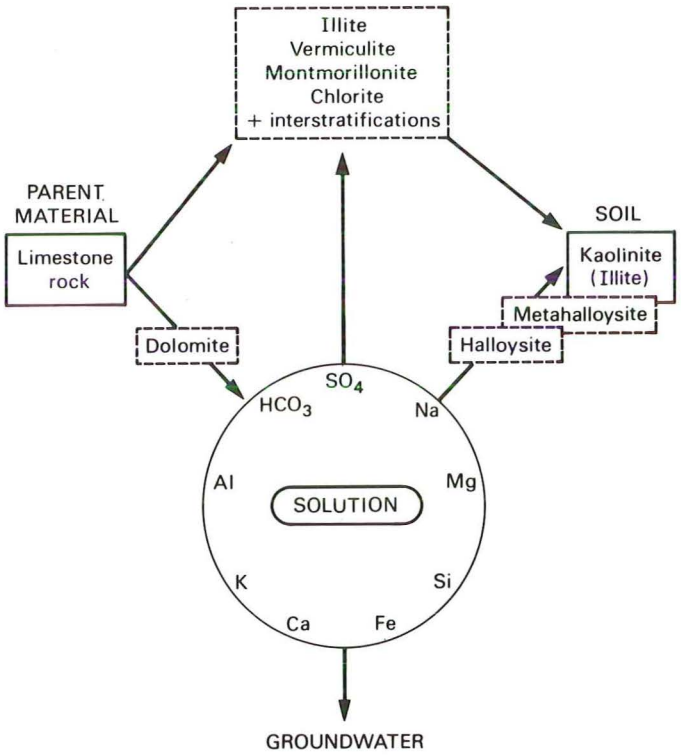

Fig. 2.36 Diagram of the various mineral (trans-)formation and (trans-)formation paths during the weathering of limestone.

CHAPTER 3 SOILS ON MIOCENE AND PLIOCENE SEDIMENTARY ROCKS

In the previous chapter soil formation on limestone and dolomite has been discussed. It has been concluded that soil formation has started at least in early Quaternary times.

Besides soils on limestone and dolomite also soils in other parent materials, viz. shales and sandstones of Miocene age and conglomerates and sandstones of Pliocene/old Quaternary age, occur (see appendix 1: soil map). These soils are discussed below as they appear to be of great help in reconstructing the landscape evolution and to obtain an insight in the soil-forming processes.

3.1 Soils on (calcareous) shales, (calcareous) sandstones and (calcareous) conglomerates: general characteristics, mineralogy and soil-forming processes.

Two major occurrences of soils on other than calcareous rocks will be discussed below. These are (1) soils on calcareous shales and calcareous sandstones of Miocene age and (2) soils on conglomerates and sandstones of Pliocene and/or old Quaternary age. These soils are located in the northern and eastern parts of the main research area and locally in the central part.

Along the Sacco River and in the valley bottoms of its tributaries alluvial and alluvio-colluvial deposits occur. They, and the soils formed in them are of little relevance for the present study. They are discussed by Sevink et al. (1979) in a larger context.

3.1.1 The soils on calcareous shales and calcareous sandstones of Miocene age.

Shales of Miocene age ("argille caotiche") border the main research area at its northern and eastern fringes (see section 1.6). Locally consolidated sandstones occur, while sandy strata were frequently observed in the shales. The area has a rolling to hilly physiography and is dissected by many streams. Most of these are fed by springs from the limestone area. The shales are susceptible to mass movements and landslides ("franas") as a result of these are found at several locations , especially in the zone between San Giovanni Incarico and Monte Lamia.

The soils in the weathering products of shales are rather uniform and were classified either as calcaric regosols (strongly affected by erosion) or as calcic cambisols (slightly affected by erosion. Northwest of San Giovanni Incarico and between this village and Pico dark colluvium derived from eroded rendzinas and lithosols on limestone covers the soils on shales. These soils were classified as calcic kastanozems (see e.g. profile Sp/106).

One of the main characteristics of the calcic cambisols is the occurrence of a distinct calcic horizon. The clayey texture and the montmorillonitic mineralogy (see e.g. profile Sp/166) contribute to a vertic character of the soils. It would be wrong, however, to attribute these vertic properties only, or even mainly, to soil-forming processes as the parent rock also shows slickensides.

Miocene sandstones have a limited extension in the main research area. They are found mainly in the eastern part as a spur from the large occurrence near Colle Tronco, approximately 2.5 km southeast of San Giovanni Incarico, and near Colle della Pece in the northwest. In general, the relief of the sandstones has steeper slopes than those in the shales and very few well developed soils occur. Soils developed on Miocene sandstones are to be classified as eutric cambisols. Also a more eroded phase on this parent rock could be distinguished and were classified as eutric regosols. Locally, where erosion is very strong, lithosols occur. In contrast to the soils on shales, formation of a calcic horizon has not been observed in the soils on calcareous sandstones. Hence decalcification must be an important process in these soils.

Five profile are described, three of these are soils on calcareous shales (profiles Sp/141, Sp/166 and Sp/191, all calcic cambisols), one a soil on calcareous sandstone

(profile Sp/258, an eutric cambisol) and one in colluviuvium derived from shales overlying a reddish brown soil on limestone (profile Sp/106, a calcic kastanozem). As well developed soils on shales and sandstones were hard to find in the main research area and good examples were studied previously (Spaargaren, 1973, 1974), these were used to illustrate the weathering and soil-forming processes on both parent rocks.

Profile descriptions and analytical data of these soils are given in appendix 2.

Soils on calcareous shales.

The soils on these shales often contain sandy strata which are of sedimentary origin. Differences in mineralogy may very well occur related to this heterogeneity of the parent material and the analytical and mineralogical data therefore have to be handled with special care.

Profile Sp/166, classified as a calcic cambisol, was described and sampled in a clay pit for brick works west of Pontecorvo. The results of the semi-quantitative X-ray diffraction analyses and norm calculations are shown in tables 3.1 and 3.2.

Table 3.1 Semi-quantitative X-ray diffraction analyses of the fraction <2 μm of profile Sp/166 (calcic cambisol).

Horizon	Depth of sample (cm)[1]	Sm	14 Å	10 Å[2]	7 Å[3]	Qtz %	Ana
Apck	10-30	+	-	(+)	(+)	1-3	tr
Bck(g)	40-55	++	tr	+	(+)	1-3	tr
Bckg	70-90	++	tr	+	(+)	1-3	tr
	120-135	++	-	+	(+)	1-3	tr
Ckg	150-170	++	-	+	(+)	1-3	tr
Cg	190-205	++	-	+	(+)	1-3	tr
R		++	-	+	(+)	1-3	tr

[1] All samples contain possibly hausmannite [2] 10 Å = probably primary muscovite [3] 7 Å = kaolinite

Table 3.2 Normative mineralogical composition of the fractions <2 mm and <2 μm of profile Sp/166 (calcic cambisol), given in weight percentages.

Fine earth fraction (<2 mm)

Horizon	Depth of sample (cm)	Sm	Ms	Kaol	Q	Ab	Go/Hm	Chl	Cc	Cp	Ru	Pr	CO_2	W
Apck	10-30	10	12	5	31	5	4	2	30	0.2	0.4	-	+0.3	+3
Bck(g)	40-55	9	12	6	28	5	4	2	33	0.2	0.5	-	+0.4	+2
Bckg	70-90	10	14	4	34	6	4	3	24	0.2	0.5	-	+1	+2
	120-135	10	12	2	33	6	4	3	29	0.3	0.4	-	+2	+2
Ckg	150-170	10	14	3	34	6	4	3	25	0.2	0.4	-	+0.3	+2
Cg	190-205	18	17	5	25	6	5	3	20	0.3	0.7	0.3	+1	+2
R		13	16	-	37	8	2	5	15	0.3	0.5	3	+1	+1

Clay fraction (<2 μm)

Horizon	Depth of sample (cm)	Sm	Ms	Kaol	Q	Go	Ab	Ru	Pr	Cc	W
Apck	10-30	32	23	10	22	8	3	0.7	-	1	+5
Bck(g)	40-55	29	22	9	23	8	3	0.6	-	5	+6
Bckg	70-90	30	23	7	19	8	4	0.6	-	8	+6
	120-135	33	24	5	18	7	4	0.6	-	8	+6
Ckg	150-170	33	26	4	18	7	4	0.6	-	7	+6
Cg	190-205	36	27	2	14	8	3	0.8	-	9	+5
R		39	28	-	14	5	4	0.8	1	8	+5

The semi-quantitative X-ray diffraction analyses do not show many differences. A slight decrease in smectite and 14 Å mineral content can be noted in the Apck horizon and the occurrence of 14 Å minerals in the Bck(g) and the top part of the Bckg horizon. The normative mineralogical composition, which is in fair agreement with the X-ray diffraction data, shows a decrease in smectite and muscovite content in the fraction < 2 μm towards the top of the profile. An increase can be observed in kaolinite and free silica content in the same direction.

The free silica content needs more explanation. The figures in table 3.2 are much higher than given by the X-ray diffraction analyses. This might suggest a high amount of amorphous silica in the soil. However, it is much more likely that at least part of the excess in free silica must be attributed ot some other mineral. Weathering of muscovite, as suggested by the normative mineralogical composition of the fraction < 2 μm, may not only produce kaolinite but also illite as intemediate stage. Introducing illite leads to a more constant figure for the 10 Å minerals (in that case muscovite+illite) as suggested by the X-ray diffraction analyses, together with lower kaolinite and free silica contents. Still free silica content remains rather high (between 15 and 18 %) with respect to the figures of table 3.1. This is mainly due to the necessary introduction of saponite in the norm calculations because of lack of normative kaolinite (van der Plas & van Schuylenborgh, 1970).

In the rock sample all normative kaolinite was used to produce normative montmorillonite from saponite according to the equation

$$28\ \text{Sap} + 68\ \text{Kaol} + 48\ \text{Q} = 144\ \text{Mm} (+ 14\ \text{W})$$

The then obtained ratio Mm/Sap was taken constant in the variant calculations of the other samples. The necessity of introducing this procedure suggest a smectite in this soil being somewhat more rich in Mg than in normative montmorillonite. The geogene origin of the smectite as deduced from its dominant occurrence in the rock, may very well explain this. Because of its deviating composition it is not unlikely that the Si-content differs as well and may be somewhat higher than in the normative montmorillonite. This however, is not introduced in the norm calculations as it is rather speculative how much free silica has to be attributed to the smectite.

Although the normative mineralogical composition of the clay fraction still shows some deficiences and bearing in mind the discussion above, some trends can be postulated from the presented figures (table 3.2). Decrease in smectite and muscovite content towards the top of the profile suggests the weathering of these minerals. However, the secondary products newly found by pedogenesis are not very well defined. The occurrence of illite as an intermediate stage of weathering cannot be excluded, as well as of some 14 Å mineral.

In this view the composition of groundwater sampled in the quarry is of interest (sp/167, see appendix 5). Fig. 3.1 shows the lg $[Mg^{2+}]$ + 2pH and lg $[H_4SiO_4^o]$ plots of the samples in $MgO - Al_2O_3 - SiO_2 - H_2O$ phase diagram. All samples appear to be situated in the Mg-chlorite stability field. As mentioned in chapter 2, Verstraten (1978) recently showed that this part of the diagram can be occupied by a vermiculite. Consequently, the formation of a vermiculite might be possible. The presence of 14 Å reflections on the X-ray films of the Bck(g) and the top part of the Bckg horizons might be an indication for this. However, these reflections are very weak and can not be attributed definitely either to chlorite or vermiculite.

The figures of the fraction <2 mm show clearly the formation of the calcic horizon. Calcite content increases from 15 % in the parent material to 33 % in the Bck(g). The formation of a calcic horizon just below the A horizon in soils with an non-flushing (hydrological) regime is a very common feature (van Schuylenborgh, 1977). Due to a higher biological activity in the A horizon, partial CO_2 pressure in the A horizon is higher than in the horizon below. Consequently, the carbonates in this horizon are more soluble and will precipitate just below the A horizon. In this soil a net transport of carbonates, however, occurs from bottom to top by capillary movements. They precipitate under the A horizon mainly because of the porous character of this horizon and of the vertic properties of the soil. Both characteristics contribute to aeration of the soil, especially in the drying-up period. By this, a soil atmosphere is created close

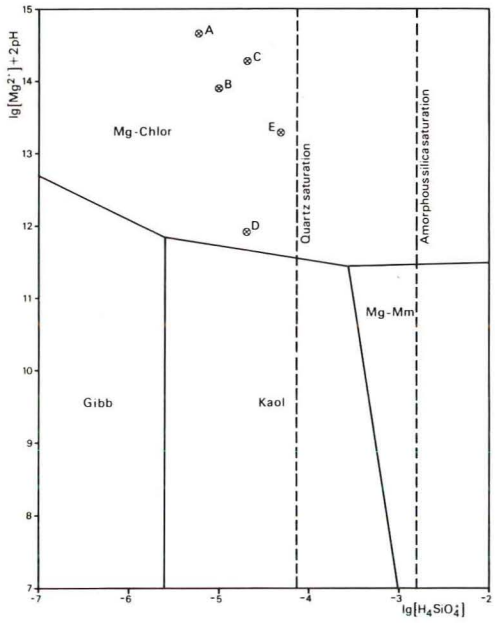

Fig. 3.1 Stability fields of Mg-chlorite (clinochlore), Mg-montmorillonite kaolinite and gibbsite in the system $MgO - Al_2O_3 - SiO_2 - H_2O$ at 15° C and 1 bar pressure. Indicated are the lg Mg^{2+} + 2pH and lg $H_4SiO_4^\circ$ plots of sample Sp/167.

to that of the air atmosphere with low partial CO_2 pressures. Hence carbonates will precipitate in the aerated parts, at first just below the A horizon.

At the time of profile description (end of June, 1971) the soil was moist from 1 m downwards. This coincides with a second peak in calcite content in the lower part of the Bckg horizon. This might be explained by differences in drying-up velocity between the top part and the lower part of the profile. At the end of the spring when the soil starts drying-up, cracking and decrease in biological activity lead to precipitation of calcium carbonate in the top part of the soil. Prolonged desiccaton is accompanied by deeper cracking and aeration of the top part of the soil. The lower part still remains moist for quite some time as is also reflected by its gleyic character. This leads to a lower zone of precipitation, whose location depends on the depth of desiccation.

Soils on calcareous sandstone.

Profile Sp/258, classified as a eutric cambisol, is located on the northern side of the Valle Latina near Coldragone. In contrast to profile Sp/166, as well as the profiles Sp/106 and Sp/191, this soil is decalcified down to a depth of approximately 2.50 m.

In the sandstones often clayey sliding planes occur. These have also been observed in the parent rock of the profile under review, but could not be detected in the solum. The sandstone itself has a very homogeneous character.

The X-ray diffraction data of the fraction < 2 μm and the normative mineralogical composition of the fractions < 2 mm, 2 - 2000 μm and < 2 μm of this soil are presented in the tables 3.3 and 3.4.

Table 3.3. Semi-quantitative X-ray diffraction analyses of the fraction < 2 μm of profile Sp/258 (eutric Cambisol)

Horizon	Depth of sample (cm)	Sm	14 Å	10.5 Å	Ill	7 Å	Qtz %	Ab	Go	1.53 A
Ap	5 - 15	+	(+)	+	++(+)	(+)	8 - 12	x	?	x
Bw	30 - 40	+	+	+	++(+)	(+)	10 - 15	x	?	x
C	50 - 70	+	+(+)	(+)	++	(+)	10 - 15	x	?	x

The X-ray diffraction data show a decrease in content of 14 Å minerals and an increase in illite content. The same holds for the normative mineralogical composition if smectite is taken constant. In the fraction 2 - 2000 μm and, consequently, in the fraction < 2 mm in table 3.4 a decrease in mica content is noted towards the surface. Weathering of 14 Å minerals and alteration of micas, the latter probably accompanied by formation of illite, can be regarded as the main weathering process. The apparent stability of the feldspars (plagioclase + orthoclase) must most likely be attributed to admixture, probably of volcanic origin.

Table 3.4 Normative mineralogical composition of the fractions < 2 mm, 2 - 2000 μm and < 2 μm of profile Sp/258 (eutric cambisol), given in weight percentages.

Fine earth fraction < 2 mm.

Horizon	Depth of sample (cm)	Q	Plag	Or	Mica	Go/Hm	Sm + Verm	Ill	Ru	Prl	W
Ap	5 - 15	50	26	9	5	3	2	4	0.5	0.1	+1
Bw	30 - 40	48	26	8	7	3	3	4	0.5	0.1	+2
C	50 - 70	48	27	6	11	3	2	2	0.5	0.1	+2

Fraction 2 - 2000 μm.

Horizon	Depth of sample (cm)	Q	Plag	Or	Mica	Hm	Ru	Prl	W
Ap	5 - 15	54	28	10	6	2	0.5	0.1	+1
Bw	30 - 40	53	28	9	8	2	0.5	0.1	+1
C	50 - 70	51	27	6	12	3	0.5	0.1	+1

Clay fraction < 2 μm.

Horizon	Depth of sample (cm)	Sm + Verm	Ill	Q	Go	Plag	Ru	Prl	W
Ap	5 - 15	30	45	3	14	7	0.7	0.4	+5
Bw	30 - 40	34	42	2	13	8	0.7	0.3	+5
C	50 - 70	37	36	2	14	10	0.6	0.2	+5

Concluding remarks.

Of the two other profiles mentioned in the introduction of this section (profiles Sp/106, a calcic kastanozem, and Sp/191, a calcic cambisol) only profile descriptions have been made. They show more or less the same characteristics as profile Sp/166.

In general the soils on Miocene shales and sandstones appear to be relatively young. They contain a high amount of weatherable minerals. The main soil forming processes are formation of a cambic horizon, formation of a calcic horizon in the soils on calcareous shales and decalcification of the soils on calcareous sandstones. The main weathering processes are alteration of smectite, 14 Å minerals and mica and most probably formation of illite. Formation of some 14 Å mineral (possibly vermiculite) in the upper horizon seems to be likely. The apparent stability of feldspars is thought to be due to admixture of volcanic material. New formation of kaolinite by pedogenesis seems to be questionable.

3.1.2 Soils on sandstones and conglomerates of Pliocene and/or Quaternary age.

In the central part and in the northwest of the main research area strongly weathered conglomerates and sandstones occur. The conglomerates bear evidence of tectonic disturbance (Angellucci, 1966) and are attributed to the Pliocene. They border the footslopes of the Monte Calvini - Monte Caruso ridge. A minor occurrence is found south of Pico. The soils on these conglomerates will be briefly discussed at the end of this section.

In the northwestern part and between Monte Nero and Monte Lamia unconsolidated sandy formations occur, which show a fluviatile character as indicated by the presence of gravel beds. Moreover just northwest of the main research area crossbedding was observed in these deposits. No evidence has been found that these sandy formations have been tectonically disturbed. This indicates a deposition after the latest orogenic movements. Therefore it is preferred to attribute these sands to old Quaternary times rather than the Pliocene in which the major tectonical movement took place (Accordi, 1965; Parotto & Praturlon, 1975).

In contrast to the soils on Miocene shales and sandstones, the soils in the Pliocene/old Quaternary deposits show a pronounced soil development. Several profiles have been studied, both on the conglomerates and in the sandy formations (profiles Sp/4

a ferric acrisol; Sp/22, Sp/41, orthic acrisols; Sp/64, a ferric luvisol; Sp/186, an eutric nitosol and C 7, a ferric luvisol. They all show a distinct argillic B formation, mostly a pseudogleyic Bgt under the Bt and, with the exception of the latter two profiles, hues of 5YR. Profile Sp/186 is regarded as a younger soil in old Quaternary deposits as will be discussed below. Profile Sp/64 probably has been truncated and this was followed by a formation of an argillic B in the Bg horizon. This probably explains the different habitus (hue 7.5YR) with respect to the reddish colours observed in the other soils. The profile descriptions of the soils mentioned above are given in appendix 2 together with their analytical data.

Soils on sandstones.

Profile Sp/4, the ferric acrisol, is regarded as an example of the most complete soil in the old Quaternary deposits. Profile Sp/22 describes a section along a footpath at Colle Arnaro, in which the major horizons were exposed, including probably the parent rock. This section is shown in fig. 3.2, with the sampling points. Near this

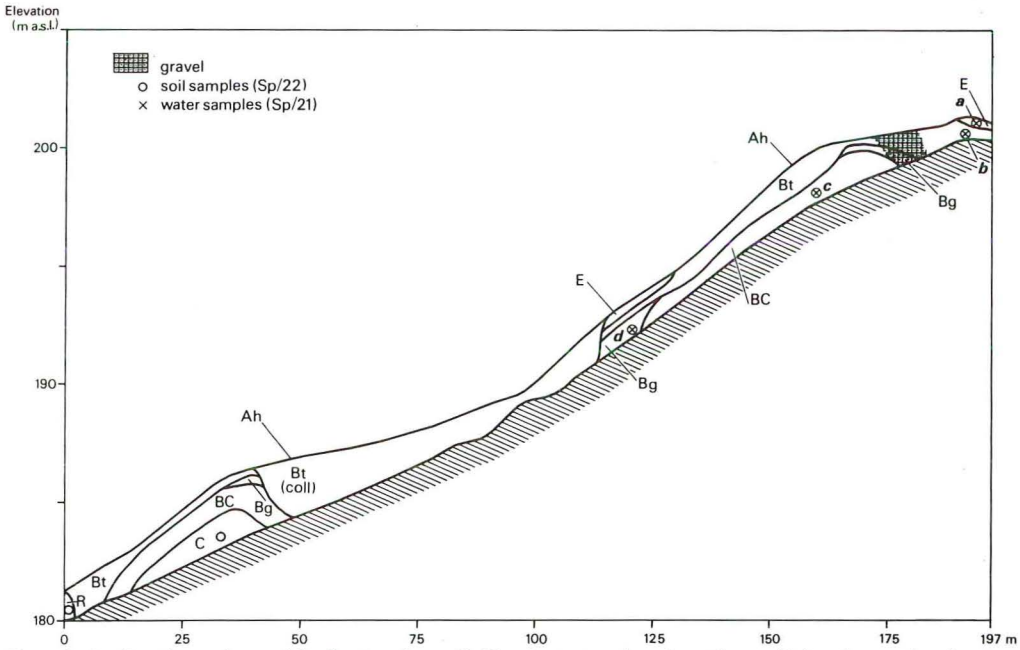

Fig. 3.2 Section alongside footpath at Colle Arnaro showing the soil horizons in the Pliocene/old Quaternary sandstones.

section also soil water samples have been collected from the E, Bt, Bg and BC horizons (samples Sp/21 a, b, c and d; see appendix 5).

Profile Sp/4 has developed in fluviatile deposits, as is indicated by the occurrence of gravelly layers. In the sandy sediments at Colle Arnaro, where section Sp/22 has been described and sampled locally gravelly strata and local gravel concentrations have been observed. Original heterogeneity therefore has to be kept in mind while interpreting the mineralogical and analytical data. It is thought however, that these possible differences are nowadays of minor importance as a long period of pedogenesis most likely has effaced the supposed heterogeneity.

The results of the X-ray diffraction analyses and the normative mineralogical calculations of profiles Sp/4 and Sp/22 are presented in the tables 3.5 and 3.6.

Table 3.5 Semi-quantitative X-ray diffraction analyses of the fraction < 2 μm of profile Sp/4 and section Sp/22.

ferric acrisol Sp/4

Horizon	Depth of sample (cm)	Mm	14 Å	10 Å (Ill)	7 Å [1]	Q %	Go	Hm	Ana
Ah	0 - 10	tr	tr	(+)	+(+)	2 - 4	x	-	tr
E	15 - 35	tr	tr	(+)	+(+)	3 - 5	x	-	tr
Bt	50 - 80	tr	tr	(+)	+(+)	2 - 4	x	-	tr
Bgt	100 - 130	tr	?	+	+(+)	3 - 5	xx	x	?
	150 - 170	tr	tr	+	+(+)	2 - 4	(x)	-	?

Section Sp/122

Horizon	Sm	14 Å	10 Å (Ill)	7 Å	Q %	Go	Ab	Cc
E	(+)	-	+	+(+) [2]	4 - 6	(x)	-	-
Bt	tr	-	+	++ [2]	4 - 6	(x)	-	-
Bgt	(+)	-	(+)	+(+) [2]	1 - 3	x	-	-
BC	(+)	(+)	+(+)	+(+) [2]	3 - 5	(x)	-	-
C	+(+)	+	+	(+) [3]	3 - 5	(x)	tr	-
R	+++	++	+	(+) [3]	3 - 5	(x)	tr	(x)

[1] 7 Å = kaolinite / halloysite [2] 7 Å = kaolinite + metahalloysite [3] 7 Å = kaolinite

The X-ray diffraction analyses of profile Sp/4 do not show much differences, though a decrease in illite content towards the top of the profile is suggested. Of interest is the appearance of a notably higher amount in goethite and haematite content in the top part of the Bgt horizon. As the chemical analyses even show a decrease in Fe_2O_3 content in the Bgt horizon with respect to the overlying horizons, this must indicate the presence of well crystalized free iron compounds, while in the overlying horizons probably more amorphous iron compounds occur.

The X-ray diffraction data of the samples of profile Sp/4 and section Sp/22 are very similar except for smectite content which is somewhat higher in section Sp/22 in comparable samples. This is also shown in the normative mineralogical composition (table 3.6). As the smectite in the samples of section Sp/22 is most probably inherited from the parent material, in which it is the dominant clay mineral, differences in parent material may be the cause of this discrepancy.

The normative mineralogical trends in the fractions < 2 μm in both profiles are essentially the same. Both show an increase in smectite + vermiculite and illite content from the Bgt horizon upwards and a decrease in kaolinite content in the same direction. Free silica is rather constant in the top part of section Sp/22 but increases towards the top in profile Sp/4.

The increase in illite content in the fraction < 2 μm upwards is not in accordance with the X-ray diffraction analyses. The most likely explanation for this is admixture with volcanic material. Increase in the top of profile Sp/4 in normative plagioclase (Ca - Na - feldspars) and mica content in the fraction 2 - 2000 μm are also indicative for this. Therefore part of the K_2O, which now is attributed totally to illite, may originate from amorphous or poorly crystalline volcanic material or from more K-rich micas. If e.g. part of the normative illite is converted into muscovite, the figure for 10 Å minerals are strongly reduced (for calculation method see preceding section).

The kaolinite content is increasing downwards in profile Sp/4. Part of this increase must of course be explained by the admixture of volcanic material in the top part of the soil. However, two other considerations have to be taken into account. In the first place and possibly related to the admixture mentioned above, micromorphological analyses revealed evidence of transportation of soil material. The E as well as the Bt samples contain papules and distinct iron-manganese nodules with a sharp boundary. The papules and nodules mentioned above are interpreted as pedorelicts, although periodic dessication also may lead to sharply limited accretionar glaebules (Drosdoff & Nikiforoff, 1940) and in situ formation can therefore not totally be excluded. Admixture with other than volcanic material, e.g. from neighbouring Miocene deposits through colluviation processes may also has taken place.

Table 3.6 Normative mineralogical composition of the fractions <2 mm, 2-2000 μm and <2 μm of profile Sp/4, a ferric acrisol, and section Sp/22, given in weight percentages.

Fine earth fraction (<2 mm).

	Hor.	Depth of sample (cm)	Q	Plag	Or	Mica[1]	Sm+Verm	Ill	Kaol	Go/Hm	Cc	Ru	Misc[2]	W
Sp/4	Ah	0-10	69	8	1	10	1	3	6	2	-	0.2	0.4	+0.3
	E	15-35	68	4	-	12	1	5	8	2	-	0.4	tr	+0.2
	Bt	50-80	50	2	-	8	2	7	25	5	-	0.5	0.4	+0.8
	Bgt	100-130	54	2	1	7	1	6	24	4	-	0.4	0.9	+0.6
		150-170	70	3	2	8	0.4	2	11	3	-	0.3	tr	+1.0
Sp/22	E		67	4	8	5	3	4	6	3	-	0.5	0.1	+1
	Bt		53	4	7	5	4	6	15	5	-	0.6	0.4	+2
	Bgt		58	3	3	10	4	4	13	4	-	0.6	0.1	+1
	BC		61	3	2	15	3	3	8	4	-	0.5	0.3	+1
	C		61	9	3	16	2	2	3	3	-	0.3	0.4	+1
	R		30	8	3	8	0.5	0.2	-	2	48	0.2	0.2	+1[3]

Fraction 2-2000 μm.

	Horizon	Depth of sample (cm)	Q	Plag	Or	Mica[1]	Hm	Cc	Ru	Misc[2]	W	CO_2
Sp/4	Ah	0-10	78	9	1	11	0.4	-	0.1	0.2	+0.1	-
	E	15-35	79	5	-	15	1	-	0.3	tr	tr	-
	Bt	50-80	80	4	-	14	1	-	0.4	0.5	+1	-
	Bgt	100-130	81	3	2	10	2	-	0.3	1	+1	-
		150-170	84	4	2	9	2	-	0.3	tr	+1	-
Sp/22	E		80	4	9	6	1	-	0.4	tr	+1	-
	Bt		75	5	10	7	2	-	0.5	0.2	+2	-
	Bgt		76	4	5	13	2	-	0.5	tr	+1	-
	BC		71	4	2	19	3	-	0.5	0.2	+1	-
	C		66	9	4	17	3	-	0.3	0.3	tr	-
	R		30	8	3	8	2	48	0.2	0.3	+1	-0.3

Clay fraction (<2 μm).

	Horizon	Depth of sample (cm)	Sm+Verm	Ill	Kaol	Q	Go	Cc		Misc[4]	W
Sp/4	Ah	0-10	6	25	50	5	10	-	0.9	3	+2
	E	15-35	6	27	48	7	10	-	1.0	1	+1
	Bt	50-80	5	17	62	4	11	-	0.7	1	+1
	Bgt	100-130	4	16	66	4	9	-	0.6	1	tr
		150-170	3	15	68	3	10	-	0.6	tr	tr
Sp/22	E		19	22	38	5	13	-	0.7	2	+3
	Bt		14	18	48	6	11	-	0.9	2	+2
	Bgt		14	15	51	5	12	-	0.7	2	+3
	BC		16	17	45	7	12	-	0.6	2	+3
	C		22	18	32	9	14	-	0.6	4	+5
	R		48	18	-	9	14	8	0.4	3	+6

[1] Mica = biotite + muscovite [2] Misc = apatite + strengite + pyrolusite [3] Shortage of CO_2 = 0.3% [4] Misc = plagioclase + apatite + strengite + pyrolusite

Table 3.7 Semi-quantitative X-ray diffraction analyses of the fraction <2 μm of some samples of profile C 7 (ferric luvisol).

Horizon	Depth of sample (cm)	Mm	14 Å	10 Å (Ill)	Kaol[1]	Qtz %	Go	Ana
Bg1	70-75	?	?	++	++	2-4	xx	(x)
	135-140	tr	?	++	++	2-4	tr	(x)
	220-230	tr	?	++	+(+)	2-4	(x)	(x)
	315-325	(+)	-	++	++(+)	2-4	(x)	(x)
Bg2	340-345	(+)	-	++	++	3-5	(x)	(x)
	440-450	+	?	++	++(+)	4-6	(x)	(x)

[1] 7 Å = kaolinite/halloysite

Table 3.8 Normative mineralogical composition of the fractions <2 mm, 2-2000 μm and <2 μm of profile C 7 (ferric luvisol), given in weight percentages.

Fine earth fraction (< 2 mm).

Horizon	Depth of sample (cm)	Q	Plag	Mica[1]	Go/Hm	Sm	Ill	Kaol	Ru	Misc[2]	W	CO_2
E	10-15	58	3	10	5	5	6	12	0.9	0.3	-0.3	-
Bt1	30-40	29	2	7	9	7	11	33	0.9	0.5	+1	-
Bt2	55-60	36	2	7	8	5	10	31	0.7	0.3	+1	-
Bg1	70-75	43	2	7	7	4	10	26	0.6	0.3	+1	-
	135-140	46	1	9	6	3	10	24	0.5	0.6	+1	+0.2
	220-230	43	2	9	6	3	9	26	0.5	1	+1	+0.1
	315-325	38	2	9	7	5	11	27	0.5	1	+0.3	+0.3
Bg2	340-345	43	3	10	6	5	12	20	0.5	1	+0.3	+0.2
	440-450	49	2	10	6	5	10	17	0.5	0.7	+0.3	+0.2

Fraction 2-2000 μm.

Horizon	Depth of sample (cm)	Q	Plag	Mica[1]	Hm	Ru	Misc[3]	W
E	10-15	79	3	15	2	0.7	0.1	-1
Bt1	30-40	72	3	19	5	0.9	0.1	+1
Bt2	55-60	76	3	15	5	0.6	-	+2
Bg1	70-75	79	3	13	4	0.5	0.2	+2
	135-140	77	2	16	4	0.4	0.3	+1
	220-230	75	3	18	3	0.4	0.9	+1
	315-325	74	3	19	3	0.4	0.8	-0.1
Bg2	340-345	73	5	19	2	0.5	0.9	-0.2
	440-450	77	3	17	2	0.3	0.5	-0.1

Clay fraction (<2 μm).

Horizon	Depth of sample (cm)	Sm	Ill	Kaol	Q	Go	Ru	Misc[2]	W	CO_2
E	10-15	16	22	42	4	13	1.2	2	+3	-
Bt1	30-40	12	18	54	1	12	1.0	2	+2	-
Bt2	55-60	10	18	57	1	11	0.8	2	+1	-
Bg1	70-75	8	21	53	6	10	0.7	1	+1	-
	135-140	6	22	52	8	9	0.6	2	+1	+0.4
	220-230	7	20	53	8	9	0.7	2	+1	+0.3
	315-325	10	21	51	5	10	0.7	2	+1	+0.5
Bg2	340-345	11	25	42	9	10	0.6	2	+1	+0.4
	440-450	11	24	41	10	11	0.6	2	+1	+0.6

[1] Mica = biotite + muscovite + traces orthoclase [2] Misc = dolomite + apatite + strengite [3] Misc = dolomite + apatite

Secondly the increase in kaolinite content downwards may also be explained by preferential eluviation of kaolinite and/or materials with similar $SiO_2Al_2O_3$ ratios (Mohr et al., 1972). Illuviation is still an important process as is clear from the thin sections of the Bt, Bgt and BC samples of section Sp/22, which in the Bgt horizon show the skeleton grains embedded in nearly perfectly orientated and birefringent ferriargilans (fig. 3.3, 3.4 and 3.5). The nature and quantity of these make neoformation of kaolinite in situ not a likely cause for the increase in clay content. Hence the most plausible explanation for the increase in kaolinite content is the above mentioned preferential eluviation.

Free silica content decreases with depth in profile Sp/4, but increases again from the Bgt "downwards" in section Sp/22.

In this view a ferric luvisol in old Quaternary alluvial fan deposits near Veroli (Province of Frosinone), which was studied in connexion with the survey project "Southern Italy", is of interest (profile C '). During the construction works for the "superstrada Frosinone - Sora" in July 1975 a section of more than 5 m deep through the strongly weathered alluvial fan deposits was exposed.

In this exposure no indications have been found on the homogeneity/heterogeneity in this section. Because a profile in alluvial fan deposits is discussed here, geogenetic differences in this soil may not be excluded. However, pedogenetic characteristics dominate so strongly, that influences of original heterogeneity most probably are of minor importance.

The qualitative X-ray diffraction analyses of a number of samples from a profile taken in this section and their normative mineralogical composition are shown in tables 3.7 and 3.8.

Both X-ray diffraction analyses and the normative mineralogical composition of the fraction <2 μm show an increase with depth in quartz c.q. free silica content. The presence of white silica concretions (see profile description, appendix 2) in the Bg1 indicates weathering of silicate minerals in the top horizons and precipitation of amorphous silica in the lower parts of the soil. Desilication can therefore be regarded as an important process in the soil.

Both X-ray diffraction analyses and normative mineralogical composition show a decrease of smectite in the lower part of the soil towards the top of the Bg1. This points not only to instability of smectite but also to its geogene origin.

Little can be said however, about the normative increase in the top part of the soil as no X-ray diffraction data are available of the upper horizons. The "increase" might as well be caused by neoformation of some big Mg-bearing 14 Å mineral, whose occurrence is already indicated by a question mark in table 3.7 and may be present in larger quantities in the upper horizons.

The increase in free silica content in the fraction <2 μm in the "lower" horizons of section Sp/22 might be explained in the same way. The mobility of silica in the Pliocene/ old Quaternary deposits is of great importance for the mineralogy of soils on other parent rocks in the neighbourhood. This has already been indicated in chapter 2, in which differences in H_4SiO_4 content in karstic springs could be related to the presence of the Pliocene/old Quaternary deposits.

The pseudogley formation in these soils (Sp/4, Sp/22) is well illustrated by the analyses of the grey and red mottles of the Bgt of profile Sp/4. Qualitative X-ray diffraction data and normative mineralogical composition of the mottles are given in table 3.9 and 3.10.

Table 3.9 Qualitative X-ray diffraction analyses of the grey and red mottles of the Bgt horizon of profile Sp/4 of the fraction <2 μm.

	Mm	14 Å	10 Å (Ill)	7 Å[1]	Qtz %	Go	Ana
Grey mottles	tr	tr	+	+(+)	3-5	xx	?
Red mottles	tr	?	+	+(+)	2-4	tr	?

[1] 7 Å = kaolinite/halloysite

Fig. 3.3

Fig. 3.4

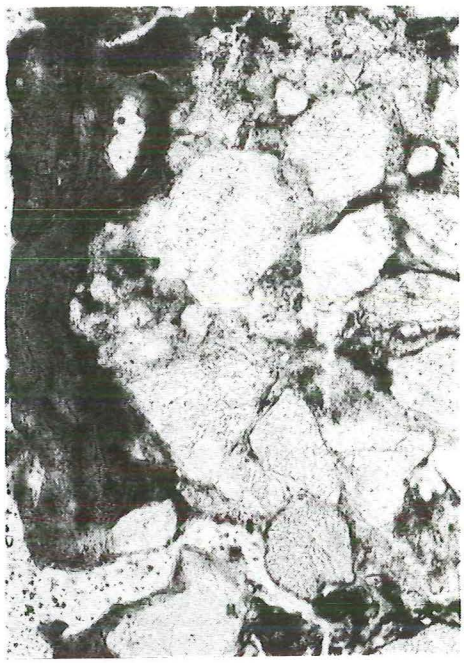

Fig. 3.5

Fig. 3.3 Bt section Sp/22. Argillan along void in porphyroskelic S-matrix. Plain light, 70x.

Fig. 3.4 Bgt section Sp/22. Ferri-argillans in porphyroskelic to agglomeroplasmic S-matrix. Plain light, 70x.

Fig. 3.5 BC section Sp/22. Interpedal ferri-argillan; agglomeroplasmic S-matrix. Plain light, 70x.

Table 3.10 Normative mineralogical composition and "free iron" content of the fractions <2 mm and <2 μm of the grey and red mottles of the Bgt horizon of profile Sp/4, given in weight percentages.

Fine earth fraction (<2 mm).

	Q	Plag	Mica[1]	Or	Go/Hm	Sm+Verm	Ill	Kaol	Ru	Str	W	"free iron"
Grey mottles	54	3	1	5	2	2	6	26	0.4	0.2	+0.5	0.9
Red mottles	60	2	5	2	8	1	4	17	0.4	0.4	+0.8	6.0

Clay fraction (<2 μm).

	Sm+Verm	Ill	Kaol	Q	Go	Ru	Str	W	"free iron"
Grey mottles	4	15	68	6	5	0.6	1	-0.6	1.4
Red mottles	4	14	58	5	19	0.4	tr	+0.5	13.7

[1] Mica = biotite + muscovite

The most striking feature is the presence of a relatively high amount of crystalline iron components (goethite) in the grey mottles and a relatively low content in the red mottles (table 3.9). Obviously the crystalline free iron (goethite) was not (strongly) affected by the deferration process, while amorphous iron compounds prevail in the red mottles. Probably redistribution of amorphous free iron compounds took place within the peds.

Besides the difference in goethite content, the normative mineralogical composition of the clay fraction does not show much differentiation. On goethite-free basis in fact, the normative content varies within 1 % for most of the minerals and for kaolinite within 2 %. This is in contrast to the mineralogy of the mottles from the soil in older limestone-derived colluvium, discussed in the preceding chapter (profile Sp/97, tables 2.28 and 2.29). Different permeability of the peds is thought to be the main cause for this difference (see 2.5.3).

A different profile in sandy deposits was described in the Monte Lamia area (profile Sp/186) Based on profile development and field observations, this profile is thought to be relatively young compared with the previously discussed soils. Fig. 3.6 shows the physiographic position of this profile and some soil relations in this area in a schematic section. The soil has been classified as eutric nitosol and arenic palexeralf (see appendix 2), the latter in analogy with the arenic paleustalfs and arenic paleudalfs (Soil Survey Staff, 1975).

No indications of sedimentary stratification have been found on the locality of the profile description. Upslope, however, a cemented gravel layer has been observed (see fig. 3.6), indicating that within the deposits mineralogical differences of geogene origin may occur.

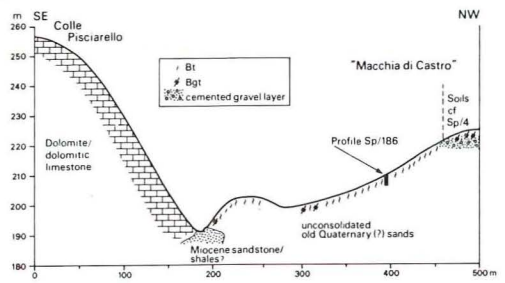

Fig. 3.6 Schematic section at the contact of the dolomitic limestone near Monte Lamia and the unconsolidated Pliocene/old Quaternary deposits of "Macchia di Castro", showing the interrelation of the older and younger soils.

On top of the ridge in the northwest, remnants were found of the Bgt as it appears in the profiles Sp/4 and Sp/22. This horizon is underlain by a horizontal gravel layer, cemented by calcium carbonate, probably a petrocalcic horizon belonging to the old soil on top of it. At other locations similar cemented gravel layers have been observed, e.g. at Colle Arnaro, but evidence of a petrocalcic formation belonging to the old soil with Bgt in Pliocene/old Quaternary sands could not be established with certainty. In other soils in south-central Italy petrocalcic horizons

have been reported recently by Remmelzwaal (1978) and Sevink et al. (1979).

From its physiographic position it is concluded that profile Sp/186 represents a relatively young soil in Pliocene/old Quaternary sands, which view is supported by the profile description and the analyses of the samples. The soil shows less red hues than the previously discussed soils, while the X-ray diffraction analyses and the chemical analyses, converted into a normative mineralogical composition indicate a relatively high amount of weatherable minerals (see tables 3.11 and 3.12).

Table 3.11 Semi-quantitative X-ray diffraction analyses of the fraction <2 μm of profile Sp/186 (eutric nitosol).

Horizon	Depth of sample (cm)	Mm	14 Å[1]	10 Å (111)	7 Å[2]	Qtz %	Fsp[3]
Ah	0-5	(+)	++	?	+	8-12	(x)
E	10-30	+	++	?	+	6-10	(x)
Bt1	40-55	+	+	tr	+	4-6	tr
Bt2	70-90	+	+	tr	+	6-10	tr
Bt3	100-120	(+)	(+)	?	(+)	4-6	tr
Bt4	140-160	?	(+)	?	(+)	3-5	?
BC		+(+)	tr	?	tr	2-4	?

[1] 14 Å = vermiculite [2] 7 Å = kaolinite [3] Fsp = albite and orthoclase

The amount of amorphous material probably increases from the Bt3 to the BC horizon.

Table 3.12 Normative mineralogical composition of the fractions <2 mm and <2 μm of profile Sp/186 (eutric nitosol), given in weight percentages.

Fine earth fraction (<2 mm).

Horizon	Depth of sample (cm)	Q	Fsp[1]	Mica[2]	Go/Hm	Sm	Verm	Kaol	Misc[3]	W
Ah	0-5	65	11	18	1	0.3	0.6	3	1	-0.4
E	10-30	59	10	19	2	1	0.8	7	1	+0.2
Bt1	40-55	51	8	19	4	2	1.2	14	0.4	+0.4
Bt2	70-90	56	7	17	4	2	1.1	12	1	+0.7
Bt3	100-120	53	9	18	4	2	1.1	12	1	+1
Bt4	140-160	49	8	22	4	2	1.0	13	1	+0.3
BC		57	7	24	4	3	0.2	4	0.4	+2

Clay fraction (<2 μm).

Horizon	Depth of sample (cm)	Sm	Verm	Kaol	Q	Go	Fsp[1]	Misc[3]	W
Ah	0-5	5	8	49	11	10	15	2	+4
E	10-30	8	7	54	7	12	11	1	+2
Bt1	40-55	8	5	57	4	14	11	1	+2
Bt2	70-90	7	5	55	7	13	11	2	+2
Bt3	100-120	7	5	58	4	12	12	2	+2
Bt4	140-160	10	4	56	4	12	12	2	+2
BC		28	1	41	3	16	9	2	+4

[1] Fsp = albite + anorthite + orthoclase [2] Mica = biotite + muscovite [3] Misc = apatite + pyrolusite + rutile + strengite

The analyses show that kaolinite has probably been translocated preferentially to the Bt horizons. This may also explain the increase with depth of normative goethite, which might be bound to the kaolinite as amorphous free iron compounds (see also the chemical analyses of this profile in appendix 2). The increase towards the surface of vermiculite, feldspar and free silica (quartz) must then, at least partial, be attributed to residual enrichment. This, however, cannot account for the total increase in feldspars and quartz in the clay fraction. Admixture of allochtonous material, i.e. airborne volcanic dust, can therefore not be excluded and may influence the mineralogy, mainly

of the upper horizons. The high amount of smectite in the BC horizon and the rapid decrease towards the surface indicates, like in other profiles (e.g. section Sp/22 and profile C 7) its geogene origin.

Soils on conglomerates.

Only two soil profiles have been described and sampled of the soils on Pliocene/old Quaternary conglomerates (profile Sp/41 and Sp/64). The former profile, an orthic acrisol is situated in the zone of the footslopes of the Monte Calvilli - Monte Caruso ridge, in which area these conglomerates have their greatest extent. Particle size distribution shows that at a depth of 1 m clay content is still increasing. This shows the pronounced development of the argillic B horizon to considerable depths in these deposits.

Profile Sp/64, classified as a ferric luvisol, is situated north of Pastena in the Piana Madonna delle Macchie. The section at time of description was over 5 m high and showed from bottom to top a strongly weathered, alluvial fan-like deposit. Throughout the soil black pisolites and, rarely, large haematite concretions were observed.

The strongly heterogenous character of this deposit may have influenced and still may influence the mineralogy of this soil. Therefore one must be very careful in interpreting the analytical data.

The normative mineralogical composition (table 3.13) shows an increase with depth of the free silica content in the fraction < 2 μm, similar to the soils described previously. No silica nodules however, have been observed in the profile such as these mentioned in the discussion of profile C 7.

The deviating normative content of smectite and in a minor sense also that of illite, compared with the X-ray diffraction analyses (table 3.14), is most probably due to the presence of vermiculite and chlorite in the clay fraction. As is discussed before, small amounts of 14 Å minerals as well as the presence of muscovite in the mode, may considerably affect the normative mineralogical figures. Therefore no conclusions may be drawn on the stability of smectite and illite minerals in this profile.

Table 3.13 Normative mineralogical composition of the fractions <2 mm and <2 μm of profile Sp/64 (ferric luvisol), given in weight percentages.

Fine earth fraction (<2 mm).

Horizon	Depth of sample (cm)	Q	Plag	Mica[1]	Sm	Ill	Kaol	Go/Hm	Ru	Misc[2]	W
Ap	0-20	57	5	8	5	7	11	6	0.7	1	+2
Bt	30-60	56	2	3	3	7	20	7	0.6	1	+2
Bg(t)	80-110	61	2	7	2	5	14	7	0.5	1	+3

Clay fraction (< 2 μm).

Horizon	Depth of sample (cm)	Sm	Ill	Kaol	Q	Go	Ru	Misc[3]	W
Ap	0-20	18	25	40	3	12	0.3	2	+4
Bt	30-60	10	23	44	9	12	0.3	2	+3
Bg(t)	80-110	11	22	40	10	15	0.2	2	+2

[1] Mica = biotite + muscovite [2] Misc = strengite + apatite + purolusite [3] Misc = albite + pyrolusite + strengite

Table 3.14 Semi-quantitative X-ray diffraction analyses of the fraction <2 μm of profile Sp/64 (ferric luvisol).

Horizon	Depth of sample (cm)	Mm	14 Å	10 Å (Ill)	7 Å (Kaol)	Qtz %
Ap	0-20	tr	tr[1]	(+)	+	3-5
Bt	30-60	(+)	tr[1]	+	+(+)	5-8
Bg(t)	80-110	(+)	tr[2]	+	+	4-6

[1] 14 Å = vermiculite [2] 14 Å = vermiculite + chlorite

The increase in plagioclase and muscovite content in the fraction <2 mm in the top part of the soil may be indicative for admixture with volcanic material. The weak development of the Bt horizon as compared with the pronounced Bt horizons in soils on other Pliocene/old Quaternary deposits and with the Bg(t) in this soil suggests a younger soil-forming phase superposed on an older one. This polycyclic character is also illustrated in the thin sections, in which in the sample of the Bt clay illuviation features have been observed in a matrix similar to that of the Bg(t) (fig. 3.7 and 3.8).

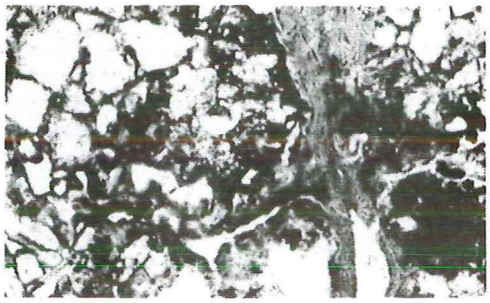

Fig. 3.7 Bt ferric luvisol (profile Sp/64). Compound argillan-ferri-argillan in agglomeroplasmic S-matrix with sharp to diffuse sesquioxidic nodules. Plain light, 45x.

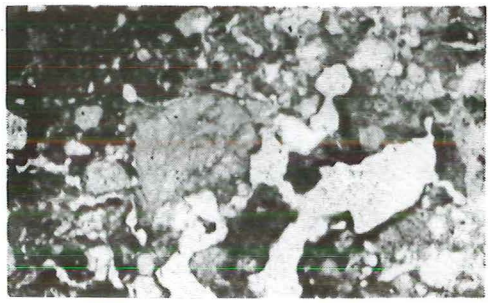

Fig. 3.8 Bg(t) ferric luvisol (profile Sp/64). Irregular ortho-vugh with ferri-argillans in agglomeroplasmic to porphyroskelic S-matrix and diffu-sesquioxidic nodules. Pl. light, 20x

The soils on Pliocene/old Quaternary deposits, in general, show a fair degree of weathering, reflected by a relatively high amount of kaolinite and quartz, and a relatively low content in weatherable minerals, e.g. micas and feldspars, as compared with the parent materials. Also the amount of titan minerals (rutile, anatase) is approximately doubled by residual enrichment. The alteration of the primary minerals is accompanied by a desilication in the top horizons, as reflected by the increase of amorphous silica in the subsoil (see e.g. profile C 7).

Except for the relatively young soils, the soils on Pliocene/old Quaternary deposits are characterized by a pronounced development of the argillic B horizon, as well as by the occurrence of pseudogleyic features. Formation of petrocalcic horizons may have taken place but could not be clearly established in the main research area.

In most of the soils indications were found of admixture with volcanic material in the top horizons. This is reflected in the analyses by a relatively high amount of K-micas and feldspars in these horizons and often also by a relatively high amount of quartz in the clay fractions (see e.g. profile Sp/186 (eutric nitosol), table 3.11).

3.1.3 Discussion and conclusions.

A great difference in soil characteristics exists between the soils on Miocene sediments on one hand and on Pliocene/old Quaternary deposits on the other hand. The former soils can be best described as relatively young soils with a high content of weatherable minerals and a profile development characterized by a cambic B horizon. In addition, the soils, depending on their parent materials, may be decalcified (calcareous sandstones), but formation of a calcic horizon (calcareous shales) also occurs.

On the contrary, the soils on Pliocene/old Quaternary deposits appear to be relatively old. They are characterized by the occurrence of a well developed argillic B horizon, often overlying horizons with pseudogleyic features. The content of weatherable minerals in the parts which are not affected by admixture with volcanic material, is rather low, and the clay fraction is dominated by 1:1 lattice layer minerals (kaolinite, halloysite). Moreover the colour of these soils is much redder than those on Miocene

sandstones and shales.

The difference between these soils can best be explained in terms of time. It is not very likely, that differences in parent material are the main cause. Most of the Pliocene/old Quaternary deposits have most probably at least for a part originated from the Miocene formations and show very similar mineral compositions, in particular when the sandstones of both are compared. Moreover, recently a reddish brown decalcified soil with an argillic B horizon on Miocene sandstone, comparable with the soils on Pliocene/old Quaternary deposits, has been found in the Volturno basin, south-east of Venafro (Tak, personal communication).

The soils on Pliocene/old Quaternary deposits are most probably a remnant of a rather stable phase in landscape development. They may have covered large areas, including the Miocene deposits. Denudation and erosion indicating a period of landscape instability, have caused removal of these soils and the underlying Miocene deposits were exposed at the surface. The susceptibility of these deposits, especially the calcareous shale, to mass movement ("franas"), frequently observed in the main research area, has most likely contributed to a great extent to this removal. It is also probably the main cause of the relatively poor soil development in the Miocene deposits.

The period of landscape instability mentioned above may be related to the tectonic and volcanic activities in mid-Pleistocene times. Deep drillings in the Valle Latina near Aquino revealed the presence of Pliocene/old Quaternary conglomerates at the base of thick lacustrine deposits (Portegies Zwart, 1974). K-Ar dating of the top of the lacustrine sediments gave an age of approximately 400 000 years (Remmelzwaal, 1978; Sevink et al., 1979). Taking into account the time necessary for the deposition of the thick (150-200 m (Devoto, 1965)) lacustrine sediments, the time of these activities must be at least be more than $\frac{1}{2}$ million years ago.

CHAPTER 4 LANDSCAPE EVOLUTION AND SOIL-FORMING PROCESSES DURING THE QUATERNARY

Soil- and landscape forming processes have acted on the area under survey since middle- and late Pliocene times. It has been discussed in 1.6.1 that in these times the definitive uplift of the Pre-Apennines took place. However, the processes insofar as they are reflected in the landscape of today, are mainly of Quaternary age. Data about possible pre-Quaternary soil- and landscape-forming processes in this region are very fragmentary and not sufficiently clear to warrant their discussion. The present chapter therefore will only deal with the soil forming processes and landscape evolution during the Quaternary.

4.1 Landscape evolution during the Quaternary.

Three main landscape-forming processes have been recognized. These are: (1) tectonical movements, most probably accompanied by volcanic activities, (2) karst development and lacustrine phases, and (3) several erosion and denudation phases.

4.1.1 Tectonical movements and volcanic activity.

As mentioned at the end of the preceding chapter, a major tectonical phase must be attributed to the mid-Pleistocene. This has been concluded from the present distribution of the Pliocene/old Quaternary deposits and from the literature.

The occurrence of the pseudogleyic features in the soils on Pliocene/old Quaternary deposits also gives a clear indication on the landscape evolution in the northern part of the main research area. The mottled horizon in profile Sp/4 indicates that this soil must have developed in a relatively flat position, e.g. an alluvial plain. The fluviatile character of the material supports this view.

At present this soil is found on a ridge between two small incisions at an elevation of approximately 155 m above the Sacco River and at the fringes of the broad Valle Latina. From this point to approximately 45 km downstream of the Sacco and Liri Rivers lacustrine deposits occur with a thickness of 100 to 150 m, locally 200 m (Arnoldus-Huyzendveld, 1973; Devoto, 1965; Portegies Zwart, 1974; Spaargaren, 1974). These deposits have been dated by K-Ar method to an age of 400 000 years (Remmelzwaal, 1978; Sevink et al., 1979). Paleontological investigations showed a fauna characteristic for colder periods (Devoto, 1965). This is also indicated by the presence of Pinularia polaris in samples of the lacustrine deposits near Pontecorvo, a diatom species indicative for relatively cold environments (< 10 °C).

The formation of the so-called Lirino Lake was caused by damming of the Valle Latina by the Roccamonfina volcano. Because of its extention it is very unlikely that erosion and denudation processes are responsible for the creation of the lacustrine basin, which has a length of 50 km and a width of 5 km and more. Therefore it must be assumed that tectonical movements are the main cause for the formation of the Valle Latina. This is in accordance with the morphological profile characteristics of the ferric acrisols (e.g. Sp/4) and gleyic acrisols in Pliocene/old Quaternary deposits, bordering the Valle Latina. As mentioned above, their pseudogleyic features indicate a soil developement in a relatively flat position, e.g. an alluvial plain.

The formation of the Valle Latina is thought to be caused by relatively quick tectonical movements. Datings of the top of the lacustrine sediments indicate an age of 0.43 million years. The base of the sediments which are locally 200 m thick (Devoto, 1965; Portegies Zwart, 1974) lies under present sea level. It has already been discussed above that erosion processes must be held responsible for the creation of the deep and wide lacustrine basin prior to the damming of the valley by the Roccamonfina volcano. On the other hand slow tectonic movements would be most probably have been accompanied by filling up of the valley with fluviatile deposits and the lacustrine facies would not have

reached its present thickness. Therefore relatively quick tectonic movements accompanied by a higher volcanic activity is believed to be the most likely explanation for the creation of the thick and deep lacustrine basin.

The large tectonical movements in the Valle Latina must undoubtedly have had influene on the surrounding limestone mountains. Reversely the dissolution of the limestone may have affected the tectonical movements. During the long stable period prior to the tectonic movements enormous amounts of limestone must have been dissolved. It is not unlikely that the loss of weight of the limestone mountains due to this dissolution may have contributed to the tectonic movements.

The tectonical movements were accompanied by volcanic activity. Three major volcanic complexes surround the main research area, viz. the Colli Albani south of Rome, the Colli Ernici, a complex of numerous small volcanos and explosion holes approximately 25 to 40 km northwest of the main research area and the Roccamonfina, approximately 40 km to the south-east.

Many K-Ar datings on these volcanic complexes are available from the literature (Evernden &Curtis, 1965; Gasperini & Adams, 1969; Basilione & Civetta, 1975; Sevink et al., 1979). The ages run from 1.2 to 0.2 million years. The K-Ar datings indicate two main periods of volcanic activity, one approximately 1 million years ago and another between 0.5 and 0.4 million years ago. With respect to the first period also volcanic activity of the Ponza Isles must be taken into account (Remmelzwaal, 1978).

The volcanic activity, as well as the tectonic movements may have resulted in an important erosion phase, which was recognized in the research area. This will be discussed in 4.1.4. Admixture with airborne volcanic dust has also been of great influence on the mineralogy of the soils as is shown in the previous chapters.

4.1.2 Karst development.

The most striking karst forms in the main research area are the large depressions near Pastena ("poljes") and the smaller basins near Monte Cervaro, of which some probably may be regarded as uvalas. Still smaller karstic features as dolines can be observed throughout the area but are concentrated mainly in the western part (see also chapter 1).

The central and northwestern part is dominated by a number of aligned depressions, of which the "Piana Madonna delle Macchie" is the largest one. The syn- or late- orogenic Pliocene conglomerates (Angelucci, 1966) are concentrated in this zone. This indicates that during their deposition this depression already existed. The geological reconstruction of Mancini (1967) also shows this depression, which is most likely of tectonical origin (fig.4.1). Studying the geological map (fig. 1.8) it is striking that at present the Pliocene conglomerates are located at the southwestern side. If the depression was already existing in its present form at the time of deposition of the Pliocene conglomerates, they most probably would have covered the whole area. Partial removal by erosion and denudation would have led to a more random distribution of the Pliocene deposits in the central depression. No remnants of them however, have been observed at the northeastern side.

On the contrary, at some locations more or less level surfaces of limestone or weathering products of limestone have been found, e.g. near the "Grotte di Pastena" (unit A5 on the Soil Map, appendix 1). These surfaces are locally dissected, are unconformous to the limestone strata and resemble the pediment-like forms observed elsewhere in south-central Italy (Sevink et al., 1979). It therefore seems to be justified to assume that the formation of e.g. the "Piana Madonna delle Macchie" is at least partly caused by dissolution of the limestone following the deposition of the Pliocene conglomerates in an existing (tectonical) depression. The same might also account for the polje southwest of Pastena ("Piana di San Andrea").

As for the other karstic basins, the start of their development is uncertain. Although they are most likely linked to tectonical zones (overthrust faults etc.), their development is much weaker than those of the poljes near Pastena. Locally colluvial deposits have

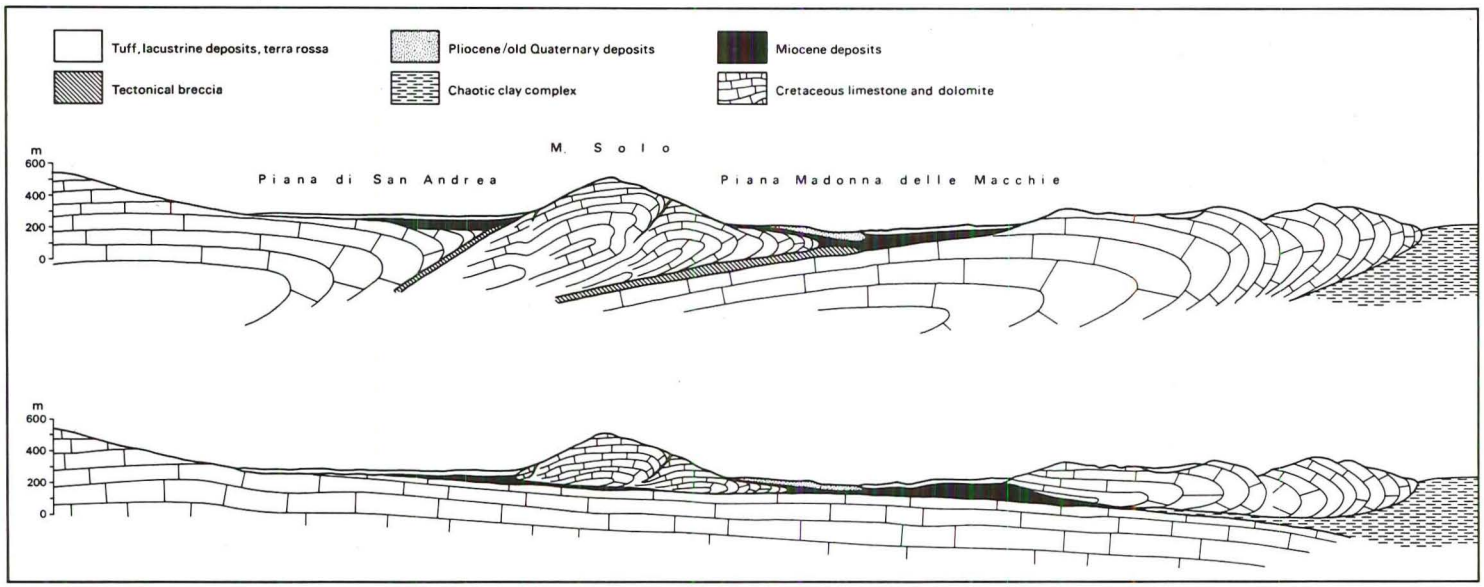

Fig. 4.1 Geological reconstruction based on geoelectrical data of a section through the Monte Ausoni along the line Pastena – Falvaterra (after Mancini, 1967).

been found which did not bear evidence of volcanic admixture (see 2.5.3, profile Sp/97); their age therefore is thought to be more than 1 million years. As, however, no Pliocene sediments have been observed in these basins, their formation has most likely to be attributed to early Quaternary times.

The formation of the present poljes is believed to be a fossil process. The distribution of lacustrine sediments in the "Piana Madonna delle Macchie" (fig. 4.2) indicates that this polje must have reached its present form at the time of deposition of the lake sediments, which are thought to be contemporaneous with the lacustrine deposits in the Valle Latina (see 4.1.3). Demangeot (1965) concludes from many observations in central Italy that the polje formation must be attributed to the period from late Tertiary to mid-Pleistocene times. The rough outline of the present limestone landscape therefore is thought to be existing since mid-Pleistocene times.

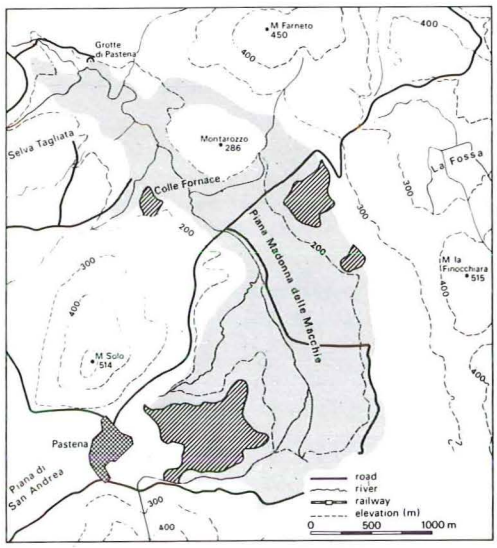

Fig. 4.2 The occurrence of lacustrine sediments (dashed areas) within 2 m of the surface of the basin floor (dotted area) of the "Piana Madonna delle Macchie".

Landscape formation during these times, as well as soil formation, is believed to have taken place under rather stable conditions. Only one (local ?) erosion phase is recognized at probably 1 million years ago. Deep weathering and pronounced soil formation in the Pliocene/old Quaternary deposits and the development of thick soils on limestone indicate this. This stable period ends with the beginning of large tectonical movements accompanied by volcanic activity. This has been discussed in 4.1.1.

Dissolution of the limestone, however, continued. Probably induced by the tectonical movements new subsurface drainage systems developed, leading to new dissolution basins. Most likely the smaller depressions, of which many are related to fault systems, have initiated from mid-Pleistocene times. This younger karst system is still active as many springs in the main research area are directly related to the dissolution depressions (Segre, 1948).

4.1.3 Lacustrine phases.

In a number of karstic basins lacustrine deposits have been observed. The largest occurrence is found in the "Piana Madonna delle Macchie", associated with volcanic deposits. The spreading of these sediments is shown in fig. 4.2, which indicates the occurrence of lacustrine deposits within 2 m of the surface. They are exposed notheast of Monte Solo, covered by a thick coherent tuff deposit (profile Sp/56).

The sediments are most likely contemporaneous with the lacustrine deposits in the Valle Latina. The exit of the "Grotte di Pastena", which drains the basin, has an altitude of 151 m a.s.l. (Segre, 1948). Just before the exit a siphon with a heigth of 20 m occurs in the cave system (Ferri-Ricchi, 1970). The altitude of the level of the Lirino Lake is estimated to have been 135 to 145 above present sea level (Arnoldus-Huyzendveld, 1973; Spaargaren, 1974). This indicates that during the existence of the Lirino Lake probably only restricted drainage occurred through the "Grotte di Pastena".

Diatom research of the lacustrine sediments in the "Piana Madonna delle Macchie" showed a dominance of Mel. arenarie and an unknown Diploneis species. The environment

was interpreted as a lake with running water, having a sandy subsoil and steep banks. No temperature indication could be found from the diatom assemblage like in those from the Lirino Lake sediments.

The age of the Lirini Lake is determined at mid-Pleistocene times. Potassium-argon dating of a tuff sample from the top of its lacustrine deposits near Rocca d' Evandro (Remmelzwaal, 1978) indicates an age of 0.43 (±0.10) million years.

In other karst basins lacustrine sediments associated with tuff have been observed (e.g. at "La Fossa"). This may indicate that volcanic eruptions, probably those between 0.5 and 0.4 million years ago (see 4.1.1) may have played a role in the creation of karst lakes. However, even at present-day seasonal flooding occurs (fig. 4.3), due to the impermeability of the colluvial deposits in the karst basins. Because blocking of the drainage system may occur anywhere and anytime, no specific lacustrine phase can be distinguished in the landscape evolution.

Fig. 4.3 Seasonal inundation of the karst basin "La Fossa". Photograph taken during the winter of 1976.

4.1.4 Erosion/denudation and colluviation.

At least three erosion/denudation phases have been recognized in the main research area. As already mentioned in 2.1.3, distinction could be made according to the admixture of allochtonous material. The following three groups have been distinguished:

- colluvial deposits with admixture of volcanic material and pottery fragments
- colluvial deposits with admixture of volcanic material without pottery fragments and
- colluvial deposits without admixture of volcanic material and pottery fragments.

Even at present-day soil erosion, mainly due to overgrazing, continues. The deep "in situ" soils at "Il Vallangero" are nowadays severely subject to erosion, caused by deforestation of the area during World War II (local information). Deforestation and overgrazing must be held responsible for the severe soil erosion which gave the landscape its present bare character.

The last erosion/denudation phase which has resulted in the colluvial deposits with pottery fragments, has been found in all karst basins and is related to human activity. Already in pre-Roman times the investigated area was populated by the Vosci tribe. Soil erosion may have started during these times, but probably reached its culmination during the Roman occupation of the area starting after the First Samnitic War (343-341 B.C.) (Hadas, 1956).

The colluvial deposits of this erosion/denudation period may reach considerable thickness. Deep-augerings in the smaller polje near Pastena ("Piana di San Andrea") showed a thickness of antropogenous colluvium of some 6 m. Down to the depth to which pottery fragments occur the material was also somewhat coarser textured as is shown in fig. 4.4. Also elsewhere in south-central Italy thick Roman colluvia has been found (Remmelzwaal, 1978).

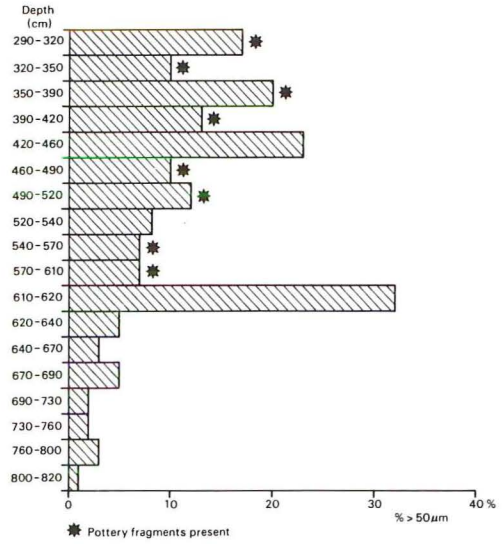

Fig. 4.4 Percentage particles>50μm and occurrence of pottery fragments in samples from a deep-augering in the "Piana di San Andrea".

No underground karstic drainage way is known to occur under the "Piana di San Andrea". It has therefore been assumed that all slope material is sedimentated in this basin. The amount of antropogenous colluvial deposits has been estimated on approximately 6 million m^3. The "effective" catchment area (viz. the adjacent slopes of the limestone mountains) has a surface of approximately 8 km^2. This may indicate a pre-erosional average soil thickness of 75 cm, assuming equal porosity in "mother" soil and colluvial deposits. In fact, porosity of the original soils may have been greater. It is therefore not unlikely that these soils have had a thickness approaching 1 m. This would represent an age of the soils of approximately 500 000 years (see 2.6.3), the time supposed to be spanning the period between the last natural erosion/denudation phase (induced by volcanism) and the antropogenous erosion.

The next older erosion phase is contemporaneous with the main volcanic activity. In many colluvial deposits tuffaceous strata occur (see fig. 4.5). Many of these tuff deposits bear evidence of translocation, as they are often mixed with material derived from limestone. Deposition of hot volcanic ashes is thought to be responsible for this erosion, as it may result in the destruction of the vegetation. Volcanic eruptions are often accompanied by heavy rains. This leads to erosion of the soils on slopes, together with the transport of the volcanic ashes and deposition of the material in the karstic basins.

Evidences of this erosion phase are found all over the main research area. The heavy mineral fraction in the soils shows a high amount of volcanic minerals. The brown/yellowish brown : colourless garnet ratio is relatively high and may reach values of 7 or more (see table 2.18).

This erosion phase is most likely related to the second period of volcanic activity between 0.5 and 0.4 million years ago. At some locations soils in these deposits have been found covering remnants of still older pseudogleyic soils and are overlain by colluvial deposits related to the youngest (antropogenous) erosion phase (see e.g. profiles Sp/118 and Sp/119).

The oldest erosion/denudation phase could only be established locally. In some karstic basins near Monte Cervaro strongly pseudogleyed buried paleosols occur. The colluvial character could be established in the thin sections of one of the soils (viz. profile

Fig. 4.5 Tuffaceous strata interbedded in alluvio-colluvial deposits at "La Fossa".

Sp/97, a chromic vertisol) and from its mineralogical composition (see 2.5.3).

The heavy mineral composition in this soil indicates a mainly limestone-derived colluvium in which volcanic minerals are almost completely lacking. The brown/yellowish brown : colourless garnet ratio is relatively low which indicates the limestone-derived character. It is believed that this erosion phase is prior to the main volcanic period, which begins at approximately 1 million years ago.

4.2 Soil-forming processes, including weathering processes, during the Quaternary.

The discussion on the weathering processes and soils in chapters 2 and 3 has revealed a number of mineralogical and pedological characteristics. They can be summarized as follows:

- with respect to the limestone area: dissolution of the carbonates, weathering of the primary minerals (mainly illite) and formation of kaolinitic products. The presence of metastable micaceous minerals in the present soils is thought to be a function of the physical properties of the weathering products. The deep soils on limestone, which are classified as eutric nitosols and chromic luvisols (FAO-Unesco, 1974), show a rather uniform expression, having dark reddish brown to reddish brown colours and an argillic B horizon. In addition they often possess vertic characteristics and pseudogleyic features, especially the "in situ" soils and those developed in the older colluvial deposits. The deep soils on dolomite, classified as chromic vertisols and chromic luvisols are rather similar to those on limestone, but vertic properties are often more pronounced. The vertic properties in the eroded soils on dolomite on the contrary are frequently less pronounced, probably due relatively dry environment compared to their counterparts on limestone.
- with respect to the Pliocene/old Quaternary conglomerates and sandstones: decalcification, if calcium carbonate was present al all, weathering of primary minerals (mainly feldspars and micas), desilication and formation of kandites and to a minor

extant of vermiculite. The soils on Pliocene/old Quaternary conglomerates and sandstones, classified as ferric/gleyic acrisols and ferric luvisols show, like the soils on limestone dark reddish brown to reddish brown colours and a pronounced argillic B horizon, especially in the older soils. Formation of petrocalcic horizons may be supposed but evidence for this could not be clearly established. Pseudogleyic features are common in these soils and are significant for the older soils.
- with respect to the Miocene sandstonesand shales as well as to the present-day weathering of and soil formation on limestone and dolomite and the Pliocene/old Quaternary deposits: decalcification or calcification, depending on the parent material, weathering of the primary minerals (mainly micas (illite) and feldspars) and formation of 10 Å and 14 Å minerals, most probably as intermediate weathering stage and to a minor extent kaolinitic products. The soils do not show the reddish colours mentioned in the two foregoing summaries. Cambic B horizons predominate in the recent soils on limestone and dolomite and in the well developed soils on Miocene sandstones and shales. The soils on Pliocene/old Quaternary sandstones on the other hand show deep developed argillic B horizons. Moreover formation of a calcic horizon in the soils on Miocene shales is very common. Pseudogleyic features lack or are very weak developed in the soils mentioned here.

This summary suggests the following main weathering and soil forming processes during the Quaternary:
- weathering of the primary minerals and formation of 1 : 1 lattice layer clays as ultimate products, probably through an intermediate stage with formation of 2 : 1 clays depending on parent material and the soil-water chemistry.
- formation of argillic B horizons in non calcareous or decalcified materials.
- formation of cambic B horizons in calcareous or decalcified materials.
- formation of pseudogleyic characteristics.
- development of vertic properties in heavy textured soils.
- "rubefaction".

In the following sections the mineralogy of the soils and their morpho-pedological characteristics will be discussed. Special attention will be paid to the stability of the weathering products, weathering intensity and soil-age implications.

4.2.1 The mineralogy of the soils, with special attention to the stability of the weathering products, weathering intensity and the soil-age implications.

The mineralogy of the soils in the main research area has been discussed comprehensively in the chapters 2 and 3 of this study. This part will focus on the mineralogical implications, espesially those observed in the clay fraction.

As discussed above the soils in the main research area can be divided into two groups, amongst others based on the mineralogy of the clay fraction ($< 2\ \mu m$). One group, which is thought to represent the reflection of a relatively long period of soil formation can be characterized by the clay fraction as "kaolinitic soils". This term refers to the soils in which the 1 : 1 clay minerals (kaolinite, halloysite, metahalloysite) dominate the fraction $< 2\ \mu m$. In the second group the clay fraction consists mainly of 2 : 1 lattice layer minerals (smectite, illite, muscovite and vermiculite) with a minor occurrence of kaolinitic clays. As discussed in the previous chapters, these minerals , with exception of vermiculite, appear to be inherited mostly from the parent materials.

The formation of kaolinitic clays, observed in the soils on limestone as well as in the soils on Pliocene/old Quaternary deposits, has been discussed by many authors (e.g. de Klimpe & Fripiat, 1968; Kittrick, 1969; Miller, 1972; Eberl & Hower, 1975, La Iglesia & Galen, 1975; Wilke & Schwertmann, 1977). A review on the formation of 1 : 1 clay minerals and their transformation mutual is given in section 2.5.

The fraction formed by the 1 : 1 minerals in the relatively old soils is dominated by kaolinite. Calculated X-ray diffraction analyses of profile Sp/122 for instance (table 2.12) show a decreasing amount of kaolinite with depth and a growing importance of the metastable phases metahalloysite and halloysite. From this the synthesis sequence of

kaolinite is suggested as halloysite→metahalloysite→kaolinite. The last transformation is most probably a very sluggish one as the structures of kaolinite and metahalloysite do not match and recrystallization must take place. Therefore the high amounts of kaolinite occurring in the soils on limestone and on Pliocene/old Quaternary conglomerates and sandstones may be indicative for a relatively old age of these soils.

The dominance of the kaolinitic clays in these soils also indicates that these minerals most probably form the stable final product of weathering. They occur in different weathering environments, both in the mild environment of weathering limestone as the moderately acid environment of weathering conglomerates and sandstones of Pliocene/old Quaternary age. Observations in the relatively young soils indicate that in general present-day weathering also leads to formation of kaolinitic products. The composition of the soil waters viewed in relation to the stable phases in the system $MgO - Al_2O_3 - SiO_2 - H_2O$ point out that kaolinite can be expected to be the stable final product in the weathering of most parent materials. Theoretical calculations on the weathering of limestone support this view (see section 2.3). The conclusion therefore seems to be justified that kaolinite is the main weathering product in this area, both in the past and the nowadays.

The accessory minerals in the clay fraction (mainly illite and smectite) must be regarded as metastable phases, although montmorillonite may form a stable phase as is indicated in section 2.4. There is evidence that the illite in the soils, especially in those on limestone, is inherited from the parent material and depletion of it is enhanced by physical properties of the soils. A second source of 10 Å minerals is thought to be airborne volcanic dust as in most topsoils increase in illite content coincidence with admixture of volcanic material.

The clay mineral distribution in the relatively young soils could in most cases be related to the parent material or to specific weathering conditions. For instance the occurrence of montmorillonite in the young soils on dolomite near Monte Lamia could be explained by a supply of aqueous silica in the soil solution from Pliocene/old Quaternary sandstones in the neighbourhood.

Weathering intensity within the soils on different parent materials can only be regarded tentatively. In general the relatively old soils show a higher amount of resistent minerals such as quartz and various titanium oxides. However, the volcanic admixture especially in the uppermost part of the soils, as mentioned previously, may influence in various proportions the weathering intensity trends. As the source of the volcanic material as well as its age is often uncertain, no correction could be introduced to estimate the original mineral assemblage. Therefore calculations on the rate of mineral weathering as an aid in determining the soil age, as e.g. was done by Ruhe (1956), could not be carried out.

There are however, sufficient mineralogical data available to assume that a distinction can be made between relatively old and relatively young soils on base of these data. An example for this may be given by comparing the figures of the normative mineralogical composition of section Sp/22 and profile Sp/186, a eutric nitosol, both on Pliocene/ old Quaternary deposits. The increase in normative free silica from the R to the E horizon in the fraction 2 – 2000 μm in section Sp/22 from 30 to 80 % (see table 3.6) together with an increase from 0.4 to 0.9 % in normative rutile in the fraction <2 μm of the same section is thought to be indicative for a relatively high rate of weathering in this soil. The same figures for a relatively young soil on Pliocene/old Quaternary sandstones, profile Sp/186, range from 62 to 70 % for free silica, while normative rutile in the clay fraction even shows a decrease towards the top of the profile.

The foregoing illustrates that although quantitative methods are not applied for various reasons, relative weathering intensity can be estimated by comparing the mineralogical and chemical data.

In the past the occurrence of specific minerals (e.g. kaolinite) has been interpreted as the result of a long and intensive weathering. Even climatic conditions have been extrapolated from the occurrence of kaolinite (Bakker & Levelt, 1964; Fränzle, 1965). If the stability relations of clay minerals are reviewed, however, it appears that kaolinite is one of the most common phases to be expected in soil environments. Its stability is mainly a function of the pH and the dissolved silica content of the interstitial soil

water. Only very high activities of especially Mg^{2+} may influence the pH dependency. At pH 7 the $[Mg^{2+}]$ must rise above approximately 1 mmol/l and at a pH 6 even above approximately 100 mmol/l to influence the stability of kaolinite. As kaolinite also forms the stable phase between dissolved silica activities of approximately 0.001 and 0.4 mmol/l, it is most probable that in many soil environments under the prevailing and related climates kaolinite can be expected as stable phase. It gives therefore little information on the age of the soil and cannot be used to indicate paleoclimates.

This is especially important in interpreting the mineralogical composition of the soils on limestone in which kaolinite forms the major constituent. It has been mentioned before that neoformation of clay minerals is inhibited by kinetic factors. Recent investigations on the experimental formation of kaolinite have also shown that e.g. organic compounds are necessary as cataclyst (Lineares & Huertas, 1971; Hem & Lind, 1974). Little is known on these factors, but the drastic mineralogical change in the soils on limestone with respect to the non-carbonate mineralogy of the limestone itself seems to justify the supposition that a considerable time is needed for this transformation.

An indication on the age of these soils can be gathered from the amount of limestone dissolved to produce the soils found (see section 2.4.2). From figure 2.35 it was preliminary concluded, that for the formation of 1 m soil ca. 500 000 years are needed. This figure seems to match with some other interpretations discussed above (see section 4.1).

4.2.2 Pedological characteristics in the soils: argillic B horizon, cambic B horizon pseudogleyic features and rubefaction.

Argillic B horizons.

Soils with argillic B horizons are very common in the research area. Evidence of clay translocation has been found in the thick soils on limestone, the soils in young colluvial deposits derived from limestone and the soils on Pliocene/old Quaternary deposits. In the latter soils the formation of an argillic B horizon can be very pronounced. In profile Sp/4 e.g. absolute increase in clay content occurs from 16 % in the eluvial E horizon to 40 % in the argillic B horizon. It also can reach considerable thickness as is illustrated by the particle size analyses of profiles Sp/41 and Sp/186.

In the deep "in situ" soils on limestone argillic B horizons are often difficult to recognize on field criteria, mostly because of the very fine texture. Granulometric analyses and study of thin sections appear to be indispensable and have shown clear evidence of translocation of clay in these soils (see e.g. profile Sp/122).

The process of clay migration and accumulation is reviewed by Mohr et al. (1972). Essential are the electro-kinetic characteristics of the clay particles and the chemistry of the percolating water. These factors determine the thickness of the double layer and thus flocculation or dispersion of the clay.

One of the favourable conditions in the formation of an argillic B horizon seems to be a climate with pronounced dry seasons in which dessication and cracking of the soils occur (Soil Survey Staff, 1975). The process is described as follows:

> "Wetting a dry soils seems to lead to disruption of the fabric and to dispersion of clay. Once dispersed, the clay is believed to move with the percolating water and to stop where the percolating water stops. Water percolating in noncapillary voids commonly is stopped by capillary withdrawal into the soil fabric. During this withdrawal the clay is believed to be deposited on the walls of the noncapillary voids. This would explain why illuvial clay commonly is plasterd on the faces of peds and on the walls of pores. Such a mechanism for movement and deposition of clay is favored in several ways by a seasonal moisture deficit. First, as already mentioned, wetting a dry soil favors dispersion of the clay; second, when a soil dries, cracks form in which gravitational water or water held at low tension can percolate; third, the halting of percolating water by capillary withdrawal is favored by the strong tendency for a dry soil to take up moisture".

The mediterranean climate provides rather well the conditions for clay translocation as described above. In the dry summer period strong dessication occurs and cracking of the soils, especially those with a clayey texture, was frequently observed during this

season. The heavy shower character of the precipitation promotes the lowering of the electrolyte content resulting in an increase of the double layer thickness (Mohr et al., 1972).

Van Schuylenborgh (1947) has shown that aggregates of kaolinite and sand were less resistent to the impact of raindrops than aggregates built up from montmorillonite and sand. Most older soils have a kaolinitic clay mineralogy and the distribution of kaolinite in the clay fraction confirms his findings of preferential translocation of kaolinite by percolating water.

Dating the process of argillic B horizon formation is rather speculative. In Western Europe it is generally believed that textural B horizons are mainly formed during relatively warm periods. This however, does not mean that during glacial times the process of argilluviation did not take place (Sevink & Vink, 1970). Whether the general rule that argillic B horizons must be attributed to interglacial times is valid in the mediterranean area is rather doubtful.

The climate during the glacial times in the mediterranean region is believed to be approximately 6-8 °C cooler than the present one but the precipitation regime was more or less the same as today, i.e. dry summers and moist winters (Fränzle, 1965; Frenzel, 1967). The amount of rainfall, however, may have been somewhat lower (Schwarzbach, 1974). The climatic change between the interglacial and glacial times have had the greatest expression on the vegetation cover. According to Frenzel the forests, which are believed to be the natural vegetation cover during interglacial periods, disappeared. Pollen analyses from several mediterranean regions indicate the presence of a cold and dry Artemesia steppe during the last Glacial (Bonatti, 1966; Frank, 1969, Wijmstra, 1969). These vegetational changes may have resulted in accelerated erosion, but the presence of relatively old soils "in situ" indicates that the presumed accelerated erosion did only affect parts of the area. Hence, soil forming processes such as argilluviation could go on though their rates may have been somewhat less.

On more or less empirical criteria the Soil Survey Staff (1975) suggests that the formation of an argillic horizon is favoured by the presence of a forest cover. The process of argilluviation, however, also takes place in soils developed in young (antropogenous) colluvium derived from limestone. Clay illuviation features have also been observed in vertisols (e.g. profile Sp/98, see fig. 2.31 and appendix 2), which are nowadays under cultivation. In these soils translocation phenomena must be very young as by the self-mulching processes in vertisols they will be frequently destroyed (see also Remmelzwaal, 1978). There is therefore no reason to assume that the process of argillic B horizon formation is limited to interglacial times due to the presence of forests during these periods.

As temperature was considerable lower during the Glacials than at present times, evapotranspiration consequently must have dropped also. The direct result on the process of argilluviation is less dessication and thus less cracking of the soils. Hence the process of textural B formation is believed to have still continued during glacial times although the rate of formation has most likely been somewhat less than during interglacial periods and at present-day.

Theoretically it would be possible to estimate the age of an argillic B horizon by calculating the quantities of clay formed and translocated as a function of time (Birkeland, 1974). Little is known, however, on the rate of clay formation and translocation. Both may vary in time, depending on e.g. climate as is shown above and in the previous chapters. It must therefore be concluded that only relative ages can be estimated by comparing the argillic B horizon development on the same parent materials. The more pronounced character of the textural B in the ferric acrisol on Pliocene/old quaternary deposits profile Sp/4) as compared to the textural B in the eutric nitosol (profile Sp/186) indicates most likely a relatively older age of the former soil with respect to the latter one.

Cambic B horizons.

Cambic B horizons are quite common in the relatively young soils. They are especially found in the well-developed soils on Miocene sandstones and shales. Locally

they can be recognized in the young soils on limestone and dolomite. Their mineralogy is characterized by a considerable amount of weatherable minerals and a clay mineralogy which can be described as the product of an intermediate stage of weathering.

The mineralogical characteristics and the appearance mainly in the younger soils appoints the development of cambic B horizons most probably to recent and subrecent times.

Special attention however must be paid in this sence to the chromic vertisols in cracks in the limestone. These soils do not show evidence of clay illuviation but do bear the characteristics significant for a cambic horizon as defined by the Soil Survey Staff (1975). The profiles are very similar to the lower parts of the deep soils on limestone and are therefore believed to be the remnants of these thicker soils. Because of the position below an argillic horizon, the lower part of the deep soils is nor regarded as a cambic horizon (Soil Survey Staff (1975), but as they come at the surface by truncation of the profile they have indeed to be regarded as such. This however, does not mean that, as stated previously, they are formed in recent to subrecent times. This is also evident from the mineralogical composition of these soils which does not show a considerable amount of weatherable minerals or intermediate weathering products. hence the age of these cambic B horizons must be much older than those developed for instance in the Miocene sandstones and shales.

Pseudogleyic features.

In this subsection the hydromorphic features are indicated as pseudogley, because the morphology of the mottled horizons in the profiles under discussion resemble very much the iron (and manganese) redistribution pattern characteristics for this pedogenetic feature. It has been shown, however, in 2.5.3 (profile sp/97, a chromic vertisol) and 3.1.2 (profile Sp/4, a ferric acrisol) that redistribution of free iron (and manganese) compounds, which has led to a pseudogleyic appearence, may have resulted from different processes.

In a number of soils, both on limestone and on Pliocene/old Quaternary deposits pseudogleyic features have been observed. As mentioned in the discussion of the profiles the pseudogleyic appearance in some older colluvial deposits derived from limestone is most probably due to loss of iron along the pedfaces. On the other hand analyses of the mottles in the soils on Pliocene/old Quaternary sandstone clearly showed a redistribution of iron compounds within the peds. It is therefore not possible to relate both appearances with each other as obviously they have resulted from different processes.

The pseudogleyic features in the oldest colluvial deposits derived from limestone are the result of a mainly vertical redistribution of iron compounds. Profile Sp/97 showed in the upper part loss of iron along the pedfaces and translocations of iron to lower parts of the profile (see also free iron contents profile Sp/97, appendix 2).

Penetrating rainwater must be held responsible for the process of deferration. Interstitial soil water samples have a pH between 6 and 7 (see appendix 4.1, sample Sp/170). These conditions imply a very low solubility of free iron compounds, if chelating by soluble organic compounds is of minor importance. Consequently, a considerable time will be needed to create a perceptible decrease in iron content.

The pseudogleyic features are the most pronounced in soils with more or less level position. They, however, have also been observed in soils on steep slopes, e.g. in profile Sp/122. This indicates that, although the physiographic position may be very important, it will not be the rate determining step. The clayey character of the soils may not be neglected in this view and might even be more important than the physiographic position.

Dating of the pseudogleyic features in the soils derived from limestone is rather difficult. They have only been observed in the relatively old soils and often they are associated with pediment-like forms at the foot of slopes (Sevink et al., 1979). These forms are relatively old and are attributed mainly to early Pleistocene times.

Summarizing, the pseudogleyic features observed in some soils are of different origin. Firstly, temporarely waterlogging due to the impermeable Miocene calcareous

shales and a probably original level position seem to be the cause of the pseudogleyic features in the ferric acrisols (e.g. profile Sp/4) in Pliocene/old Quaternary deposits. Redistribution of free iron compounds has mainly taken place within the peds ("horizontal").

Secondly, pseudogleyic features may be closely related to the permeability of the soil material, while the physiographic position seem to be of minor importance. Redistribution of the free iron compounds is thought to occur mainly in "vertical" direction.

Rubefaction.

Most of the studied soils show reddish colours, with hues of 5YR and 2.5YR. Only the soils on Miocene sandstones and shales as well as the younger soils on limestone and dolomite have yellower hues.

It is generally accepted that red colours in soils are due to specific iron compounds. It is however still under discussion which iron compound causes the bright reddish colour, characteristic for many soils in the mediterranean area. Buringh (1970), Segalen (1964) and Schwertmann & Taylor (1977) attribute the reddish colours simply to the presence of haematite. On the other hand some authors have discussed that it must be due to amorphous iron hydroxides, bound to clay particles (Duchaufour, 1977; Lamouroux, 1972).

Roughly a distinction can be made between red and non-red soils, delimiting the red soils between hues of 10R and 5YR. Reddish colours are common in soils on limestone and dolomite, on volcanic rocks and in well-developed soils on Pliocene/old Quaternary deposits. Recently also a reddish-brown soil was found on Miocene sandstone near Venafro (Tal, personal communication).

On the other hand, the soils on lacustrine deposits in the Valle Latina and the soils in alluvial deposits of the Sacco and Liri Rivers, as well as most of the soils on Miocene sandstones and shales do not show reddish colours. Also the younger soils on Pliocene/old Quaternary sandstone near Monte Lamia (e.g. profile Sp/186) have hues yellower than other soils on similar deposits.

Because "reddish" and "non-reddish" soils have been observed developed on the same parent material (viz. on Miocene sandstones and on Pliocene/old Quaternary sandy deposits), the process of aging of the free iron compounds is thought to be the most important factor influencing the degree of reddening (cf. Duchaufour, 1977). Secondary factors may be paleoclimates (Birkeland, 1974), the presence of relatively high amounts of easily weatherable, Fe(II)-rich minerals and a very porous character of the soil material.

A relatively large amount of iron is produced upon weathering and iron oxides and -hydroxides will be formed. Extreme drying out, which can be expected during the summer in materials with a relatively high porosity will lead to increase in modality of the soil solution. Consequently, the activity of water will be lowered which in its turn affects the chemical equilibria, for instance those between the main iron oxides and -hydroxides. Rubefaction in relatively young materials as reported by Remmelzwaal (1978) and Sevink et al. (1979) in some volcanic deposits and marine and eolian sands in south-central Italy may very well be caused by the extreme aptitude to reddening as described above.

As the redness of the soil material obviously depends on a number of factors, whose influence and interrelationship cannot be determined accurately, rubefaction cannot be used as soil-age indicator. The degree of reddining may only be used within a group of soils developed in the same homogenous parent material to estimate their relative ages.

4.3 Synthesis of landscape evolution and soil formation during the Quaternary.

In table 4.1 a synthesis of the main landscape- and soil-forming processes with their results is shown. With respect to the time scale used, preference is given to indicate the absolute ages obtained from K - Ar datings rather than a relative time table. However, because of lack of data on absolute ages younger than 70 000 B.P. the Last Glacial and Holocene have been introduced.

Table 4.1 Synthesis of the landscape- and soil-forming processes and their results.

LANDSCAPE		SOIL		TIME SCALE
Process	Result	Process	Result	
Erosion/ Denudation	Colluvia	Soil erosion	Soils in colluvia Soils in young surfaces	Holocene
Stable		Mollic horizons Soil formation	"Pseudogley" Luvisols/Nitosols/ Vertisols	
Dissolution of the limestone	Karstic features (caves, dolines, etc.)	Soil formation	"Pseudogley" Luvisols/Nitosols/ Vertisols Rubefaction	Last Glacial 70 000 B.P.
Tectonics: Volcanism and erosion. Stagnating drainage to the "Valle Latina"	Tuff deposits Colluvia Lacustrine deposits ("Lake of Pastena")	Soil erosion Tuff admixture Colluviation	1) Truncated soils 2) Truncated soils on slopes 3) Soils in tuff and colluvial deposits	400 000 B.P.
Tectonics: Dissolution of the limestone		Soil formation	"Pseudogley" Nitosols/Vertisols Rubefaction	
Start of volcanism and erosion	Tuff deposits Colluvia	Soil erosion Tuff admixture Colluviation	1) Truncated soils 2) Truncated soils on slopes 3) Soils in colluvia	1 000 000 B.P.
Dissolution of the limestone	Poljes, pediments, lapies karst	First limestone weathering and soil formation Soil formation in Pliocene deposits	Nitosols/Vertisols without tuff Rubefaction	
Tectonics	Alluvial fans ("Molasse")	Start of soil formation		Pliocene

REFERENCES

Accordi, B. (1966) - La componente traslativa nella tettonica dell' Appennino Laziale - Abruzzese. Geol. Rom., Vol. V, pp 355-406. Roma.

Accordi, B., A. Angelucci & G. Sirna (1967) - Note illustrative della Carta Geologica d' Italia alla scala 1:100000: F° 159 & 160 (Frosinone e Cassino). 76 pp. Servizio Geologico d' Italia, Roma.

Ahmad, A., R.L. Jones & A.H. Beavers (1966) - Genesis, mineralogy and related properties of West Indian soils: I. Bauxitic soils of Jamaica. Soil Sc. Soc. Am. Proc., Vol. 30, pp 719-722. Madison.

Angelucci, A. (1966) - Tectonic marks on pebbles of middle Valle Latina (Central Italy). Geol. Rom., Vol. V, pp 312-322. Roma.

Arnoldus-Huyzendveld, A.M.H. (1973) - Verslag van een bodemkartering in de Ciociaria, het gebied rond Frosinone (Italië). Int. Rep. Fys. Geogr. Bod. Lab. Univ. Amsterdam, 126 pp. Amsterdam.

Bakker, J.P. & Th.W.M. Levelt (1964) - An inquiry into the probability of a polyclimatic development of peneplains and pediments (etchplains) in Europe during the Senonian and Tertiary period. Publ. Serv. geol. du Lux., Vol. XIV, pp. 27-75. Luxembourg.

Barnes, I. & J.R. O'Neil (1971) - Calcium-magnesium carbonate solid solutions from Holocene conglomerate cements and travertines in the Coast Range of California. Geoch. et Cosmoch. Acta, Vol. 35, pp 699-718. Pergamon Press.

Basilone, P. & L. Civetta (1975) - Datazione K-Ar dell7 actività dei Monte Ernici. Rend. Soc. It. Min. Petr., Vol. 31, pp 175-179.

Beaven, P.J. & M.J. Dumbleton (1966) - Clay minerals and geomorphology in four Caribean islands. Clay Min. (1966), no. 6, pp 371-382.

Birkeland, P.W. (1974) - Pedology, weathering and geomorphological research. 285 pp. New York-London-Toronto.

Birot, P. (1953) - Le problème des terres rouges. In: Birot, P. & J. Dresch - La Méditerranée et le Moyen Orient, pp 80-82. Paris.

Blanc, E. (1930) - Die Mediterran-Roterde (Terra Rossa). In: Blanck, E. - Handbuch der Bodenlehre, Dritter Band, pp 194-257. Berlin.

de Boer, R.B. (1977) - Stability of Mg-Ca carbonates. Geoch. et Cosmoch. Acta, Vol. 41, pp 265-270. Pergamon Press.

Bolt, G.H. & M.G.M. Bruggenwert (Ed.) (1976) - Soil chemistry. A. Basic elements. 281 pp. Amsterdam.

Bonatti, E. (1966) - North mediterranean climate during the last Würm glaciation. Nature, Vol. 209, pp 984-985.

Boni, C.F. (1975) - The relationships between the geology and hydrogeology of the Latium-Abruzzi Apennines. In: Ogniben, L., M. Parotto & A Praturlon (Ed.) - Structural model of Italy, pp 301-311. Roma.

Bottner, P. & P. Lossaint (1966) - Etat de nos connaissances sur les sols rouges du bassin Méditerranéen. Ann. Agric. 1967, no. 1.

van Breemen, N. (1976) - Genesis and solution chemistry of acid sulphate soils in Thailand. Thesis Agricultural University Wageningen, 263 pp. Wageningen.

Brewer, R. (1976) - Fabric and mineral analysis of soils. 482 pp. New York.

Brugger, H (1974) - Umwandlung der Silikate bei der Bodenbildung aus Dolomit im schweizerischen Nationalpark. Thesis Technische Hochschule Zürich, 65 pp. Zürich.

de Bruin, J.H.S. (1970) - A correlation study of red and yellow soils in areas with a Mediterranean climate. FAO-Unesco World Soil Resources Report no. 39, 95 pp. Rome.

Buringh, P. (1970) - Introduction to the study of soils in tropical and subtropical regions. 99 pp. Wageningen.

Burton, J.D., T.M. Leatherland & P.S. Liss (1970) - The reactivity of dissolved silicon in some natural waters. Limn. and Oceanogr., Vol. 15, no. 3, pp 473-476.

Carroll, D. & J.C. Hathaway (1954) - Clay minerals in a limestone soil profile. Clays and clay minerals, Proceedings of the Second National Conference on clays and clay minerals, University of Missouri, Col, October 15-17, 1953. Publication 327, National Academy of Sciences - National Research Council, pp 171-182. Washington D.C.
Chilingar, G.V., H.J. Bissell & R.W. Fairbridge (Ed.) (1967) - Carbonate rocks. Origin, occurrence and classification. Developments in sedimentology 9A. 471 pp. Amsterdam - London - New York.
Clayton, R.N., B.F. Jones & R.A. Berner (1968) - Isotope studies of dolomite formation under sedimentary conditions. Geoch. et Cosmoch. Acta, Vol. 32, pp 415-432. Pergamon Press.
Clemency, Ch.V. & A.F. Wagner (1961) - Titrimetric determination of ferrous iron in silicate rocks and minerals. Anal. Chem., Vol. 33, pp 888-892.
Cvijic, J. (1893) - Das Karstphänomen. Geogr. Abh. V. 3. Wien.

Demangeot, J. (1965) - Géomorphologie des Abruzzes adriatiques. Mémoires et documents, Centre de recherches et documentation cartographiques et géographiques. 403 pp. Paris.
Devoto, G. (1965) - Lacustrine Pleistocene in the lower Liri Valley. Geol. Rom. Vol. IV, pp 291-368. Roma.
Dirven, J.M.C., J. van Schuylenborgh & N. van Breemen (1976) - Weathering of serpentinite in Mantanzas Province, Cuba: Mass transfer calculations and irreversible weathering pathways. Soil Sc. Soc. Am. J., Vol. 40, no. 6, pp 901-907. Madison.
Dixon, J.B. & S.B. Weed (Ed.) (1977) - Minerals in soil environments. 948 pp. Madison.
Drosdoff, M. & C.C. Nikiforoff (1940) - Iron-manganese nodules in Dayton soils. Soil Sci. Vol. 49, pp 333-345.
Duchaufour, P. (1977) - Pédologie. Tome I - Pédogenèse et classification. 477 pp. Paris - New York - Barcelone - Milan.
Durand, R. & P. Dutil (1971) - Premier résultats sur l' altération expérimentale de roches calcaire et dolomitiques. Ann. Agron. Vol. 22, pp 397-424. Paris.

Eberl, D. & J. Hower (1975) - Kaolinite synthesis: The role of the Si/Al and (alkali)/(H^+) ratio in hydrothermal systems. Clays and clay min., Vol. 23, pp 301-309. Pergamon Press.
Emberger, Gaussen, Kassas & de Philippis (1962) - Bioclimatic map of the Mediterranean region, 1:5 000 000. Unesco/FAO. Paris.
Eridia, F. (1942) - Distribuzione della temperature dell' aria in Italia nel decennio 1926-1935. Min. Lav. Pubbl. Serv. Idrogr., no. 21.
Evernden, J.F. & G.H. Curtis (1965) - The potassium-argon dating of Late Cenozoic rocks in East Africa and Italy. Curr. Anthr., Vol. 6, pp 343-385.
FAO (1977) - FAO Guidelines for soil profile description. Second edition, 66 pp. Roma.
FAO-Unesco (1971) - Soil Map of the World 1:5 000 000, Volume IV South America. 193 pp. Paris.
FAO-Unesco (1974) - Soil Map of the World 1:5 000 000, Volume I Legend. 59 pp. Paris.
FAO-Unesco (1975 a) - Soil Map of the World 1:5 000 000, Volume II North America. 210 pp. Paris.
FAO-Unesco (1975 b) - Soil Map of the World 1:5 000 000, Volume III Mexico and Central America. 96 pp. Paris.
FAO-Unesco (1977 a) - Soil Map of the World 1:5 000 000, Volume VI Africa. 299 pp. Paris.
FAO-Unesco (1977 b) - Soil Map of the World 1:5 000 000. Volume VII South Asia. 117 pp. Paris
Fazzini, P., R. Gelmini, M.P. Mantovani & M. Pelligrini (1972) - Geologia dei Monti della Tolfa (Lazio settentrionale, provincia di Viterbo e Roma). Mem. Soc. Geol. It., Vol. 11, pp 65-144. Bologna.
Fenaroli, L. (1970) - Note illustrative della Carta della Vegetazione reale d' Italia. 127 pp. Roma.
Ferri-Ricchi, L. (1970) - Spéléologie nouvelle, science d' une aventure. I Des spéléonautes en plongée. Atlas, juin 1970, pp 40-51. Paris.

Frank, A.H.E. (1969) - Pollen stratigraphy of the Lake of Vico (cental Italy). Paleog. Paleocl., Paleoec., Vol. 6, pp 67-85. Amsterdam.
Fränzle, O. (1965) - Die pleistozäne Klima- und Landschaftentwicklung der nördlichen Po-Ebene im Lichte bodengeographischer Untersuchungen. Akademie der Wissenschaften und der Literatur, Abhandlungen der Mathematisch-Naturwissenschaftlichen Klasse, Jahrgang 1965, no. 8. 146 pp. Wiesbaden.
Frenzel, B. (1967) - Die Klimaschwankungen des Eiszeitalters. 291 pp. Braunsweig.
Fritz, B. (1975) - Etude thermodynamique et simulation des réactions entre mineraux et solutions. Application a la géochimie des altérations et des eaux continentales. Mem. 41, Sciences Géologiques, Université Louis Pasteur de Strasbourg , Institut de Géologie.

Gal, M. (1966) - Clay mineralogy in the study of the genesis of terra rossa and rendzina originating from calcareous rocks. Proc. Int. Clay Conf. Jerusalem, Vol. 1, pp 199-207.
Gasperini, D. & J.A.S. Adams (1969) - K-Ar dating of Italian Plio-Pleistocene rocks. Earth Plan. Sc. L., Vol. 6, pp 225-230.
Graf, D.L. & J.R. Goldsmith (1956) - Some hydrothermal synthesis of dolomite and protodolomite. J. Geol., Vol. 64, pp 173-186.
Graf zu Leinigen, W. (1930) - Die Roterde als Lösungsrest mariner Kalkgesteine. Chem. der Erde, Vol. 4, pp 178-187. Jena.
Grandjaquet, C. (1963) - Importance de la tectonique tangentielle en Italie méridionale. Rev. Géogr. phys. Géol. dyn., Vol. V (1962), fasc. 2, pp 109-113. Paris.
van der Grinten, P.M.E.M. & J.M.H. Lenoir (1973) - Statistische procesbeheersing. 598 pp. Utrecht-Antwerpen.
Grontmij N.V. (1963) - Nomogrammen voor bepaling van de verdamping. 57-801 Serie A. 38 pp. de Bilt.

Hadas, M. (1956) - A history of Rome from its origins to 529 A.D. as told by the Roman historians. 308 pp. New York.
Helgeson, H.C. (1968) - Evaluation of irreversible reactions in geochemical processes involving minerals and aqueous solutions - I. Thermodynamic relations. Geoch. et Cosmoch. Acta, Vol. 32, pp 853-877. Pergamon Press.
Helgeson, H.C. (1969) - Thermodynamics of hydrothermal systems at elevated temperatures and pressures. Am. J. Sc., Vol. 267, pp 729-804.
Helgeson, H.C. (1971) - Kinetics of mass transfer among silicates and aqueous solutions. Geoch. et Cosmoch. Acta, Vol. 35, pp 421-469. Pergamon Press.
Helgeson, H.C. (1972) - Kinetics of mass transfer among silicates and aqueous solutions: Correction and clarification. Geoch. et Cosmoch. Acta, Vol. 36, pp 1067-1070. Pergamon Press.
Helgeson, H.C., R. M. Garrels & F.T. Mackenzie (1969) - Evaluation of irreversible reactions in geochemical processes involving minerals and aqueous solutions - II. Applications. Geoch. et Cosmoch. Acta, Vol. 33, pp 455-481. Pergamon Press.
Hem, J.D. & C.J. Lind (1974) - Kaolinite synthesis at 25 °C. Science, Vol. 184, pp 1171-1173. Washington D.C.

Istituto Geografico Militare (1961) - Fº 159 I S.E. (Ceccano), Fº 159 II N.E. (Vallecorsa), Fº 160 III N.O. (Pico), Fº 160 IV S.O. (Ceprano) della Carta d' Italia alla scala di 1:25000. Firenze.
Jacobson, R.L. & D. Langmuir (1970) - The chemical history of some spring waters in carbonate rocks. Ground Water, Vol. 8, no.3.
Katz, A. & A. Matthews (1977) - The dolomitization of $CaCO_3$: an experimental study at 252-295 °C. Geoch. et Cosmoch. Acta, Vol. 41, pp 297-308. Pergamon Press.
Khan, D.H. (1960) - Clay mineral distribution in some rendzinas, red-brown soils and terra rossa on limestones of different geological ages. Soil Sc., Vol. 90, pp 312-319.
Kharaka, Y.K. & I. Barnes (1973) - SOLMNEQ: solution-mineral equilibrium computations. Rep. U.S. Geol. Survey, Water Res. Div., no. 73-002. 82 pp.

de Kimpe (1969) - Crystallization of kaolinite at low temperatures from an alumino-silisic gel. Clays and Clay Min., Vol. 17, pp 37-38.
de Kimpe, C.R., M.C. Castuche & G.W. Brindley (1964) - Low-temperature synthesis of kaolin minerals. Am. Min., Vol. 49, pp 1-16.
de Kimpe, C.R. & J.J. Fripiat (1968) - Kaolinite crystallization from H-exchanged zeolites. Am. Min., Vol. 53, pp 216-230.
Kittrick, J.A. (1970) - Precipitation of kaolinite at 25 °C and 1 atm. Clays and Clay Min., Vol. 18, pp 261-267. Pergamon Press.
Klinge, H. (1957) - Über spanische Terra rossa - Vorkommen und die Möglichkeiten ihrer zeitlichen Einordnung auf Grund bodengeografischer Studien. Z. Pfl. Düng. Bodenk., Vol. 76, pp 223-231. Weinheim.
Köppen, W. (1936) - Das geographisches System der Klimate. In: Köppen, W. & R. Geiger, Handbuch der Klimatologie, Bd 1, Teil 3. 44 pp. Berlin.
Kovda, V.A., C. van den Bergh & R.M. Hagan (1973) - Irrigation, drainage and salinity. 510 pp. Paris.
Ku S-Y. & Hsü C-C. (1963) - Soil colloid researches. V. Clay minerals and their transformation in rendzina, terra fusca and terra rossa of Yunnan and Kwangsi. Acta Pedologica Sinica, Vol. 14, no. 4, pp 411-416. (Translated in english by Wen T-T.)

Laboratory of Physical Geography and Soil Science (1971) - Methods of soil and rock analyses. 85 pp.
La Iglesia, A. & E. Galen (1975) - Halloysite-kaolinite transformation at room temperature. Clays and Clay Min., Vol. 23, pp 109-113. Pergamon Press.
Lamouroux, M. (1965) - Observations sur l' altération des roches calcaires sous climate méditerranéen humide. Cah. Ped. III, fasc. 1, pp 21-41. ORSTOM Paris.
Lamouroux, M. (1967) - Contribution à l' étude de pédogenèse en sols rouges méditerranéens. Sc. du Sol, 1967-2, pp 55-86. Versailles.
Lamouroux, M. (1972) - Etude de sols formés sur roches carbonatées. Pédogenèse fersiallitique au Liban. Mém. ORSTOM, no. 56. 266 pp. Paris.
Langmuir, D. (1971) - The geochemistry of some carbonate ground waters in central Pennsylvania. Geoch. et Cosmoch. Acta, Vol. 35, pp 1023-1045. Pergamon Press.
Linares, J. & F. Huertas (1971) - Kaolinite synthesis at room temperature. Science, Vol. 171, pp 896-898. Washington D.C.
Lippi-Boncambi, C., R.C. Mackenzie & A. Mitchel (1955) - The mineralogy of some soils from Central Italy. Clay Min. Bull., Vol. 2, no. 3, pp 281-288.
Lippman, F. (1973) - Sedimentary carbonate minerals. Minerals, rocks and organic materials. Monograph Series of Theoretical and Experimental Studies No. 6. 228 pp. Heidelberg-New York.

Maignien, R. (1959) - Les sols subarides au Sénégal. L' Agron. trop. 5, pp 536-571.
Mancini, M. (1967) - Rilevamento geologico e studio geoelettrico di una zona compresa fra le tavolette Pico (III N.O.) e Ceprano (IV S.O.), foglio 160 (Cassino). Tese di Laurea Università di Roma. 54 pp. Roma.
Marković-Marjanović, J. (1972) - Mogućnost odredivanja relativne hronologije različitih tipova zemljišta u Jugoslaviji (Possibility of determining the relative chronology of various soil types in Yougoslavia). IV Kongres Jugoslovenskog Društva za Proučavanje Zemljišta - Plenarni, Referati i Izvodi (IVth Congress of Yougoslav Society of Soil Science - Introduction, lecture and abstracts), pp 192-195. Beograd.
Marshall, C.E. (1977) - The physical chemistry and mineralogy of soils. Vol. II - Soils in place. 313 pp. New York-London-Sydney-Toronto.
Mensching, H. (1955) - Karst und Terra Rossa auf Mallorca. Erdkunde Bd IX, pp 188-196.
Miller, B. (1972) - Relationship of soil properties to transformation of carbonate rocks into soils. Thesis University of Tennessee, 203 pp.
Ministero dei Lavori Pubblici (1955) - Precipitazioni medie mensili ed annue e numero dei giorni piovosi per il trentennio 1921-1950. Bacine con foce al litorale tirrenico dal Fiora al Lago di Fondi. Sezione idrografico di Roma, Pubbl. no. 24 del Servizio, Fasc. I. 233 pp. Roma.

Ministero dei Lavori Pubblici (1958) - Precipitazione medie mensili ed annue e numero dei giorni piovosi per il trentennio 1921-1950. Bacini con foce al litorale tirrenico dal Garigliano al Bussento. Sezione idrografico di Napoli. Pubbl. no. 24 del Servizio, Fasc. X. 237 pp. Roma.

Misra, U.K. (1973) - Mineral equilibria in a soil system under natural and modified conditions as shown by the physical chemistry of the aqueous phase. Ph. D. Thesis, University of Missouri, Columbia.

Mohr, E.C.J., F.A. van Baren & J. van Schuylenborgh (1972) - Tropical soils. A comprehensive study of their genesis. 481 pp. Den Haag-Pari-Djakarta.

Mueller, R.F. & S.K. Saxena (1977) - Chemical petrology. 394 pp. New York-Heidelberg-Berlin.

Murakami, H. (1966) - Some problems on the oxidation of oxidizable sulphur. Characteristics and improvement of acid sulphate soils (part 3). Abstract in: Soil Sc. Pl. Nutr., Vol. 14 (1968), pp 83-84. Tokyo.

Negretti, G.C., G. Lombardi & L. Morbidelli (1966) - Studio geopetrografico del complesso vulcanico Tolfetano-Cerite (Lazio). IV. Le manifestazioni vulcaniche acide del settore Civitavecchia-Tolfetano. Atti Ist. Petr. Univ. Roma.

Norrish, K. & L.E.R. Rogers (1956) - The mineralogy of some terra rossa and rendzinas of South Australia. J. Soil Sc., Vol. 7, no. 2, pp 294-301. Oxford.

Oyama, M. & H. Takehara (1967) - Revised Standard Soil Color Charts. Research Council for Agriculture, Forestry and Fisheries, Ministry of Agriculture and Forestry. 74 pp. Tokyo.

Parotto, M. & A. Praturlon (1975)- Geological summary of the Central Apennines. In: Ogniben, L., M. Parotto & A. Praturlon (Ed.) - Structural Model of Italy. Quaderni de "La Ricerca Scientifica" no. 90. 502 pp. Roma.

van der Plas, L. & J. van Schuylenborgh (1970) - Petrochemical calculations applied to soils - with special reference to soil formation. Geoderma, Vol. 4, pp 357-385. Amsterdam.

Portegies Zwart, R. & O.C. Spaargaren (1973) - De waterhuishouding van het stroomgebied van de Liri-Garigliano. Int. Rep. Dept. Civ. Eng. Agr. Univ. Wageningen. 35 pp. Amsterdam.

Portegies Zwart, R. (1974) - Bodems en landschap in het Liridal benedenstrooms van Pontecorvo (Lazio, Italië). Int. Rep. Fys. Geogr. Bod. Lab. Univ. Amsterdam.

Reifenberg, A. (1929) - Die Entstehung der Mediterran-Roterde (Terra Rossa). Ein Beitrag zur angewandten Kolloidchemie. Sonderausgabe aus Kolloidchemische Beihefte. 93 pp. Dresden-Leipzig.

Reifenberg, A. (1947) - Some observations on red soils. C.R. Conf. Péd. Med., pp 161-163. Paris.

Remmelzwaal, A. (1978) - Soil genesis and Quaternary landscape development in the Tyrrhenian coastal area of south-central Italy. Thesis Univ. Amsterdam. 309 pp. Amsterdam.

Robbins, C. & W.D. Keller (1952) - Clay and other non-carbonate minerals in some limestones. J. Sed. Petr., Vol. 22, no. 3, pp 146-152.

Robie, R.A. & D.R. Waldbaum (1968) - Thermodynamic properties of minerals and related substances at 298.15 °K (25.0 °C) and 1 atmosphere (1.013 bars) pressure and at higher temperatures. Geol. Survey Bull. no. 1259. 256 pp. Washington D.C.

Robie, R.A., B.S. Hemingway & J.R. Fisher (1978) - Thermodynamic properties of minerals and related substances at 298.15 °K and 1 bar (10^5 Pascals) pressure and at higher temperatures. Geol. Survey Bull. no. 1452. 456 pp. Washington D.C.

Rosenberg, P.E., D.M. Burt & H.D. Holland (1967) - Calcite-dolomite-magnesite stability relations in solutions: the effect of ionic strength. Geoch. et Cosmoch. Acta, Vol. 31, pp 391-396. Pergamon Press.

Ross, C.S. & S.B. Hendrick (1945) - Minerals of the montmorillonite group, their origin and relation to soils and clays. U.S. Geol. Survey Prof. Paper 205-B, pp 23-79. Washington D.C.

Rottini, O.T., G. Lotti & P.V. Baldacci (1965) - Recherches sur les argiles de la terra rossa italiene. La Ricerca Scientifica, Anno 35-Serie 2, Rediconti B, Vol. 6, no. 1, pp 59-65.
Ruhe, R.V. (1956) - Geomorphic surfaces and the nature of soils. Soil Sc., Vol. 82, pp 441-455.
Scheffer, F. & P. Schachtschabel (1976) - Lehrbuch der Bodenkunde, 9e Auflage. 394 pp. Stuttgart.
Schlichting, E. & H.-P. Blume (1966) - Bodenkundliches Praktikum. Hamburg-Berlin.
van Schuylenborgh, J. (1947) - A study on soil structure. Thesis Agricultural University Wageningen. 110 pp. Wageningen.
van Schuylenborgh, J. (1977) - Verwering en bodemvorming. Lecture notes Fys. Geogr. Bod. Lab. Univ. Amsterdam, revised by J.M. Verstraten. 212 pp. Amsterdam.
Schwarzbach, M. (1974) - Das Klima der Vorzeit. Eine Einführung in die Paläoklimatologie. 380 pp. Stuttgart.
Schwertmann, U. & R.M. Taylor (1977) - Iron oxides. Chapter 5 in: Dixon, J.B. & S.B. Weed (Ed.) - Minerals in soil environments, pp 145-180. Madison.
Segalen, P. (1964) - Le fer dans les sols. Initiations-documentations techniques no. 4 de l' ORSTOM. 150 pp. Paris.
Segre, A.G. (1948) - I fenomeni carsici e la speleologia del Lazio. Pubbl. dell' Istituto di Geografia dell' Università di Roma, Serie A, no. 7. 239 pp. Roma.
Servizio Geologico d' Italia (1966) - Carta geologica d' Italia, F° 159 (Frosinone) and F° 160 (Cassino). Firenze.
Sestini, G. (1970) - Development of the Northern Apennines geosyncline. Sed. Geol., Vol. 4, pp 201-648. Amsterdam.
Sevink, J. & A.P.A. Vink (1969) - Some banded soils on the southern Veluwe (the Netherlands). Geoderma, Vol. 3, pp 157-173. Amsterdam.
Sevink, J., A. Remmelzwaal, O.C. Spaargaren & A.P.A. Vink (1979) - The soils of southern Lazio and adjacent Campania (Agro Pontino, Volsci Range, Garigliano Basin and Valle Latina). Geol. Rom. (in preparation).
Sinno, R. (1963) - Studio sulle terre rosse dell' Italia centrale e meridionale. La terra rossa di Gaeta (Nota I). Estratto dal "Bolletino dalla Società dei Naturalisti in Napoli", Vol. LXXII.
Soil Survey (1970) - Selected chapters from the unedited text of the Soil Taxonomy of the National Cooperative Soil Survey. Soil Conservation Service, U.S.D.A. 499 pp. Washington D.C.
Soil Survey Staff (1951) - Soil Survey Manual. Soil Conservation Service, U.S.D.A. 503 pp. Washington D.C.
Soil Survey Staff (1975) - Soil Taxonomy. A basic system of soil classification for making and interpreting soil surveys. Agricultural Handbook no. 436. Soil Conservation Service, U.S.D.A. 754 pp. Washington D.C.
Spaargaren, O.C. (1973) - Verslag van een pedogenetisch onderzoek van twee bodemprofielen in het Valle Latina (Zuid Italië). Int. Rep. Fys. Geogr. Bod. Lab. Univ. Amsterdam. 20 pp. Amsterdam.
Spaargaren, O.C. (1974) - Bodemkundig en hydrologisch onderzoek in de Oost-Ciociaria (Lazio, Italië). Int. Rep. Fys. Geogr. Bod. Lab. Univ. Amsterdam. 158 pp. Amsterdam.
Stumm, W. & J.J. Morgan (1970) - Aquatic Chemistry. 583 pp. New York.
Tamura, T. & M.L. Jackson (1953) - Structural and energy relationships in the formation of iron and aluminium oxides, hydroxides and silicates. Science, Vol. 117, pp 381-383.
Thornthwaite, C.W. & J.R. Mather (1955) - The water balance. Publ. in Climatology, Vol. VIII, no. I. Drexel Institute of Technology. 104 pp. Centerton, New Jersey.
Thorstenson, D.C. & L.N. Plummer (1977) - Equilibrium criteria for two-component solids reacting with fixed composition in an aqueous phase - Example: the magnesium calcites. Am. J. of Sc., Vol. 277. pp 1203-1223.

Tombesi, L., E. Romano & E. Lauciani (1965) - Misura di evapotraspirazione potentiale e bilanci idrologici di alcune colture. Annali della stazione chimico-agrario sperimentale di Roma, Serie III, Pubbl. 234. 24 pp. Roma.

Valeton, I. (1972) - Bauxites. Developments in soil science 1. 226 pp. Amsterdam.

Verstraten, J.M. (1978) - Water-rock interactions in (very) low-grade metamorphic shales. A case study in a catchment in the Oesling, Luxembourg. Thesis Univ. Amsterdam. 249 pp. Amsterdam.

Vink, A.P.A. (1963) - Planning of soil surveys in land development. Publ. ILRI no. 10. 55 pp. Wageningen.

de Waart, J.P. (1971) - Reconstruction of the Cenozoic evolution of a polygenetic landscape near Cannes, S.E. France. A paleogeomorphological study. Thesis Univ. Amsterdam. 123 pp. Amsterdam.

Weast, R.C. (Ed.) (1975) - Handbook of chemistry and physics. 55th Edition (1974-1975). Cleveland.

Weaver, C.E. & L.D. Pollard (1973) - The chemistry of clay minerals. Developments in sedimentology no. 15. 213 pp. Amsterdam.

Wilke, B.-M. & U. Schwertmann (1977) - Gibbsite and halloysite decomposition in strongly acid podzolic soils developed from granitic saprolite of the Bayerischer Wald. Geoderma, Vol. 19, pp 51-61. Amsterdam.

Wood, W.W. (1973) - A technique using porous cups for water sampling at any depth in the unsaturated zone. Water Resource Res., Vol. 9, pp 486-488.

Wijmstra, T.A. (1969) - Palynology of the first 30 metres of a 120 m deep section in northern Greece. Acta Bot. Neerl., Vol. 18, pp 511-527.

Zen, E-an (1972) - Gibbs free energy, enthalpy and entropy of ten rock-forming minerals. Calculations, discrepances, implications. Am. Min., Vol. 57, pp 524-553.

APPENDICES

APPENDIX 2 SOIL PROFILE DESCRIPTIONS AND ANALYSES.

Profile descriptions were made according to the Guidelines for Soil Profile Description (FAO, 1977). Soil names are given both in terms of the Legend of the Soil Map of the World (FAO-UNESCO, 1974) as well according to the USDA Soil Taxonomy (SOIL SURVEY STAFF, 1975). Classification according to the Soil Taxonomy is given down to the fifth or "family" level, while to the "Soil Map of the World"-name the textural class is added.

Soil horizons have been named according to the FAO Guidelines for Soil Profile Description. Because this horizon designation is not yet commonly used, it must be emphasized here, that this notation indicates properties and does not have a genetic meaning. For instance, an argillic B horizon, indicated by Bt, can be subdivided into Bt1, Bt2, Bt3 .... etc. In former notations the symbol B2t e.g. was attributed to that part of the argillic B horizon, in which the clay illuviation was the most pronounced. This interpretation should not be given to the Bt2 notation of the new FAO-system, as it only indicates a morphological subdivision of the argillic B horizon, which may be based on other profile characteristics than clay illuviation features.

The following suffix letters have been used to qualify the master horizons (FAO, 1977):

- c: accumulation in concretionary form
- g: mottling reflecting variations in oxidation and reduction
- h: accumulation of organic matter in mineral horizons
- k: accumulation of calcium carbonate
- m: strongly cemented, consolidated, indurated
- p: disturbed by ploughing or other tillage practises
- t: illuvial accumulation of clay
- w: alteration in situ as reflected by clay content, colour, structure

Arabic prefixes have been used to indicate lithological discontinuities. They are also used to distinguish soil horizons with admixture of volcanic material from those without this admixture.

The coordinates given in the profile descriptions are the coordinates used on the italian topographic maps. They differ from the international coordinate system by another zero meridian, which is in the italian system the meridian over Monte Mario at Rome. This meridian is situated 12^{o} 27' 10" east of Greenwich (see also section 1.2).

Together with the profile descriptions the physical and chemical analyses of the soil samples are given. The analysing procedures are summarized in appendix 3. The figures have been rounded off to one decimal. Amounts less than 0.05% are indicated by tr (trace), not detectable by a bar (-) and blank means not determined.

Profilenumber: Sp/4
Classification: FERRIC ACRISOL, medium textured (FAO-UNESCO, 1974)
ULTIC HAPLOXERALF, fine kaolinitic, mesic (SOIL SURVEY STAFF, 1975)
Location: approximately 1.5 km north-east of Castro dei Volsci (Fr., Italy) alongside road Madonna del Piano-Ceprano; topographical map Ceccano, F° 159 I S.E. della Carta d' Italia 1 : 25 000, 41° 31' 04" N.L. and 0° 57' 58" east of Monte Mario (Rome)
Elevation: approximately 155 m a.s.l.
Physiographic position: convex slope near the crest of a ridge
Slope: sloping (10 %)
Vegetation: oak wood with poor groundcover
Parent material: fluviatile sands with gravel layers of probably old Quaternary age
Drainage conditions: (moderately) well drained
Moisture conditions: dry throughout profile

Ah 0-10 cm; brownish black (10YR 2/2, moist) sandy clay loam; weak fine crumb; soft when dry; many very fine and fine pores; non calcareous; many fine and few medium and coarse roots; pH 6.6; clear and wavy boundary to

E 10-40 cm; bright brown (7.5YR 5/6, moist) loam; common coarse faint clear orange (7.5YR 6/6, moist) mottles; moderate fine to medium angular blocky; hard when dry; patchy moderately thick brown (7.5YR 4/4, moist) clay-iron-humus cutans in some pores; very few rounded fresh quartz gravels; non calcareous; common very fine and fine roots; pH 5.2; gradual and wavy boundary to

Bt 40-100 cm; reddish brown (5YR 4/6, moist) clay; moderate very fine to fine angular blocky; slightly hard when dry; continuous moderately thick to thick dull reddish brown (5YR 4/4, moist) clay-iron cutans on most of the pedfaces, in pores and around nodules; common very fine pores; very few rounded fresh quartz gravels; very few large hard spherical black iron-manganese and brown iron nodules; non calcareous; common very fine and fine roots; pH 4.9; clear and wavy boundary to

Bgt 100->190 cm; mottled clay loam, light grey (2.5Y 8/2), bright brown (7.5YR 5/8) and red (10R 4/8), all when moist; weak medium to thick platy; hard when dry; broken moderately thick bright brown (7.5YR 5/6, moist) clay-iron cutans, mainly in vertical voids; common very fine pores; very few to few rounded fresh quartz gravels; non calcareous; very few fine roots; pH 4.6

ANALYSES PROFILE Sp/4

Horizon	Depth of sample (cm)	TEXTURE (µm in weight %) >2 mm	Sand 2000-1000	Sand 1000-500	Sand 500-250	Sand 250-100	Sand 100-50	Sand 50-2	Silt Clay <2	pH H_2O	pH $CaCl_2$	Org. C %
Ah	0- 10	0.6	2.0	2.0	10.0	28.5	19.0	26.5	12.0	6.6	6.0	7.8
E	15- 35	2.1	1.5	1.5	8.0	26.0	17.0	29.5	16.5	5.2	4.1	0.7
Bt	50- 80	0.6	1.0	1.0	5.0	18.0	13.0	22.0	40.0	4.9	3.8	0.6
Bgt	100-130	0.1	0.5	0.8	5.0	20.5	12.0	25.0	36.0	4.6	3.1	0.2
	150-170	14.1	4.5	9.5	30.0	20.5	5.0	15.0	16.0	4.6	3.4	0.1
Bgt	grey mot.	0.0	0.2	0.3	4.0	19.0	15.0	24.0	38.0	4.8	2.8	0.2
	red mot.	0.0	0.3	0.7	9.0	34.0	9.5	17.0	29.5	4.8	3.4	0.1

ELEMENTAL COMPOSITION OF THE FINE EARTH FRACTION (weight %)

Horizon	Depth of sample (cm)	SiO_2	Al_2O_3	Fe_2O_3	FeO	MnO	MgO	CaO	Na_2O	K_2O	TiO_2	P_2O_5	H_2O	"Free" Fe_2O_3
Ah	0- 10	83.3	9.0	1.5	0.6	tr	0.4	0.9	0.5	1.6	0.2	0.1	1.9	1.2
E	15- 35	82.1	9.8	2.3	0.5	0.1	0.3	0.1	0.5	1.7	0.4	tr	2.4	1.7
Bt	50- 80	70.3	15.6	5.0	0.5	tr	0.5	0.1	0.3	1.4	0.5	0.2	5.7	3.9
Bgt	100-130	72.8	14.5	4.4	0.1	tr	0.4	tr	0.2	1.5	0.4	0.4	5.2	3.1
	150-170	82.9	9.0	2.5	0.1	tr	0.3	0.1	0.3	1.4	0.3	tr	3.2	1.6
Bgt	grey mot.	75.7	14.5	2.1	0.1	tr	0.5	tr	0.4	1.5	0.4	tr	4.9	0.9
	red mot.	74.8	10.9	7.2	0.2	0.1	0.3	tr	0.2	1.3	0.4	0.2	4.5	6.0

ELEMENTAL COMPOSITION OF THE CLAY FRACTION (weight %)

Horizon	Depth of sample (cm)	SiO_2	Al_2O_3	Fe_2O_3	FeO	MnO	MgO	CaO	Na_2O	K_2O	TiO_2	P_2O_5	H_2O	"Free" Fe_2O_3
Ah	0- 10	44.8	28.8	9.2	0.6	0.1	1.2	tr	0.2	1.8	0.8	0.5	12.1	6.1
E	15- 35	47.0	28.5	9.0	0.7	0.1	1.2	tr	0.1	2.0	0.9	tr	10.5	7.4
Bt	50- 80	43.8	30.8	10.3	0.4	0.1	1.0	tr	tr	1.3	0.7	0.2	11.5	7.6
Bgt	100-130	45.8	31.8	8.2	0.1	0.1	1.0	tr	0.1	1.2	0.7	tr	11.2	5.0
	150-170	44.1	32.4	9.1	0.1	tr	0.9	tr	tr	1.1	0.6	tr	11.8	6.0
Bgt	grey mot.	47.8	33.1	5.1	0.1	0.1	1.0	tr	tr	1.1	0.7	0.2	10.8	1.4
	red mot.	41.1	28.1	17.0	0.1	0.2	0.9	tr	tr	1.0	0.3	tr	11.4	13.7

MOLAR RATIOS

		SOIL				CLAY			
Horizon	Depth of sample (cm)	$\frac{SiO_2}{R_2O_3}$	$\frac{SiO_2}{Al_2O_3}$	$\frac{SiO_2}{Fe_2O_3}$	$\frac{Al_2O_3}{Fe_2O_3}$	$\frac{SiO_2}{R_2O_3}$	$\frac{SiO_2}{Al_2O_3}$	$\frac{SiO_2}{Fe_2O_3}$	$\frac{Al_2O_3}{Fe_2O_3}$
Ah	0- 10	14.2	15.7	145.7	9.3	2.2	2.6	13.0	4.9
E	15- 35	12.4	14.3	94.4	6.6	2.3	2.8	13.9	5.0
Bt	50- 80	6.4	7.7	37.5	4.9	2.0	2.4	11.3	4.7
Bgt	100-130	7.1	8.5	43.6	5.1	2.1	2.4	14.9	6.1
	150-170	13.3	15.7	88.2	5.6	2.0	2.3	12.9	5.6
Bgt	grey mot.	8.1	8.9	95.0	10.7	2.2	2.5	24.7	10.1
	red mot.	8.2	11.6	27.5	2.4	1.8	2.5	6.4	2.6

Profilenumber: Sp/22 (section along footpath)
Classification: not relevant
Location: at Colle Arnaro, approximately 5.5 km north-north-west of Pastena (Fr., Italy); topographical map Ceprano, F° 160 IV S.O. della Carta d' Italia 1 : 25 000, approximately 41° 30' 37" N.L. and 1° 00' 32" east of Monte Mario (Rome)
Elevation: approximately 200 m a.s.l.
Vegetation: oak wood and shrub ("macchia")
Parent material: sandstone of Pliocene/old Quaternary age
Moisture conditions: moist along the entire section

Ah brownish black (7.5YR 2/2, moist) clay loam; moderate medium crumb; very friable when moist; many very fine and fine pores; non calcareous; few wormholes

E brown (7.5YR 4/6, moist) sandy loam; moderate medium angular blocky; friable when moist; patchy moderately thick brown (7.5YR 4/6, moist) clay-iron cutans along some pores; common very fine and fine pores; very few rounded and angular fresh chert gravels; very few small soft spherical black iron-manganese nodules; non calcareous; few wormholes; pH 5.3

Bt bright reddish brown (5YR 5/8, moist) clay loam; moderate medium to coarse angular blocky; firm when moist; continuous moderately thick to thick bright reddish brown (5YR 5/6, moist) clay-iron cutans on most of the pedfaces and in pores; common very fine and fine and few medium pores; very few small soft spherical black iron-manganese nodules; non calcareous; few wormholes; pH 5.2

Bgt mottled sandy clay loam, reddish brown (2.5YR 4/6), brown (7.5YR 4/4 and 7.5YR 4/6), bright yellowish brown (10YR 6/6) and bluish black (5PB 2/1), all when moist; moderate coarse to very coarse subangular blocky; friable when moist; broken moderately thick orange (7.5YR 6/6, moist) clay-iron cutans on some pedfaces; common very fine and fine pores; very few small soft spherical black iron-manganese nodules; non calcareous; few wormholes; pH 5.4

BC yellow orange (7.5YR 7/8, moist) sandy loam; few medium prominent clear light grey (2.5Y 7/1, moist) mottles; very weak coarse to very coarse subangular blocky; very friable when moist; continuous thick reddish brown (5YR 4/6, moist) clay-iron cutans in voids and on large pedfaces; few very fine and fine pores; non calcareous; very few wormholes; pH 4.7

C yellow orange (10YR 7/8, moist) sandy loam; single grain; very friable when moist; few very fine and fine and very few medium pores; non calcareous; few wormholes; pH 5.3

R pale yellow (5Y 8/3, moist) sand; massive; extremely firm when moist; weakly cemented; strongly calcareous; pH 8.3

ANALYSES PROFILE Sp/22

	TEXTURE (µm in weight %)											
	Sand					Silt	Clay	pH		Org.	"Free" Fe_2O_3	
Horizon	2000 1000	1000 500	500 250	250 100	100 50	50 2	<2	H_2O	$CaCl_2$	C %	Soil	Clay
E	0.4	1.0	12.5	37.5	10.5	21.5	16.5	5.3	4.3	0.3	1.3	6.5
Bt	0.2	0.6	7.5	27.0	7.0	26.5	31.0	5.2	4.3	0.0	2.4	6.3
Bgt	0.0	0.2	7.5	37.0	9.0	20.5	26.0	5.4	4.2	0.2	1.9	6.5
BC	0.2	0.5	8.5	34.5	8.0	31.5	16.5	4.7	3.4	0.3	2.2	6.3
C	0.0	0.1	22.5	33.5	8.0	26.5	9.0	5.3	4.0	0.7	1.1	5.8
R	3.5	6.5	30.5	38.0	7.5	13.0	1.0	8.3	7.5	0.0	0.5	3.8

ELEMENTAL COMPOSITION OF THE FINE EARTH FRACTION (weight %)

Horizon	SiO_2	Al_2O_3	Fe_2O_3	FeO	MnO	MgO	CaO	Na_2O	K_2O	TiO_2	P_2O_5	H_2O	CO_2
E	83.2	7.9	2.6	0.2	0.1	0.3	0.1	0.4	2.1	0.4	tr	2.7	-
Bt	74.4	12.1	4.5	0.1	0.2	0.6	0.2	0.4	2.1	0.7	tr	4.8	-
Bgt	76.4	11.8	4.0	0.1	tr	0.5	0.3	0.2	2.0	0.5	tr	4.1	-
BC	77.5	10.9	4.1	0.1	0.2	0.6	0.1	0.4	2.4	0.5	tr	3.4	-
C	79.4	10.1	3.4	tr	0.2	0.8	0.2	1.0	2.6	0.4	tr	2.0	-
R	41.4	4.9	1.6	tr	0.1	0.7	26.6	0.9	1.4	0.2	tr	1.8	20.5

ELEMENTAL COMPOSITION OF THE CLAY FRACTION (weight %)

Horizon	SiO_2	Al_2O_3	Fe_2O_3	FeO	MnO	MgO	CaO	Na_2O	K_2O	TiO_2	P_2O_5	H_2O	CO_2
E	47.3	25.5	11.1	0.2	0.2	1.5	0.2	0.1	1.6	0.7	0.3	11.4	-
Bt	47.1	27.0	10.0	0.1	0.2	1.2	0.3	0.1	1.3	0.9	0.2	11.5	-
Bgt	46.4	27.4	10.5	0.1	0.1	1.1	0.3	0.1	1.1	0.6	0.2	12.1	-
BC	47.6	25.9	10.6	0.1	0.3	1.3	0.2	0.1	1.2	0.6	0.3	11.9	-
C	48.8	22.5	11.8	0.1	0.7	1.7	0.2	0.2	1.3	0.6	0.3	12.3	-
R	48.9	14.8	11.8	0.1	0.3	3.7	4.5	0.2	1.2	0.4	0.2	10.3	3.4

MOLAR RATIOS

	SOIL				CLAY			
Horizon	$\frac{SiO_2}{R_2O_3}$	$\frac{SiO_2}{Al_2O_3}$	$\frac{SiO_2}{Fe_2O_3}$	$\frac{Al_2O_3}{Fe_2O_3}$	$\frac{SiO_2}{R_2O_3}$	$\frac{SiO_2}{Al_2O_3}$	$\frac{SiO_2}{Fe_2O_3}$	$\frac{Al_2O_3}{Fe_2O_3}$
E	14.8	17.9	86.1	4.8	2.5	3.2	11.4	3.6
Bt	8.4	10.5	43.8	4.2	2.4	3.0	12.5	4.2
Bgt	9.0	11.0	51.2	4.7	2.3	2.9	11.7	4.1
BC	9.7	12.1	50.7	4.2	2.5	3.1	11.0	3.8
C	11.0	13.3	62.3	4.7	2.7	3.6	10.8	3.0
R	11.9	14.5	67.9	4.7	3.7	5.6	11.0	2.0

Profilenumber: Sp/41
Classification: ORTHIC ACRISOL, medium textured (FAO-UNESCO, 1974)
ULTIC HAPLOXERALF, fine-loamy, mixed, mesic (SOIL SURVEY STAFF, 1975)
Location: at locality "I Castagneti", approximately 5 km north-west of Pastena (Fr., Italy); topographical map Ceprano, F° 160 IV S.O. della Carta d' Italia 1 : 25 000, 41° 30' 11" N.L. and 1° 00' 22" east of Monte Mario (Rome)
Elevation: approximately 175 m a.s.l.
Physiographic position: straight slope in rolling to hilly country
Slope: very steep (60 %)
Vegetation: oak trees with poor groundcover
Parent material: conglomerates of Pliocene age
Drainage conditions: well drained
Moisture conditions: dry throughout profile
Presence of stones: (slightly) gravelly and stony

AB 0-25 cm; reddish brown (5YR 5/6, moist) slightly gravelly sandy loam; moderate medium to coarse subangular blocky; slightly hard when dry; common fine and medium pores; few rounded and angular strongly weathered Miocene sandstone, chert and quartz gravels; non calcareous; somw biopores; common fine and medium roots; pH 5.0; clear and smooth boundary to

Bt1 25-65 cm; reddish brown (5YR 4/6, moist) gravelly loam; common medium prominent sharp bluish black (5PB 2/1, moist) mottles; moderate coarse subangular blocky; slightly hard when dry; broken moderately thick reddish brown (2.5YR 4/6, moist) clay-iron cutans on all pedfaces, around gravels and in pores; many fine and medium pores; many rounded and angular strongly weathered Miocene sandstone, chert and quartz gravels; non calcareous; some biopores; common fine and medium roots; pH 5.6; gradual and smooth boundary to

Bt2 60->100 cm; reddish brown (5YR 4/6, moist) (slightly) gravelly and stony clay (loam); few fine prominent sharp bluish black (5PB 2/1, moist) mottles; weak coarse prismatic, breaking into moderate to strong fine to medium subangular blocky; slightly hard when dry; continuous moderately thick to thick dull reddish brown (2.5YR 4/4, moist) clay-iron cutans on all pedfaces and in pores; common fine and medium pores; many rounded and angular strongly weathered Miocene sandstone chert and quartz gravels and few rounded strongly weathered Miocene sandstone stones; non calcareous; common fine and medium roots; pH 5.6-5.8

ANALYSES PROFILE Sp/41

		TEXTURE (µm in weight %)									
	Depth of		Sand					Silt	Clay		
Horizon	sample (cm)	>2 mm	2000 1000	1000 500	500 250	250 100	100 50	50 2	<2	pH H_2O	pH $CaCl_2$	Org. C %
AB	5- 20	12.5	5.5	4.5	10.5	23.0	12.0	28.0	17.0	5.0	4.3	0.8
Bt1	35- 45	22.5	3.0	3.5	8.0	17.0	9.5	32.5	26.0	5.6	5.0	0.7
Bt2	55- 70	11.0	3.5	3.0	7.0	13.0	7.0	30.5	36.5	5.6	5.1	0.5
	90-100	18.5	3.0	2.5	6.0	11.5	5.5	29.0	42.5	5.8	5.1	0.6

Profilenumber: Sp/56
Classification: CALCARIC PHAEOZEM, medium textured (FAO-Unesco, 1974)
LITHIC HAPLOXEROLL, coarse-loamy, mixed, mesic (SOIL SURVEY STAFF, 1975)
Location: approx. 2 km north of Pastena (Fr., Italy) at the locality "Colle Fornace" in the Piana Madonna delle Macchie; topographical map Pico, F° 160 III N.O. della Carta d' Italia 1:25 000, 41° 29' 11" N.L. and 1° 02' 27" east of Monte Mario (Rome)
Elevation: approx. 195 m a.s.l.
Physiographic position: small plateau in polje in limestone mountains
Vegetation: cereals
Parent material: calcareous, strongly cemented tuff, overlying finely stratified lacustrine deposits
Drainage conditions: well drained
Moisture conditions: moist throughout profile
Human influence: ploughing

Ap 0-32 cm; dark brown (7.5YR 3/3, moist) silt loam; moderate fine to medium subangular blocky; friable when moist; patchy moderately thick dark brown (7.5YR 3/3, moist), probably pressure cutans cuased by faunal activity in some biopores; common very fine and fine and few medium pores; very few small soft spherical black iron-manganese nodules; calcareous; common worm excrements; common fine and medium roots; pH 7.6; abrupt and smooth boundary to

Cm 32-210 cm; olive black (5Y 3/2, moist) loamy sand; massive; extremely firm when moist; strongly cemented; few fine pores; strongly calcareous; very few fine roots in fissures; abrupt and smooth boundary to

2C1 210-235 cm; yellowish grey (2.5Y 5/3, moist), alternating with dull yellowish brown (10YR 5/4, moist) finely stratified silt loam showing shrinking cracks; very friable when moist; common prints of organic material (leaves, stems, etc.); few thin tuff layers at approximately 230 cm; calcareous; abrupt and wavy boundary to

2C2 235-265 cm; dull brown (7.5YR 5/4, moist), alternating with brown (7.5YR 4/4, moist) and yellowish grey (2.5Y 5/3, moist) finely stratified silt loam showing shrinking cracks; very friable when moist; common prints of organic material (leaves, stems, etc.); calcareous; abrupt and smooth boundary to

2C3 265->350 cm; brownish black (7.5YR 3/2, moist) finely stratified silt loam; very friable when moist; few prints of organic material (leaves, stems, etc.); calcareous

ANALYSES PROFILE Sp/56

		TEXTURE (µm in weight %)									
	Depth of		Sand					Silt	Clay		
Horizon	sample (cm)	>2 mm	2000 1000	1000 500	500 250	250 100	100 50	50 2	<2	pH H_2O	pH $CaCl_2$	Org. C %
Ap	10- 30	0.9	1.0	2.0	7.0	15.0	9.0	52.0	14.0	7.6	7.4	2.3
Cm	50- 80	0.0	4.0	10.0	44.5	24.0	3.5	10.0	4.0			0.1
2C1	215-230	0.0			0.1			84.0	16.0			0.2
2C2	240-260	0.0	0.5	1.0	3.0	8.0	4.5	65.0	18.0			0.5
2C3	275-300	0.0	1.0	1.0	4.5	11.0	6.0	51.0	25.5			0.6

Profilenumber: Sp/64
Classification: FERRIC LUVISOL, medium textured (FAO-UNESCO, 1974)
MOLLIC HAPLOXERALF, fine-loamy, mixed, mesic (SOIL SURVEY STAFF, 1975)
Location: approximately 2 km northwest of Pastena (Fr., Italy), alongside road Pastena-Falvaterra; topographical map Pico, F° 160 III N.O. della Carta d' Italia 1 : 25 000, 41° 28' 56" N.L. and 1° 02' 55" east of Monte Mario (Rome)
Elevation: approximately 200 m a.s.l.
Physiographic position: plateau (former alluvial fan?)
Slope: gently sloping (3 %)
Vegetation: vine and cereals
Parent material: conglomerate, probably of Pliocene/old Quaternary age
Drainage conditions: well drained
Moisture conditions: moist throughout profile
Presence of stones: very gravelly and stony
Human influence: ploughing

Ap 0-20 cm; dark brown (7.5YR 3/3, moist) gravelly loam; weak fine crumb; very friable when moist; many very fine and fine pores; many rounded strongly weathered Miocene sandstone and quartz gravel and few rounded strongly weathered granite gravel; non calcareous; many fine and medium roots; pH 6.9; clear and smooth boundary to

Bt 20-70 cm; brown (7.5YR 4/4, moist) gravelly, stony and bouldery clay loam; moderate fine to medium subangular blocky; friable when moist; broken moderately thick dark brown (7.5YR 3/4, moist) clay-iron(-humus) cutans on most of the pedfaces and in pores; many gravels, stones and boulders, consisting of rounded strongly weathered Miocene sandstone and quartz and very few rounded strongly weathered granite gravel; very few large hard spherical black pisolites; non calcareous; common fine and few medium roots; pH 6.9; diffuse and smooth boundary to

Bg(t) 70->350 cm; bright brown (7.5YR 5/8, moist) gravelly, stony and bouldery loam; common coarse prominent sharp light grey (10YR 8/2) and bluish black (5PB 2/1) mottles, both when moist; moderate medium angular blocky; friable when moist; patchy moderately thick bright brown (7.5YR 5/6, moist) clay-iron cutans on some vertical pedfaces; few fine pores; many gravel, stones and boulders, consisting of rounded strongly weathered Miocene sandstone and quartz and very few rounded strongly weathered granite gravel; few large hard spherical black pisolites and very few haematite nodules; non calcareous; few fine roots; pH 7.4

ANALYSES PROFILE Sp/64

Horizon	Depth of sample (cm)	TEXTURE (µm in weight %) Sand 2000-1000	Sand 1000-500	Sand 500-250	Sand 250-100	Sand 100-50	Silt 50-2	Clay <2	pH H_2O	pH $CaCl_2$	Org. C %	"Free" Fe_2O_3 Soil	"Free" Fe_2O_3 Clay
		1000	500	250	100	50	2						
Ap	0- 20	4.5	3.5	7.5	16.0	10.5	31.0	27.0	6.9	6.4	1.7	4.5	8.3
Bt	30- 60	4.0	4.0	7.0	14.5	9.5	30.0	31.5	6.9	6.3	0.4	5.1	8.2
Bg(t)	80-110	6.0	5.5	10.5	16.5	10.0	30.0	21.0	7.4	6.8	0.0	5.0	9.3

ELEMENTAL COMPOSITION OF THE FINE EARTH FRACTION (weight %)

Horizon	Depth of sample (cm)	SiO_2	Al_2O_3	Fe_2O_3	FeO	MnO	MgO	CaO	Na_2O	K_2O	TiO_2	P_2O_5	H_2O
Ap	0- 20	74.0	10.9	5.7	0.3	0.4	0.6	0.7	0.3	1.4	0.7	0.3	4.9
Bt	30- 60	72.7	11.9	6.8	0.1	0.4	0.5	0.4	tr	0.8	0.6	0.1	5.5
Bg(t)	80-110	74.2	10.5	6.5	tr	0.4	0.6	0.4	tr	1.2	0.5	0.1	5.6

ELEMENTAL COMPOSITION OF THE CLAY FRACTION (weight %)

Horizon	Depth of sample (cm)	SiO_2	Al_2O_3	Fe_2O_3	FeO	MnO	MgO	CaO	Na_2O	K_2O	TiO_2	P_2O_5	H_2O
Ap	0- 20	45.6	26.1	10.5	1.0	0.2	1.0	-	0.1	1.8	0.3	0.4	13.0
Bt	30- 60	47.7	25.9	10.8	0.3	0.2	0.9	-	0.1	1.6	0.3	0.2	11.8
Bg(t)	80-110	47.9	24.6	13.1	0.1	0.3	1.2	-	0.1	1.6	0.2	0.2	10.7

MOLAR RATIOS

Horizon	Depth of sample (cm)	SOIL $\frac{SiO_2}{R_2O_3}$	SOIL $\frac{SiO_2}{Al_2O_3}$	SOIL $\frac{SiO_2}{Fe_2O_3}$	SOIL $\frac{Al_2O_3}{Fe_2O_3}$	CLAY $\frac{SiO_2}{R_2O_3}$	CLAY $\frac{SiO_2}{Al_2O_3}$	CLAY $\frac{SiO_2}{Fe_2O_3}$	CLAY $\frac{Al_2O_3}{Fe_2O_3}$
Ap	0- 20	8.6	11.5	34.3	3.0	2.4	3.0	11.5	3.9
Bt	30- 60	7.6	10.3	28.4	2.8	2.5	3.1	11.7	3.8
Bg(t)	80-110	8.6	12.0	30.2	2.5	2.5	3.3	9.7	2.9

Profilenumber: Sp/66
Classification: CHROMIC VERTISOL, fine textured (FAO-Unesco, 1974)
TYPIC CHROMOXERERT, very fine, mixed, mesic (SOIL SURVEY STAFF, 1975)
Location: approx. 500 m northeast of Pastena (Fr., Italy), alongside road Pastena-Falvaterra; topographical map Pico, F° 160, III N.O. della Carta d' Italia 1 : 25 000, 41° 28' 18" N.L. and 1° 02' 33" east of Monte Mario (Rome)
Elevation: approx. 250 m a.s.l.
Physiographic position: slope at fringe of tectonic karst basin ("polje")
Slope: steep (48 %)
Vegetation: olive trees and shrub
Parent material: light grey hard limestone (soil developed in fissure)
Drainage conditions: well drained
Moisture conditions: dry throughout profile
Presence of rock outcrops: very rocky
Human influence: terracing (locally A horizon removed)

AB 0-45 cm; dark reddish brown (5YR 3/6, moist) slightly gravelly clay; weak medium subangular blocky, breaking into moderate fine angular blocky, locally wedgeshaped; hard when dry; patchy moderately thick reddish brown (5YR 4/6, moist) clay-iron cutans in some pores and common small slickensides; common fine and medium pores; few angular and rounded fresh limestone gravel; non calcareous; pH 7.8; clear and smooth boundary to

Bw 45-150 cm; dull reddish brown (2.5YR 4/4, moist) slightly gravelly and stony clay; moderate coarse subangular blocky, breaking into strong fine angular blocky, locally wedgeshaped; very hard when dry; patchy moderately thick reddish brown (2.5YR 4/4, moist) clay-iron cutans on some pedfaces and common small and medium intersecting slickensides; few fine pores; few angular and rounded fresh limestone gravel and stones; non calcareous; pH 7.8; lateral abrupt and broken boundary to R and diffuse and smooth boundary to

2Bwck 150-170 cm; reddish brown (2.5YR 4/6, moist) slightly gravelly and stony clay; few fine prominent sharp bluish black (5PB 2/1, moist) mottles; moderate coarse prismatic, breaking into strong medium angular blocky, wedgeshaped; very hard when dry; patchy moderately thick reddish brown (2.5YR 4/6, moist) clay-iron cutans on some pedfaces and large intersecting slickensides; few fine and medium pores; few angular and rounded fresh limestone gravel and stones; few large hard knobby reddish brown calcium carbonate nodules and very few small soft spherical black iron-manganese nodules; non calcareous; few fine roots; pH 7.8; abrupt and broken boundary to

R > 170 cm; light grey hard limestone

ANALYSES PROFILE Sp/66

		TEXTURE (µm in weight %)										
	Depth of		Sand					Silt	Clay	pH		Org.
Horizon	sample (cm)	>2 mm	2000 1000	1000 500	500 250	250 100	100 50	50 2	<2	H_2O	$CaCl_2$	C %
AB	10- 30	0.1	0.2	0.3	0.9	2.0	2.0	12.5	82.0	7.8	7.4	0.7
Bw	70-100	0.1	0.2	0.3	0.9	2.0	2.0	18.5	76.0	7.8	7.4	0.7
2Bwck	150-170	4.0	0.1	0.1	0.5	4.5	4.5	10.5	80.5	7.8	7.6	0.4

ELEMENTAL COMPOSITION OF THE FINE EARTH FRACTION (weight %)

Horizon	Depth of sample (cm)	SiO_2	Al_2O_3	Fe_2O_3	FeO	MnO	MgO	CaO	Na_2O	K_2O	TiO_2	P_2O_5	H_2O
AB	10- 30	48.8	26.3	8.3	0.5	0.2	1.7	1.2	0.2	2.1	0.8	0.3	9.7
Bw	70-100	48.4	26.5	8.2	0.7	0.2	1.8	1.0	0.3	2.2	0.8	0.2	9.4
2Bwck	150-170	48.4	26.4	8.4	0.4	0.3	1.7	1.3	0.6	1.6	0.8	0.2	10.1

ELEMENTAL COMPOSITION OF THE CLAY FRACTION (weight %)

Horizon	Depth of sample (cm)	SiO_2	Al_2O_3	Fe_2O_3	FeO	MnO	MgO	CaO	Na_2O	K_2O	TiO_2	P_2O_5	H_2O
AB	10- 30	41.4	30.3	9.7	0.4	0.3	1.8	0.2	0.3	2.0	0.8	tr	12.7
Bw	70-100	43.2	29.5	9.4	0.4	0.1	1.8	0.2	0.1	2.6	0.8	-	12.0
2Bwck	150-170	43.9	30.6	9.5	0.3	0.1	1.8	tr	tr	1.3	0.7	-	11.7

MOLAR RATIOS

Horizon	Depth of sample (cm)	SOIL $\frac{SiO_2}{R_2O_3}$	SOIL $\frac{SiO_2}{Al_2O_3}$	SOIL $\frac{SiO_2}{Fe_2O_3}$	SOIL $\frac{Al_2O_3}{Fe_2O_3}$	CLAY $\frac{SiO_2}{R_2O_3}$	CLAY $\frac{SiO_2}{Al_2O_3}$	CLAY $\frac{SiO_2}{Fe_2O_3}$	CLAY $\frac{Al_2O_3}{Fe_2O_3}$
AB	10- 30	2.6	3.2	15.7	5.0	1.9	2.3	11.4	4.9
Bw	70-100	2.6	3.1	15.6	5.1	2.1	2.5	12.2	4.9
2Bwck	150-170	2.6	3.1	15.3	4.9	2.0	2.4	12.3	5.1

Profilenumber: Sp/93
Classification: CHROMIC VERTISOL, fine textured (FAO-Unesco, 1974)
TYPIC CHROMOXERERT, very fine, mixed, mesic (SOIL SURVEY STAFF, 1975)
Location: approx. 2 km south of Falvaterra (Fr., Italy), alongside road Falvaterra-Pastena at road pass between two karst basins; topographical map Pico, F° 160, III N.O. della Carta d' Italia 1 : 25 000, 41° 29' 25" N.L. and 1° 03' 47" east of Monte Mario (Rome)
Elevation: approx. 300 m a.s.l.
Physiographic position: pass between two karst basins in limestone mountains
Slope: sloping (12 %)
Vegetation: shrub (mainly Ampelodesma tenax Link)
Parent material: hard grey limestone (soil developed in narrow fissure)
Drainage conditions: well drained
Moisture conditions: dry throughout profile
Presence of rock outcrops: extremely rocky

AB 0-40 cm; dark reddish brown (5YR 3/2, moist) gravelly and stony clay; moderate fine subangular blocky; hard when dry; patchy thin dark reddish brown (5YR 3/2, moist) clay-iron-humus cutans on some pedfaces; very porous; many irregular fresh limestone gravel and stones; very few small hard spherical black iron-manganese nodules; slightly calcareous; very few pottery fragments; many fine and medium and few coarse roots; pH 6.9; clear and wavy boundary to

Bt 40-55 cm; dark reddish brown (5YR 3/3, moist) slightly gravelly and stony clay; moderate fine subangular blocky; hard when dry; broken thick dark reddish brown (5YR 3/2, moist) cutans, probably matrans, scattered over pedfaces, broken moderately thick dull reddish brown (5YR 4/4, moist) clay-iron cutans, mainly on vertical pedfaces and few medium slickensides; few fine pores; few irregular fresh limestone gravel and stones; very few small hard spherical black iron-manganese nodules; slightly calcareous; very few pottery fragments; few fine roots; pH 7.3; clear and smooth boundary to

Bw1 55-100 cm; reddish brown (5YR 4/6, moist) slightly gravelly and stony clay; moderate coarse to very coarse angular blocky, often wedgeshaped; hard when dry; patchy moderately thick dull reddish brown (5YR 4/4, moist) clay-iron cutans on some pedfaces and in pores and common medium and few large intersecting slickensides; few fine pores; very few irregular fresh limestone gravel and stones; very few small soft spherical white calcium carbonate nodules and very few small soft spherical black iron-manganese nodules; slightly calcareous; few fine roots; pH 7.6; gradual and wavy boundary to

Bw2 100-160 cm; dark reddish brown (5YR 3/6, moist) slightly gravelly and stony silty clay; few fine distinct clear bluish black (5PB 2/1, moist) mottles; coarse to very coarse angular blocky, wedgeshaped; patchy moderately thick reddish brown (5YR 4/6, moist) clay-iron cutans on some vertical pedfaces and common large intersecting slickensides; few fine pores; few irregular fresh limestone gravel and stones; very few small hard spherical black iron-manganese nodules; slightly calcareous; very few fine roots; pH 6.9; abrupt and broken boundary to

R > 160 cm; hard grey limestone

ANALYSES PROFILE Sp/93

		TEXTURE (µm in weight %)										
	Depth of	Sand					Silt	Clay	pH		Org.	%
Horizon	sample (cm)	2000 1000	1000 500	500 250	250 100	100 50	50 2	<2	H_2O	$CaCl_2$	C %	CO_2
AB	10- 30	0.3	0.4	1.0	3.0	2.0	17.5	75.5	6.9	6.6	4.0	0.6
Bt	40- 50			2.5			11.0	86.5	7.3	6.9	1.7	0.4
Bw1	60- 80			2.0			7.0	91.0	7.6	7.0	0.4	0.3
Bw2	120-150			2.0			43.5	54.5	6.9	6.7	0.4	0.2

Profilenumber: Sp/97
Classification: CHROMIC VERTISOL, fine textured (FAO-Unesco, 1974)
AQUIC CHROMOXERERT, very fine, mixed, mesic (SOIL SURVEY STAFF, 1975)
Location: approx. 1.5 km south of Falvaterra (Fr., Italy), alongside road Falvaterra-Capodicolle; topographical map Pico, F° 160, III N.O. della Carta d' Italia 1 : 25 000, 41° 29' 33" N.L. and 1° 04' 38" east of Monte Mario (Rome)
Elevation: approx. 300 m a.s.l.
Physiographic position: concave slope in karst basin
Slope: sloping (10 %)
Microrelief: some gilgai relief
Vegetation: grass with scattered fruit and oak trees
Parent material: older colluvial deposits, covered by young colluvial deposits, both derived from limestone with some admixture of volcanic material in the young colluvial deposits
Drainage conditions: imperfectly drained
Moisture conditions: dry down to 1.5 m, lower moist

AB 0-35 cm; dark reddish brown (5YR 3/3, moist) clay; few fine distinct sharp bluish black (5PB 2/1, moist) mottles; strong coarse to very coarse prismatic; hard when dry; continuous thick dark reddish brown (5YR 3/6, moist) clay-iron cutans on most of the pedfaces, patchy thick dark reddish brown (5YR 3/2, moist) clay-iron(-humus) cutans in some pores and few small slickensides; common very fine and fine and few medium pores; very few small soft spherical black iron-manganese nodules; non calcareous; very few pottery fragments; common medium and few fine roots; some worm holes; pH 6.0; abrupt and smooth boundary to

2Bg(t)1 35-70/80 cm; dark reddish brown (5YR 3/6, moist) clay; common coarse prominent clear light grey (10Y 7/2) and orange (7.5YR 6/8) mottles, few medium prominent sharp bluish black (5PB 2/1) mottles and common medium to coarse faint diffuse red (10R 3/6) mottles all when moist; strong medium to coarse prismatic; hard to very hard when dry; patchy moderately thick reddish brown (5YR 3/2, moist) clay-iron-humus cutans on some vertical pedfaces and in pores, patchy moderately thick dark reddish brown (2.5YR 3/6, moist) clay-iron cutans on some pedfaces and common medium intersecting slickensides; common very fine and fine pores; non calcareous; few fine and very few medium roots; pH 5.8; gradual and smooth inclined[1] boundary to

2Bg(t)2 70/80-105/130 cm; dark reddish brown (5YR 3/6, moist) clay; many sharp coarse prominent light grey (7.5Y 7/2) and yellow orange (10YR 7/8) mottles and common medium distinct diffuse dark red (10R 3/6) mottles, all when moist; strong coarse to very coarse (sub-)angular blocky, peds locally wedgeshaped; patchy moderately thick dark reddish brown (5YR 3/6, moist) clay-iron cutans on some pedfaces and in pores and many large intersecting slickensides; few very fine and fine pores; non calcareous; few fine roots; pH 5.4; gradual and smooth inclined[1] boundary to

2Bg(t)3 105/130-155/170 cm; dark reddish brown (5YR 3/6, moist) clay; many medium distinct dark greyish yellow (2.5Y 5/2) and bright yellowish brown (10YR 6/6) mottles, common medium distict diffuse dark reddish brown (2.5YR 3/6) mottles and few medium prominent sharp bluish black (5PB 2/1) mottles, all when moist; strong coarse angular blocky, wedgeshaped; hard to very hard when dry; patchy moderately thick greyish brown (5YR 4/2, moist) clay-iron cutans in pores and many medium intersecting slickensides; few very fine and fine pores; non calcareous; few very fine and fine roots; pH 5.2; abrupt and smooth inclined[1] boundary to

2Bg 155/170-170/185 cm; dark reddish brown (2.5YR 3/4, moist) clay; common coarse faint diffuse light grey (5Y 7/2, moist) mottles and few fine distinct orange (7.5YR 6/8, moist) mottles; strong fine to medium angular blocky, peds locally wedgeshaped; firm when moist; many small intersecting slickensides; few fine pores; non calcareous; few very fine roots; pH 5.0; clear and wavy inclined[1] boundary to

3B(t) 170/185-280[2] cm; dark reddish brown (5YR 3/4, moist) clay; many coarse prominent sharp bluish black (5PB 2/1, moist) mottles on most of the pedfaces and few medium prominent sharp bright brown (2.5YR 5/8, moist) mottles inside the peds; moderate fine to medium angular blocky; firm when moist; patchy thin dark reddish brown (5YR 3/6, moist) clay-iron cutans mainly on vertical pedfaces and few small intersecting slickensides; very few very fine pores; non calcareous; very few medium roots; pH 5.2; with locally

4Bg; 225-260 cm; pocket of mottled clay, bluish black (5PB 2/1), yellow orange (7.5YR 7/8) and reddish brown (2.5YR 4/8), all when moist; weak fine angular blocky; friable when moist; few small slickensides; very few very fine pores; non calcareous; very few very fine roots; pH 5.0

[1]inclined with respect to the surface [2]depth obtained by augering; from this depth down to 360 cm the mottled clay as described in 4Bg re-appeared

ANALYSES PROFILE Sp/97

Horizon	Depth of sample (cm)	TEXTURE (µm in weight %) Sand 2000 50	Silt 50 2	Clay <2	pH H_2O	pH $CaCl_2$	Org. C %	"Free" Fe_2O_3 Soil	"Free" Fe_2O_3 Clay
AB	5- 25	5.5	23.0	71.5	6.0	5.5	1.6	5.9	7.1
2Bg(t)1	45- 65	0.5	8.0	91.5	5.8	5.2	0.5	4.8	3.9
2Bg(t)2	90-105	0.0	6.5	93.5	5.4	4.5	0.3	5.0	3.9
2Bg(t)3	130-150	0.5	5.5	94.0	5.2	4.2	0.4	5.8	4.7
2Bg	160-170	0.5	7.5	92.0	5.0	4.1	0.3	5.4	5.9
3B(t)	180-200	4.0	25.0	71.0	5.3	4.3	0.4	5.3	5.2
	200-220	3.0	21.5	75.5	5.2	4.2	0.3	5.7	5.9
4Bg	230-250	0.0	5.5	94.5	5.0	4.2			
2Bg(t)1	Grey m.	0.0	9.5	90.5	4.8	4.1	0.5	3.4	2.2
	Red m.	0.5	7.5	92.0	5.2	4.4	0.3	5.6	5.7

ELEMENTAL COMPOSITION OF THE FINE EARTH FRACTION (weight %)

Horizon	Depth of sample (cm)	SiO_2	Al_2O_3	Fe_2O_3	FeO	MnO	MgO	CaO	Na_2O	K_2O	TiO_2	P_2O_5	H_2O
AB	5- 25	51.3	24.3	8.5	1.0	0.2	0.9	0.5	0.3	2.3	1.2	0.2	9.5
2Bg(t)1	45- 65	47.3	28.3	7.6	0.6	0.1	1.3	0.5	0.2	2.4	0.8	0.1	10.9
2Bg(t)2	90-105	46.3	29.2	8.0	0.4	tr	1.3	0.4	0.1	2.2	0.8	0.1	11.2
2Bg(t)3	130-150	46.3	28.9	8.4	0.6	0.1	1.0	0.3	0.1	1.8	0.9	0.2	11.5
2Bg	160-170	45.6	29.5	8.2	0.3	0.1	1.0	0.2	0.2	1.9	0.8	0.2	11.1
3B(t)	180-200	48.2	27.3	7.7	0.4	0.2	0.6	0.2	0.3	1.7	1.0	0.2	12.0
	200-220	47.7	27.7	8.0	0.5	0.2	0.7	0.2	0.3	1.7	1.0	0.2	11.8
2Bg(t)1	Grey m.	49.6	25.9	6.6	0.4	0.1	2.3	0.7	0.1	4.1	1.0	0.1	9.1
	Red m.	45.8	29.6	8.1	0.4	0.1	1.1	0.4	0.2	2.1	0.7	0.1	11.6

ELEMENTAL COMPOSITION OF THE CLAY FRACTION (weight %)

Horizon	Depth of sample (cm)	SiO_2	Al_2O_3	Fe_2O_3	FeO	MnO	MgO	CaO	Na_2O	K_2O	TiO_2	P_2O_5	H_2O
AB	5- 25	44.4	29.0	9.9	0.2	0.1	0.8	0.1	0.1	1.7	1.2	0.4	12.2
2Bg(t)1	45- 65	47.4	29.2	6.8	0.2	tr	1.2	0.1	0.1	2.5	0.8	0.2	11.4
2Bg(t)2	90-105	46.6	30.1	6.9	0.2	tr	1.1	0.1	0.1	2.4	0.8	0.2	11.6
2Bg(t)3	130-150	46.2	30.0	7.7	0.1	tr	0.9	0.1	0.1	1.9	0.9	0.3	11.9
2Bg	160-170	45.5	30.2	8.8	0.1	tr	0.8	0.1	0.1	1.8	0.8	0.3	11.5
3B(t)	180-200	44.4	32.2	7.5	0.1	0.1	0.5	0.1	0.1	0.8	0.9	0.4	13.1
	200-220	44.0	31.8	8.1	0.1	0.1	0.5	0.1	tr	0.9	1.0	0.5	13.0
2Bg(t)1	Grey m.	49.9	26.9	6.0	0.3	tr	2.3	0.1	0.1	4.5	0.9	0.1	9.1
	Red m.	45.4	29.8	8.5	0.2	tr	1.0	0.1	0.1	2.0	0.8	0.2	11.9

MOLAR RATIOS

Horizon	Depth of sample (cm)	SOIL $\frac{SiO_2}{R_2O_3}$	SOIL $\frac{SiO_2}{Al_2O_3}$	SOIL $\frac{SiO_2}{Fe_2O_3}$	SOIL $\frac{Al_2O_3}{Fe_2O_3}$	CLAY $\frac{SiO_2}{R_2O_3}$	CLAY $\frac{SiO_2}{Al_2O_3}$	CLAY $\frac{SiO_2}{Fe_2O_3}$	CLAY $\frac{Al_2O_3}{Fe_2O_3}$
AB	5- 25	2.9	3.6	16.1	4.5	2.1	2.6	11.9	4.6
2Bg(t)1	45- 65	2.4	2.8	16.5	5.8	2.4	2.8	18.4	6.7
2Bg(t)2	90-105	2.3	2.7	15.4	5.7	2.3	2.6	18.1	6.9
2Bg(t)3	130-150	2.3	2.7	14.7	5.4	2.3	2.6	15.9	6.1
2Bg	160-170	2.2	2.6	14.8	5.6	2.2	2.6	13.7	5.3
3B(t)	180-200	2.5	3.0	16.6	5.5	2.0	2.3	15.7	6.7
	200-220	2.5	2.9	15.8	5.4	2.0	2.4	14.5	6.2
2Bg(t)1	Grey m.	2.8	3.3	20.0	6.2	2.8	3.2	22.2	7.1
	Red m.	2.2	2.6	15.0	5.7	2.2	2.6	14.2	5.5

Profilenumber: Sp/98
Classification: CHROMIC LUVISOL, fine textured (FAO-UNESCO, 1974)
TYPIC HAPLOXERALF, very-fine, kaolinitic, mesic (SOIL SURVEY STAFF, 1975)
Location: approx. 1.2 km south of Falvaterra (Fr., Italy), alongside road Falvaterra-Capodicolle; topographical map Pico, F° 160 III N.O. della Carta d' Italia 1 : 25 000, 41° 29' 38" N.L. and 1° 04' 39" east of Monte Mario (Rome)
Elevation: approx. 300 m a.s.l.
Physiographic position: concave slope in karst basin
Slope: gently sloping to sloping (6 %)
Vegetation: oak and fruit trees with groundcover of grasses
Parent material: colluvial deposits derived from limestone with admixture of volcanic material
Drainage conditions: moderately well drained
Moisture conditions: dry throughout profile
Erosion conditions: slight sheet erosion

Ap 0-35 cm; dark brown (7.5YR 3/4, moist) clay; massive; very hard when dry; continuous thick dark brown (7.5YR 3/3, moist) clay-humus cutans along the walls of biopores; common medium pores; very few small soft spherical black iron-manganese nodules; few volcanic minerals; non calcareous; few pottery fragments; many biopores and wormholes; common fine and medium roots; abrupt and smooth boundary to

B 35-40 cm; dark brown (7.5YR 3/3, moist) clay; common fine prominent sharp bluish black (5PB 2/1, moist) mottles; moderate medium platy; very hard when dry; few very fine and fine pores; very few small soft spherical black iron-manganese nodules; continuous platy pan, probably caused by sheet erosion deposition; few volcanic minerals; non calcareous; few pottery fragments; very few biopores; common fine and medium roots; pH 5.9; abrupt and smooth boundary to

Bt1 40-80 cm; dark reddish brown (5YR 3/4, moist) clay; weak coarse subangular blocky, breaking into moderate medium angular blocky; hard when dry; broken moderately thick dark reddish brown (5YR 3/6, moist) clay-iron(-humus) cutans on most of the pedfaces and in most of the pores; many very fine, fine, medium and coarse pores; very few small soft spherical black iron-manganese nodules; few volcanic minerals; non calcareous; few pottery fragments; some biopores; many fine, medium and coarse roots; pH 5.8; diffuse and smooth boundary to

Bt2 80-140 cm; dark reddish brown (5YR 3/4, moist) clay; moderate coarse prismatic, breaking into strong medium subangular blocky; hard when dry; continuous thick dark reddish brown (5YR 3/4, moist) clay-iron(-humus) cutans on all pedfaces and in pores and few small, weakly developed slickensides; many very fine, fine and medium pores; very few small soft spherical black iron-manganese nodules; few volcanic minerals; non calcareous; few pottery fragments; few biopores; few fine and medium roots; pH 5.3-5.4; gradual and smooth boundary to

Bt3 140->170 cm; dark reddish brown (5YR 3/4, moist) clay; common medium prominent sharp bluish black (5PB 2/1, moist) mottles; strong fine to medium prismatic, breaking into strong medium subangular blocky; hard when dry; continuous moderately thick dark reddish brown (5YR 3/6, moist) clay-iron cutans on all pedfaces and few small, weakly developed slickensides; common fine pores; few small soft spherical black iron-manganese nodules; few volcanic minerals; non calcareous; few pottery fragments; very few biopores; very few fine roots; pH 5.4

ANALYSES PROFILE Sp/98

		TEXTURE (µm in weight %)									
	Depth of	┌ Sand ┐					Silt	Clay			
Horizon	sample (cm)	2000 1000	1000 500	500 250	250 100	100 50	50 2	<2	pH H_2O	pH $CaCl_2$	Org. C %
B	35- 40	0.2	0.5	1.5	3.5	2.0	29.5	63.0	5.9	5.3	0.9
Bt1	50- 70	———		4.0	———		24.0	71.5	5.8	5.2	0.9
Bt2	85-100	0.2	0.4	0.8	2.0	1.5	26.5	68.5	5.4	4.8	0.8
	120-135	0.1	0.3	0.6	1.5	3.5	31.5	62.5	5.3	4.6	1.1
Bt3	145-160	0.2	0.5	1.5	3.0	2.0	32.0	60.5	5.4	4.6	1.0

ELEMENTAL COMPOSITION OF THE FINE EARTH FRACTION (weight %)

Horizon	Depth of sample (cm)	SiO_2	Al_2O_3	Fe_2O_3	FeO	MnO	MgO	CaO	Na_2O	K_2O	TiO_2	P_2O_5	H_2O	"Free" Fe_2O_3
B	35- 40	50.5	24.2	9.1	0.5	0.3	0.8	0.5	0.3	2.4	1.2	0.2	10.0	6.0
Bt1	50- 70	47.6	27.0	9.7	0.3	0.2	0.8	0.4	0.2	1.9	1.1	0.3	10.4	6.3
Bt2	85-100	49.1	26.0	9.9	0.2	0.2	0.8	0.3	0.2	1.9	1.2	0.2	9.9	6.3
	120-135	51.3	24.5	9.3	0.5	0.3	0.8	0.4	0.3	2.1	1.2	0.2	9.0	6.3
Bt3	145-160	53.1	23.4	8.8	0.4	0.4	0.9	0.4	0.4	2.1	1.3	0.2	8.7	6.3

ELEMENTAL COMPOSITION OF THE CLAY FRACTION (weight %)

Horizon	Depth of sample (cm)	SiO_2	Al_2O_3	Fe_2O_3	FeO	MnO	MgO	CaO	Na_2O	K_2O	TiO_2	P_2O_5	H_2O	"Free" Fe_2O_3
B	35- 40	44.8	29.3	10.0	0.2	0.1	0.9		0.1	1.5	1.1	0.3	11.6	7.7
Bt1	50- 70	44.1	30.5	9.8	0.2	0.1	0.8		0.1	1.3	1.0	0.3	11.7	7.6
Bt2	85-100	44.3	30.1	10.1	0.1	0.1	0.9		0.1	1.4	1.1	0.3	11.5	7.7
	120-135	44.0	29.6	10.5	0.1	0.1	0.9		0.1	1.6	1.2	0.3	11.4	8.0
Bt3	145-160	44.0	29.5	10.6	0.1	0.2	1.0		0.1	1.6	1.2	0.4	11.4	7.9

MOLAR RATIOS

Horizon	Depth of sample (cm)	SOIL $\frac{SiO_2}{R_2O_3}$	SOIL $\frac{SiO_2}{Al_2O_3}$	SOIL $\frac{SiO_2}{Fe_2O_3}$	SOIL $\frac{Al_2O_3}{Fe_2O_3}$	CLAY $\frac{SiO_2}{R_2O_3}$	CLAY $\frac{SiO_2}{Al_2O_3}$	CLAY $\frac{SiO_2}{Fe_2O_3}$	CLAY $\frac{Al_2O_3}{Fe_2O_3}$
B	35- 40	2.3	3.5	14.0	4.0	2.1	2.6	11.8	4.5
Bt1	50- 70	2.4	3.0	12.5	4.2	2.0	2.5	11.8	4.8
Bt2	85-100	2.6	3.2	13.0	4.0	2.1	2.5	11.6	4.6
	120-135	2.8	3.6	13.8	3.9	2.1	2.5	11.0	4.4
Bt3	145-160	3.1	3.9	15.3	4.0	2.1	2.5	10.9	4.3

Profilenumber: Sp/99
Classification: CALCARIC PHAEOZEM, fine textured (FAO-Unesco, 1974)
LITHIC/TYPIC HAPLOXEROLL, very fine, mixed, mesic (SOIL SURVEY STAFF, 1975)
Location: approx. 1 km south of Falvaterra (Fr., Italy) alongside road Falvaterra-Pastena; topographical map Pico, F° 160, III N.O. della Carta d' Italia 1 : 25 000, 41° 29' 42" N.L. and 1° 04' 42" east of Monte Mario (Rome)
Elevation: approx. 300 m a.s.l.
Physiographic position: slightly concave slope in limestone mountains
Slope: moderately steep (18 %)
Vegetation: shrub (mainly Ampelodesma tenax Link)
Parent material: light grey to grey hard limestone
Drainage conditions: excessively drained
Moisture conditions: dry throughout profile
Presence of rock outcrops: extremely rocky

Ah 0-20/30 cm; brownish black (5YR 2/2, moist) clay; moderate fine to medium crumb; slightly hard when dry; many very fine and fine pores; few angular fresh limestone gravel; very few small hard spherical black iron-manganese nodules; non calcareous; few pottery fragments; some wormholes; many fine roots; pH 6.8; abrupt and broken boundary to R and clear and smooth boundary to

Bw 20/30-40/80 cm; dark reddish brown (5YR 3/6, moist) clay; moderate very fine to fine angular blocky; slightly hard when dry; patchy thin dark reddish brown (5YR 3/3, moist) clay-iron(-humus) cutans on some vertical pedfaces; few angular fresh limestone boulders and stones; very few small hard spherical black iron-manganese nodules; slightly calcareous; few wormholes; few medium roots; pH 7.2; abrupt and broken boundary to

R >40/80 cm; light grey to grey hard limestone

ANALYSES PROFILE Sp/99

Horizon	Depth of sample (cm)	TEXTURE (µm in weight %) Sand 2000-1000	Sand 1000-500	Sand 500-250	Sand 250-100	Sand 100-50	Silt 50-2	Clay <2	pH H_2O	pH $CaCl_2$	Org. C %	% CO_2
		1000	500	250	100	50	2					
Ah	5- 25	0.5	0.5	1.5	3.5	2.0	26.5	66.0	6.8	6.5	3.3	0.0
Bw	30- 45			1.5			6.0	92.5	7.2	6.8	1.6	0.1

Profilenumber: Sp/106
Classification: CALCIC KASTANOZEM, fine textured (FAO-Unesco, 1974)
TYPIC CALCIXEROLL, fine-silty, mixed, mesic (SOIL SURVEY STAFF,
Location: south of San Giovanni Incarico (Fr., Italy), approx. 200 m south of km stone 90 of the S;S; della Valle del Liri (N^{O} 82); topographical map Pico, F^{O} 160, III N.O. della Carta d' Italia 1 : 25 000, 41^{O} 29' 44" N.L. and 1^{O} 06' 21" east of Monte Mario (Rome)
Elevation: approx. 185 m a.s.l.
Physiographic position: concave slope in rolling country
Slope: sloping (11 %)
Vegetation: grass and shrub
Parent material: colluvial material derived from Miocene shales, covering a dark reddish brown soil on limestone
Drainage conditions: moderately well drained
Moisture conditions: dry down to 2 m, then moist

Apck 0-35 cm; dark brown (10YR 3/3, moist) slightly gravelly clay; moderate medium crumb; slightly hard when dry; common very fine and fine pores; many rounded fresh limestone gravel; few small soft spherical white calcium carbonate segregations; strongly calcareous; few pottery fragments; few wormholes; few medium and common fine roots; pH 7.2; abrupt and wavy boundary to

Bck 35-65 cm; grey (5Y 6/1, moist) slightly gravelly silt loam; moderate fine subangular blocky; hard when dry; many very fine and fine pores; many large soft irregular white calcium carbonate segregations; strongly calcareous; few worm holes; common fine roots; pH 7.3; clear and wavy boundary to

Cck1 65-110 cm; grey (7.5Y 6/1, moist) slightly gravelly loam; few medium clear distinct yellowish brown (10YR 5/6, moist) mottles; massive; soft when dry; many large soft irregular white calcium carbonate segregations; strongly calcareous; few fine pores; few fine roots; pH 7.6; clear and wavy boundary to

Cck2 110-140 cm; grey (7.5Y 6/1, moist) slightly gravelly silty clay; very weak fine angular blocky; slightly hard when dry; common large soft irregular white calcium carbonate segregations; strongly calcareous; few very fine and very few fine pores; very few fine roots; pH 7.5; abrupt and smooth boundary to

2Btck 140->220 cm; dark reddish brown (2.5YR 3/4, moist) slightly gravelly silty clay; few medium prominent sharp bluish black (5PB 2/1, moist) mottles; strong coarse angular blocky, locally wedgeshaped; very hard when dry; broken moderately thick dark reddish brown (2.5YR 3/6, moist) clay-iron cutans on some pedfaces and in some pores and few medium slickensides; common fine and few medium pores; from 170 cm downwards very many rounded and angular fresh limestone boulders; few large soft irregular yellow calcium carbonate segregations; matrix non calcareous; very few fine roots; pH 7.6

ANALYSES PROFILE Sp/106

		TEXTURE (µm in weight %)									
	Depth of		Sand					Silt	Clay		
Horizon	sample (cm)	>2 mm	2000 1000	1000 500	500 250	250 100	100 50	50 2	<2	pH H_2O	pH $CaCl_2$
Apck	10- 30	6.5	3.0	2.0	3.0	6.5	4.5	38.5	42.5	7.2	6.9
Bck	40- 60	4.5	1.5	1.5	2.5	5.5	7.0	55.5	26.0	7.3	6.9
Cck1	80-100	7.0	2.5	3.0	5.0	11.5	9.5	46.0	22.5	7.6	7.0
Cck2	110-130	9.5	3.5	3.5	4.0	4.5	3.0	40.5	40.5	7.5	7.0
2Btck	160-180	4.0	0.2	0.2	0.5	3.0	2.0	43.5	50.5	7.6	7.1

Profilenumber: Sp/111
Classification: CHROMIC LUVISOL, fine textured (FAO-Unesco, 1974)
MOLLIC HAPLOXERALF, very-fine, kaolinitic, mesic (SOIL SURVEY STAFF, 1975)
Location: approx. 1 km southwest of San Giovanni Incarico (Fr., Italy) in a karst basin; topographical map Pico, F° 160, III N.O. della Carta d' Italia 1 : 25 000, 41° 29' 36" N.L. and 1° 05' 44" east of Monte Mario (Rome)
Elevation: approx. 450 m a.s.l.
Physiographic position: at the fringe of a karst basin in limestone mountains
Slope: (moderately) steep (25 %)
Vegetation: shrub (mainly Ampelodesma tenax Link)
Parent material: colluvial deposits derived from limestone, mixed with tuff
Drainage conditions: moderately well drained
Moisture conditions: dry throughout profile
Erosion conditions: severe gully erosion

Ah 0-25 cm; dark reddish brown (5YR 3/4, moist) clay; moderate fine to mrdium subangular blocky; slightly hard when dry; patchy thin clay-humus cutans on horizontal pedfaces and continuous thick clay-humus cutans in biopores, both dark reddish brown (5YR 3/3, moist); many fine and medium pores; very few volcanic minerals; few pottery fragments; non calcareous; common fine roots; pH 5.7; abrupt and smooth boundary to

Bt 25-50 cm; dark reddish brown (5YR 3/6, moist) clay; common coarse prominent sharp bluish black (5PB 2/1, moist) mottles; weak medium prismatic, breaking into moderate angular blocky; broken moderately thick to thick red (2.5YR 4/6, moist) clay-iron cutans on vertical pedfaces and few oblique slickensides; few fine pores; non calcareous; common volcanic minerals; common fine roots; pH 5.1; gradual and wavy boundary to

2BC 50-70 cm; yellow orange (7.5YR 7/8, rubbed and moistened) clay; few fine prominent clear bluish black (5PB 2/1, moist) mottles; weak fine to medium subangular blocky; soft when dry; few continuous thick dark reddish brown (5YR 3/6, moist) clay-iron cutans in mainly vertical voids; many fine pores; few soft spherical black iron-manganese nodules and common volcanic minerals; non calcareous; few wormholes; few fine roots; pH 5.2; abrupt and broken boundary to

3Bw 70->450 cm; mottled clay, dark reddish brown (5YR 3/3), dull reddish brown (5YR 4/4), bright reddish brown (5YR 5/8), light grey (5Y 7/2) and bluish black (5PB 2/1), all when moist; weak coarse angular blocky, wedgeshaped, breaking into fine to medium angular blocky; hard when dry; continuous large intersecting slickensides; few fine pores; non calcareous; few fine to medium roots; pH 5.1 - 5.3

ANALYSES PROFILE Sp/111

		TEXTURE (µm in weight %)									
	Depth of	← Sand →					Silt	Clay			
Horizon	sample (cm)	2000 1000	1000 500	500 250	250 100	100 50	50 2	<2	pH H_2O	pH $CaCl_2$	Org. C %
Ah	5- 20	0.4	0.7	1.5	3.5	2.0	28.0	64.0	5.7	5.1	1.3
Bt	30- 45	0.5	0.8	2.0	4.5	1.5	28.0	62.5	5.1	4.5	0.3
2BC	50- 70	1.5	2.0	6.0	6.0	2.0	36.0	46.5	5.2	4.4	0.3
3Bw	90-120	0.2	0.5	2.0	4.0	1.5	36.5	55.0	5.1	4.3	0.3
	180-220	0.1	0.2	2.0	4.5	1.0	25.5	66.5	5.1	4.3	0.3
	280-310	0.3	1.0	3.0	3.5	1.5	29.5	61.0	5.3	4.3	0.2
	380-420	0.0	0.1	0.6	2.0	1.0	26.5	69.5	5.2	4.4	0.2

Profilenumber: Sp/118
Classification: CHROMIC LUVISOL, fine textured (FAO-UNESCO, 1974)
TYPIC HAPLOXERALF, fine, mixed, mesic (SOIL SURVEY STAFF, 1975)
Location: approx. 2.5 km south-west of San Giovanni Incarico (Fr., Italy) in karst basin "La Fossa"; topographical map Pico, F° 160, III N.O. della Carta d' Italia 1 : 25 000, 41° 29' 15" N.L. and 1° 04' 33" east of Monte Mario (Rome)
Physiographic position: lower part of alluvial fan
Slope: sloping (10.5 %)
Vegetation: grass with scattered oak trees
Parent material: alluvial deposits derived from weathering material of limestone
Drainage conditions: moderately well drained
Moisture conditions: dry throughout profile
Erosion conditions: moderate to severe gully erosion

Ap 0-35 cm; reddish brown (5YR 4/6, moist) clay; moderate fine to medium subangular blocky; slightly hard when dry; many fine pores; very few volcanic minerals; non calcareous; few pottery fragments; few wormholes; common fine to medium roots; clear and smooth boundary to

Bt1 35-90 cm; dull reddish brown (5YR 4/4, moist) clay; common coarse prominent sharp bluish black (5PB 2/1, moist) mottles; moderate coarse prismatic, breaking into strong fine to medium angular blocky; hard when dry; broken moderately thick reddish brown (5YR 4/6, moist) clay-iron cutans on some pedfaces and in pores; common fine and medium pores; very few volcanic minerals; very few small soft hard spherical red iron nodules; non calcareous; common medium and few fine roots; gradual and smooth boundary to

Bt2 90-130 cm; dull reddish brown (5YR 4/4, moist) clay; common medium distinct clear dull reddish brown (5YR 5/4, moist) and common coarse prominent sharp bluish black (5PB 2/1, moist) mottles; moderate coarse prismatic, breaking into strong medium angular blocky; hard when dry; continuous moderately thick reddish brown (5YR4/6, moist) clay-iron cutans on most of the pedfaces and in pores; few fine pores; very few volcanic minerals; few small hard irregular yellowish red iron nodules; non calcareous; few fine and medium roots; clear and smooth boundary to

2C 130-170 cm; weathered tuff layer with continuous thick reddish brown (5YR 4/8, moist) clay-iron cutans in vertical voids; non calcareous;

Profilenumber: Sp/119a
Classification: CHROMIC CAMBISOL, fine textured (FAO-Unesco, 1974)
TYPIC XEROCHREPT, fine,mesic (SOIL SURVEY STAFF, 1975)
Location: at the fringe of karst basin "La Fossa", approximately 2.5 km south-west of San Giovanni Incarico (Fr., Italy); topographical map Pico, F° 160, III N.O. della Carta d' Italia 1 : 25 000, 41° 29' 14" N.L. and 1° 04' 37" east of Monte Mario (Rome)
Elevation: approx. 280 m a.s.l.
Physiographic position: top of alluvial fan
Slope: sloping (10.5 %)
Vegetation: grass
Parent material: alluvial material derived from weathered limestone
Drainage conditions: moderately well drained
Moisture conditions: dry throughout profile
Evidence of erosion: moderate to severe gully erosion

Ah 0-15 cm; dark reddish brown (5YR 3/3, moist) slightly gravelly clay; moderate fine angular blocky; hard when dry; few angular and rounded fresh limestone gravel and stones; very few small soft spherical black iron-manganese nodules; non calcareous; some pottery fragments; many fine and few coarse roots; clear and smooth boundary to

Bw1 15-95 cm; dark reddish brown (5YR 3/4, moist) slightly gravelly clay; few coarse faint clear dark reddish brown (5YR 3/6, moist) mottles; weak coarse prismatic, breaking into strong fine angular blocky; hard when dry; common fine and medium pores and few coarse pores; few angular slightly weathered limestone gravel and stones; few small soft spherical black iron-manganese nodules; non calcareous; some pottery and charcoal fragments; some wormholes; common medium and few fine roots; gradual and smooth boundary to

Bw2 95- 170 cm; dark reddish brown (5YR 3/4, moist) gravelly clay; weak coarse subangular blocky breaking into strong fine angular blocky; hard when dry; common fine pores; common angular and rounded slightly weathered limestone gravel and stones; few small soft spherical black iron-manganese nodules; non calcareous; some pottery and charcoal fragments; some wormholes; few fine to medium roots; gradual and smooth boundary to

Bw3 170-250 cm; dark reddish brown (5YR 3/6, moist) gravelly clay; slightly hard when dry; moderate coarse prismatic, breaking into moderate fine to medium angular blocky, locally wedgeshaped; many small intersecting slickensides; common fine pores; common angular and rounded slightly weathered limestone gravel and stones; few small soft spherical black iron-manganese nodules; non calcareous; few pottery and charcoal fragments; few fine roots; lateral abrupt and broken boundary to R and clear and smooth boundary to

2Bw4 250-270 cm; dark red (2.5YR 3/6, moist) very gravelly clay; moderate fine to medium angular blocky; slightly hard when dry; broken thin clay-iron cutans on top of the peds; few fine pores; many rounded slightly weathered limestone gravel and stones; calcareous; abrupt and broken boundary to

R >270 cm; hard light grey dolomitic limestone

Profilenumber: Sp/119b (Profile located at a distance of approximately 10 m of profile Sp/119a)

0-80 cm; CALCIC CAMBISOL in very gravelly clay, developed in recent alluvial fan deposits (see profilenumber Sp/119a); abrupt and smooth boundary to

2Bg 80-95 cm; dark reddish brown (5YR 3/6, moist) clay; common coarse prominent clear olive yellow (5Y 6/4, moist) mottles and few fine prominent sharp bluish black (5PB 2/1, moist) mottles; moderate very coarse angular blocky, breaking into strong very fine to fine angular blocky, wedgeshaped; hard when dry; many medium intersecting slickensides; few fine pores; non calcareous; clear and broken boundary to

2B(g) 95->125 cm; dark reddish brown (2.5YR 3/6, moist) slightly gravelly clay; common fine to medium prominent sharp bluish black (5PB 2/1, moist) mottles; weak medium subangular blocky, breaking into strong very fine to fine angular blocky, wedgeshaped; hard when dry; many small intersecting slickensides; few fine pores; very few rounded weathered limestone gravel; non calcareous; some wormholes; few fine roots

Profilenumber: Sp/122
Classification: EUTRIC NITOSOL, fine textured (FAO-Unesco, 1974)
MOLLIC PALEXERALF, very-fine, kaolinitic, mesic (SOIL SURVEY STAFF, 1975)
Location: approx 2.5 km southwest of San Giovanni Incarico (Fr., Italy) at the locality "Il Vallangero"; topographical map Pico, F° 160, III N.O. della Carta d' Italia 1 : 25 000, 41° 29' 12" N.L. and 1° 05' 05" east of Monte Mario (Rome)
Elevation: approx. 325 m a.s.l.
Physiographic position: convex slope in limestone mountains
Slope: steep (29 %)
Vegetation: oak trees, grass and shrub ("macchia")
Parent material: residual material derived from limestone with probably admixture of volcanic material in the top part of the profile
Drainage conditions: (moderately) well drained
Moisture conditions: moist throughout profile
Erosion conditions: severe gully erosion

Ah 0-5 cm; very dark reddish brown (5YR 2/3, moist) clay; moderate very fine to fine subangular blocky; friable when moist; common very fine and fine pores; very few volcanic minerals; very few small soft spherical black iron-manganese nodules; non calcareous; very few pottery fragments; few wormholes; common fine and medium roots; pH 6.3; abrupt and smooth boundary to

E 5-15 cm; dark reddish brown (5YR 3/4, moist) clay; moderate fine to medium subangular blocky; friable when moist; common very fine and fine pores; very few volcanic minerals; very few small soft spherical black iron-manganese nodules; non calcareous; common fine and medium roots; pH 5.9; clear and smooth boundary to

Bt1 15-40 cm; dark reddish brown (5YR 3/6, moist) clay; moderate fine to medium angular blocky; firm when moist; patchy moderately thick very dark reddish brown (5YR 2/4, moist) clay-iron-humus cutans on some pedfaces and in some pores; common very fine and fine pores; very few volcanic minerals; non calcareous; common fine and medium roots; pH 5.9; gradual and smooth boundary to

Bt2 40-80 cm; dark reddish brown (2.5YR 3/6, moist) clay; weak coarse prismatic, breaking into moderate fine to medium angular blocky; firm when moist; broken moderately thick dark reddish brown (2.5YR 3/4, moist) clay-iron cutans on some pedfaces and in some pores, and few small slickensides; common very fine and fine pores; very few volcanic minerals; non calcareous; very few wormholes; common fine and medium roots; pH 5.6; gradual and smooth boundary to

2Bt3 80-140 cm; reddish brown (2.5YR 4/6, moist) clay; few fine prominent sharp bluish black (5PB 2/1, moist) and fine distinct clear dark olive brown (2.5Y 3/3, moist) mottles; moderate fine to medium angular blocky, locally wedgeshaped; firm when moist; broken moderately thick reddish brown (2.5YR 4/6, moist) clay-iron cutans on some pedfaces and in some pores, and common medium intersecting slickensides; few very fine and fine pores; very few small soft spherical black iron-manganese nodules; non calcareous; common fine and medium roots; pH 5.1; diffuse and smooth boundary to

2Bt(g) 140->300 cm; red (10R 4/6, moist) clay; common fine to medium faint to distinct clear mottles, dark reddish brown (5YR 3/6), bright brown (2.5YR 5/8), red (10R 4/8) and bluish black (5PB 2/1), all when moist; moderate fine angular blocky, locally wedgeshaped; firm when moist; patchy moderately thick red (10R 4/6, moist) clay-iron cutans on some pedfaces and in some pores, and common large intersecting oblique sli-

ckensides; few very fine and fine pores; very few small soft spherical black iron-manganese nodules; non calcareous; few fine roots; pH 5.0 - 5.3

ANALYSES PROFILE Sp/122

Horizon	Depth of sample (cm)	TEXTURE (µm in weight %) Sand 2000-1000	Sand 1000-500	Sand 500-250	Sand 250-100	Sand 100-50	Silt 50-2	Clay <2	pH H_2O	pH $CaCl_2$	Org. C %	"Free" Fe_2O_3 Soil	"Free" Fe_2O_3 Clay
Ah	0- 5	0.7	0.8	1.5	4.0	3.0	32.0	58.0	6.4	5.8	4.4	6.9	7.6
E	5- 15	0.5	0.6	1.0	3.5	2.0	29.5	63.0	5.9	5.2	2.3	6.9	8.0
Bt1	20- 35	0.0	0.0	0.2	5.0	0.5	23.0	71.5	5.9	5.3	2.4	7.2	8.0
Bt2	50- 70			3.0			12.5	84.5	5.6	4.9	0.7	7.9	6.6
2Bt3	100-130			3.0			21.0	76.0	5.1	4.2	0.5	7.9	6.5
2Bt(g)	180-210			5.5			18.0	76.5	5.2	4.1	0.4	7.1	6.1
	240-260			4.5			19.0	76.5	5.3	4.2	0.5	7.5	6.3
	290-300			3.0			16.0	81.0	5.0	4.0	0.3	6.8	6.1

ELEMENTAL COMPOSITION OF THE FINE EARTH FRACTION (weight %)

Horizon	Depth of sample (cm)	SiO_2	Al_2O_3	Fe_2O_3	FeO	MnO	MgO	CaO	Na_2O	K_2O	TiO_2	P_2O_5	H_2O
Ah	0- 5	53.6	22.3	8.4	0.6	0.3	0.8	0.6	0.4	2.4	1.2	0.2	9.2
E	5- 15	52.3	23.5	8.8	0.3	0.3	0.8	0.3	0.3	2.3	1.3	0.2	9.5
Bt1	20- 35	49.3	25.2	9.1	0.3	0.2	0.7	0.8	0.3	2.0	1.2	0.2	10.6
Bt2	50- 70	44.3	30.1	9.2	0.3	0.1	0.5	0.3	0.1	1.1	1.0	0.3	12.6
2Bt3	100-130	45.4	29.2	9.8	0.2	tr	0.5	0.3	0.1	1.3	1.0	0.3	12.0
2Bt(g)	180-210	47.8	27.8	9.4	0.2	0.1	0.7	0.3	0.1	1.5	1.0	0.2	11.0
	240-260	47.1	28.4	9.1	0.2	0.2	0.5	0.2	0.1	1.4	1.0	0.2	11.5
	290-300	49.0	27.1	9.0	0.1	0.1	0.9	0.3	0.1	1.7	1.0	0.2	10.6

ELEMENTAL COMPOSITION OF THE CLAY FRACTION (weight %)

Horizon	Depth of sample (cm)	SiO_2	Al_2O_3	Fe_2O_3	FeO	MnO	MgO	CaO	Na_2O	K_2O	TiO_2	P_2O_5	H_2O
Ah	0- 5	42.8	29.1	10.4	0.3	0.1	0.8	tr	0.1	1.4	1.1	0.4	13.5
E	5- 15	42.7	29.4	10.5	0.2	0.1	0.8	0.1	0.1	1.4	1.2	0.5	13.0
Bt1	20- 35	42.6	30.1	10.2	0.2	0.1	0.7	tr	tr	1.2	1.1	0.5	13.3
Bt2	50- 70	42.1	32.0	8.9	0.2	0.1	0.5	tr	tr	0.8	0.9	0.3	14.1
2Bt3	100-130	42.7	31.9	8.9	0.1	tr	0.5	tr	tr	0.8	0.9	0.3	13.9
2Bt(g)	180-210	43.9	31.0	8.8	0.1	0.2	0.7	tr	tr	1.2	0.9	0.3	13.0
	240-260	42.9	31.7	8.8	0.1	0.1	0.5	tr	tr	0.9	0.9	0.3	13.8
	290-300	44.5	30.4	8.9	0.1	tr	0.9	tr	tr	1.5	0.9	0.2	12.5

MOLAR RATIOS

Horizon	Depth of sample (cm)	SOIL $\frac{SiO_2}{R_2O_3}$	SOIL $\frac{SiO_2}{Al_2O_3}$	SOIL $\frac{SiO_2}{Fe_2O_3}$	SOIL $\frac{Al_2O_3}{Fe_2O_3}$	CLAY $\frac{SiO_2}{R_2O_3}$	CLAY $\frac{SiO_2}{Al_2O_3}$	CLAY $\frac{SiO_2}{Fe_2O_3}$	CLAY $\frac{Al_2O_3}{Fe_2O_3}$
Ah	0- 5	3.3	4.1	17.0	4.2	2.0	2.5	11.0	4.4
E	5- 15	3.1	3.8	15.7	4.4	2.0	2.5	10.8	4.4
Bt1	20- 35	2.7	3.3	14.4	4.3	2.0	2.4	11.1	4.6
Bt2	50- 70	2.1	2.5	12.8	5.1	1.9	2.2	12.6	5.6
2Bt3	100-130	2.2	2.6	12.3	4.7	1.9	2.3	12.8	5.7
2Bt(g)	180-210	2.4	2.9	13.5	4.6	2.0	2.4	13.2	5.5
	240-260	2.3	2.8	13.7	4.9	2.0	2.3	13.0	5.7
	290-300	2.5	3.1	14.6	4.8	2.1	2.5	13.3	5.3

Profilenumber: Sp/123
Classification: CHROMIC LUVISOL, fine textured (FAO-Unesco, 1974)
MOLLIC HAPLOXERALF, very-fine, kaolinitic, mesic (SOIL SURVEY STAFF, 1975)
Location: approx. 2.5 km southwest of San Giovanni Incarico (Fr., Italy) at the locality "Il Vallangero"; topographical map Pico, F° 160, III N.O. della Carta d' Italia 1 : 25 000, 41° 29' 09" N.L. and 1° 05' 03" east of Monte Mario (Rome)
Elevation: approx. 370 m a.s.l.
Physiographic position: convex slope in limestone mountains
Slope: steep (27 %)
Vegetation: grass and shrub ("macchia")
Parent material: residual material derived from limestone with admixture of volcanic material
Drainage conditions: (moderately) well drained
Moisture conditions: dry throughout profile
Erosion conditions: severe gully erosion

Ah 0-30 cm; dark reddish brown (5YR 3/6, moist) clay; weak coarse subangular blocky, breaking into strong medium subangular blocky; slightly hard when dry; common fine pores; very few volcanic minerals; non calcareous; common wormholes; common fine and medium roots; pH 5.6; clear and smooth boundary to

Bt 30-110 cm; reddish brown (5YR 4/6, moist) clay; moderate coarse prismatic, breaking into moderate medium angular blocky; slightly hard when dry; broken moderately thick to thick dark reddish brown (5YR 3/3, moist) clay-iron (-humus) cutans on horizontal pedfaces and in coarse (bio-)pores; common small intersecting slickensides; many fine and medium and few coarse pores; very few volcanic minerals; non calcareous; common wormholes; few medium roots; pH 5.7; diffuse and smooth boundary to

2Bw1 110-220 cm; dark reddish brown (5YR 3/4, moist) clay; common fine and medium prominent sharp bluish black (5PB 2/1, moist) mottles; weak coarse prismatic, breaking into moderate fine angular blocky, locally wedgeshaped; hard when dry; few large and common small intersecting slickensides; few fine pores; few volcanic minerals; non calcareous; few fine roots; pH 6.0; clear and smooth boundary to

3Bw2 220-250/300 cm; dark reddish brown (2.5YR 3/6, moist) clay; few medium prominent sharp bluish black (5PB 2/1, moist) mottles; moderate coarse prismatic, breaking into strong fine angular blocky, wedgeshaped; hard when dry; common large continuous intersecting slickensides; few fine pores; non calcareous; pH 5.6 - 6.3; abrupt and broken boundary to

3Bk white silt loam, consisting of secondary powdery calcium carbonate, thickness up to 5 cm; pH 7.1; abrupt and irregular boundary to

R white hard limestone

ANALYSES PROFILE Sp/123

Horizon	Depth of sample (cm)	TEXTURE (µm in weight %) Sand 2000–1000	1000–500	500–250	250–100	100–50	Silt 50–2	Clay <2	pH H_2O	pH $CaCl_2$	Org. C %	% CO_2 Soil	% CO_2 Clay
Ah	5- 25	0.2	0.3	0.7	3.0	1.5	15.0	79.5	5.7	5.1	1.4	0.0	0.0
Bt	40- 60			4.0			12.0	84.0	5.7	5.1	0.9	0.0	0.0
	80-100			4.5			14.0	81.5	5.8	5.2	0.5	0.0	0.0
2Bw1	130-150	0.4	0.7	1.5	5.5	3.0	30.0	59.0	6.1	5.4	0.5	0.0	0.0
	180-200	0.4	0.5	1.0	4.5	3.0	22.5	68.0	6.0	4.9	0.5	0.0	0.0
3Bw2	230-250			3.5			12.0	84.5	5.6	5.2	0.4	0.0	0.0
	270-290			0.0			5.0	95.0	6.4	5.7	0.8	0.0	0.0
3Bk	300-305	2.0	1.5	2.0	6.0	5.5	67.0	16.0	7.2	7.0	0.5	37.0	18.4
R											0.2	42.3	

ELEMENTAL COMPOSITION OF THE FINE EARTH FRACTION AND ROCK (weight %)

Horizon	Depth of sample (cm)	SiO_2	Al_2O_3	Fe_2O_3	FeO	MnO	MgO	CaO	Na_2O	K_2O	TiO_2	P_2O_5	H_2O	"Free" Fe_2O_3
Ah	5- 25	46.2	29.0	9.8	0.2	0.1	0.6	0.4	0.2	1.7	1.1	0.2	10.6	7.0
Bt	40- 60	44.6	29.9	10.1	0.2	0.1	0.6	0.3	0.1	1.4	1.1	0.2	11.5	7.1
	80-100	44.5	29.2	10.6	0.2	0.1	0.6	0.4	0.2	1.7	1.2	0.2	11.3	7.6
2Bw1	130-150	51.2	24.8	10.6	0.2	0.2	0.7	0.3	0.3	2.0	0.7	0.2	9.0	7.5
	180-200	48.8	26.5	10.6	0.2	0.2	0.6	0.3	0.2	1.7	0.6	0.2	10.1	7.5
3Bw2	230-250	45.9	29.3	9.4	0.1	0.1	0.6	0.4	0.2	1.6	1.0	0.1	11.2	6.2
	270-290	45.5	29.6	8.8	0.2	0.1	0.8	0.2	0.1	1.6	0.9	0.2	12.1	5.8
3Bk	300-305	7.2	4.3	1.1	0.2	tr	0.3	46.8	0.1	0.2	0.1	tr	3.1	0.8
R		1.6	1.3	0.3	tr	tr	0.5	53.4	0.1	0.1	tr	tr	0.5	0.1

ELEMENTAL COMPOSITION OF THE CLAY FRACTION (weight %)

Horizon	Depth of sample (cm)	SiO_2	Al_2O_3	Fe_2O_3	FeO	MnO	MgO	CaO	Na_2O	K_2O	TiO_2	P_2O_5	H_2O	"Free" Fe_2O_3
Ah	5- 25	43.6	30.6	9.3	0.2	0.1	0.6	tr	0.1	1.2	1.0	0.2	13.2	6.6
Bt	40- 60	43.6	30.8	8.8	0.2	0.1	0.6	tr	tr	1.2	0.9	0.2	13.7	6.2
	80-100	43.4	30.6	9.3	0.1	0.1	0.6	tr	tr	1.2	1.0	0.2	13.5	6.6
2Bw1	130-150	43.6	29.4	10.6	0.2	0.1	0.7	0.1	0.1	1.4	1.2	0.3	12.4	7.7
	180-200	43.8	30.3	9.5	0.2	0.1	0.6	0.1	tr	1.3	1.1	0.3	12.7	6.7
3Bw2	230-250	45.0	31.0	8.0	0.1	0.1	0.7	0.1	tr	1.3	0.9	0.2	12.7	5.1
	270-290	44.6	29.8	8.7	0.2	0.1	0.8	0.1	0.1	1.5	0.9	0.2	13.2	5.7
3Bk	300-305	26.7	15.5	4.8	0.2	0.1	0.4	23.5	0.1	0.8	0.5	0.2	8.9	3.3

MOLAR RATIOS

Horizon	Depth of sample (cm)	SOIL $\frac{SiO_2}{R_2O_3}$	SOIL $\frac{SiO_2}{Al_2O_3}$	SOIL $\frac{SiO_2}{Fe_2O_3}$	SOIL $\frac{Al_2O_3}{Fe_2O_3}$	CLAY $\frac{SiO_2}{R_2O_3}$	CLAY $\frac{SiO_2}{Al_2O_3}$	CLAY $\frac{SiO_2}{Fe_2O_3}$	CLAY $\frac{Al_2O_3}{Fe_2O_3}$
Ah	5- 25	2.2	2.7	12.5	4.7	2.0	2.4	12.5	5.2
Bt	40- 60	2.1	2.5	11.7	4.6	2.0	2.4	13.2	5.5
	80-100	2.1	2.6	11.2	4.3	2.0	2.4	12.4	5.2
2Bw1	130-150	2.8	3.5	12.9	3.7	2.1	2.5	11.0	4.4
	180-200	2.5	3.1	12.3	3.9	2.0	2.5	12.2	5.0
3Bw2	230-250	2.2	2.7	13.0	4.9	2.1	2.5	15.1	6.1
	270-290	2.2	2.6	13.7	5.3	2.1	2.5	13.7	5.4
3Bk	300-305	2.5	2.9	17.0	6.0	2.4	2.9	14.8	5.1

Profilenumber: Sp/141
Classification: CALCIC CAMBISOL, medium textured (FAO-UNESCO, 1974)
CALCIXEROLLIC XEROCHREPT, fine-loamy, mixed, mesic (SOIL SURVEY STAFF, 1975)
Location: approx. 500 m east-north-east of Pico (Fr., Italy), alongside road Pico-Pontecorvo, 60 m east of junction with road to San Giovanni Incarico (S.S. della Valle del Liri, n° 82); topographical map Pico, F° 160 III N.O. della Carta d' Italia 1 : 25 000, 41° 27' 09" N.L. and 1° 06' 51" east of Monte Mario (Rome)
Elevation: approx. 140 m a.s.l.
Physiographic position: concave slope in rolling country
Slope: sloping (8 %)
Vegetation: vine and cereals
Parent material: Miocene shales
Drainage conditions: moderately well drained
Moisture conditions: dry down to 90 cm, than moist

Ap 0-40 cm; dull yellowish brown (10YR 4/3, moist) loam; weak fine crumb; slightly hard when dry; common very fine and fine pores; very few angular fresh limestone and sandstone gravel; calcareous; very few pottery fragments; many fine, medium and coarse roots; abrupt and wavy boundary to

Bck 40-100 cm; greyish to light yellow (2.5Y 7/2 to 2.5Y 7/3, moist) loam; common coarse prominent bright brown (7.5YR 5/8, moist) mottles; weak coarse to very coarse angular blocky; hard when dry; common very fine pores; few small soft irregular and spherical white calcium carbonate nodules; strongly calcareous; common fine, medium and coarse roots; clear and wavy boundary to

Cg 100->140 cm; greyish olive (5Y 5/2, moist) sandy loam; common coarse prominent clear orange (7.5YR 6/8, moist) mottles; massive; very friable when moist; few very fine pores; calcareous; few fine to medium roots

Profilenumber:Sp/164
Classification: CHROMIC LUVISOL, fine textured (FAO-UNESCO, 1974)
TYPIC HAPLOXERALF, fine, mixed, mesic (SOIL SURVEY STAFF, 1975)
Location: approx. 2.2 km south-west of San Giovanni Incarico (Fr., Italy) at "Il Vallangero"; topographical map Pico, F° 160 III N.O. della Carta d' Italia 1 : 25 000, 41° 29' 16" N.L. and 1° 05' 07" east of Monte Mario (Rome)
Elevation: approx. 275 m a.s.l.
Physiographic position: concave slope of limestone mountains
Slope: steep (27 %)
Vegetation: shrub ("macchia")
Parent material: residual material derived from limestone mixed with tuff layers
Drainage conditions: well drained
Moisture conditions: dry throughout profile
Erosion conditions: severe gully erosion

Ah 0-20 cm; dark reddish brown (5YR 3/2, moist) clay; weak coarse subangular blocky, breaking into very fine to fine angular blocky; hard when dry; patchy to broken moderately thick dark reddish brown (5YR 3/2, moist) clay-humus cutans on some pedfaces; many fine to medium pores; non calcareous; many fine, medium and coarse roots; clear and smooth boundary to

AB 20-35 cm; dark reddish brown (5YR 3/4, moist) clay; moderate fine to medium angular blocky; slightly hard when dry; patchy moderately thick dark reddish brown (5YR 3/2, moist) clay-humus(-iron) cutans on some pedfaces; non calcareous; some wormholes; common fine and medium roots; gradual and smooth boundary to

Bt 35-55 cm; dark reddish brown (2.5YR 3/4, moist) clay; moderate medium to coarse angular blocky; slightly hard when dry; broken moderately thick dark reddish brown (2.5YR 3/4, moist) clay-iron cutans on most of the pedfaces and in pores; common fine and medium pores; very few small hard spherical black iron-manganese nodules; non calcareous; common fine and few medium and coarse roots; gradual and smooth boundary to

2Bt1 55-75 cm; bright brown (7.5YR 5/6, moist) clay; few medium prominent sharp bluish black (5PB 2/1, moist) mottles; weak medium to coarse prismatic, breaking into moderate medium angular blocky; slightly hard when dry; continuous thick reddish brown (2.5YR 4/6, moist) clay-iron cutans on all pedfaces and in pores; common fine and medium pores; common volcanic minerals; very few small hard spherical black iron-manganese nodules; non calcareous; few wormholes; few fine and medium roots; clear and smooth boundary to

2Bt2 75-90 cm; bright brown (7.5YR 5/6, moist) clay; few prominent sharp bluish black (5PB 2/1, moist) mottles; weak medium to coarse subangular blocky; slightly hard when dry; continuous moderately thick to thick dull reddish brown (2.5YR 4/4, moist) clay-iron cutans on all pedfaces and in pores; common fine and medium pores; many rounded weathered tuff gravel; very few small hard spherical black iron-manganese nodules; non calcareous; few fine to meium roots; clear and smooth boundary to

2BC 90->150 cm; layers of weathered tuff; few very coarse prominent sharp dark bluish grey (5PB 4/1) and bluish black (5PB 2/1), both when moist, mottles; broken moderately thick to thick reddish brown (2.5YR 4/6, moist) clay-iron cutans on some pedfaces and in mainly vertical voids; weak thick platy to weak coarse prismatic; few fine roots; locally many biopores; soft when dry; sample Sp/164

Profilenumber: Sp/166
Classification: CALCIC CAMBISOL, medium textured (FAO-Unesco, 1974)
CALCIXEROLLIC XEROCHREPT, fine-loamy, mixed, mesic (SOIL SURVEY STAFF, 1975)
Location: in clay pit "San Bartolomeo, Fornaci Pontecorvo" at the locality "Tordone", approx. 3.5 km west of Pontecorvo (Fr., Italy); topographical map Pontecorvo, F° 160, III N.E. della Carta d' Italia 1 : 25 000, 41° 27' 20" N.L. and 1° 10' 21" east of Monte Mario (Rome)
Elevation: approx. 100 m a.s.l.
Physiographic position: crest between two small incisions
Slope: gently sloping (5 %)
Vegetation: grass
Parent material: shales with sandy inclusions of Miocene age ("argille caotiche")
Drainage conditions: moderately well drained
Moisture conditions; dry down to 1 m, then moist

Apck 0-35 cm; dull yellow (2.5Y 6/4, moist) clay loam; moderate medium subangular blocky; hard when dry; very porous; few angular non calcareous gravel and few rounded fresh calcareous gravel; few large hard irregular calcium carbonate concretions; common fine roots; pH 7.2; abrupt and smooth boundary to

Bck(g) 35-60 cm; dull yellow (2.5Y 6/4, moist) clay loam with sandy inclusions; few fine distinct sharp bright brown (7.5YR 5/6, moist) mottles; weak medium prismatic, breaking into strong medium to coarse angular blocky, wedgeshaped; hard when dry; broken moderately thick grey (5Y 6/1, moist) cutans, probably calcitans, on vertical and oblique pedfaces; few slickensides; few very fine pores; very few large hard irregular calcium carbonate concretions and many large soft calcium carbonate segregations, both white; few very fine roots; pH 7.6; diffuse and wavy boundary to

Bckg 60-140 cm; greyish yellow to greyish olive (2.5Y 6/2 to 5Y 5/2, both moist) clay loam with sandy inclusions; many medium distinct sharp bright brown (7.5YR 5/6, moist) mottles; weak coarse prismatic, breaking into strong medium and coarse angular blocky, wedgeshaped; extremely firm when moist; continuous thick grey (5Y 6/1, moist) cutans, probaly calcitans, on vertical and oblique pedfaces; common slickensides; few very fine pores; very few small hard irregular calcium carbonate concretions and few small soft calcium carbonate segregations, both white, also pseudomiscelia; few very fine roots; pH 8.0; gradual and wavy boundary to

Ckg 140-180 cm; yellowish grey to dull yellow (2.5Y 6/1 to 2.5Y 6/4, both moist) clay loam with banded sandy inclusions; many coarse prominent sharp orange (7.5YR 6/6, moist) mottles; massive; in clayey parts many continuous large intersecting slickensides; clay loam firm, sand extremely firm when moist; very few small soft white calcium carbonate segregations; pH 8.2; gradual and wavy boundary to

Cg 180->230 cm; yellowish grey to dull yellow (2.5Y 6/1 to 2.5Y 6/4, both moist) silty clay with banded sandy inclusions; many coarse prominent sharp orange (7.5YR 6/6, moist) mottles; massive; in clayey parts many continuous large intersecting slickensides; silty clay firm, sand extremely firm when moist; strongly calcareous; pH 8.3

R grey (5Y 4/1, moist) clay loam with banded sandy inclusions; massive; extremely firm when moist; calcareous; pH 8.0

ANALYSES PROFILE Sp/166

Horizon	Depth of sample (cm)	TEXTURE (µm in weight %) >2 mm	Sand 2000-1000	Sand 1000-500	Sand 500-250	Sand 250-100	Sand 100-50	Silt 50-2	Clay <2	pH H_2O	pH $CaCl_2$	Org. C %	% CO_2 Soil	% CO_2 Clay
Apck	10- 30	0.8	1.5	1.0	3.5	12.5	10.0	40.5	31.0	7.2	6.8	0.9	13.2	0.3
Bck(g)	40- 55	0.8	2.5	2.0	4.0	9.0	10.0	41.5	31.0	7.6	7.0	0.2	14.8	2.2
Bckg	70- 90	0.7	1.5	1.0	4.0	12.5	10.5	40.0	30.5	7.9	7.2	0.1	11.7	3.5
	120-135	0.6	2.5	2.0	3.5	13.0	9.0	39.5	30.5	8.1	7.2	0.2	13.7	3.3
Ckg	150-170	0.2	1.0	1.0	3.5	18.0	10.0	37.0	29.5	8.2	7.4	tr	11.3	2.9
Cg	190-205	0.0	0.5	0.5	0.5	1.5	2.0	43.0	52.0	8.3	7.5	0.2[1]	9.3	3.9
R		0.0	1.0	1.0	2.5	10.0	11.5	39.5	34.5	8.0	7.4	0.8[1]	8.4	3.4

ELEMENTAL COMPOSITION OF THE FINE EARTH FRACTION (weight %)

Horizon	Depth of sample (cm)	SiO_2	Al_2O_3	Fe_2O_3	FeO	MnO	MgO	CaO	Na_2O	K_2O	TiO_2	P_2O_5	S	H_2O
Apck	10- 30	48.4	9.8	3.4	0.4	0.1	1.1	16.5	0.6	1.4	0.4	0.1	-	4.8
Bck(g)	40- 55	45.3	10.1	3.3	0.4	0.1	1.1	18.4	0.6	1.4	0.4	0.1	-	4.1
Bckg	70- 90	52.0	10.6	4.0	0.4	0.1	1.3	13.3	0.7	1.5	0.5	0.1	-	3.8
	120-135	49.4	9.4	3.4	0.5	0.1	1.4	15.7	0.7	1.4	0.4	0.1	-	3.9
Ckg	150-170	51.8	10.2	3.7	0.5	0.1	1.4	14.2	0.7	1.5	0.5	0.1	-	4.1
Cg	190-205	50.6	13.8	4.5	0.7	0.1	2.0	11.5	0.7	1.9	0.6	0.1	0.2	3.9
R		58.2	11.1	1.9	2.3	0.1	2.0	8.6	0.9	1.8	0.5	0.1	1.4	2.7

ELEMENTAL COMPOSITION OF THE CLAY FRACTION (weight %)

Horizon	Depth of sample (cm)	SiO_2	Al_2O_3	Fe_2O_3	FeO	MnO	MgO	CaO	Na_2O	K_2O	TiO_2	P_2O_5	S	H_2O
Apck	10- 30	57.0	18.4	7.1	0.5	0.1	2.3	0.4	0.4	2.5	0.6		-	10.5
Bck(g)	40- 55	55.5	17.4	6.4	0.3	0.1	2.3	2.8	0.3	2.5	0.6		-	9.6
Bckg	70- 90	52.3	17.4	6.6	0.5	0.1	2.2	4.4	0.4	2.6	0.6		-	9.5
	120-135	52.8	17.4	6.3	0.6	0.1	2.4	4.3	0.4	2.7	0.7		-	9.2
Ckg	150-170	53.1	17.7	6.3	0.6	0.1	2.4	3.7	0.4	2.9	0.7		-	9.1
Cg	190-205	50.3	17.9	6.6	0.7	0.1	2.5	5.0	0.4	3.1	0.7		-	9.0
R		52.3	18.3	4.3	1.6	0.1	2.7	4.3	0.4	3.2	0.7		0.7	7.9

MOLAR RATIOS

Horizon	Depth of sample (cm)	SOIL $\frac{SiO_2}{R_2O_3}$	SOIL $\frac{SiO_2}{Al_2O_3}$	SOIL $\frac{SiO_2}{Fe_2O_3}$	SOIL $\frac{Al_2O_3}{Fe_2O_3}$	CLAY $\frac{SiO_2}{R_2O_3}$	CLAY $\frac{SiO_2}{Al_2O_3}$	CLAY $\frac{SiO_2}{Fe_2O_3}$	CLAY $\frac{Al_2O_3}{Fe_2O_3}$	"Free" Fe_2O_3 Soil	"Free" Fe_2O_3 Clay
Apck	10- 30	6.9	8.4	37.4	4.5	4.2	5.2	21.5	4.1	1.6	2.7
Bck(g)	40- 55	6.3	7.6	36.4	4.8	4.4	5.4	22.9	4.2	1.1	2.1
Bckg	70- 90	6.7	8.3	34.6	4.2	4.1	5.1	21.1	4.1	1.8	2.9
	120-135	7.2	8.9	38.5	4.3	4.2	5.1	22.4	4.4	1.1	2.5
Ckg	150-170	7.0	8.6	37.7	4.4	4.2	5.1	22.3	4.4	1.6	2.3
Cg	190-205	5.2	6.2	29.6	4.8	3.9	4.8	20.4	4.3	1.9	2.4
R		8.0	8.9	80.2	9.0	4.2	4.8	32.3	6.7	0.6	0.7

[1] high value mainly due to oxidation of sulfide minerals

Profilenumber: Sp/183
Classification: CALCIC CAMBISOL, fine textured (FAO-Unesco, 1974)
TYPIC XEROCHREPT, clayey over loamy, mixed, mesic (SOIL SURVEY STAFF, 1975)
Location: alongside road San Giovanni Incarico-Madonna della Piana (Fr., Italy) near "Fontana Pisciarella", approx. 1 km northwest of Monte Lamia; topographical map Ceprano, F° 160, IV S.O. della Carta d' Italia 1 : 25 000, 41° 30' 11" N.L. and 1° 01' 53" east of Monte Mario (Rome)
Elevation: approx. 180 m a.s.l.
Physiographic position: at break of slope from steeply dissected limestone mountains to rolling country with Miocene shales
Slope: very steep (70 %)
Vegetation: oak trees and shrub
Parent material: dolomitic limestone
Drainage conditions: moderately well drained
Moisture conditions: moist throughout profile
Groundwater table: approx. 1.30 cm deep

O 1-0 cm; partly decomposed leave litter; abrupt and smooth boundary to

AB 0-10 cm; brown (10YR 4/4, moist) clay; moderate fine to medium subangular blocky; friable when moist; patchy moderately thick dark brown (10YR 3/3, moist) clay-iron-humus cutans on some pedfaces; few flat and subangular weathered dolomitic gravel; very few small soft spherical black iron-manganese nodules; (slightly) calcareous; common fine and medium roots; pH 7.2; clear and smooth boundary to

B 10-35 cm; brown (10YR 4/4, moist) clay; weak medium prismatic, breaking into moderate fine to medium subangular blocky; friable to firm when moist; patchy moderately thick brown (10YR 4/4, moist) clay-iron cutans on some pedfaces and in some pores; very few subangular weathered dolomitic gravel; very few small soft spherical black iron-manganese nodules; (slightly) calcareous; few wormholes; common fine and medium roots; pH 7.3; clear and smooth boundary to

BC 35-60 cm; yellowish brown (10YR 5/6, moist) sandy loam; few fine prominent sharp bluish black (5PB 2/1, moist) mottles; weak medium to coarse subangular blocky; very friable when moist; patchy moderately thick brown (10YR 4/4, moist) clay-iron cutans on some pedfaces and in some pores; common fine and medium and few coarse pores; many angular weathered dolomitic gravel; very few small soft spherical black iron-manganese nodules; strongly calcareous; few wormholes; few fine and medium roots; pH 7.9; gradual and smooth boundary to

BCg 60-105 cm; bright yellowish brown (10YR 7/6, moist) loamy sand; common medium to coarse prominent clear to sharp mottles, reddish brown (5YR 4/8), brownish grey (10YR 6/1), light grey (2.5Y 8/2) and bluish black (5PB 2/1), all when moist; very weak medium to coarse angular blocky; loose when moist; patchy moderately thick transparent clay cutans in some large pores; many strongly weathered angular dolomitic gravel; strongly calcareous; few wormholes; pH 8.3; diffuse and irregular boundary to

Cg 105->160 cm; pale yellow (2.5Y 8/4, moist) sand; common medium to coarse prominent clear mottles, yellow orange (7.5YR 7/8), dull orange (7.5YR 7/3) and dark bluish grey (5PB 3/1), all when moist; single grain; loose when moist; very few medium pores; many strongly weathered angular dolomitic gravel; strongly calcareous; few wormholes; pH 8.6

ANALYSES PROFILE Sp/183

Horizon	Depth of sample (cm)	TEXTURE (µm in weight %) Sand 2000–1000	Sand 1000–500	Sand 500–250	Sand 250–100	Sand 100–50	Silt 50–2	Clay <2	pH H_2O	pH $CaCl_2$	Org. C %	% CO_2 Soil	% CO_2 Clay
AB	0- 10	1.5	0.3	1.0	3.0	1.5	24.0	68.0	7.2	6.9	6.7	1.9	0.1
B	15- 30	0.4	0.5	2.5	6.5	2.5	20.0	67.5	7.3	7.2	2.8	6.2	0.2
BC	40- 55	0.1	0.7	25.5	49.0	5.0	4.0	16.0	7.9	7.6	0.7	40.9	0.6
BCg	75- 90	0.2	1.0	24.0	53.5	7.5	4.0	10.0	8.3	7.4	0.2	44.4	1.3
Cg	120-140	0.1	0.1	9.0	70.0	10.0	6.0	4.5	8.6	7.7	0.2	45.0	2.2

ELEMENTAL COMPOSITION OF THE FINE EARTH FRACTION (weight %)

Horizon	Depth of sample (cm)	SiO_2	Al_2O_3	Fe_2O_3	FeO	MnO	MgO	CaO	Na_2O	K_2O	TiO_2	P_2O_5	H_2O	"Free" Fe_2O_3
AB	0- 10	53.3	21.6	5.9	0.6	0.2	2.4	2.9	0.4	2.3	1.0	0.1	7.4	3.2
B	15- 30	49.0	20.0	5.9	0.3	0.3	4.1	4.7	0.4	2.1	0.8	0.1	6.3	3.0
BC	40- 55	5.3	3.4	1.1	0.1	0.1	18.6	27.4	0.1	0.2	0.1	0.1	2.3	0.3
BCg	75- 90	2.8	1.1	0.7	0.1	tr	19.4	30.1	0.1	0.1	0.1	tr	1.1	0.3
Cg	120-140	2.4	1.4	0.3	tr	tr	19.4	30.8	0.1	0.1	tr	tr	0.5	0.1

ELEMENTAL COMPOSITION OF THE CLAY FRACTION (weight %)

Horizon	Depth of sample (cm)	SiO_2	Al_2O_3	Fe_2O_3	FeO	MnO	MgO	CaO	Na_2O	K_2O	TiO_2	P_2O_5	H_2O	"Free Fe_2O_3
AB	0- 10	44.8	25.8	8.4	0.5	0.1	2.2	0.1	0.1	1.8	0.9	0.2	15.1	5.0
B	15- 30	43.2	27.3	9.2	0.4	0.2	2.3	0.1	0.1	2.1	0.8	0.2	14.1	5.4
BC	40- 55	43.7	26.1	9.0	0.4	0.3	2.5	0.4	0.1	2.0	0.8	0.3	14.1	5.1
BCg	75- 90	45.0	24.9	10.7	0.2	0.3	2.8	0.8	tr	2.5	0.8	0.2	10.7	6.0
Cg	120-140	44.3	24.3	9.2	0.1	0.7	3.3	1.4	tr	2.5	0.7	0.2	11.1	4.8

MOLAR RATIOS

Horizon	Depth of sample (cm)	$\frac{SiO_2}{R_2O_3}$	$\frac{SiO_2}{Al_2O_3}$	$\frac{SiO_2}{Fe_2O_3}$	$\frac{Al_2O_3}{Fe_2O_3}$	$\frac{SiO_2}{R_2O_3}$	$\frac{SiO_2}{Al_2O_3}$	$\frac{SiO_2}{Fe_2O_3}$	$\frac{Al_2O_3}{Fe_2O_3}$
AB	0- 10	3.6	4.2	24.2	5.8	2.4	3.0	14.2	4.8
B	15- 30	3.5	4.2	22.2	5.3	2.2	2.7	12.5	4.7
BC	40- 55	2.2	2.6	12.7	4.9	2.3	2.8	13.0	4.6
BCg	75- 90	3.1	4.3	10.4	2.4	2.4	3.1	11.2	3.7
Cg	120-140	2.6	3.0	22.9	7.7	2.5	3.1	12.8	4.1

Profilenumber: Sp/186
Classification: EUTRIC NITOSOL, coarse textured (FAO-UNESCO, 1974)
ARENIC PALEXERALF, coarse-loamy, mixed, mesic (SOIL SURVEY STAFF, 1975)
Location: approx. 4 km west of Falvaterra (Fr., Italy) at the "Macchia di Castro"; topographical map Ceprano, F° 160, IV S.O. della Carta d' Italia 1 : 25 000, 41° 30' 37" N.L. and 1° 01' 37" E.L.
Physiographic position: concave slope near small incision
Slope: steep (27 %)
Elevation: approx. 230 m a.s.l.
Vegetation: oak wood and shrub ("macchia")
Parent material: sandstone of Pliocene/old Quaternary age
Drainage conditions: well drained
Moisture conditions: moist throughout profile
Erosion conditions: moderate gully erosion

Ah 0-5 cm; very dark brown (7.5YR 2/3, moist) to brownish black (7.5YR 2/2, moist) sandy loam; weak very fine subangular blocky; very friable when moist; many very fine and fine pores; non calcareous; common fine roots; pH 6.3; abrupt and smooth boundary to

E 5-35 cm; brown (7.5YR 4/6, moist) sandy loam; moderate medium to coarse subangular blocky; very friable when moist; patchy moderately thick brown (7.5YR 4/4, moist) clay-iron-humus cutans on some pedfaces; common very fine and fine and few medium pores; non calcareous; few wormholes; common fine, medium and coarse roots; pH 5.6; gradual and smooth boundary to

Bt1 35-65 cm; bright brown (7.5YR 5/6, moist) sandy clay loam; few medium prominent clear bluish black (5PB 2/1, moist) mottles; coarse subangular blocky; friable when moist; broken moderately thick bright brown (5YR 5/8, moist) clay-iron cutans on some pedfaces and in most of the pores; very few small soft spherical black iron-manganese nodules; non calcareous; few wormholes; common fine and medium roots; pH 5.1; gradual and smooth boundary to

Bt2 65-95 cm; brown (7.5YR 4/6, moist) sandy clay loam; few fine to medium prominent clear bluish black (5PB 2/1) mottles; weak coarse to very coarse prismatic, breaking into moderate medium to coarse subangular blocky; broken moderately thick bright brown (7.5YR 5/6, moist) clay-iron cutans on most of the pedfaces and in pores; common fine and medium pores; very few small soft spherical black iron-manganese nodules; non calcareous; few fine and medium roots; pH 5.2; gradual and smooth boundary to

Bt3 95-130 cm; dark brown (7.5YR 3/4, moist) sandy clay loam; common coarse distinct clear brown (7.5YR 4/6, moist) mottles and few medium prominent sharp bluish black (5PB 2/1, moist) mottles; moderate to strong very coarse prismatic; friable to firm when moist; broken moderately thick to thick dark reddish brown (5YR 3/4, moist) clay-iron cutans on most of the pedfaces and in pores; common fine and medium pores; non calcareous; few wormholes; few fine and medium roots; pH 5.2; gradual and smooth boundary to

Bt4 130->175 cm; dark brown (7.5YR 3/4, moist) sandy clay loam; common coarse distinct clear brown (7.5YR 4/6, moist) mottles and few medium prominent sharp bluish black (5PB 2/1, moist) mottles; moderate medium to coarse angular blocky; friable when moist; broken moderately thick dull reddish brown (5YR 4/4, moist) clay-iron cutans on most of the pedfaces and in some pores; few very fine to fine pores; very few small soft spherical black iron-manganese nodules; non calcareous; few fine roots; pH 5.4

ANALYSES PROFILE Sp/186

Horizon	Depth of sample (cm)	TEXTURE (µm in weight %) Sand 2000–1000	Sand 1000–500	Sand 500–250	Sand 250–100	Sand 100–50	Silt 50–2	Clay <2	pH H_2O	pH $CaCl_2$	Org. C %
Ah	0- 5	1.0	2.5	22.5	36.0	9.0	21.5	7.0	6.3	5.7	2.4
E	10- 30	0.6	1.0	20.5	36.5	9.0	20.0	12.5	5.6	4.4	0.7
Bt1	40- 55	0.3	1.0	14.5	30.5	7.5	21.0	24.5	5.1	3.8	0.3
Bt2	70- 90	0.4	1.5	18.5	31.0	6.5	19.5	22.5	5.2	3.9	0.2
Bt3	100-120	0.4	1.0	16.0	29.0	7.0	24.5	22.0	5.2	4.0	0.2
Bt4	140-160	0.4	1.0	16.0	27.5	6.5	26.0	22.5	5.3	4.2	0.3
BC[1]		0.2	0.8	27.0	35.0	6.0	21.0	10.5	5.4	4.5	0.3

ELEMENTAL COMPOSITION OF THE FINE EARTH FRACTION (weight %)

Horizon	Depth of sample (cm)	SiO_2	Al_2O_3	Fe_2O_3	FeO	MnO	MgO	CaO	Na_2O	K_2O	TiO_2	P_2O_5	H_2O	"Free" Fe_2O_3
Ah	0- 5	83.2	10.0	0.8	0.6	0.2	0.4	0.5	1.0	2.3	0.3	tr	0.8	0.6
E	10- 30	80.8	10.3	2.0	0.2	0.2	0.4	0.3	1.1	2.7	0.2	tr	1.9	1.1
Bt1	40- 55	73.9	14.1	3.7	0.1	0.1	0.8	0.5	0.7	2.5	0.1	0.1	3.5	2.0
Bt2	70- 90	76.5	12.5	3.3	tr	0.1	0.7	0.3	0.7	2.2	0.2	tr	3.4	1.8
Bt3	100-120	75.9	12.1	3.3	0.1	0.2	0.7	0.4	0.9	2.6	0.3	0.1	3.6	1.8
Bt4	140-160	72.8	15.4	3.3	tr	0.2	0.6	0.4	0.8	2.6	0.3	0.1	3.6	1.9
BC[1]		76.5	12.5	3.3	tr	0.1	0.7	0.3	0.7	2.2	0.2	tr	3.4	1.4

ELEMENTAL COMPOSITION OF THE CLAY FRACTION (weight %)

Horizon	Depth of sample (cm)	SiO_2	Al_2O_3	Fe_2O_3	FeO	MnO	MgO	CaO	Na_2O	K_2O	TiO_2	P_2O_5	H_2O	"Free" Fe_2O_3
Ah	0- 5	48.3	23.3	9.2	0.7	0.2	2.3	0.1	0.3	2.1	0.5	0.3	12.8	4.9
E	10- 30	46.8	25.2	11.0	0.4	0.1	2.2	0.1	0.1	1.8	0.4	0.2	11.9	6.0
Bt1	40- 55	45.0	26.4	12.2	0.2	tr	1.9	0.1	0.1	1.7	0.3	0.2	12.1	7.0
Bt2	70- 90	46.0	25.5	11.6	0.2	0.4	1.9	tr	0.1	1.7	0.6	0.2	12.0	6.7
Bt3	100-120	45.2	26.5	10.9	0.2	0.3	1.8	0.1	0.1	1.8	0.6	0.2	12.3	6.3
Bt4	140-160	45.5	26.7	10.4	0.1	0.6	1.8	0.1	0.1	1.8	0.7	0.3	12.1	6.1
BC[1]		45.6	23.1	14.3	0.1	0.3	1.9	0.1	tr	1.5	0.2	0.3	12.6	9.0

MOLAR RATIOS

Horizon	Depth of sample (cm)	SOIL $\frac{SiO_2}{R_2O_3}$	SOIL $\frac{SiO_2}{Al_2O_3}$	SOIL $\frac{SiO_2}{Fe_2O_3}$	SOIL $\frac{Al_2O_3}{Fe_2O_3}$	CLAY $\frac{SiO_2}{R_2O_3}$	CLAY $\frac{SiO_2}{Al_2O_3}$	CLAY $\frac{SiO_2}{Fe_2O_3}$	CLAY $\frac{Al_2O_3}{Fe_2O_3}$
Ah	0- 5	13.5	14.1	279.9	19.8	2.8	3.5	14.1	4.0
E	10- 30	11.9	13.3	109.6	8.3	2.5	3.2	11.3	3.6
Bt1	40- 55	7.6	8.9	53.4	6.0	2.2	2.9	9.8	3.4
Bt2	70- 90	8.9	10.4	61.1	5.9	2.4	3.1	10.5	3.4
Bt3	100-120	9.1	10.7	61.2	5.7	2.3	2.9	11.0	3.8
Bt4	140-160	7.1	8.0	59.0	7.8	2.3	2.9	11.7	4.0
BC[1]		8.9	10.4	61.1	5.9	2.4	3.4	8.5	2.5

[1] sample BC taken from spot near profile

Profilenumber: Sp/191
Classification: CALCIC CAMBISOL, medium textured (FAO- UNESCO, 1974)
AQUIC CALCIXEROLLIC XEROCHREPT, coarse-loamy, mixed, mesic (SOIL SURVEY STAFF, 1975)
Location: approx. 1 km north of Monte Lamia, alongside road Madonna della Piana-San Giovanni Incarico (Fr., Italy); topographical map Ceprano, F° 160, IV S.O. della Carta d' Italia 1 : 25 000, 41° 30' 50" N.L. and 1° 02' 11" east of Monte Mario (Rome)
Elevation: approx. 160 m a.s.l.
Physiographic position: slightly convex slope near watershed between two small incisions
Slope: moderately steep (23 %)
Vegetation: grass with scattered olive trees
Parent material: Miocene sandstones and shales
Drainage conditions: well drained
Moisture conditions: moist throughout profile

Ap 0-20 cm; yellowish brown (2.5Y 5/4, moist) loam; weak medium crumb to very fine to fine angular blocky; very friable when moist; many very fine and fine pores; calcareous; few wormholes; common very fine and fine roots; pH 7.5; abrupt and smooth boundary to

Bgck1 20-35 cm; dull yellow (2.5Y 6/4, moist) loam; few fine distinct clear yellowish grey (2.5Y 6/1, moist) and bright yellowish brown (10YR 6/6, moist) mottles; moderate fine to medium angular blocky; very friable when moist; common very fine and fine pores; very few small soft irregular white calcium carbonate nodules; strongly calcareous; common fine and medium and few coarse roots; few wormholes; pH 7.7; clear and smooth boundary to

Bgck2 35-50 cm; yellowish brown (2.5Y 5/4, moist) sandy loam; few fine distinct clear yellowish grey (2.5Y 6/1, moist) and bright yellowish brown (10YR 6/6, moist) mottles; moderate fine to medium prismatic; friable to firm when moist; few very fine and fine pores; very few small soft irregular and spherical white calcium carbonate nodules; (strongly) calcareous; very few very fine roots; pH 8.0; gradual and irregular boundary to

BCck 50->90cm; yellowish brown (2.5Y 5/4, moist) sandy loam; moderate coarse to very coarse subangular blocky; friable to firm when moist; few fine and medium pores; few angular weathered Miocene sandstone gravel; very few small soft irregular and spherical white calcium carbonate nodules; (strongly) calcareous; few wormholes; pH 8.0

ANALYSES PROFILE Sp/191

		TEXTURE (µm in weight %)									
	Depth of		Sand					Silt	Clay		
Horizon	sample (cm)	>2 mm	2000 1000	1000 500	500 250	250 100	100 50	50 2	<2	pH H_2O	pH $CaCl_2$
Ap	5- 15	0.3	0.3	1.0	10.0	28.0	12.0	30.0	18.0	7.5	7.1
Bgck1	20- 30	0.3	0.2	0.3	3.0	14.0	12.5	47.5	22.5	7.7	7.4
Bgck2	35- 45	0.0	0.3	0.6	8.0	42.0	13.0	26.5	9.5	8.0	7.6
BCck	60- 70	0.0	1.0	3.5	18.5	34.5	11.0	23.5	7.5	8.0	7.7

Profilenumber: Sp/234
Classification: CHROMIC VERTISOL, fine textured (FAO-Unesco, 1974)
ENTIC PALEXEROLLIC CHROMOXERERT, very-fine, kaolinitic, mesic (SOIL SURVEY STAFF, 1975)
Location: approx. 3.5 km south of Pico (Fr., Italy), alongside the road Pico-San Oliva; topographical map Pico, F° 160, III N.O. della Carta d' Italia 1 : 25 000, 41° 25' 04" N.L. and 1° 05' 23" east of Monte Mario)Rome)
Elevation: approx. 500 m a.s.l.
Physiographic position: concave slope in limestone mountains
Slope: (moderately) steep (25 %)
Vegetation: oak trees and grass
Parent material: dolomitic limestone; top part of the profile may be of colluvial origin
Drainage conditions: moderately well drained
Moisture conditions: dry throughout profile
Presence of rock outcrops: very rocky

Ah 0-20 cm; reddish brown (5YR 4/6, moist) clay; moderate fine to medium crumb; slightly hard when dry; common fine and medium pores; non calcareous; common fine and medium roots; pH 7.3; clear and smooth boundary to

Bt 20-45 cm; bright reddish brown (5YR 5/8, moist) clay; few fine faint clear bright reddish brown (5YR 5/6, moist) and few coarse distinct clear reddish brown (2.5YR 4/6, moist) mottles; weak coarse prismatic, breaking into strong fine to medium angular blocky; hard when dry; broken moderately thick dull reddish brown (2.5YR 4/4, moist) clay-iron(-humus) cutans on vertical pedfaces and in pores, and few oblique slickensides; common fine and few medium pores; few small hard spherical black iron-manganese nodules; non calcareous; very few wormholes; common fine and medium roots; pH 7.3; gradual and smooth boundary to

Bw1 45-105 cm; dark reddish brown (5YR 3/6, moist) clay; very few fine prominent sharp bluish black (5PB 2/1, moist) mottles; fine to medium angular blocky, wedgeshaped; hard when dry; very many large intersecting slickensides and patchy moderately thick dull reddish brown (2.5YR 4/4, moist) clay-iron (-humus) cutans in some pores; few fine and medium pores; non calcareous; common medium and few coarse roots; pH 7.1; gradual and smooth boundary to

Bw2 105-160 cm; dark reddish brown (2.5YR 3/6, moist) clay; many coarse prominent sharp bluish black (5PB 2/1, moist) mottles; weak coarse to very coarse angular blocky, breaking into strong fine angular blocky, wedgeshaped; slightly hard when dry; many continuous intersecting slickensides and patchy moderately thick reddish brown (2.5YR 4/6, moist) clay-iron cutans in some pores; few fine pores; non calcareous; few medium roots; pH 6.5; gradual and smooth boundary to

Bw3 160-250 cm; reddish brown (2.5YR 4/6, moist) clay; many coarse prominent sharp bluish black (5PB 2/1, moist) mottles; strong fine angular blocky, wedgeshaped; slightly hard when dry; many continuous intersecting slickensides; few fine pores; non calcareous; few medium roots; pH 4.9; diffuse and smooth boundary to Bw4 with lateral a sharp and irregular boundary to C

Bw4 250-300 cm; reddish brown (2.5YR 4/6, moist) clay; very few fine prominent sharp bluish black (5PB 2/1, moist) mottles; weak medium to coarse angular blocky, breaking into strong fine angular blocky, wedgeshaped; slightly hard when dry; many contnuous intersecting slickensides; few fine pores; slightly calcareous; few medium roots; pH 7.1; sharp and irregular boundary to

C 300-330/350 cm; light yellow orange (10YR 8/4, moist) sand; few coarse prominent clear reddish brown (5YR 4/8, moist) mottles; structureless; soft when dry; calcareous; pH 8.5; abrupt and irregular boundary to

R 330/350 cm +; hard dolomitic limestone

ANALYSES PROFILE Sp/234

Horizon	Depth of sample (cm)	TEXTURE (µm in weight %) >2 mm	Sand 2000-1000	Sand 1000-500	Sand 500-250	Sand 250-100	Sand 100-50	Silt 50-2	Clay <2	pH H_2O	pH $CaCl_2$	Org. C %	% CO_2 Soil	% CO_2 Clay
Ah	5- 15	0.2			2.5			24.0	73.5	7.3	7.1	1.3	-	-
Bt	25- 40	-			2.0			25.0	73.0	7.3	6.9	0.4	-	-
Bw1	70- 90	-			1.5			13.0	85.5	7.1	6.7	0.2	-	-
Bw2	120-140	-			0.5			3.5	96.0	6.5	6.1	0.3	-	-
Bw3	200-220	-			1.0			7.5	91.5	4.9	4.4	0.3	-	-
Bw4	270-290	-			0.5			3.5	96.0	7.1	6.8	0.5	0.7	-
C	310-325	-	0.0	0.0	1.0	80.5	12.0	3.5	3.0	8.5	8.2	0.1	41.8	0.7
R												0.1	42.5	

ELEMENTAL COMPOSITION OF THE FINE EARTH FRACTION AND ROCK (weight %)

Horizon	Depth of sample (cm)	SiO_2	Al_2O_3	Fe_2O_3	FeO	MnO	MgO	CaO	Na_2O	K_2O	TiO_2	P_2O_5	H_2O	"Free" Fe_2O_3
Ah	5- 15	47.7	27.7	8.9	0.3	0.1	0.9	0.6	0.1	1.6	1.0	0.1	11.1	5.5
Bt	25- 40	49.7	26.5	8.9	0.3	0.1	0.8	0.3	0.2	1.9	1.1	0.2	10.2	5.5
Bw1	70- 90	46.0	29.6	8.7	0.2	0.1	0.9	0.4	0.1	1.6	0.9	0.2	11.3	5.4
Bw2	120-140	44.9	29.8	9.4	0.2	0.1	0.8	0.3	0.1	1.4	0.9	0.2	12.1	5.8
Bw3	200-220	45.1	30.5	8.9	0.2	0.1	0.8	0.2	0.1	1.5	0.9	0.2	11.5	5.9
Bw4	270-290	43.9	30.4	9.2	0.3	0.1	1.1	0.7	0.1	1.3	0.8	0.2	11.4	5.8
C	310-325	5.0	1.1	0.4	0.1	tr	16.0	33.1	0.1	tr	tr	tr	2.5	0.3
R		4.1	0.2	0.2	tr	tr	17.4	32.8	0.1	tr	tr	tr	2.7	tr

ELEMENTAL COMPOSITION OF THE CLAY FRACTION (weight %)

Horizon	Depth of sample (cm)	SiO_2	Al_2O_3	Fe_2O_3	FeO	MnO	MgO	CaO	Na_2O	K_2O	TiO_2	P_2O_5	H_2O	"Free" Fe_2O_3
Ah	5- 15	45.0	30.4	8.9	0.1	0.1	0.8	0.1	0.2	1.3	0.9	0.4	11.8	6.5
Bt	25- 40	45.6	30.0	8.9	0.1	0.1	0.9	tr	0.2	1.7	0.9	0.3	11.4	6.4
Bw1	70- 90	45.2	30.4	8.8	0.1	0.1	0.8	0.1	0.3	1.5	0.8	0.2	11.7	6.3
Bw2	120-140	44.8	30.6	9.3	0.1	0.1	0.7	tr	0.2	1.3	0.8	0.3	11.9	6.8
Bw3	200-220	45.2	30.1	9.2	0.1	0.1	0.8	tr	0.1	1.4	0.8	0.3	12.0	6.7
Bw4	270-290	44.0	30.4	9.3	0.1	0.1	0.8	0.1	0.3	1.3	0.8	0.3	12.6	6.7
C	310-325	44.3	29.9	8.9	0.2	0.1	1.1	0.5	0.1	1.7	0.8	0.5	11.3	6.4

MOLAR RATIOS

Horizon	Depth of sample (cm)	SOIL $\frac{SiO_2}{R_2O_3}$	SOIL $\frac{SiO_2}{Al_2O_3}$	SOIL $\frac{SiO_2}{Fe_2O_3}$	SOIL $\frac{Al_2O_3}{Fe_2O_3}$	CLAY $\frac{SiO_2}{R_2O_3}$	CLAY $\frac{SiO_2}{Al_2O_3}$	CLAY $\frac{SiO_2}{Fe_2O_3}$	CLAY $\frac{Al_2O_3}{Fe_2O_3}$
Ah	5- 15	2.4	2.9	14.3	4.9	2.1	2.5	13.4	5.3
Bt	25- 40	2.6	3.2	14.9	4.7	2.2	2.6	13.6	5.3
Bw1	70- 90	2.2	2.6	14.0	5.3	2.1	2.5	13.6	5.4
Bw2	120-140	2.1	2.6	12.7	5.0	2.1	2.5	12.9	5.2
Bw3	200-220	2.1	2.5	13.5	5.4	2.1	2.5	13.1	5.1
Bw4	270-290	2.1	2.5	12.7	5.2	2.1	2.5	12.5	5.1
C	310-325	6.4	7.8	34.9	4.5	2.1	2.5	13.2	5.2
R		21.4	38.8	47.6	1.2				

Profilenumber: Sp/235
Classification: CHROMIC VERTISOL, fine textured (FAO-Unesco, 1974)
TYPIC CHROMOXERERT, very fine, kaolinitic, mesic (SOIL SURVEY STAFF, 1975)
Location: approx. 5 km south-south-west of Pico (Fr., Italy) alongside road Pico-San Oliva; topographical map Esperia, F° 160, III S.E. della Carta d'Italia 1 : 25 000, 41° 24' 48" N.L. and 1° 07' 31" east of Monte Mario (Rome)
Elevation: approx. 280 m a.s.l.
Physiogrphic position: concave slope in limestone mountains
Slope: steep (32 %)
Vegetation: oak trees and shrub ("macchia")
Parent material: white to light grey hard limestone
Drainage conditions: well drained
Moisture conditions: dry throughout profile
Presence of rock outcrops: very rocky

Ah 0-5 cm; dark reddish brown (5YR 3/3, moist) clay; strong very fine angular blocky; hard when dry; many fine pores; non calcareous; many fine and medium roots; abrupt and wavy boundary to

AB 5-30 cm; dark reddish brown (5YR 3/4, moist) clay; strong fine to medium angular blocky; hard when dry; many small intersecting slickensides; many fine and medium pores; slightly calcareous; some insect- and wormholes; many fine and medium roots; pH 6.5; lateral abrupt and broken boundary to R and clear and smooth boundary to

Bw 30-90 cm; dark reddish brown (2.5YR 3/4, moist) clay; moderate medium prismatic, breaking into strong fine angular blocky, wedgeshaped; hard when dry; many small intersecting slickensides; common fine and medium and few coarse pores; slightly calcareous; many coarse wormholes; pH 7.1-7.3; abrupt and broken boundary to

R 90 cm +; white to light grey limestone, showing fissures and cracks

ANALYSES PROFILE Sp/235

		TEXTURE (µm in weight %)										
	Depth of	Sand					Silt	Clay	pH		Org.	%
Horizon	sample (cm)	2000 1000	1000 500	500 250	250 100	100 50	50 2	<2	H_2O	$CaCl_2$	C %	CO_2
AB	10- 25			3.0			13.5	83.5	6.5	6.2	3.6	0.1
Bw	40- 55			0.5			4.5	95.0	7.1	6.6	1.7	0.1
Bw	70- 90			0.5			10.5	89.0	7.3	6.9	2.0	0.2

Profilenumber: Sp/258
Classification: EUTRIC CAMBISOL, medium textured (FAO-Unesco, 1974)
TYPIC XEROCHREPT, coarse-loamy, mixed, mesic (SOIL SURVEY STAFF, 1975)
Location: approx. 600 m east of Coldragone (Fr. Italy) at locality "Colfelice", topographical map Roccasecca, F° 160 IV S.E. della Carta d'Italia 1 : 25 000, 41° 39' 15" N.L. and 1° 09' 01" east of Monta Mario (Rome)
Elavation: approx. 175 m a.s.l.
Physiographic position: nearly summit of isolated hill
Slope: gently sloping (5 %)
Vegetation: grass
Parent material: sandstone of Miocene age
Drainage conditions: somewhat excessively drained
Moisture conditions: dry throughout profile

Ap 0-25 cm; yellowish brown (2.5Y 5/4, moist) sandy loam; moderate medium crumb; slightly hard when dry; few fine and very few medium pores; non calcareous; some pottery fragments; common medium roots; pH 7.0; clear and smooth boundary to

Bw 25-45 cm; olive brown (2.5Y 7/4, moist) sandy loam; moderate medium angular blocky; few medium roots; pH 7.1; clear and smooth boundary to

C 45-250 cm; light yellow (2.5Y 7/4, moist) sandy loam; massive; slightly hard when dry; few fine and very few medium pores; non calcareous; few fine roots; pH 7.1; diffuse and wavy boundary to

R 250 cm +; calcareous coherent sandstone of Miocene age

ANALYSES PROFILE Sp/258

		TEXTURE (µm in weight %)									
	Depth of	Sand						Silt	Clay		
Horizon	sample (cm)	2000 1000	1000 500	500 250	250 100	100 50	50 2	<2	pH H_2O	pH $CaCl_2$	Org. C %
Ap	5- 15	0.1	0.6	8.0	30.0	17.0	36.0	8.5	7.0	6.4	1.0
Bw	30- 40	0.6	0.5	7.5	27.0	16.5	38.5	9.5	7.1	6.4	0.5
C	50- 70	0.1	0.4	11.5	36.0	13.0	34.0	5.0	7.1	6.7	0.2

ELEMENTAL COMPOSITION OF THE FINE EARTH FRACTION (weight %)

Horizon	Depth of sample (cm)	SiO_2	Al_2O_3	Fe_2O_3	FeO	MnO	MgO	CaO	Na_2O	K_2O	TiO_2	P_2O_5	H_2O	"Free" Fe_2O_3
Ap	5- 15	76.9	10.7	2.7	0.2	0.1	0.9	1.2	2.3	2.4	0.5		2.0	1.0
Bw	30- 40	75.7	11.4	2.9	0.3	0.1	1.0	1.4	2.2	2.4	0.5		2.4	1.0
C	50- 70	75.5	11.3	3.0	0.3	0.1	1.1	1.2	2.4	2.4	0.5		2.4	1.1

ELEMENTAL COMPOSITION OF THE CLAY FRACTION (weight %)

Horizon	Depth of sample (cm)	SiO_2	Al_2O_3	Fe_2O_3	FeO	MnO	MgO	CaO	Na_2O	K_2O	TiO_2	P_2O_5	H_2O	"Free" Fe_2O_3
Ap	5- 15	49.5	20.8	11.8	0.2	0.3	3.0	0.2	0.6	3.2	0.7		9.7	5.9
Bw	30- 40	50.5	20.9	11.4	0.2	0.3	2.8	0.3	0.7	3.0	0.7		9.4	5.9
C	50- 70	51.5	19.4	11.9	0.3	0.2	2.6	0.3	1.0	2.5	0.5		9.8	7.0

MOLAR RATIOS

		SOIL				CLAY			
Horizon	Depth of sample (cm)	$\frac{SiO_2}{R_2O_3}$	$\frac{SiO_2}{Al_2O_3}$	$\frac{SiO_2}{Fe_2O_3}$	$\frac{Al_2O_3}{Fe_2O_3}$	$\frac{SiO_2}{R_2O_3}$	$\frac{SiO_2}{Al_2O_3}$	$\frac{SiO_2}{Fe_2O_3}$	$\frac{Al_2O_3}{Fe_2O_3}$
Ap	5- 15	10.5	12.2	74.6	6.1	2.7	4.0	11.2	2.8
Bw	30- 40	9.7	11.3	69.9	6.2	3.1	4.1	11.8	2.9
C	50- 70	9.7	11.3	67.6	6.0	3.3	4.5	11.6	2.6

Profilenumber: C 7 (from SEVINK et al., 1980)
Classification: FERRIC LUVISOL, fine textured (FAO-UNESCO, 1974)
AQUIC HAPLOXERALF, fine, mixed, mesic (SOIL SURVEY STAFF, 1975)
Date of examination: 30th July 1975
Authors: O.C.Spaargaren & J.C.Tijmons
Location: approx. 3 km south-east of Veroli (Fr., Italy) alongside "Superstrada" Frosinone-Sora, at locality "Casino Novelli"; topographical map Alatri, F° 151 II S.E. della Carta d' Italia 1 : 25 000, 41° 40' 06" N.L. and 0° 51' 59" east of Monte Mario (Rome)
Elevation: approx. 360 m a.s.l.
Physiographic position: convex summit of dissected terrace
Slope: gently sloping (3 %)
Vegetation: open woodland (oak and olive trees with grasses and shrub)
Parent material: probably old Quaternary alluvial fan deposits
Drainage conditions: (moderately) well drained
Moisture conditions: dry throughout profile
Erosion conditions: slight sheet erosion

E 0-15 cm; dull orange to orange (5YR 7/5, dry) to reddish brown (5YR 4/6, moist) sandy clay loam; moderate fine to medium subangular blocky; slightly hard when dry; very few fine pores; very few small hard spherical black iron-manganese nodules; non calcareous; few fine and medium roots; pH 5.1; clear and smooth boundary to

Bt1 15-50 cm; bright reddish brown (5YR 5/7, dry) to reddish brown (5YR 4/8, moist) clay; common medium prominent sharp bluish black (5PB 2/1, both dry and moist) mottles; moderate coarse prismatic, breaking into strong fine to medium subangular blocky; hard when dry; continuous moderately thick reddish brown (2.5YR 4/6, both dry and moist) clay-iron cutans on all pedfaces; few fine pores; few small hard spherical black iron-manganese nodules; non calcareous; common fine and medium roots; pH 5.0; gradual and smooth boundary to

Bt2 50-65 cm; orange (7.5YR 6/8, dry) to bright brown (7.5YR 5/8, moist) clay; moderate medium to coarse angular blocky, locally wedgeshaped; hard when dry; broken moderately thick bright reddish brown (5YR 5/6,dry) to reddish brown (5YR 4/6, moist) clay-iron cutans on some pedfaces and common small slickensides; common fine and medium pores; non calcareous; few fine and medium roots; pH 5.1; gradual and smooth boundary to

Bg1 65-325 cm; mottled clay, light grey (5Y 8/1, dry; 5Y 7/1, moist), brownish grey (10YR 6/1, dry; 10YR 5/1, moist), orange (7.5YR 6/8, dry) to bright brown (7.5YR 5/8, moist) and bright brown (2.5YR 5/6, dry) to dark reddish brown (2.5YR 3/6, moist); from 210 cm downwards also common coarse distinct sharp bluish black (5PB 2/1, both dry and moist) mottles; strong coarse angular blocky, locally wedgeshaped; hard when dry; patchy thin brownish grey (5YR 6/1, both dry and moist) clay cutans and common small slickensides; few fine pores; very few small hard irregular white silica nodules; slightly calcareous; pH 5.1; gradual and smooth boundary to

Bg2 325->450 cm; orange (7.5YR 6/6, dry) to bright brown (7.5YR 5/6, moist) clay; many coarse prominent bluish black (5PB 2/1, both dry and moist) and few coarse distinct prominent light brownish grey (5YR 7/1, dry) to brownish grey (5YR 6/1, moist) mottles; strong medium to coarse angular blocky, locally wedgeshaped; hard when dry; common medium slickensides, sometimes intersecting; few fine pores; very few strongly weathered, probably Miocene sandstone gravel; slightly calcareous; pH 7.2

ANALYSES PROFILE C 7

Horizon	Depth of sample (cm)	TEXTURE (µm in weight %) Sand 2000–1000	1000–500	500–250	250–100	100–50	Silt 50–2	Clay <2	pH H_2O	pH $CaCl_2$	Org. C %	% CO_2 Soil	% CO_2 Clay
E	10- 15	1.5	1.0	4.5	13.5	6.5	44.5	28.5	5.1	4.3	2.6	-	-
Bt1	30- 40	0.5	0.7	2.0	6.5	2.5	27.0	61.0	5.0	4.1	0.8	-	-
Bt2	55- 60	0.3	0.8	3.0	11.0	3.5	27.5	54.0	5.1	4.0	0.5	-	-
Bg1	70- 75	0.0	0.2	2.0	9.0	9.0	31.0	49.0	5.2	4.1	0.5	tr	-
	135-140	0.4	0.9	4.0	14.0	8.0	27.5	45.0	4.8	3.8	0.4	0.3	0.5
	220-230	0.7	1.0	4.0	11.5	9.5	25.0	48.0	5.1	4.2	0.4	0.5	0.5
	315-325	0.5	1.0	3.5	9.5	8.0	25.0	53.0	5.8	5.2	0.4	0.5	0.6
Bg2	340-350	0.3	0.6	3.0	10.5	9.5	29.0	47.0	7.4	7.0	0.4	0.6	0.7
	440-450	0.9	1.0	5.0	14.0	9.0	29.0	41.5	7.0	6.5	0.3	0.4	0.7

ELEMENTAL COMPOSITION OF THE FINE EARTH FRACTION (weight %)

Horizon	Depth of sample (cm)	SiO_2	Al_2O_3	Fe_2O_3	FeO	MnO	MgO	CaO	Na_2O	K_2O	TiO_2	P_2O_5	H_2O	"Free" Fe_2O_3
E	10- 15	76.2	11.7	4.9	0.4	0.3	0.5	0.2	0.2	1.6	0.9	0.1	3.2	3.7
Bt1	30- 40	58.9	20.6	8.4	0.4	0.1	0.6	0.1	0.2	1.7	0.9	0.2	7.9	5.9
Bt2	55- 60	62.8	18.7	7.5	0.4	0.1	0.6	0.2	0.1	1.6	0.7	0.1	7.3	5.5
Bg1	70- 75	66.4	17.0	6.9	0.1	tr	0.6	0.2	0.1	1.5	0.6	tr	6.6	5.2
	135-140	68.5	16.3	5.8	0.2	tr	0.6	0.2	0.1	1.8	0.5	tr	5.7	4.1
	220-230	66.8	17.2	5.9	0.1	0.1	0.7	0.3	0.1	1.9	0.5	0.1	5.9	3.8
	315-325	65.5	17.8	6.2	0.1	0.2	0.8	0.3	0.1	2.0	0.5	0.1	5.7	4.3
Bg2	340-350	68.5	15.9	5.6	0.1	0.1	0.9	0.5	0.2	2.2	0.5	0.1	4.7	3.5
	440-450	71.1	14.5	5.5	0.1	0.2	0.8	0.3	0.1	2.0	0.5	0.1	4.4	3.7

ELEMENTAL COMPOSITION OF THE CLAY FRACTION (weight %)

Horizon	Depth of sample (cm)	SiO_2	Al_2O_3	Fe_2O_3	FeO	MnO	MgO	CaO	Na_2O	K_2O	TiO_2	P_2O_5	H_2O	"Free" Fe_2O_3
E	10- 15	45.7	26.1	11.4	0.2	0.5	1.0	0.1	0.1	1.6	1.2	0.3	11.8	8.2
Bt1	30- 40	44.3	29.2	10.7	0.1	0.1	1.0	tr	0.1	1.3	1.0	0.3	11.9	7.6
Bt2	55- 60	44.6	30.2	9.9	0.1	tr	0.9	0.1	0.1	1.3	0.8	0.2	11.7	6.9
Bg1	70- 75	47.2	29.0	9.3	0.1	0.1	0.8	tr	0.1	1.5	0.7	0.2	11.0	6.6
	135-140	49.0	28.7	7.7	0.1	tr	0.9	0.1	0.1	1.6	0.6	0.2	10.5	4.8
	220-230	47.6	28.3	9.2	tr	0.1	0.9	tr	0.1	1.4	0.7	0.4	10.9	6.2
	315-325	47.0	28.3	9.6	0.1	0.2	1.0	0.1	0.1	1.5	0.7	0.4	10.5	6.7
Bg2	340-350	49.3	26.5	9.7	0.1	0.2	1.3	0.1	0.1	1.8	0.6	0.2	9.6	6.4
	440-450	49.4	25.8	10.4	tr	0.2	1.2	tr	0.1	1.8	0.6	0.3	9.6	7.3

MOLAR RATIOS

Horizon	Depth of sample (cm)	SOIL $\frac{SiO_2}{R_2O_3}$	$\frac{SiO_2}{Al_2O_3}$	$\frac{SiO_2}{Fe_2O_3}$	$\frac{Al_2O_3}{Fe_2O_3}$	CLAY $\frac{SiO_2}{R_2O_3}$	$\frac{SiO_2}{Al_2O_3}$	$\frac{SiO_2}{Fe_2O_3}$	$\frac{Al_2O_3}{Fe_2O_3}$
E	10- 15	8.8	11.1	41.5	3.7	2.3	3.0	10.7	3.6
Bt1	30- 40	3.8	4.8	18.7	3.9	2.1	2.6	11.0	4.3
Bt2	55- 60	4.5	5.7	22.2	3.9	2.1	2.5	12.0	4.8
Bg1	70- 75	5.3	6.7	25.7	3.9	2.3	2.8	13.5	4.9
	135-140	5.8	7.1	31.6	4.4	2.5	2.9	16.9	5.8
	220-230	5.4	6.6	30.1	4.6	2.4	2.9	13.8	4.8
	315-325	5.1	6.2	27.9	4.5	2.3	2.8	13.0	4.6
Bg2	340-350	6.0	7.3	32.3	4.4	2.6	3.2	13.5	4.3
	440-450	6.7	8.4	34.1	4.1	2.6	3.2	12.7	3.9

Horizon	Depth of sample (cm)	Exchangeable cations Ca	Mg	K	Na	Sum	Exch. ac.	CEC Soil	Clay	BS %
		meq/100 g								
Bt1	30- 45	2.6	2.1	0.4	0.4	5.5	1.3	6.8	10.8	81
Bg1	70- 75	3.6	2.3	0.3	0.4	6.6	1.3	7.9	16.0	84
	135-140	3.2	2.5	0.3	0.4	6.4	1.1	7.5	16.9	85

Profilenumber: E 80
Classification: CHROMIC LUVISOL, fine textured (FAO-Unesco, 1974)
MOLLIC HAPLOXERALF, clayey over sandy, kaolinitic, mesic (SOIL SURVEY STAFF, 1975)
Date of examination: 12-8-1975
Authors: O.C.Spaargaren & J.C.Tijmons
Location: alongside road Itri-Sperlonga, approx. 3 km east of Sperlonga (Lt., Italy); topographical map Itri, F° 171 IV N.O. della Carta d'Italia 1 : 25 000, 41° 15" 38" N.L. and 1° 01' 06" east of Monte Mario (Rome)
Elevation: approx. 250 m a.s.l.
Physiographic position: concave slope in dolomitic limestone mountains
Slope: steep (32 %)
Vegetation: shrub (mainly Ampelodesma tenax Link)
Parent material: dolomitic limestone (soil developed in fissure)
Drainage conditions: well drained
Moisture conditions: dry throughout profile
Presence of rock outcrops: very rocky

Ah 0-20 cm; dark reddish brown (5YR 3/2, dry) to brownish black (5YR 3/1, moist) slightly gravelly clay; moderate fine crumb; slightly hard when dry; many very fine and fine pores; very few slightly weathered angular dolomitic limestone gravel; slightly calcareous; moderate ant activity; many fine and medium and few coarse roots; pH 6.9; clear and smooth boundary to

AB 20-30 cm; dark reddish brown (2.5YR 3/4, dry; 2.5YR 3/3, moist) clay; strong very fine angular blocky; hard when dry; broken moderately thick dark reddish brown (5YR 3/3, dry; 5YR 3/2, moist) clay-iron-humus cutans on most of the pedfaces; common very fine and fine pores; slightly calcareous; many fine and medium and few coarse roots; pH 6.9; clear and smooth boundary to

Bt1 30-65 cm; reddish brown (2.5YR 4/6, dry) to dull reddish brown (2.5YR 4/4, moist) slightly gravelly clay; weak medium to coarse prismatic, breaking into moderate to strong very fine (sub-)angular blocky; hard when dry; continuous moderately thick dull reddish brown (2.5YR 4/4, dry; 2.5YR 4/3, moist) clay-iron cutans on all pedfaces; common very fine and fine pores; very few slightly weathered angular and rounded dolomitic limestone gravel; slightly calcareous; common fine and medium and few coarse roots; pH 6.8; clear and wavy boundary to

Bt2 65-125 cm; orange (5YR 6/8, dry) to bright reddish brown (5YR 5/8, moist) slightly gravelly and stony sandy loam; moderate fine to medium subangular blocky; very hard when dry; broken moderately thick dull reddish brown (2.5YR 4/4, dry and moist) clay-iron cutans on most of the pedfaces; few very fine and medium pores; very slightly weathered (sub-)angular and knobby dolomitic limestone gravel and stones; calcareous; few medium roots; pH 7.4; clear and irregular boundary to

R 125 cm +; hard coherent dolomitic limestone with secondary calcium carbonate precipitations on the boundary between B and R

ANALYSES PROFILE E 80

Horizon	Depth of sample (cm)	TEXTURE (µm in weight %) Sand 2000–1000	1000–500	500–250	250–100	100–50	Silt 50–2	Clay <2	pH H_2O	pH $CaCl_2$	Org. C %	% CO_2 Soil	% CO_2 Clay
Ah	5- 15	0.3	0.4	0.7	3.0	0.8	24.0	70.5	6.9	6.7	7.2	1.3	0.5
AB	20- 30	0.5	0.1	0.5	3.0	0.9	13.0	82.0	6.9	6.6	2.6	0.5	0.6
Bt1	35- 55	0.1	0.1	0.4	1.0	0.4	6.5	91.5	6.8	6.4	1.3	0.6	0.7
Bt2	80-100	0.5	0.3	2.0	53.5	7.0	27.0	9.5	7.4	7.1	0.6	34.5	0.6

ELEMENTAL COMPOSITION OF THE FINE EARTH FRACTION (weight %)

Horizon	Depth of sample (cm)	SiO_2	Al_2O_3	Fe_2O_3	FeO	MnO	MgO	CaO	Na_2O	K_2O	TiO_2	P_2O_5	H_2O	"Free" Fe_2O_3
Ah	5- 15	49.4	24.5	6.8	1.4	0.2	1.5	2.6	0.4	2.2	0.8	0.1	8.8	4.3
AB	20- 30	48.2	28.0	7.8	0.7	0.2	1.1	1.0	0.4	2.1	0.8	0.1	9.2	4.7
Bt1	35- 55	45.6	29.9	8.5	0.4	0.2	1.0	0.8	0.2	1.8	0.8	0.1	10.2	4.9
Bt2	80-100	19.3	3.4	2.9	0.1	0.1	14.7	23.5	0.1	0.5	0.2	tr	0.9	1.7

ELEMENTAL COMPOSITION OF THE CLAY FRACTION (weight %)

Horizon	Depth of sample (cm)	SiO_2	Al_2O_3	Fe_2O_3	FeO	MnO	MgO	CaO	Na_2O	K_2O	TiO_2	P_2O_5	H_2O	"Free" Fe_2O_3
Ah	5- 15	43.8	29.4	8.8	0.2	0.1	1.0	0.4	0.1	1.5	0.8	0.2	13.3	5.7
AB	20- 30	43.7	30.3	8.8	0.2	0.2	1.0	0.1	0.1	1.5	0.8	0.2	12.6	5.6
Bt1	35- 55	44.5	30.4	8.9	0.2	0.1	1.0	0.1	0.1	1.4	0.7	0.2	11.7	5.5
Bt2	80-100	45.2	29.2	8.9	0.2	0.1	1.2	0.3	0.1	1.5	0.7	0.2	11.8	5.5

MOLAR RATIOS

Horizon	Depth of sample (cm)	SOIL $\frac{SiO_2}{R_2O_3}$	SOIL $\frac{SiO_2}{Al_2O_3}$	SOIL $\frac{SiO_2}{Fe_2O_3}$	SOIL $\frac{Al_2O_3}{Fe_2O_3}$	CLAY $\frac{SiO_2}{R_2O_3}$	CLAY $\frac{SiO_2}{Al_2O_3}$	CLAY $\frac{SiO_2}{Fe_2O_3}$	CLAY $\frac{Al_2O_3}{Fe_2O_3}$
Ah	5- 15	2.9	3.4	19.2	5.6	2.1	2.5	13.3	5.3
AB	20- 30	2.5	2.9	16.4	5.6	2.1	2.4	13.2	5.4
Bt1	35- 55	2.2	2.6	14.2	5.5	2.1	2.5	13.3	5.4
Bt2	80-100	6.3	9.7	17.8	1.8	2.2	2.6	13.5	5.2

ANALYSES SAMPLES Sp/30, Sp/68, Sp/117 and Sp/227

Sp/ 30: weathering dolomite near profile Sp/183, related to water sampling point Sp/31.

Sp/ 68: hard limestone and soil in fissure of the limestone in a quarry near Pastena.
Sp/68a: hard limestone; Sp/68b: non-carbonate residue of the limestone;
Sp/68c: soil in fissure of the limestone

Sp/117: soil sample in karst basin "La Fossa" of limestone-derived colluvium with admixture of volcanic material, related to water sampling point Sp/116.

Sp/227: samples of weathering limestone and related soil at "Il Vallangero" of water sampling point Sp/189. These samples may be regarded as the lower part of profile Sp/122.
Sp/227a: soil sample; Sp/227b: sample of weathering limestone

Sample nr.	TEXTURE (µm in weight %) Sand 2000–1000	1000–500	500–250	250–100	100–50	Silt 50–2	Clay <2	pH H_2O	pH $CaCl_2$	Org. C %	"Free" Fe_2O_3 Soil	"Free" Fe_2O_3 Clay
Sp/ 30	1.0	4.0	29.5	36.5	10.0	15.5	3.0	8.6	7.6	-		
Sp/ 68a										0.0[5]	0.1	
Sp/ 68b			3.5			28.5	68.0			6.1[1]	4.6	4.4
Sp/ 68c			2.5			14.5	83.0	7.0	6.3	0.9	5.9	6.0
Sp/117	0.3	0.6	1.0	3.5	2.0	39.5	53.0	6.6	5.6	0.6		
Sp/227a			0.1			2.0	98.0	6.2	5.8	1.0		
Sp/227b	7.5	4.5	6.5	10.5	5.0	38.5	27.5	7.7	7.2	0.6		

ELEMENTAL COMPOSITION OF THE FINE EARTH FRACTION AND ROCK (weight %)

Sample nr.	SiO_2	Al_2O_3	Fe_2O_3	FeO	MnO	MgO	CaO	Na_2O	K_2O	TiO_2	P_2O_5	H_2O	CO_2	S
Sp/ 30	1.6	0.9	0.2	tr	tr	20.1	29.3	0.3	0.1	0.1	0.2	1.2	46.1	
Sp/ 68a	0.5	0.2	0.1	tr	tr	9.5	44.0	tr	0.1	tr	tr	45.5[2]	46.8	
Sp/ 68b	43.4	19.0	8.6	1.4	0.1	3.4	2.2	0.3	4.8	0.9	0.4	15.3[2]	2.2	1.5
Sp/ 68c	45.6	27.6	8.6	0.4	0.2	2.0	1.0	0.2	2.7	0.8	0.2	10.7	-	
Sp/117	51.4	24.1	10.2	0.3	0.3	1.0	0.5	0.3	2.3	1.0	0.3	8.3	-	
Sp/227a	41.8	30.5	10.1	0.5	0.2	1.3	0.6	tr	1.5	0.7	0.4	12.4	-	
Sp/227b	12.1	8.8	2.8	0.1	0.1	0.8	38.4	tr	0.5	0.7	tr	3.6	32.1	

ELEMENTAL COMPOSITION OF THE CLAY FRACTION (weight %)

Sample nr.	SiO_2	Al_2O_3	Fe_2O_3	FeO	MnO	MgO	CaO	Na_2O	K_2O	TiO_2	P_2O_5	H_2O	CO_2	S
Sp/ 30	47.2	25.1	10.8	0.6	0.1	2.8	0.1	tr	2.6	0.6	0.1	9.9	-	
Sp/ 68b	46.3	25.4	6.1	1.1	0.1	3.1	tr	0.1	5.6	0.6	0.4	9.9	-	1.2
Sp/ 68c	44.1	31.2	8.1	0.4	0.1	1.9	0.1	tr	2.0	0.3	-	11.9	-	
Sp/117	41.5	28.9	12.2	0.4	0.2	1.2	tr	0.2	1.9	1.2	0.3	12.1	-	
Sp/227a	42.0	30.6	9.7	0.4	0.1	1.4	tr	0.1	1.7	0.6	0.2	13.2	-	
Sp/227b	41.3	30.2	10.7	0.6	0.1	1.5	0.1	tr	1.7	0.7	0.2	12.8	0.1	

MOLAR RATIOS

Sample nr.	SOIL $\frac{SiO_2}{R_2O_3}$	$\frac{SiO_2}{Al_2O_3}$	$\frac{SiO_2}{Fe_2O_3}$	$\frac{Al_2O_3}{Fe_2O_3}$	CLAY $\frac{SiO_2}{R_2O_3}$	$\frac{SiO_2}{Al_2O_3}$	$\frac{SiO_2}{Fe_2O_3}$	$\frac{Al_2O_3}{Fe_2O_3}$
Sp/ 30	2.6	3.0	20.5	6.9	2.5	3.2	11.7	3.6
Sp/ 68a	3.0	3.9	13.4	3.5				
Sp/ 68b	3.0	3.9	13.4	3.5	2.7	3.1	20.2	6.6
Sp/ 68c	2.3	2.8	14.1	5.0	2.1	2.4	14.5	6.0
Sp/117	2.9	3.6	13.4	3.7	1.9	2.4	9.0	3.7
Sp/227a	1.9	2.3	11.0	4.7	1.9	2.3	11.6	5.0
Sp/227b	1.9	2.3	11.5	5.0	1.9	2.3	10.2	4.4

BULK DENSITY

Sp/68a 2.77 g/cm^3
Sp/68d 2.78 "
Sp/68e 2.68 "

APPENDIX 3 ANALYTICAL METHODS

The analyses were carried out according the prescriptions given by the "Methods of soil and rock analyses" of the Laboratory of Physical Geography and Soil Science (1971). The essences of the methods are described below.

3.1 Soil and rock samples.

- GRANULOMETRIC ANALYSIS: the fine earth fraction was pretreated wit H_2O_2 in order to remove organic compounds. Salts were removed by filtering the suspension through suction. The silt and clay fractions were obtained by wet-sieving of the suspended fine earth. Peptization was carried out by Na-pyrophosphate (3 mmol/l) before wet-sieving. The fractions <2 µm and 2-50 µm were obtained by pipetting method. The fraction >50 µm were obtained by dry-sieving.
- ORGANIC MATTER: organic matter was oxidized in the air-dry state by $K_2Cr_2O_7$ in H_2SO_4 96 % under steady heating up to 175° C for 90 seconds. The colour intensity of the formed chromo-ions was measured colorimetrically.
- pH: pH has been measured potentiometrically in a 25 ml aqua dest. c.q. 0.01 M $CaCl_2$ - extract of 10 g fine earth
- "FREE IRON": free iron content was determined according the method of Jackson in a Na-citate/Na-bicarbonate/Na-dithionate extract of 1 g fine earth c.q. 0.2 g clay. Iron content in the extract was estimated colorimetrically.
- CO_2 CONTENT: CO_2 content was estimated after destruction of the carbonate by 4 M HCl in a weighed apparatus, which is open to the air. Determination by loss of weight was carried out after the reaction had ceased.
- SEPARATION OF THE CLAY FRACTION FOR ELEMENTAL ANALYSES: the clay fraction <2 µm of the fine earth fraction was separated after oxidation of organic matter with H_2O_2 and peptization with 4 M NaOH (to pH=8). The clay-separate was saturated with Li c.q. Ba with a 2 M LiCl (pH=7) c.q 2 M $BaCl_2$ (pH=7) solution. Li-saturated clays were used for colorimetrical analyses, Ba-saturated clays for analyses with an argon plasma spectrometer ("Spectraspan"). The Li- and Ba-saturated samples were dialyzed against distilled water until completely free of Cl-ions and recovered by freeze-drying.
- ELEMENTAL ANALYSES OF THE ROCK, FINE EARTH AND CLAY FRACTION: total Al, Fe, Mn, Ca, Mg, Na, K, Ti, P (and occasionally S) were estimated after destruction of the sample with HF and H_2SO_4. Total Al was estimated with pyrocatachol violet; total Fe colorimetrically with orthophenanthroline; total Mn colorimetrically with formaldoxim; total Ca colorimetrically with glyoxal bis (2-hydroxyanil); total Mg colorimetrically with titan yellow; total Ti colorimetrically with tiron; total P colorimetrically as phosphorus-molybdenum complex; total Na and K were estimated by flame photometry; total Li in the Li-saturated clay fraction was measured by flame-photometry; total S was estimated turbidimetrically as $BaSO_4$ stabilized by "Tween 8C". For Fe (II) and Fe (III) analyses, the rock, fine earth or clay sample was destructed with HF and H_2SO_4 for exactly 10 minutes on a hot place already heated for half an hour at 180 °C. After transferring the obtained solution into a mixture of saturated boric acid and 4 M HCl and gently boiling for 2 minutes Fe (II) was determined colorimetrically after cooling and filtration of the sample. Total iron was measured afterwards in the same solution upon adding a solid reductant (hydroquinone).
  Loss on ignition was determined by heating an absolute dry rock, fine earth or clay sample for 3 hours at 950 °C. Total Si was calculated by substraction the total amount of determined oxides from 100.

  A number of elemental analyses were carried out on an Argon Plasma Spectrometer, equipped with a Multi-Channel Readout Module. For this, the sample (fine earth fraction or Ba-saturated clay) was dissolved at room temperature in a mixture of aqua regia and HF (50 %) in a closed polyethylene bottle. To bind free fluoride, present after the dissolution of the sample, an excess of boric

acid is added; finally $LiNO_3$ is added to serve as matrix and as stabilizer of the flame temperature. The "Spectraspan" analyses covered the determinations of total Si, Al, Mn, Mg, Ca, Na, Ti, P and Ba, the latter in the case of clay samples.

- X-RAY DIFFRACTION ANALYSES: X-ray diffraction analyses on disorientated clay samples were carried out by means of a quadruple Guinier-de Wolff camera using Co-K^{α} radiation. Diffractograms were obtained with a Philips vertical diffractometer with Cu-K^{α} radiation, using well orientated clay samples. Diffractograms were made of clay samples saturated with Mg, Mg-ethylene glycol, heated to 300° and to 550° C. The diffractograms were used to calculate the intensity percentages of the clay minerals. Guinier films were interpreted semi-quantitatively and the results are expressed in the form of + (for clay minerals) or x (for non-clay minerals). Their number indicates the relative importance of the reflections, with a maximum indication of +++++.
- BULK DENSITY: the bulk density of the limestone was determined according to the parafine method (SCHLICHTING & BLUME, 1966). A rock sample was weighed, coated with melted parafine (melting point approx. 45° C) and weighed again in order to determine the amount of parafine. Afterwards it was weighed in water of known temperature and the volume of the rock sample, after correction for the parafine, was calculated.
- POROSITY OF THE SOIL: the porosity of the soil was calculated from the bulk density of undisturbed soil aggregates and finely ground soil material (SCHEFFER & SCHACHTSCHABEL, 1976). To determine the bulk density of the soil aggregates, the same method was followed as described above, with a slight modification. Instead of melted parafine, nearly congealed parafine was used as it appeared that in this way the parafine did not pierce into the sample. By using the viscose parafine method a thick layer was formed around the soil aggregate and therefore the volume of the parafine was determined as well, using the bulk density and weight of the parafine around the clod. The bulk density of the finely ground soil material was determined in a picnometer.

3.2 Water samples.

3.2.1 Field determinations.

In the field the pH and the alkalinity of the water samples were determined immediately after sampling. The pH was measured potentiometrically and alkalinity was estimated by titration with 0.01 M H_2SO_4 to pH 4.5. A part of the sample, after filtering by pressure filtration through an 0.45 µm Millipore filter, was acidified with concentrated HNO_3 to pH 2-3. This part of the sample was used to estimate Na, K, Ca, Mg, total Fe, total Al and aqueous silica. NH_4, Cl, NO_3 + NO_2 and SO_4 were determined in the non-acidified part of the sample.

3.2.2 Laboratory determinations.

In the laboratory the cat- and anions and aqueous silica mentioned above were estimated colorimetrically, turbidimetrically and by using flame-photometry. The colorimetrical analyses covered the determination of Ca (with glyoxal bis (2-hydroxyanil)), Mg (with titan yellow), total Fe (with orthophenantroline), total Al (with pyrocatacholviolet), H_4SiO_4 (as the blue coloured β-silico-molybdenic acid, after adding ammonium molybdate and a reductant (Na_2SO_3 + metol + $K_2S_2O_5$) in a medium of sulphuric acid and tartaric acid), NH_4 (indophenol-blue method) and NO_3 + NO_2 (as NO_2-sulphanilic acid complex). Na and K were estimated by flame-photometry, using $Al(NO_3)_3$ to prevent interference of calcium. Cl was determined by titration with 0.02 M $Hg(NO_3)_2$, using diphenyl-carbazone and bromphenol blue in ethanol as mixed indicator. The turbidimetrical determinations covered the estimation of SO_4 (as $BaSO_4$ stabilized by "Tween 80").

3.3 Miscellaneous analyses.

The non-carbonate part (insoluble residue) of the limestone was obtained by dissolving ground limestone, which has been passed through a 2 mm sieve, in water, to which approx. 10 % HCl was added by means of a dropping bottle. The solution was buffered by an excess of ammonium acetate and care was taken that the pH did not drop below 5.5, in order to prevent dissolution of the non-carbonate minerals. Moreover, the dissolution process was carried out as rapidly as possible to avoid neoformation of minerals. The residue was dialyzed against distilled water until it was free of Cl-ions and recovered by freeze-drying.

During the dissolution of the non-carbonate residue of the limestone in aqua regia and HF for elemental analyses, a part appeared to be "insoluble". This residue was separated from the dissolved sample, washed five times in distilled water and freeze-dried. Because this sample contains a relatively high amount of organic C and because of the dark brown colour of this residue, it was thought that this residue consists of organic substances incorporated in the limestone rock.

Determinations on the nature of this material were carried out by mass spectrometric methods at the Laboratory for Organic Chemistry of the University of Amsterdam. The measurements were performed on a Varian MAT 711 double focussing mass spectrometer equipped with a combined EI/FI/FD source. Samples were introduced into the ion source (200° C) via a direct insertion probe (0-300° C). Electron impact ionization (EI) showed that the sample contains, besides traces of HCl and phtalates (softeners, used in plastics, therefore probably drawn from the plastic beakers used during the dissolution process), alkanes (saturated C-H compounds). Field ionization (FI) probes showed molecular weights of these compounds between 250 and 500, corresponding with (assuming a non-branching structure) $C_{18}H_{38}$ to $C_{36}H_{74}$. As alkanes with a molecular formula of $C_{18}H_{38}$ and higher are solid at room temperature (WEAST, 1975) and because of the sudden appearance of these compounds in the FI-diagram at 250, it is very well possible that initially als alkanes with a lower molecular formula than $C_{18}H_{38}$ are present in the limestone, but that these are removed during the dissolution process.

APPENDIX 4 WEATHERING PATHWAY DESCRIPTIONS AND GIBBS FREE ENERGIES OF THE SPECIES INVOLVED IN KCAL/MOL.

Weathering model I: $P_{CO_2} = 10^{-3.52}$ bar.

(In)variant point	pH	Chemical reaction
	5.68	Congruent dissolution of the limestone rock.
		$\{Ca_{365}Mg_{110}(CO_3)_{475} + Mg_{0.25}K_{0.6}Al_{2.3}Si_{3.5}O_{10}(OH)_2\} +$ $(485-b-d-i)H_2O + (483-b-d-e-2f-3g-4h-i)CO_2(g) \longrightarrow$ $(365-a-b)Ca^{2+} + aCaHCO_3^+ + bCaCO_3^o + (110.25-c-d)Mg^{2+} + cMgHCO_3^+ +$ $dMgCO_3^o + 0.6K^+ + (2.3-e-f-g-h)Al^{3+} + eAlOH^{2+} + fAl(OH)_2^+ +$ $gAl(OH)_3^o + hAl(OH)_4^- + 3.5H_4SiO_4^o + (958-a-2b-c-2d-e-2f-3g-4h-2i)$ $HCO_3^- + iCO_3^{2-}$
A	8.06	Incongruent dissolution of the limestone rock; formation of Mg-chlorite (clinochlore).
		$2\{Ca_{365}Mg_{110}(CO_3)_{475} + Mg_{0.25}K_{0.6}Al_{2.3}Si_{3.5}O_{10}(OH)_2\} +$ $(947-b-d-e)H_2O + (929.2-b-d-e)CO_2(g) \longrightarrow$ $2.3Mg_5Al_2Si_3O_{10}(OH)_8(s) + (730-a-b)Ca^{2+} + aCaHCO_3^+ + bCaCO_3^o +$ $(209-c-d)Mg^{2+} + cMgHCO_3^+ + dMgCO_3^o + 1.2K^+ + 0.1H_4SiO_4^o +$ $(1879.2-a-2b-c-2d-2e)HCO_3^- + eCO_3^{2-}$
B	8.18	Incongruent dissolution of the limestone rock; formation of Mg-chlorite (clinochlore); residual enrichment of dolomite.
		$2\{Ca_{365}Mg_{110}(CO_3)_{475} + Mg_{0.25}K_{0.6}Al_{2.3}Si_{3.5}O_{10}(OH)_2\} +$ $(529-b-c)H_2O + (511.2-b-c)CO_2(g) \longrightarrow$ $2.3Mg_5Al_2Si_3O_{10}(OH)_8(s) + 209CaMg(CO_3)_2(s) + (521-a-b)Ca^{2+} +$ $aCaHCO_3^+ + bCaCO_3^o + 1.2K^+ + 0.1H_4SiO_4^o + (1043.2-a-2b-2c)HCO_3^- +$ cCO_3^{2-}
C	8.35	Equilibrium between the limestone rock and the solution.

Weathering model I': variant calculation, assuming partial equilibrium between the solution and dolomite, starting in variant point B of weathering model I. $P_{CO_2} = 10^{-3.52}$ bar.

(In)variant point	pH	Chemical reaction
B	8.18	Incongruent dissolution of the limestone rock; formation of Mg-chlorite (clinochlore) and dolomite.
		$2\{Ca_{365}Mg_{110}(CO_3)_{475} + Mg_{0.25}K_{0.6}Al_{2.3}Si_{3.5}O_{10}(OH)_2\} + aMg^{2+} +$ $(529-2a-c-d)H_2O + (511.2-2a-c-d)CO_2(g) \longrightarrow$ $2.3Mg_5Al_2Si_3O_{10}(OH)_8(s) + (209+a)CaMg(CO_3)_2(s) + (521-a-b-c)$ $Ca^{2+} + bCaHCO_3^+ + cCaCO_3^o + 1.2K^+ + 0.1H_4SiO_4^o + dCO_3^{2-} +$ $(1043.2-4a-b-2c-2d)HCO_3$

Note: coefficient a must be determined by "trial and error".

Weathering model I' (continued)

(In)variant point	pH	Chemical reaction
C'	8.33	Incongruent dissolution of the limestone rock; formation of Mg-chlorite (clinochlore), dolomite and calcite.
		$2\{Ca_{365}Mg_{110}(CO_3)_{475} + Mg_{0.25}K_{0.6}Al_{2.3}Si_{3.5}O_{10}(OH)_2\} + (8-a-b)H_2O \rightarrow$
		$2.3Mg_5Al_2Si_3O_{10}(OH)_8(s) + 209CaMg(CO_3)_2(s) + 521CaCO_3(s) + 1.2K^+ + (0.1-a)H_4SiO_4^o + aH_3SiO_4^- + bCO_3^{2-} + (1.2-a-2b)HCO_3^- + (9.8+a+b)CO_2(g)$
D	9.61	Incongruent dissolution of the limestone rock; formation of Mg-chlorite (clinochlore), dolomite, calcite and amorphous silica.
		$2\{Ca_{365}Mg_{110}(CO_3)_{475} + Mg_{0.25}K_{0.6}Al_{2.3}Si_{3.5}O_{10}(OH)_2\} + (6-a)H_2O \rightarrow$
		$2.3Mg_5Al_2Si_3O_{10}(OH)_8(s) + 209CaMg(CO_3)_2(s) + 521CaCO_3(s) + 0.1SiO_2(a) + 1.2K^+ + aCO_3^{2-} + (1.2-2a)HCO_3^- + (9.8+2a)CO_2(g)$
	10.50	End of calculation; ionic strength >0.5 M.

Weathering model II: $P_{CO_2} = 10^{-2.80}$ bar.

(In)variant point	pH	Chemical reaction
	5.32	Congruent dissolution of the limestone rock.
		$\{Ca_{365}Mg_{110}(CO_3)_{475} + Mg_{0.25}K_{0.6}Al_{2.3}Si_{3.5}O_{10}(OH)_2\} + (485-b-d-i)H_2O + (483-b-d-e-2f-3g-4h-i)CO_2(g) \rightarrow$
		$(365-a-b)Ca^{2+} + aCaHCO_3^+ + bCaCO_3^o + (110.25-c-d)Mg^{2+} + cMgHCO_3^+ + dMgCO_3^o + 0.6K^+ + (2.3-e-f-g-h)Al^{3+} + eAlOH^{2+} + fAl(OH)_2^+ + gAl(OH)_3^o + hAl(OH)_4^- + 3.5H_4SiO_4^o + (958-a-2b-c-2d-e-2f-3g-4h-2i)HCO_3^- + iCO_3^{2-}$
F	7.70	Incongruent dissolution of the limestone rock; formation of Mg-chlorite (clinochlore).
		$2\{Ca_{365}Mg_{110}(CO_3)_{475} + Mg_{0.25}K_{0.6}Al_{2.3}Si_{3.5}O_{10}(OH)_2\} + (947-b-d-e)H_2O + (929.2-b-d-e)CO_2(g) \rightarrow$
		$2.3Mg_5Al_2Si_3O_{10}(OH)_8(s) + (730-a-b)Ca^{2+} + aCaHCO_3^+ + bCaCO_3^o + (209-c-d)Mg^{2+} + cMgHCO_3^+ + d\,MgCO_3^o + 1.2K^+ + 0.1H_4SiO_4^o + (1879.2-a-2b-c-2d-2e)HCO_3^- + eCO_3^{2-}$

Weathering model II (continued)

(In)variant point	pH	Chemical reaction
G	7.71	Incongruent dissolution of the limestone rock; formation of Mg-chlorite (clinochlore); residual enrichment of dolomite.

$$2\{Ca_{365}Mg_{110}(CO_3)_{475} + Mg_{0.25}K_{0.6}Al_{2.3}Si_{3.5}O_{10}(OH)_2\} + (529\text{-}b\text{-}c)H_2O + (511.2\text{-}b\text{-}c)CO_2(g) \rightarrow 2.3Mg_5Al_2Si_3O_{10}(OH)_8(s) + 209CaMg(CO)_3(s) + (521\text{-}a\text{-}b)Ca^{2+} + aCaHCO_3^+ + bCaCO_3^o + 1.2K^+ + 0.1H_4SiO_4^o + (1043.2\text{-}a\text{-}2b\text{-}2c)HCO_3^- + cCO_3^{2-}$$

H	7.88	Equilibrium between the limestone rock and the solution.

Weathering model III: $P_{CO_2} = 10^{-2.00}$ bar.

(In)variant point	pH	Chemical reaction
	4.92	Congruent dissolution of the limestone rock.

$$\{Ca_{365}Mg_{110}(CO_3)_{475} + Mg_{0.25}K_{0.6}Al_{2.3}Si_{3.5}O_{10}(OH)_2\} + (485\text{-}b\text{-}d\text{-}i)H_2O + (483\text{-}b\text{-}d\text{-}e\text{-}2f\text{-}3g\text{-}4h\text{-}i)CO_2(g) \rightarrow (365\text{-}a\text{-}b)Ca^{2+} + aCaHCO_3^+ + bCaCO_3^o + (110.25\text{-}c\text{-}d)Mg^{2+} + cMgHCO_3^+ + dMgCO_3^o + 0.6K^+ + (2.3\text{-}e\text{-}f\text{-}g\text{-}h)Al^{3+} + eAlOH^{2+} + fAl(OH)_2^+ + gAl(OH)_3^o + hAl(OH)_4^- + 3.5H_4SiO_4^o + (958\text{-}a\text{-}2b\text{-}c\text{-}2d\text{-}e\text{-}2f\text{-}3g\text{-}4h\text{-}2i)HCO_3^- + iCO_3^{2-}$$

K	6.89	Incongruent dissolution of the limestone rock; formation of gibbsite.

$$\{Ca_{365}Mg_{110}(CO_3)_{475} + Mg_{0.25}K_{0.6}Al_{2.3}Si_{3.5}O_{10}(OH)_2\} + (485\text{-}b\text{-}d\text{-}e)H_2O + (476.1\text{-}b\text{-}d\text{-}e)CO_2(g) \rightarrow 2.3Al(OH)_3(s) + (365\text{-}a\text{-}b)Ca^{2+} + aCaHCO_3^+ + bCaCO_3^o + (110.25\text{-}c\text{-}d)Mg^{2+} + cMgHCO_3^+ + dMgCO_3^o + 0.6K^+ + 3.5H_4SiO_4^o + eCO_3^{2-} + (951.1\text{-}a\text{-}2b\text{-}c\text{-}2d\text{-}2e)HCO_3^-$$

L	7.18	Incongruent dissolution of the limestone rock; formation of gibbsite; residual enrichment of dolomite.

$$\{Ca_{365}Mg_{110}(CO_3)_{475} + Mg_{0.25}K_{0.6}Al_{2.3}Si_{3.5}O_{10}(OH)_2\} + (276\text{-}b\text{-}d\text{-}e)H_2O + (267.1\text{-}b\text{-}d\text{-}e)CO_2(g) \rightarrow 2.3Al(OH)_3(s) + 104.5CaMg(CO_3)_2(s) + (260.5\text{-}a\text{-}b)Ca^{2+} + aCaHCO_3^+ + bCaCO_3^o + (5.75\text{-}c\text{-}d)Mg^{2+} + cMgHCO_3^+ + dMgCO_3^o + 0.6K^+ + 3.5H_4SiO_4^o + (533.1\text{-}a\text{-}2b\text{-}c\text{-}2d\text{-}2e)HCO_3^- + eCO_3^{2-}$$

Weathering model III (continued)

(In)variant point	pH	Chemical reaction
M	7.22	Incongruent dissolution of the limestone rock; transformation of gibbsite; formation of kaolinite; residual enrichment of dolomite.

$$2\{Ca_{365}Mg_{110}(CO_3)_{475} + Mg_{0.25}K_{0.6}Al_{2.33}Si_{3.5}O_{10}(OH)_2\} + 2.4Al(OH)_3(s) + (534.5-b-d-e)H_2O + (534.2-b-d-e)CO_2(g) \rightarrow 3.5Al_2Si_2O_5(OH)_4(s) + 209CaMg(CO_3)_2(s) + (521-a-b)Ca^{2+} + aCaHCO_3^+ + bCaCO_3^o + (11.5-c-d)Mg^{2+} + cMgHCO_3^+ + dMgCO_3^o + 1.2K^+ + (1066.2-a-2b-c-2d-2e)HCO_3^- + eCO_3^{2-}$$

N	7.34	Equilibrium between the limestone rock and the solution.

Weathering model IV: $P_{CO_2} = 10^{-1.30}$ bar.

(In)variant point	pH	Chemical reaction
	4.57	Congruent dissolution of the limestone rock.

$$\{Ca_{365}Mg_{110}(CO_3)_{475} + Mg_{0.25}K_{0.6}Al_{2.3}Si_{3.5}O_{10}(OH)_2\} + (485-b-d-i)H_2O + (483-b-d-e-2f-3g-4h-i)CO_2(g) \rightarrow (365-a-b)Ca^{2+} + aCaHCO_3^+ + bCaCO_3^o + (110.25-c-d)Mg^{2+} + cMgHCO_3^+ + dMgCO_3^o + 0.6K^+ + (2.3-e-f-g-h)Al^{3+} + eAlOH^{2+} + fAl(OH)_2^+ + gAL(OH)_3^o + hAl(OH)_4^- + 3.5H_4SiO_4^o + (958-a-2b-c-2d-e-2f-3g-4h-2i)HCO_3^- + iCO_3^{2-}$$

P	6.23	Incongruent dissolution of the limestone rock; formation of gibbsite.

$$\{Ca_{365}Mg_{110}(CO_3)_{475} + Mg_{0.25}K_{0.6}Al_{2.3}Si_{3.5}O_{10}(OH)_2\} + (485-b-d-e)H_2O + (476.1-b-d-e-)CO_2(g) \rightarrow 2.3Al(OH)_3(s) + (365-a-b)Ca^{2+} + aCaHCO_3^+ + bCaCO_3^o + (110.25-c-d)Mg^{2+} + cMgHCO_3^+ + dMgCO_3^o + 0.6K^+ + 3.5H_4SiO_4^o + eCO_3^{2-} + (951.1-a-2b-c-2d-2e)HCO_3^-$$

Q	6.54	Incongruent dissolution of the limestone rock; transformation of gibbsite; formation of kaolinite.

$$2\{Ca_{365}Mg_{110}(CO_3)_{475} + Mg_{0.25}K_{0.6}Al_{2.3}Si_{3.5}O_{10}(OH)_2\} + 2.4Al(OH)_3(s) + (952.5-b-d-e)H_2O + (952.2-b-d-e)CO_2(g) \rightarrow 3.5Al_2Si_2O_5(OH)_4(s) + (730-a-b)Ca^{2+} + aCaHCO_3^+ + bCaCO_3^o + (220.5-c-d)Mg^{2+} + cMgHCO_3^+ + dMgCO_3^o + 1.2K^+ + eCO_3^{2-} + (1902.2-a-2b-c-2d-2e)HCO_3^-$$

Weathering model IV (continued)

(In)variant point	pH	Chemical reaction
R	6.72	Incongruent dissolution of the limestone rock; transformation of gibbsite; formation of kaolinite; residual enrichment of dolomite.
		$2\{Ca_{365}Mg_{110}(CO_3)_{475} + Mg_{0.25}K_{0.6}Al_{2.3}Si_{3.5}O_{10}(OH)_2\} +$ $2.4Al(OH)_3(s) + (534.5-b-d-e)H_2O + (534.2-b-d-e)CO_2(g) \rightarrow$ $3.4Al_2Si_2O_5(OH)_4(s) + 209CaMg(CO_3)_2(s) + (521-a-b)Ca^{2+} +$ $aCaHCO_3^+ + bCaCO_3^o + (11.5-c-d)Mg^{2+} + cMgHCO_3^+ + dMgCO_3^o + 1.2K^+ +$ $(1066.2-a-2b-c-2d-2e)HCO_3^- + eCO_3^{2-}$
S	6.79	Incongruent dissolution of the limestone rock; formation of kaolinite; residual enrichment of dolomite.
		$2\{Ca_{365}Mg_{110}(CO_3)_{475} + Mg_{0.25}K_{0.6}Al_{2.3}Si_{3.5}O_{10}(OH)_2\} +$ $(540.5-b-d-e)H_2O + (534.2-b-d-e)CO_2(g) \rightarrow$ $2.3Al_2Si_2O_5(OH)_4(s) + 209CaMg(CO_3)_2(s) + (521-a-b)Ca^{2+} +$ $aCaHCO_3^+ + bCaCO_3^o + (11.5-c-d)Mg^{2+} + cMgHCO_3^+ + dMgCO_3^o + 1.2K^+ +$ $2.4H_4SiO_4^o + (1066.2-a-2b-c-2d-2e)HCO_3^- + eCO_3^{2-}$
T	6.89	Equilibrium between the limestone rock and the solution.

Weathering model V: $P_{CO_2} = 10^{-0.80}$ bar.

(In)variant point	pH	Chemical reaction
	4.32	Congruent dissolution of the limestone rock.
		$\{Ca_{365}Mg_{110}(CO_3)_{475} + Mg_{0.25}K_{0.6}Al_{2.3}Si_{3.5}O_{10}(OH)_2\} +$ $(485-b-d-i)H_2O + (483-b-d-e-2f-3g-4h-i)CO_2(g) \rightarrow$ $(365-a-b)Ca^{2+} + aCaHCO_3^+ + bCaCO_3^o + (110.25-c-d)Mg^{2+} + cMgHCO_3^+ +$ $dMgCO_3^o + 0.6K^+ + (2.3-e-f-g-h)Al^{3+} + eAlOH^{2+} + fAl(OH)_2^+ +$ $gAl(OH)_3^o + hAl(OH)_4^- + 3.5H_4SiO_4^o + (958-a-2b-c-2d-e-2f-3g-4h-2i)$ $HCO_3^- + iCO_3^{2-}$
V	5.85	Incongruent dissolution of the limestone rock; formation of gibbsite.
		$\{Ca_{365}Mg_{110}(CO_3)_{475} + Mg_{0.25}K_{0.6}Al_{2.3}Si_{3.5}O_{10}(OH)_2\} +$ $(485-b-d-e)H_2O + (476.1-b-d-e)CO_2(g) \rightarrow$ $2.3Al(OH)_3(s) + (365-a-b)Ca^{2+} + aCaHCO_3^+ + bCaCO_3^o + (110.25-c-d)$ $Mg^{2+} + cMgHCO_3^+ + dMgCO_3^o + 0.6K^+ + 3.5H_4SiO_4^o + eCO_3^{2-} +$ $(951.1-a-2b-c-2d-2e)HCO_3^-$

Weathering model V (continued)

(In)variant point	pH	Chemical reaction
W	6.05	Incongruent dissolution of the limestone rock; transformation of gibbsite; formation of kaolinite.

$$2\{Ca_{365}Mg_{110}(CO_3)_{475} + Mg_{0.25}K_{0.6}Al_{2.3}Si_{3.5}O_{10}(OH)_2\} + 2.4Al(OH)_3(s) + (952.5\text{-}b\text{-}d\text{-}e)H_2O + (952.2\text{-}b\text{-}d\text{-}e)CO_2(g) \rightarrow 3.5Al_2Si_2O_5(OH)_4(s) + (730\text{-}a\text{-}b)Ca^{2+} + aCaHCO_3^- + bCaCO_3^o + (220.5\text{-}c\text{-}d)Mg^{2+} + cMgHCO_3^+ + dMgCO_3^o + 1.2K^+ + eCO_3^{2-} + (1902.2\text{-}a\text{-}2b\text{-}c\text{-}2d\text{-}2e)HCO_3^-$$

X	6.28	Incongruent dissolution of the limestone rock; formation of kaolinite.

$$2\{Ca_{365}Mg_{110}(CO_3)_{475} + Mg_{0.25}K_{0.6}Al_{2.3}Si_{3.5}O_{10}(OH)_2\} + (958.5\text{-}b\text{-}d\text{-}e)H_2O + (952.2\text{-}b\text{-}d\text{-}e)CO_2(g) \rightarrow 2.3Al_2Si_2O_5(OH)_4(s) + (730\text{-}a\text{-}b)Ca^{2+} + aCaHCO_3^+ + bCaCO_3^o + (220.5\text{-}c\text{-}d)Mg^{2+} + cMgHCO_3^+ + dMgCO_3^o + 1.2K^+ + 2.4H_4SiO_4^o + (1902.2\text{-}a\text{-}2b\text{-}c\text{-}2d\text{-}2e)HCO_3^- + eCO_3^{2-}$$

Y	6.40	Incongruent dissolution of the limestone rock; formation of kaolinite; residual enrichment of dolomite.

$$2\{Ca_{365}Mg_{110}(CO_3)_{475} + Mg_{0.25}K_{0.6}Al_{2.3}Si_{3.5}O_{10}(OH)_2\} + (540.5\text{-}b\text{-}d\text{-}e)H_2O + (534.2\text{-}b\text{-}d\text{-}e)CO_2(g) \rightarrow 2.3Al_2Si_2O_5(OH)_4(s) + 209CaMg(CO_3)_2(s) + (521\text{-}a\text{-}b)Ca^{2+} + aCaHCO_3^+ + bCaCO_3^o + (11.5\text{-}c\text{-}d)Mg^{2+} + cMgHCO_3^+ + dMgCO_3^o + 1.2K^+ + 2.4H_4SiO_4^o + (1066.2\text{-}a\text{-}2b\text{-}c\text{-}2d\text{-}2e)HCO_3^- + eCO_3^{2-}$$

Z	6.56	Equilibrium between the limestone rock and the solution.

Equilibrium constants of various aqueous species.

Aqueous species	Reaction	Lg $K_{298.15^oK}$, 1 bar pressure
H_2O	$H_2O \rightleftarrows H^+ + OH^-$	- 14.00
$H_2CO_3^*$	$H_2CO_3^* \rightleftarrows CO_2(g) + H_2O$	1.47
$H_2CO_3^*$	$H_2CO_3^* \rightleftarrows H^+ + HCO_3^-$	- 6.37
HCO_3^-	$HCO_3^- \rightleftarrows H^+ + CO_3^{2-}$	- 10.33
$CaHCO_3^+$	$CaHCO_3^+ \rightleftarrows Ca^{2+} + HCO_3^-$	- 1.26
$CaCO_3^o$	$CaCO_3^o \rightleftarrows Ca^{2+} + CO_3^{2-}$	- 3.20
$MgHCO_3^+$	$MgHCO_3^+ \rightleftarrows Mg^{2+} + HCO_3^-$	- 1.16
$MgCO_3^o$	$MgCO_3^o \rightleftarrows Mg^{2+} + CO_3^{2-}$	- 3.40

$H_2CO_3^* = H_2CO_3^o + CO_2^o$

Equilibrium constants of various aqueous species (continued).

Aqueous species	Reaction	Lg $K_{298.15^{o}\ K}$, 1 bar pressure
$AlOH^{2+}$	$AlOH^{2+} + H^{+} \rightleftarrows Al^{3+} + H_2O$	4.75
$Al(OH)_2^{+}$	$Al(OH)_2^{+} + H^{+} \rightleftarrows AlOH^{2+} + H_2O$	5.02
$Al(OH)_3^{o}$	$Al(OH)_3^{o} + H^{+} \rightleftarrows Al(OH)_2^{+} + H_2O$	5.36
$Al(OH)_4^{-}$	$Al(OH)_4^{-} + H^{+} \rightleftarrows Al(OH)_3^{o} + H_2O$	8.14
$H_4SiO_4^{o}$	$H_4SiO_4^{o} \rightleftarrows H_3SiO_4^{-} + H^{+}$	- 9.93

Gibbs free energies of formation of various minerals and species used in the calculations of the theoretical weathering models.

Mg-chlorite (clinochlore)	$Mg_5Al_2Si_3O_{10}(OH)_8$	- 1974.0 kcal/mol	[1]
Mg-montmorillonite	$Mg_{0.167}Al_{2.33}Si_{3.67}O_{10}(OH)_2$	- 1275.3 "	[2]
Kaolinite	$Al_2Si_2O_5(OH)_4$	- 903.0 "	[2]
Gibbsite (cc)	$Al(OH)_3$	- 273.5 "	[2]
Illite	$Mg_{0.25}K_{0.6}Al_{2.3}Si_{3.5}O_{10}(OH)_2$	- 1301.0 "	[2]
Calcite	$CaCO_3$	- 269.9 "	[3]
Dolomite	$CaMg(CO_3)_2$	- 518.7 "	[3]
Magnesite	$MgCO_3$	- 246.1 "	[3]
Amorphous silica	SiO_2	- 203.0 "	[3]
H_2O		- 56.7 "	[3]
$CO_2(g)$		- 94.3 "	[3]
Ca^{2+}		- 132.2 "	[3]
Mg^{2+}		- 108.9 "	[3]
K^{+}		- 67.7 "	[3]
Al^{3+}		- 116.0 "	[3]
$H_4SiO_4^{o}$		- 312.6 "	[4]
H^{+}		0	

Sources: [1]Zen, 1972; [2]Helgeson, 1969; [3]Robie & Waldbaum, 1968; [4]Robie et al., 1978.

APPENDIX 5 COMPOSITION OF THE WATER SAMPLES AND CALCULATED ION ACTIVITIES.

Origin of water sample.

Sp/ 19 Spring at contact of the limestone and Pliocene conglomerates alongside road Madonna di Piana - Pastena.
Sp/ 21a E horizon ferric acrisol at Colle Arnaro.
Sp/ 21b Bt horizon ferric acrisol at Colle Arnaro.
Sp/ 21c Bgt horizon ferric acrisol at Colle Arnaro.
Sp/ 21d BC horizon ferric acrisol at Colle Arnaro.
Sp/ 31 Weathering dolomite near spring "Pisciarello" alongside road Madonna di Piana - San Giovanni Incarico.
Sp/ 32 Spring "Pisciarello" alongside road Madonna di Piana - San Giovanni Inc.
Sp/ 59 Entrance of the "Grotte di Pastena".
Sp/ 63 Pliocene conglomerates at the foot of Monte Solo near Pastena.
Sp/108 Spring south of San Giovanni Incarico alongside road to Pico.
Sp/116 Young, Holocene colluvial deposits derived from limestone at "La Fossa".
Sp/167 Miocene shales in clay-pit west of Pontecorvo.
Sp/168 Spring near San Oliva alongside road San Oliva - Pico.
Sp/169 Young, Holocene colluvial deposits derived from limestone near sampling point Sp/168.
Sp/170 Older, Pleistocene colluvial deposits derived from limestone at "La Fossa".
Sp/189 Weathering limestone at "Il Vallangero.
Sp/193 Exit of the "Grotte di Pastena.
Sp/233 Rain water sampled west of Pontecorvo.
Sp/238 Sea water sampled Sperlonga.

Date of sampling.

	July 1971	Aug. 1974	June 1975	Aug. 1975	14-2-1976	15-2-1976	16-2-1976	19-2-1976	21-2-1976	22-2-1976	24-2-1976	27-2-1976	28-2-1976	29-2-1976
Sp/ 19			a	b			c						d	
Sp/ 21a					a		b					c		d
Sp/ 21b								a	b					c
Sp/ 21c			a					b						c
Sp/ 21d								a						b
Sp/ 31			a					b			c		d	
Sp/ 32	a		b	c			d				e		f	
Sp/ 59	a					b				c			d	
Sp/ 63	x													
Sp/108		x												
Sp/116		a	b	c				d						e
Sp/167	a		b	c		d							e	
Sp/168		a	b	c		d							e	
Sp/169			a	b				c					d	
Sp/170								a				b		
Sp/189										a	b	c		d
Sp/193										a			b	
Sp/233						a		b						

Sp/238 was collected in the summer of 1976 by Mr. Wen Ting-Tiang.

APPENDIX 5.1 CHEMICAL COMPOSITION OF THE WATER SAMPLES IN MMOL/L.

Sample number	pH_f	pH_l	K^+	Na^+	NH_4^+	Ca^{2+}	Mg^{2+}	$Fe(II)_t$	Al_t	$H_4SiO_4^o$	NO_3^-	Cl^-	HCO_3^- fld	HCO_3^- lab	CO_3^{2-} fld	SO_4^{2-}	EC_{25^o} x 10^6
Sp/ 19a	6.98	7.44	0.041	0.625	0.001	3.273	0.269	-	0.0006	0.185	0.223	0.955	6.354	4.440	-	0.064	536
/ 19b	6.98	7.24	0.070	0.614		3.488	0.318	-	0.0012	0.187	0.304	1.169	6.590	4.850	-	0.067	586
/ 19c	7.23		0.021	0.280	0.002	1.667	0.292	0.0002	-	0.105	0.132	0.300	3.982		-	0.084	366
/ 19d	7.38		0.021	0.326	0.002	2.232	0.300	0.0018	0.0026	0.138	0.070	0.396	5.040		-	0.068	432
Sp/ 21aa	5.65		0.057	0.191	0.001	0.077	0.047	0.0043	0.0141	0.082	0.025	0.203	0.130		-	0.185	55
/ 21ab	6.23		0.059	0.166	0.001	0.056	0.033	0.0108	0.0267	0.075	0.039	0.117	0.300		-	0.232	43
/ 21ac	5.49		0.037	0.419	0.015	0.217	0.149	0.0019	0.0114	0.236	0.042	0.411	0.289		-	0.311	124
/ 21ad	5.62		0.022	0.359		0.173	0.136	0.0012	0.0065	0.219	0.029	0.409	0.236		-	0.285	109
Sp/ 21ba	6.40		0.024	0.310		0.095	0.082	0.0004	0.0016	0.155	0.019	0.379	0.209		-	0.149	73
/ 21bb	5.28		0.033	0.320		0.084	0.080	0.0121	0.0197	0.151	-	0.379	0.125		-	0.104	76
/ 21bc	5.82		0.037	0.320		0.085	0.061	-	-	0.155	-	0.366	0.183		-	0.077	72
Sp/ 21ca	5.97	7.32	0.016	0.299	0.004	0.133	0.062	-	0.0154	0.229	-	0.290	0.257	0.355	-	0.036	67
/ 21cb	5.89		0.017	0.321	-	0.178	0.082	0.0038	0.0070	0.193	0.009	0.379	0.302		-	0.077	81
/ 21cc	5.78		0.008	0.348	0.004	0.105	0.082	0.0005	-	0.214	0.008	0.398	0.283		-	0.077	80
Sp/ 21da	5.81		0.010	0.291	-	0.031	0.074	0.0010	0.0034	0.220	0.008	0.391	0.121		-	0.067	62
/ 21db	5.61		0.008	0.291		0.027	0.072	0.0018	0.0015	0.220	0.025	0.353	0.095		-	0.070	60
Sp/ 31a	7.18	8.44	0.015	0.253	-	2.817	1.305	-	0.0010	0.111	0.002	0.305	7.801	3.160	-	0.062	322
/ 31b	6.97		0.013	0.302	-	2.787	1.254	0.0019	0.0038	0.135	0.008	0.353	7.768		-	0.097	441
/ 31c	7.13		0.008	0.288	0.002	2.768	1.275	0.0013	0.0017	0.125	0.005	0.353	7.896		-	0.116	504
/ 31d	7.27		0.013	0.302	-	2.735	1.254	0.0006	0.0005	0.108	0.006	0.374	7.847		-	0.127	469
Sp/ 32a		8.39	0.023	0.391		1.016	1.364		-	0.181	0.020	0.490		3.310		0.052	755
/ 32b	7.09	7.57	0.016	0.321	0.002	2.968	1.493	-	-	0.171	-	0.364	8.499	6.310	-	0.044	582
/ 32c	7.19	7.51	0.009	0.302	-	3.005	1.531	-	0.0007	0.169	-	0.382	8.691	6.558	-	0.060	612
/ 32d	7.20		0.018	0.342	0.001	2.802	1.460	0.0001	0.0003	0.164	0.022	0.378	7.955		-	0.104	631
/ 32e	6.91		0.029	0.345	0.001	2.767	1.428	0.0002	-	0.172	0.023	0.374	8.544		-	0.076	645
/ 32f	7.11		0.023	0.337	0.001	2.793	1.491	0.0004	-	0.177	0.030	0.379	8.425		-	0.054	668
Sp/ 59a	7.85	7.20	0.018	0.348		0.909	0.198		0.0004	0.055	0.179	0.416		1.500		0.052	367
/ 59b	7.09		0.055	0.228	0.008	0.947	0.192	0.0025	0.0114	0.099	0.123	0.240	2.159		-	0.099	245
/ 59c	7.82		0.055	0.236	-	1.464	0.330	0.0023	0.0106	0.083	0.085	0.249	3.614		-	0.078	352
/ 59d	8.08		0.052	0.263	-	1.621	0.372	-	-	0.081	0.111	0.305	3.876		-	0.088	390
Sp/ 63		8.11	0.066	0.478		0.767	0.164		0.0002	0.045	-	0.336		1.780		0.193	237
Sp/108		6.91	0.013	0.315	0.008	1.707	0.188										

/116b	6.82	7.09	0.011	0.188	-	0.537	0.047	-	0.0017	0.160	-	0.154	1.093	1.130	-	0.034	130
/116c	6.58	7.39	0.021	0.237	-	0.896	0.077	-	0.0053	0.174	1.529	0.310	0.500	0.490	-	0.047	252
/116d	7.52		0.015	0.160	0.003	0.868	0.093	0.0023	0.0061	0.101	0.540	0.224	1.506		-	0.076	206
/116e	7.27		0.006	0.141	0.003	0.669	0.065	0.0032	0.0085	0.087	0.170	0.177	1.131		-	0.079	154
Sp/167a	9.0	7.98	0.194	5.089		0.580	0.868		0.0070	0.007	0.226	1.580		1.650		2.347	808
/167b	8.50	7.87	0.559	17.127	0.001	1.295	1.885	-	0.0026	0.010	0.089	6.703	2.822	2.700	0.056	7.146	2226
/167c	8.79	7.34	0.448	9.039		0.685	0.984	-	0.0015	0.022	0.033	3.527	1.196	1.155	0.095	4.355	1383
/167d	7.65		0.223	4.513	0.010	0.600	0.697	0.0018	0.0025	0.020	0.086	1.382	1.478		-	2.287	728
/167e	8.35		0.150	5.110	-	0.690	0.687	0.0004	0.0347	0.050	0.099	1.853	2.632		-	1.758	808
Sp/168a		7.13	0.013	0.133	0.001	1.009	0.327	0.0001	-	0.076	0.033	0.149		2.620	-	0.023	249
/168b	7.26	7.88	0.020	0.177	0.001	1.668	0.476	-	0.0006	0.076	0.021	0.229	4.125	4.120	-	-	382
/168c	7.72	7.75	0.033	0.163	-	1.423	0.611	-	0.0015	0.069	0.011	0.258	4.056	3.872	-	0.016	375
/168d	6.90		0.011	0.185	0.002	1.486	0.271	0.0005	0.0016	0.056	0.014	0.220	3.315		-	0.069	313
/168e	7.20		0.023	0.217	0.003	1.776	0.409	0.0014	0.0007	0.090	0.036	0.241	4.338		-	0.048	380
Sp/169a	7.49	7.80	0.020	0.233	-	2.469	0.559	-	0.0006	0.156	0.002	0.275	5.861	3.055	-	0.076	313
/169b	7.21	7.46	0.025	0.250	-	2.859	0.731	-	0.0015	0.192	-	0.263	6.379	3.770	-	0.284	409
/169c	7.12		0.017	0.212	0.001	2.927	0.675	0.0121	0.0001	0.190	0.810	0.171	4.759		-	0.928	585
/169d	7.12		0.015	0.223	-	2.444	0.580	0.0002	0.0002	0.149	0.127	0.175	5.072		-	0.475	399
Sp/170a	6.28		0.004	0.277	-	0.289	0.099	0.0006	0.0002	0.098	0.446	0.174	0.200		-	0.061	130
/170b	6.87		0.002	0.288	-	0.228	0.078	0.0010	0.0005	0.140	0.516	0.177	0.181		-	0.039	105
Sp/189a	7.14		0.008	0.250	0.002	0.925	0.057	0.0086	0.0121	0.158	-	0.327	1.650		-	0.116	208
/189b	7.48		0.008	0.223	0.001	0.741	0.039	0.0014	0.0024	0.174	-	0.318	1.442		-	0.061	170
/189c	7.68		0.006	0.212	-	0.681	0.027	0.0019	0.0053	0.148	-	0.317	1.331		-	0.054	160
/189d	7.70		0.006	0.196	0.001	0.665	0.029	0.0014	0.0006	0.125	-	0.313	1.237		-	0.024	156
Sp/193a	7.38		0.043	0.470	0.001	1.919	0.336	0.0004	0.0032	0.091	0.091	0.265	4.332		-	0.083	412
/193b	7.42		0.036	0.263	0.001	2.046	0.360	0.0003	0.0011	0.095	0.088	0.253	4.843		-	0.060	461
Sp/233a	7.32		0.004	0.078	0.021	0.100	0.056	-	-	0.001	0.006	0.077	0.226		-	0.036	
/233b	8.28		0.002	0.045	0.012	0.180	0.053	-	-	0.002	0.007	0.053	0.417		-	0.025	
Sp/238[1]		7.80	0.011	0.496	-	0.011	0.060	-		0.002[2]	-	0.573		2.728[2]		0.031	

[1]Concentrations are given in mol/l. [2]Concentrations in mmol/l.

APPENDIX 5.2 ION ACTIVITIES IN THE WATER SAMPLES, EXPRESSED AS NEGATIVE LOGARITHMS (pX = -lg X), CALCULATED ACCORDING THE PROGRAM SOLMNEQ (KHARAKA & BARNES, 1973), AT 15° C (288.15° K).

Sample number	pP_{CO_2}	pH	pNa	pK	pNH_4	pCa	pMg	pFe	pAl	pSi	pCl	pNO_3	pSO_4	pOH	$pHCO_3$	pCO_3
Sp/ 19a	1.47	6.98	3.25	4.43	6.05	2.68	3.75	-	10.59	3.73	3.07	3.70	4.48	7.37	2.25	5.70
/ 19b	1.46	6.98	3.26	4.20		2.66	3.68	-	10.29	3.73	2.98	3.57	4.47	7.37	2.24	5.69
/ 19c	1.91	7.23	3.59	4.71	5.74	2.94	3.68	6.86	-	3.98	3.56	3.92	4.29	7.12	2.44	5.64
/ 19d	1.97	7.38	3.53	4.72	5.74	2.83	3.68	5.92	11.02	3.86	3.44	4.20	4.41	6.97	2.35	5.39
Sp/ 21aa	1.89	5.65	3.73	4.26	6.02	4.18	4.39	5.44	6.51	4.09	3.71	4.62	3.80	8.70	4.00	8.78
/ 21ab	2.09	6.23	3.80	4.25	6.02	4.33	4.55	5.05	7.35	4.13	3.95	4.42	3.70	8.12	3.62	7.82
/ 21ac	1.32	5.49	3.40	4.45	4.85	3.76	3.92	5.83	6.32	3.63	3.41	4.40	3.61	8.86	3.59	8.53
/ 21ad	1.53	5.62	3.47	4.68		3.86	3.95	6.02	6.80	3.66	3.41	4.56	3.64	8.73	3.67	8.48
Sp/ 21ba	2.34	6.40	3.53	4.64		4.10	4.16	6.48	8.91	3.81	3.44	4.74	3.90	7.95	3.71	7.73
/ 21bb	1.56	5.28	3.51	4.50		4.14	4.16	4.99	5.72	3.82	3.44	-	4.05	9.07	4.04	9.19
/ 21bc	1.81	5.82	3.51	4.45		4.13	4.28	-		3.81	3.45	-	4.18	8.53	3.75	8.36
Sp/ 21ca	1.87	5.97	3.54	4.81	5.41	3.94	4.26	-	7.08	3.64	3.55	-	4.51	8.38	3.66	8.12
/ 21cb	1.69	5.89	3.51	4.79	-	3.82	4.15	5.49	7.27	3.71	3.44	5.06	4.19	8.46	3.56	8.09
/ 21cc	1.58	5.78	3.47	5.11	5.41	4.05	4.15	6.37	-	3.67	3.42	5.11	4.19	8.57	3.57	8.21
Sp/ 21da	2.00	5.81	3.55	5.01	-	4.57	4.19	6.06	7.42	3.66	3.42	5.11	4.23	8.54	3.96	8.57
/ 21db	1.90	5.61	3.55	5.11		4.63	4.20	5.80	7.40	3.66	3.47	4.62	4.21	8.74	4.05	8.87
Sp/ 31a	1.58	7.18	3.65	4.87	-	2.76	3.08	-	10.87	3.95	3.57	5.75	4.51	7.17	2.17	5.41
/ 31b	1.38	6.97	3.57	4.94	-	2.77	3.09	5.91	9.77	3.87	3.50	5.15	4.31	7.38	2.17	5.62
/ 31c	1.53	7.13	3.59	5.15	5.75	2.77	3.09	6.08	10.51	3.90	3.50	5.35	4.23	7.22	2.16	5.46
/ 31d	1.67	7.27	3.57	4.94	-	2.78	3.10	6.42	11.41	3.97	3.48	5.27	4.19	7.08	2.16	5.32
Sp/ 32a	3.17	8.39	3.45	4.68		3.16	3.03		-	3.76	3.35	4.74	4.51	5.96	2.54	4.57
/ 32b	1.46	7.09	3.54	4.85	5.75	2.75	3.02	-	-	3.77	3.49	-	4.67	7.26	2.13	5.47
/ 32c	1.55	7.19	3.57	5.10	-	2.74	3.02	-	11.05	3.77	3.47	-	4.54	7.16	2.12	5.36
/ 32d	1.60	7.20	3.52	4.80	6.05	2.77	3.03	7.20	11.44	3.78	3.47	4.71	4.29	7.15	2.16	5.39
/ 32e	1.28	6.91	3.51	4.59	6.05	2.77	3.04	6.89	-	3.76	3.48	4.69	4.42	7.44	2.13	5.64
/ 32f	1.48	7.11	3.52	4.69	6.05	2.77	3.02	6.60	-	3.75	3.47	4.57	4.57	7.24	2.14	5.45
Sp/ 59a	2.95	7.85	3.49	4.77		3.16	3.82		13.48	4.26	3.41	3.78	4.44	6.50	2.86	5.44
/ 59b	2.03	7.09	3.67	4.29	5.13	3.15	3.83	5.73	9.56	4.01	3.65	3.94	4.17	7.26	2.71	6.04
/ 59c	2.55	7.82	3.66	4.30	-	2.99	3.63	5.83	11.94	4.09	3.64	4.11	4.31	6.53	2.49	5.10
/ 59d	2.78	8.08	3.62	4.32	-	2.95	3.59	-	-	4.10	3.55	3.99	4.27	6.27	2.46	4.80
Sp/ 63	3.14	8.11	3.35	4.21		3.24	3.91		14.79	4.36	3.50	-	3.87	6.24	2.79	5.10
Sp/108	1.63	6.91	3.54	4.92	5.74	2.90	4.05	-	-	3.91	3.73	4.81	4.27	7.44	2.48	6.00

/116b	2.05	6.82	3.75	4.98	-	3.36	4.41	-	9.76	3.80	3.83	-	4.58	7.53	2.99	6.59
/116c	2.16	6.58	3.65	4.71	-	3.16	4.22	-	8.77	3.76	3.54	2.84	4.48	7.77	3.34	7.19
/116d	2.62	7.52	3.82	4.85	5.55	3.18	4.14	5.78	11.09	4.00	3.68	3.29	4.27	6.83	2.86	5.77
/116e	2.49	7.27	3.87	5.25	5.55	3.27	4.28	5.61	10.16	4.06	3.78	3.79	4.23	7.08	2.98	6.14
Sp/167a	4.12	9.0	2.35	3.67		3.50	3.32		>15	5.22	2.85	3.69	2.86	5.35	2.88	4.31
/167b	3.38	8.50	1.85	3.33	6.11	3.28	3.09	-	>15	5.02	2.25	4.12	2.50	5.85	2.64	4.57
/167c	4.04	8.79	2.11	3.41		3.49	3.31	-	>15	4.70	2.51	4.54	2.64	5.56	3.01	4.65
/167d	2.77	7.65	2.40	3.70	5.05	3.47	3.38	6.04	11.95	4.70	2.91	4.11	2.86	6.70	2.88	5.66
/167e	3.25	8.35	2.34	3.87	-	3.40	3.39	6.78	13.52	4.32	2.78	4.05	2.98	6.00	2.66	4.73
Sp/168a	1.99	7.13	3.91	4.92	6.03	3.09	3.61	7.13	-	4.12	3.86	4.51	4.82	7.22	2.62	5.91
/168b	1.93	7.26	3.79	4.74	6.04	2.93	3.47	-	11.30	4.12	3.68	4.72	-	7.09	2.43	5.59
/168c	2.40	7.72	3.82	4.52	-	3.00	3.36	-	12.42	4.16	3.63	5.00	5.01	6.63	2.44	5.14
/168d	1.66	6.90	3.77	4.99	5.73	2.97	3.70	6.44	9.97	4.25	3.69	4.89	4.36	7.45	2.52	6.05
/168e	1.85	7.20	3.70	4.68	5.56	2.91	3.54	6.01	11.06	4.05	3.66	4.48	4.54	7.15	2.41	5.63
Sp/169a	2.01	7.49	3.68	4.74	-	2.79	3.43	-	12.01	3.81	3.60	5.74	4.38	6.86	2.29	5.22
/169b	1.70	7.21	3.65	4.65	-	2.75	3.32	-	10.77	3.72	3.63	-	3.82	7.14	2.25	5.47
/169c	1.74	7.12	3.72	4.82	6.05	2.75	3.37	5.14	11.71	3.72	3.81	3.14	3.32	7.23	2.38	5.69
/169d	1.71	7.12	3.70	4.87	-	2.81	3.42	6.89	11.40	3.83	3.80	3.94	3.59	7.23	2.35	5.65
Sp/170a	2.24	6.28	3.58	5.42	-	3.61	4.08	6.30	9.58	4.01	3.78	3.37	4.31	8.07	3.72	7.87
/170b	2.87	6.87	3.56	5.72	-	3.71	4.18	6.08	10.40	3.85	3.77	3.31	4.49	7.48	3.77	7.32
Sp/189a	2.20	7.14	3.63	5.12	5.73	3.15	4.35	5.19	9.66	3.80	3.51	-	4.09	7.21	2.82	6.11
/189b	2.59	7.48	3.68	5.12	6.03	3.23	4.51	5.98	11.36	3.76	3.52	-	4.35	6.87	2.87	5.82
/189c	2.83	7.68	3.70	5.25	-	3.27	4.66	5.86	11.71	3.83	3.52	-	4.40	6.67	2.91	5.66
/189d	2.88	7.70	3.73	5.25	6.03	3.27	4.63	5.99	12.73	3.91	3.53	-	4.75	6.65	2.94	5.66
Sp/193a	2.03	7.38	3.37	4.41	6.04	2.88	3.63	6.57	10.92	4.04	3.62	4.08	4.31	6.97	2.41	5.46
/193b	2.02	7.42	3.62	4.48	6.04	2.86	3.60	6.70	10.51	4.02	3.64	4.10	4.46	6.93	2.37	5.37
Sp/233a	3.22	7.32	4.12	5.41	4.69	4.05	4.30	-	-	6.00	4.13	5.23	4.50	7.03	3.66	6.77
/233b	3.92	8.28	4.36	5.71	4.96	3.80	4.33	-	-	5.71	4.29	5.17	4.67	6.07	3.40	5.55
Sp/238	2.78	7.80	0.49	2.17	-	2.62	1.84	-		5.63	0.45	-	2.58	6.56	2.81	5.43

- indicates not detected in the analyses; blank indicates not determined.

APPENDIX 6.2 ΔG_{diff} VALUES IN KCAL/MOL AT 15°C OF THE KARSTIC WATERS FOR A NUMBER OF MINERALS (WITH ΔG_{tol} VALUES)

Sample number	Kaolinite $\Delta G_{tol}=\pm1.55$ kcal/mol	Halloysite $\Delta G_{tol}=\pm1.51$ kcal/mol	Illite $\Delta G_{tol}=\pm1.75$ kcal/mol	Muscovite $\Delta G_{tol}=\pm1.87$ kcal/mol	Ca-Montmorillonite $\Delta G_{tol}=\pm1.93$ kcal/mol	Mg-Montmorillonite $\Delta G_{tol}=\pm2.04$ kcal/mol	K-Montmorillonite $\Delta G_{tol}=\pm2.02$ kcal/mol	Na-Montmorillonite $\Delta G_{tol}=\pm1.91$ kcal/mol	Pyrophyllite $\Delta G_{tol}=\pm3.40$ kcal/mol	Mg-Chlorite $\Delta G_{tol}=\pm2.49$ kcal/mol	Boehmite $\Delta G_{tol}=\pm0.63$ kcal/mol	Gibbsite(cc) $\Delta G_{tol}=\pm0.33$ kcal/mol	Gibbsite(cr) $\Delta G_{tol}=\pm0.43$ kcal/mol	Calcite $\Delta G_{tol}=\pm0.39$ kcal/mol	Aragonite $\Delta G_{tol}=\pm0.43$ kcal/mol	Dolomite $\Delta G_{tol}=\pm0.64$ kcal/mol	Magnesite $\Delta G_{tol}=\pm0.49$ kcal/mol	Siderite $\Delta G_{tol}=\pm0.53$ kcal/mol
Sp/ 19a	6.08	1.08	4.33	4.91	6.60	6.47	5.72	5.85	4.84	-2.37	1.37	0.08	0.58	-0.12	-0.17	-1.35	-2.05	
/ 19b	6.89	1.88	5.46	6.19	7.55	7.43	6.76	6.19	5.65	-1.12	1.76	0.48	0.97	-0.07	-0.12	-1.19	-1.95	
/ 19c														-0.37	-0.42	-1.42	-1.88	-2.35
/ 19d	7.79	2.78	6.46	7.62	8.50	8.42	7.53	7.67	6.20	4.89				0.10	0.05	-0.64	-1.56	-0.98
Sp/ 31a	6.36	1.35	4.46	5.01	6.59	6.64	5.54	5.70	4.53	4.70	1.80	0.51	1.01	0.16	0.11	0.20	-0.78	
/ 31b	7.81	2.81	6.35	6.38	8.35	8.39	7.27	7.49	6.21	3.39	2.41	1.13	1.62	-0.13	-0.17	-0.39	-1.08	-1.27
/ 31c	7.04	2.04	5.04	5.62	7.47	7.51	6.30	6.60	5.35	4.73	2.08	0.79	1.28	0.09	0.04	0.05	-0.86	-1.27
/ 31d	5.59	0.59	3.64	3.90	5.72	5.73	4.64	4.86	3.73	4.99	1.43	0.15	0.64	0.26	0.21	0.40	-0.52	-1.54
Sp/ 32a														0.74	0.69	1.95	0.38	
/ 32b														0.11	0.06	0.14	-0.79	
/ 32c	6.44	1.43	4.59	4.84	7.02	7.07	5.86	6.15	5.08	5.56	1.60	0.31	0.80	0 25	0.21	0.45	-0.63	
/ 32d	5.44	0.44	3.78	3.76	5.83	5.89	4.82	4.99	4.06	4.57	1.12	-0.23	0.33	0.19	0.14	0.32	-0.69	-2.65
/ 32e														-0.16	-0.21	-0.38	-1.04	-2.59
/ 32f														0.10	0.05	0.16	-0.76	-1.94
Sp/ 59a	3.92	-1.05	2.02	2.43	3.46	3.43	2.54	2.72	1.31	5.85	1.01	-0.28	0.22	-0.40	-0.45	-1.37	-1.79	
/ 59b	8.95	3.95	7.45	9.56	9.41	9.37	8.69	8.58	6.99	1.06	3.16	1.88	2.37	-1.18	-1.23	-2.97	-2.61	-1.58
/ 59c	8.23	3.23	7.61	9.43	8.78	8.75	8.03	7.92	6.06	11.20	2.91	1.62	2.12	0.28	0.23	0.01	-1.09	-0.47
/ 59d														0.71	0.66	0.88	-0.65	
Sp/108														-0.80	-0.85	-2.82	-2.84	
Sp/116a	7.25	2.25	4.87	7.33	6.49	6.39	5.70	5.61	3.61	2.27	3.15	1.87	2.36	-1.25	-1.30	-3.51	-3.08	-2.16
/116b	6.84	1.84	4.22	5.12	7.15	7.03	6.19	6.34	5.43	-0.15	1.83	0.55	1.04	-2.19	-2.23	-5.46	-4.10	
/116c	7.65	2.65	5.14	6.39	8.10	7.98	7.21	7.29	6.43	-9.19	2.19	0.91	1.40	-2.70	-2.75	-6.51	-4.63	
/116d	8.35	3.34	6.84	8.47	8.89	8.83	7.94	8.01	6.40	4.11	2.85	1.57	2.06	-0.85	-0.90	-2.68	-2.65	-1.28
/116e	8.64	3.64	6.36	8.07	9.00	8.89	7.90	8.11	6.53	0.09	3.08	1.80	2.29	-1.47	-1.52	-3.98	-3.33	-1.55

Sp/168a														-0.93	-0.98	-2.25	-2.14	-3.26
/168b	5.42	0.41	3.22	3.89	5.21	5.20	4.25	4.29	3.15	2.03	1.55	0.26	0.76	-0.31	-0.36	-1.02	-1.54	
/168c	5.98	0.97	4.66	5.62	5.97	6.00	5.12	5.12	3.59	9.29	1.89	0.60	1.10	0.20	0.15	0.22	-0.80	
/168d	5.71	0.71	2.54	3.51	5.15	5.10	4.09	4.24	3.09	-4.15	1.87	0.58	1.08	-0.96	-1.00	-2.57	-2.44	-2.52
/168e	5.75	0.74	3.65	4.39	5.70	5.68	4.77	4.81	3.68	1.20	1.62	0.33	0.82	-0.34	-0.38	-1.20	-1.68	-1.41
Sp/169a	6.18	1.17	4.92	5.32	6.77	6.75	5.79	5.87	4.73	6.51	1.52	0.23	0.73	0.37	0.32	0.20	-0.99	
/169b	7.48	2.47	6.27	7.03	8.34	8.33	7.38	7.44	6.27	4.92	2.05	0.76	1.25	0.11	0.06	-0.30	-1.18	
/169c	4.99	-0.02	2.29	1.88	4.56	4.53	3.53	3.62	3.06	0.21	0.45	-0.83	-0.34	-0.19	-0.24	-0.89	-1.53	-0.33
/169d	4.80	-0.21	2.67	2.60	4.97	4.95	3.93	4.06	3.30	0.29	0.85	-0.43	0.06	-0.22	-0.27	-0.94	-1.55	-2.60
Sp/170a	2.49	-2.52	-2.15	-2.70	1.41	1.42	0.31	0.73	0.51	-17.71	-0.07	-1.35	-0.86	-4.20	-4.25	-8.72	-5.34	-4.74
/170b	5.41	0.40	2.04	2.07	6.00	5.33	4.11	4.67	3.84	-7.46	1.19	-0.09	0.40	-3.61	-3.66	-7.54	-4.75	-3.80
Sp/189a	9.62	4.62	7.78	9.53	10.57	10.42	9.49	9.76	8.19	-0.77	3.23	1.95	2.44	-1.28	-1.32	-3.83	-3.38	-0.95
/189b	7.94	2.94	6.36	7.46	8.81	8.64	7.75	8.00	6.62	1.06	2.33	1.05	1.55	-1.00	-1.05	-3.38	-3.21	-1.62
/189c	8.40	3.40	6.91	8.25	9.30	9.10	8.20	8.49	6.89	3.03	2.66	1.38	1.83	-0.83	-0.88	-3.20	-3.20	-1.24
/189d	5.68	0.67	3.70	4.19	6.00	5.82	4.90	5.18	3.97	0.71	1.40	0.11	0.61	-0.85	-0.89	-3.18	-3.16	-1.42
Sp/193a	7.08	2.07	6.17	7.68	7.89	7.84	7.07	7.14	5.49	4.79	2.51	1.23		-0.06	-0.11	-0.80	-1.57	-1.91
/193b	9.00	3.99	7.87	9.80	9.63	9.58	8.77	8.77	6.99	6.96	3.21	1.93	2.42	0.08	0.04	-0.51	-1.42	-1.97

APPENDIX 7 CALCULATION METHOD FOR THE CONSTRUCTION OF THE ACTIVITY DIAGRAMS AT 15°C AND 1 BAR PRESSURE AND THE RELEVANT EQUATIONS.

The activity diagrams used in this study to plot the composition of the water samples, give the stability fields for the phases at 15° C (288.15° K) and 1 bar pressure. The equilibrium constants for the reactions, necessary to construct the activity diagrams at the temperature and preesure mentioned above, were calculated from the appropriate equilibrium constants for the phases, given by the computer according the program "SOLMNEQ" (KHARAKA & BARNES, 1973).

The value for lg $KT_{muscovite}$ in this program appeared to be not correct. An adequate value at 15° C and 1 bar pressure was extrapolated from the figures presented by HELGESON (1969) for lg $KT_{muscovite}$ at temperatures from 25 to 300° C and 1 bar pressure. For the reaction

$$KAl_3Si_3O_{10}(OH)_2(s) + 10H^+ \rightleftarrows K^+ + 3Al^{3+} + 3H_4SiO_4^o$$

lg $KT_{288.15^o\ K\ muscovite}$, used to compute the equilibrium constants between muscovite and other phases, was estimated on 18.9.

An example of the calculation method can be given by the stability relation between clinochlore (Mg-chlorite, $Mg_5Al_2Si_3O_{10}(OH)_8$) and kaolinite ($Al_2Si_2O_5(OH)_4$):

167[1] $Mg_5Al_2Si_3O_{10}(OH)_8(s) + 16H^+ \rightleftarrows 5Mg^{2+} + 2Al^{3+} + 3H_4SiO_4^o + 6H_2O$ (a)

219[1] $2Al^{3+} + 2H_4SiO_4^o + H_2O \rightleftarrows Al_2Si_2O_5(OH)_4(s) + 6H^+$ (b)

$Mg_5Al_2Si_3O_{10}(OH)_8(s) + 10H^+ \rightleftarrows Al_2Si_2O_5(OH)_4(s) + 5Mg^{2+} + H_4SiO_4^o + 5H_2O$ (c)

Lg $KT_{reaction\ c}$ = lg $KT_{reaction\ a}$ + lg $KT_{reaction\ b}$. For 15° C and 1 bar pressure the lg $KT_{reaction\ c}$ = 62.3350 + (-8.6176) = 53. 7174. The equilibrium state between clinochlore (Mg-chlorite) and kaolinite is therefore given by the equation

$$5(\lg[Mg^{2+}] + 2pH) + \lg[H_4SiO_4^o] = 53.72$$

When hydroxides as gibbsite were involved, also the water equilibrium constant was introduced in the calculations (e.g. clinochlore to gibbsite ($Al(OH)_3$):

167[1] $Mg_5Al_2Si_3O_{10}(OH)_8(s) + 16H^+ \rightleftarrows 5Mg^{2+} + 2Al^{3+} + 3H_4SiO_4^o + 6H_2O$ (d)

208[1] $2Al^{3+} + 6OH^- \rightleftarrows 2Al(OH)_3(s)$ (e)

2[1] $6H_2O \rightleftarrows 6H^+ + 6OH^-$ (f)

$Mg_5Al_2Si_3O_{10}(OH)_8(s) + 10H^+ \rightleftarrows 2Al(OH)_3(s) + 5Mg^{2+} + 3H_4SiO_4^o$ (g)

[1] Numbers refer to table 1 in KHARAKA & BARNES (1973).

Lg $KT_{\text{reaction g}}$ = lg $KT_{\text{reaction d}}$ + lg $KT_{\text{reaction e}}$ + lg $KT_{\text{reaction f}}$. For 15° C (288.15° K) and 1 bar pressure lg $KT_{\text{reaction g}}$ = 62.3350 + 2(+33.1423) + + 6(-14.3510) = 42.5136. The equilibrium state between clinochlore (Mg-chlorite) and gibbsite is therefore given by the equation

$$5(\lg[Mg^{2+}] + 2pH) + 3\lg[H_4SiO_4^o] = 42.51$$

The following equations were used to construct the activity diagrams for the several systems:

A. The $MgO-Al_2O_3-SiO_2-H_2O$ system.

Clinochlore (Mg-chlorite) → Mg-montmorillonite

$$2.33Mg_5Al_2Si_3O_{10}(OH)_8(s) + 22.64H^+ + 0.35H_4SiO_4^o \rightarrow$$
$$2Mg_{0.167}Al_{2.33}Si_{3.67}O_{10}(OH)_2(s) + 11.32Mg^{2+} + 19.34H_2O$$
$$11.32(\lg[Mg^{2+}] + 2pH) - 0.35\lg[H_4SiO_4^o] = 130.88$$

Clinochlore (Mg-chlorite) → kaolinite

$$Mg_5Al_2Si_3O_{10}(OH)_8(s) + 10H^+ \rightarrow Al_2Si_2O_5(OH)_4(s) + 5Mg^{2+} + H_4SiO_4^o + 5H_2O$$
$$5(\lg[Mg^{2+}] + 2pH) + \lg[H_4SiO_4^o] = 53.72$$

Clinochlore (Mg-chlorite) → gibbsite

$$Mg_5Al_2Si_3O_{10}(OH)_8(s) + 10H^+ \rightarrow 2Al(OH)_3(s) + 5Mg^{2+} + 3H_4SiO_4^o$$
$$5(\lg[Mg^{2+}] + 2pH) + 3\lg[H_4SiO_4^o] = 42.51$$

Mg-montmorillonite → kaolinite

$$2Mg_{0.167}Al_{2.33}Si_{3.67}O_{10}(OH)_2(s) + 0.66H^+ + 7.69H_2O \rightarrow$$
$$2.33Al_2Si_2O_5(OH)_4(s) + 0.33Mg^{2+} + 2.68H_4SiO_4^o$$
$$0.33(\lg[Mg^{2+}] + 2pH) + 2.68\lg[H_4SiO_4^o] = -5.72$$

Mg-montmorillonite → gibbsite

$$Mg_{0.167}Al_{2.33}Si_{3.67}O_{10}(OH)_2(s) + 0.33H^+ + 9.67H_2O \rightarrow$$
$$2.33Al(OH)_3(s) + 0.167Mg^{2+} + 3.67H_4SiO_4^o$$
$$0.167(\lg[Mg^{2+}] + 2pH) + 3.67\lg[H_4SiO_4^o] = -15.91$$

Kaolinite → gibbsite

$$Al_2Si_2O_5(OH)_4(s) + 5H_2O \rightarrow 2Al(OH)_3(s) + 2H_4SiO_4^o$$
$$2\lg[H_4SiO_4^o] = -11.20$$

B. The K_2O-Al_2O_3-SiO_2-H_2O system.

K-feldspar (microcline) → muscovite

$$3KAlSi_3O_8(s) + 2H^+ + 12H_2O \rightarrow KAl_3Si_3O_{10}(OH)_2(s) + 2K^+ + 6H_4SiO_4^o$$

$$2(\lg[K^+] + pH) + 6\lg[H_4SiO_4^o] = -14.11$$

K-feldspar → K-montmorillonite

$$2.33KAlSi_3O_8(s) + 2H^+ + 6.64H_2O \rightarrow K_{0.33}Al_{2.33}Si_{3.67}O_{10}(OH)_2(s) + 2K^+ + 3.32H_4SiO_4^o$$

$$2(\lg[K^+] + pH) + 3.32\lg[H_4SiO_4^o] = -3.19$$

K-feldspar → kaolinite

$$2KAlSi_3O_8(s) + 2H^+ + 9H_2O \rightarrow Al_2Si_2O_5(OH)_4(s) + 2K^+ + 4H_4SiO_4^o$$

$$2(\lg[K^+] + pH) + 4\lg[H_4SiO_4^o] = -5.42$$

K-feldspar → gibbsite

$$KAlSi_3O_8(s) + H^+ + 7H_2O \rightarrow Al(OH)_3(s) + K^+ + 3H_4SiO_4^o$$

$$\lg[K^+] + pH + 3\lg[H_4SiO_4^o] = -8.31$$

Muscovite → K-montmorillonite

$$2.33KAl_3Si_3O_{10}(OH)_2(s) + 1.34H^+ + 4.02H_4SiO_4^o \rightarrow 3K_{0.33}Al_{2.33}Si_{3.67}O_{10}(OH)_2(s) + 1.34K^+ + 8.04H_2O$$

$$1.34(\lg[K^+] + pH) - 4.02\lg[H_4SiO_4^o] = 23.29$$

Muscovite → kaolinite

$$2KAl_3Si_3O_{10}(OH)_2(s) + 2H^+ + 3H_2O \rightarrow 3Al_2Si_2O_5(OH)_4(s) + 2K^+$$

$$2(\lg[K^+] + pH) = 11.95$$

Muscovite → gibbsite

$$KAl_3Si_3O_{10}(OH)_2(s) + H^+ + 9H_2O \rightarrow 3Al(OH)_3(s) + K^+ + 3H_4SiO_4^o$$

$$\lg[K^+] + pH + 3\lg[H_4SiO_4^o] = -10.83$$

K-montmorillonite → kaolinite

$$2K_{0.33}Al_{2.33}Si_{3.67}O_{10}(OH)_2(s) + 0.66H^+ + 7.69H_2O \rightarrow 2.33Al_2Si_2O_5(OH)_4(s) + 0.66K^+ + 2.68H_4SiO_4^o$$

$$0.66(\lg[K^+] + pH) + 2.68\lg[H_4SiO_4^o] = -6.25$$

K-montmorillonite → gibbsite

$$K_{0.33}Al_{2.33}Si_{3.67}O_{10}(OH)_2(s) + 0.33H^+ + 9.67H_2O \rightarrow 2.33Al(OH)_3(s) + 0.33K^+ + 3.67H_4SiO_4^o$$

$$0.33(\lg[K^+] + pH) + 3.67\lg[H_4SiO_4^o] = -16.18$$

Kaolinite → gibbsite

$$Al_2Si_2O_5(OH)_4(s) + 5H_2O \rightarrow 2Al(OH)_3 + 2H_4SiO_4^o$$

$$2\lg[H_4SiO_4^o] = -11.20$$

C. The K_2O-MgO-Al_2O_3-SiO_2-H_2O system[1]

Muscovite → clinochlore (Mg-chlorite)

$$2KAl_3Si_3O_{10}(OH)_2(s) + 15Mg^{2+} + 3H_4SiO_4^o + 18H_2O \rightarrow 3Mg_5Al_2Si_3O_{10}(OH)_8(s) + 28H^+ + 2K^+$$

$$2(\lg[K^+] + pH) - 15(\lg[Mg^{2+}] + 2pH) - 3\lg[H_4SiO_4^o] = -149.21$$

Muscovite → K-montmorillonite

$$2.33KAl_3Si_3O_{10}(OH)_2(s) + 0.5Mg^{2+} + 4.02H_4SiO_4^o + 1.34H^+ \rightarrow 3Mg_{0.167}Al_{2.33}Si_{3.67}O_{10}(OH)_2(s) + 2.33K^+ + 8.04H_2O$$

$$2.33(\lg[K^+] + pH) - 0.5(\lg[Mg^{2+}] + 2pH) - 4.02\lg[H_4SiO_4^o] = 22.50$$

Muscovite → illite

$$2.3KAl_3Si_3O_{10}(OH)_2(s) + 0.75Mg^{2+} + 3.6H_4SiO_4^o \rightarrow K_{0.6}Mg_{0.25}Al_{2.3}Si_{3.5}O_{10}(OH)_2(s) + 0.5K^+ + H^+ + 6H_2O$$

$$0.5(\lg[K^+] + pH) - 0.75(\lg[Mg^{2+}] + 2pH) - 3.6\lg[H_4SiO_4^o] = 8.87$$

Illite → clinochlore (Mg-chlorite)

$$2K_{0.6}Mg_{0.25}Al_{2.3}Si_{3.5}O_{10}(OH)_2(s) + 11Mg^{2+} + 17.8H_2O \rightarrow 2.3Mg_5Al_2Si_3O_{10}(OH)_8(s) + 1.2K^+ + 0.1H_4SiO_4^o + 20.8H^+$$

$$1.2(\lg[K^+] + pH) - 11(\lg[Mg^{2+}] + 2pH) + 0.1\lg[H_4SiO_4^o] = -120.30$$

Illite → Mg-montmorillonite

$$2.33K_{0.6}Mg_{0.25}Al_{2.3}Si_{3.5}O_{10}(OH)_2(s) + 0.286H_4SiO_4^o + 1.804H^+ \rightarrow 2.3Mg_{0.167}Al_{2.33}Si_{3.67}O_{10}(OH)_2(s) + 1.398K^+ + 0.198Mg^{2+} + 1.504H_2O$$

$$1.398(\lg[K^+] + pH) + 0.198(\lg[Mg^{2+}] + 2pH) - 0.286\lg[H_4SiO_4^o] = 10.36$$

Illite → K-montmorillonite

$$2.33K_{0.6}Mg_{0.25}Al_{2.3}Si_{3.5}O_{10}(OH)_2(s) + 0.286H_4SiO_4^o + 1.804H^+ \rightarrow 2.3K_{0.33}Al_{2.33}Si_{3.67}O_{10}(OH)_2(s) + 0.639K^+ + 0.5825Mg^{2+} + 1.504H_2O$$

$$0.639(\lg[K^+] + pH) + 0.5825(\lg[Mg^{2+}] + 2pH) - 0.286\lg[H_4SiO_4^o] = 10.97$$

Illite → kaolinite

$$2K_{0.6}Mg_{0.25}Al_{2.3}Si_{3.5}O_{10}(OH)_2(s) + 2.2H^+ + 6.3H_2O \rightarrow 2.3Al_2Si_2O_5(OH)_4(s) + 1.2K^+ + 0.5Mg^{2+} + 2.4H_4SiO_4^o$$

$$1.2(\lg[K^+] + pH) + 0.5(\lg[Mg^{2+}] + 2pH) + 2.4\lg[H_4SiO_4^o] = 3.25$$

Illite → gibbsite

$$K_{0.6}Mg_{0.25}Al_{2.3}Si_{3.5}O_{10}(OH)_2(s) + 1.1H^+ + 8.9H_2O \rightarrow 2.3Al(OH)_3(s) + 0.6K^+ + 0.25Mg^{2+} + 3.5H_4SiO_4^o$$

$$0.6(\lg[K^+] + pH) + 0.25(\lg[Mg^{2+}] + 2pH) + 3.5\lg[H_4SiO_4^o] = -11.26$$

K-montmorillonite → clinochlore (Mg-chlorite)

$$2K_{0.33}Al_{2.33}Si_{3.67}O_{10}(OH)_2(s) + 11.65Mg^{2+} + 19.34H_2O \rightarrow$$
$$2.33Mg_5Al_2Si_3O_{10}(OH)_8(s) + 0.66K^+ + 0.35H_4SiO_4^o + 22.64H^+$$

$$0.66(\lg[K^+] + pH) - 11.65(\lg[Mg^{2+}] + 2pH) + 0.35\lg[H_4SiO_4^o] = -131.41$$

K-montmorillonite → Mg-montmorillonite

$$K_{0.33}Al_{2.33}Si_{3.67}O_{10}(OH)_2(s) + 0.167Mg^{2+} \rightarrow$$
$$Mg_{0.167}Al_{2.33}Si_{3.67}O_{10}(OH)_2(s) + 0.33K^+$$

$$0.33(\lg[K^+] + pH) - 0.167(\lg[Mg^{2+}] + 2pH) = -0.26$$

[1]This system includes also the equations mentioned under A and B.

APPENDIX 8 LIST OF NORM MINERALS USED.

Symbol	Mineral name	Formula
Ab	Albite	$6SiO_2.Al_2O_3.Na_2O$
AF	Alkali feldspars	Mixture of Ab - Or
Alm	Almandine	$3SiO_2.Al_2O_3.3FeO$
An	Anorthite	$2SiO_2.Al_2O_3.CaO$
Apa	Apatite	$3P_2O_5.9CaO.CaF_2$
Aug	Augite	$12SiO_2.8(Mg,Fe)O.4CaO$
Bi	Biotite	$6SiO_2.Al_2O_3.6(Mg,Fe)O.K_2O.2H_2O$
Cc	Calcite	$CaO.CO_2$
Chlor	Chlorite	$3SiO_2.Al_2O_3.5(Mg,Fe)O.4H_2O$
Dol	Dolomite	$CaO.MgO.2CO_2$
Ep	Epidote	$6SiO_2.2Al_2O_3.Fe_2O_3.4CaO.H_2O$
Fer	Ferrihydrite	$Fe_2O_3.3H_2O$
Gibb	Gibbsite	$Al_2O_3.3H_2O$
Go	Goethite	$Fe_2O_3.H_2O$
Hm	Haematite	Fe_2O_3
Ill	Illite	$K_{0.6}Mg_{0.25}Al_{2.3}Si_{3.5}O_{10}(OH)_2$
Kaol	Kaolinite	$2SiO_2.Al_2O_3.2H_2O$
Mica		Mixture of Bi - Ms
Ms	Muscovite	$6SiO_2.3Al_2O_3.K_2O.2H_2O$
Or	Orthoclase	$6SiO_2.Al_2O_3.K_2O$
Plag	Plagioclase	Mixture of Ab - An
Prl	Pyrolusite	MnO_2
Pyr	Pyrite	FeS_2
Q	Quartz (free silica)	SiO_2
Ru	Rutile	TiO_2
Sil	Sillimanite	$SiO_2.Al_2O_3$
Sm	Smectite (montmorillonite)	$16SiO_2.3Al_2O_3.2(Mg,Fe)O.4H_2O$
Str	Strengite	$Fe_2O_3.P_2O_5.4H_2O$
Verm	Vermiculite	$6SiO_2.Al_2O_3.6MgO.4H_2O$
W	Water	H_2O

Druk: Boek- en Offsetdrukkerij Verweij Wageningen b.v.